# THE INTRUSIVE HISTORY OF THE LITTLE CHIEF GRANITE PORPHYRY STOCK, CENTRAL PANAMINT RANGE, CALIFORNIA

## I. STRUCTURAL RELATIONSHIPS

## II. PETROGENESIS, BASED ON ELECTRON MICROPROBE ANALYSES OF THE FELDSPARS

Thesis by

Stewart Douglas McDowell

In Partial Fulfillment of the Requirements

For the Degree of

Doctor of Philosophy

California Institute of Technology

Pasadena, California

1967

(Submitted September 19, 1966)

ACKNOWLEDGMENTS

I am especially grateful to Dr. Arden L. Albee; who originally suggested this thesis topic, for his aid and encouragement throughout the duration of this investigation, and for his unending fund of patience. I would also like to thank Dr. L. T. Silver, Dr. C. R. Allen, Dr. L. S. Hollister, and Mr. T. McGetchin for much rewarding discussion and assistance.

Electron microprobe analyses were obtained with the able assistance of A. A. Chodos, and standards were supplied by Drs. J. V. Smith and H. P. Taylor.

Mr. Rudolf Von Huene prepared polished thin sections for microprobe analysis, and Bep Bingham performed wet chemical analyses on microprobe standards and stock samples. Finally, I would here like to thank the staff of the Geology Department in general for their timely aquisition of an electron microprobe.

Drs. Lauren A. Wright and Bennie W. Troxel provided much very useful information on the geologic relationships in the Death Valley area, and, along with Dr. John H. Stewart, greatly aided the decifering of the stratigraphic relationships in the Panamint Range. Drs. David B. Stewart and J. V. Smith provided many insights into the complexities of feldspar phase relationships, and Dr. Barclay Kamb kindly made available single crystal X-ray equipment. I am also indebted to H. Starr Curtis, Charlie Carter, and Roger LeBaron Hooke for geologic mapping in the Happy Canyon-Pleasant Canyon area.

The staff of the Death Valley National Monument offered much useful information on access to various parts of the area, and added greatly to the safety of mapping alone by providing a check-out system during extended periods of field work.

Funds covering the expenses of field work were made available by the Geological Society of America Penrose Bequest Grant 975-63 and 64. Laboratory expenses were provided by National Science Foundation Grant GP-2807. Research funds and equipment were also provided by the Geology Department of the California Institute of Technology.

The able assistance of Miss Susan House in innumerable matters directly or indirectly related to the thesis in question is most gratefully acknowledged.

## ABSTRACT

The Little Chief stock of Upper Miocene (?) age, located in the central Panamint Range near Death Valley, California, crops out over an area of 2.5 by 4.5 miles and through an elevation range of 6300 feet. It is a crosscutting diapir-like body with contact attitudes ranging from vertical to 80° outward except along the eastern margin, where the contact attitudes range from 45° outward to 35° inward. The stock appears to neck downward into a thin, east-west, dike-like body at a depth of less than 6000 feet below the present surface.

The stock has lifted a nearly rectangular "trapdoor" of later Precambrian and Precambrian (?) rocks bounded by vertical faults on the north, west, and south. The trapdoor opens to the west with a vertical throw of 3000 feet on the western margin and with a roughly north-south hinge line located just east of the stock. East of the hinge line, the trapdoor has been slightly depressed. The trapdoor offsets an earlier set of westward-dipping normal faults along which a porphyry dike swarm has been intruded.

The stock consists of two intrusive phases, a south and a slightly later north phase. The stock magma moved to a position roughly 6000 feet below the present surface and formed the westward-dipping normal faults by stretching the sedimentary rocks over the magma chamber roof, which were immediately injected by the porphyry dikes. The magma moved to the present level, truncating the normal faults and associated dikes, forming the trapdoor, and doming the sediments of the roof. The interior of the north phase then moved

slightly upward to the present level, disrupting the eastern part of the trapdoor and renewing movement on some of the trapdoor faults.

The stock is a hornblende-biotite granite porphyry with 2-10mm normally-zoned sanidine and plagioclase in a quartz-alkali feldspar-plagioclase groundmass. Detailed electron microprobe analyses yield the following feldspar compositions. The plagioclases have distinct normally-zoned layers separated by abrupt compositional gaps. The gaps formed by sporadic, abrupt water pressure decreases as the magma moved upward. Assimilation of water-rich calcic material caused large calcic oscillations on the plagioclase zones. Zonation in the outermost edges of the plagioclase phenocrysts to very low-Or plagioclase could be due to $P_{H_2O}$ increase and/or the effect of the peristerite solvus on the ternary feldspar solvus.

Sanidine coexisted with $An_{20}$ plagioclase in a magma chamber 12,000 feet below the present level, which had an undifferentiated, unsaturated ($P_{H_2O}$ = 1-1.5 Kb., T = 715°C) core surrounded by a differentiated, saturated ($P_{H_2O}$ = 2-2.5 Kb., T = 680°C) exterior. This $P_{H_2O}$ variation was equalized as the magma moved up to its present position, where the groundmass crystallized at $P_{H_2O}$ = 0.5 Kb., $P_{fluid} = P_{total}$ = 0.7 Kb., T=775°C, some 7000 feet below the contemperaneous ground surface.

Sanidine was removed from equilibrium, due to its rapid crystallization and shift of the feldspar boundary on $P_{H_2O}$ increase, at different times. It was rimmed by $An_{20}$ plagioclase in the water-poor core of the magma chamber before the magma started to move upward. Toward the exterior sanidine began to be replaced by sodic oligoclase

as the magma moved upward, and in the water-rich exterior parts sanidine exsolved to a patch perthite while the system was 50 percent melt, and the K-phase was then replaced by sodic oligoclase. In the very water-rich parts, sanidine crystallized in equilibrium until the groundmass was formed.

During upward movement assimilation of dolomitic rock formed a contaminated marginal phase which was then intruded by uncontaminated magma and carried upward as inclusions.

Fracturing of the roof of the present stock led to volatile concentration in certain restricted portions of the stock, and formation of quartz macrocyrsts, graphic textures, pegmatitic pods, coarse lamellar perthite in the sanidine, and numerous vugs.

TABLE OF CONTENTS

PART I : STRUCTURAL RELATIONSHIPS.

# LIST OF ILLUSTRATIONS

# LIST OF PLATES

# I. STRUCTURAL RELATIONSHIPS

## INTRODUCTION

The main objective of this investigation is to reconstruct in as much detail as possible the intrusive history, both structural and petrologic, of a shallow acidic intrusive igneous body. Of prime concern is the determination of the mechanisms through which the crystal-melt equilibrium adjusted to keep pace with changes in physical conditions.

Two things provided the impetus for this investigation. With the advent of the electron microprobe, it is now possible to obtain quite easily and directly vast amounts of compositional information on the crystalline phases, and hence the crystallization history can be determined in far greater detail that has been possible in the past. Secondly, the large amount of recent experimental work on feldspar phases relationships has provided a backlog of information which has not been compared in any great detail with naturally crystallizing feldspars.

The Little Chief stock was chosen for detailed study for three reasons. First, its composition is such that it can be treated accurately in the Or-Ab-An-Q-water system. Second, the feldspar textural relationships are exceedingly complex; and, finally, the stock is well exposed in all three dimensions.

The mapped area (Fig. 1) comprises some 55 square miles of the eastern flank of the Panamint Range, which defines the western side of Death Valley, California. It is roughly outlined by the meridians $117^{\circ}00'$ and $117^{\circ}07'$ west longitude and the parallels $36^{\circ}04'$ and $36^{\circ}12'$ north latitude, and lies 105 miles west of Las Vegas, Nevada

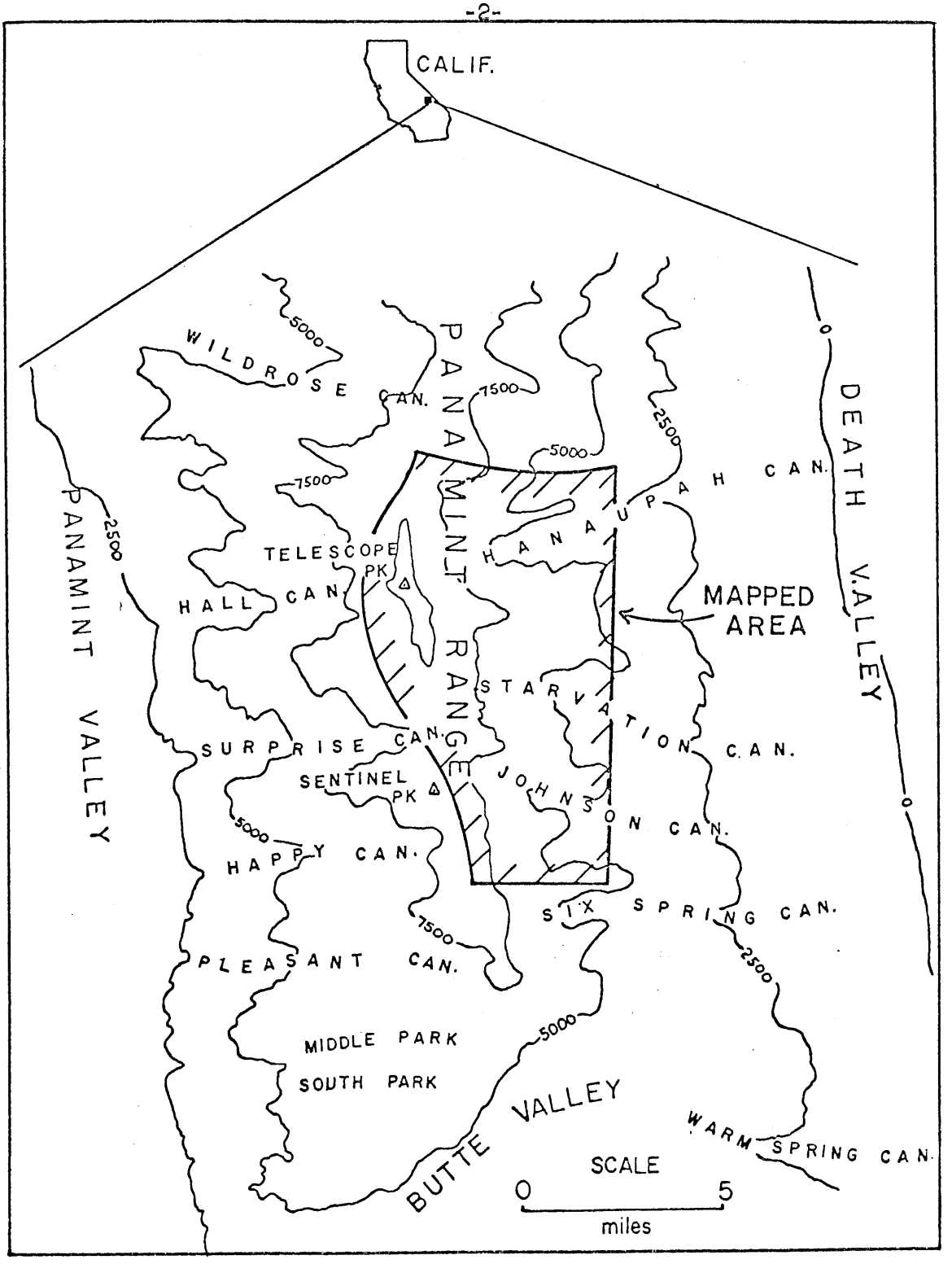


Fig. 1. Location of mapped area, Central Panamint Range near Death Valley, California.

and 118 miles east-northeast of Bakersfield, California. The stock occupies the central 15 square miles of the mapped area. The western boundary of Death Valley National Monument passes through the western part of the area, and the area itself occupies the northeastern portion of the Telescope Peak 15-minute Quadrangle.

The eastern edge of the area can be reached by jeep roads in Hanaupah and Johnson Canyons from the Death Valley side, and the western edge by a graded road leading up Surprise Canyon to Panamint City, an abandoned mining town, from the Panamint Valley side of the Panamint Range. The higher parts of the area can be reached from the Telescope Peak trail which comes into the mapped area from the north side along the crest of the range.

The roughly north-south oriented Panamint Range drainage divide passes through the western portion of the mapped area, and Bennett Peak (elevation 9980 feet), Telescope Peak (11049 feet) and Sentinel Peak (9636 feet) occur along this divide, respectively, at the north edge, in the west-central part, and at the south edge of the mapped area. The eastern edge of the mapped area, some 3 to 4 miles east of the divide, lies at elevations of 3000 feet in the canyon bottoms. Three evenly spaced east-west canyons extend eastward from the range divide: These are, from north to south, Hanaupah, Starvation, and Johnson Canyons. The local relief of the ridges between the canyons ranges from 2000 feet to 3500 feet. The topography is extremely rugged within the outcrop area of the stock, and vertical elevation changes of 2000 feet in the same horizontal distance are quite common.

The area was mapped over a period of 80 actual field days by the author working alone in the period from the summer of 1963 to the spring of 1964. The higher elevations were mapped during the summer from a base camp located on the east face of Telescope Peak at an elevation of roughly 8000 feet, and during this period, temperatures seldom exceeded 85°F. The lower elevations were mapped during the fall through spring months from base camps located at Hanaupah Spring in Hanaupah Canyon, at the springs at 4000 feet elevation in Starvation Canyon, and at the corral just below Hungry Bill's Ranch in Johnson Canyon. Most of the specimens from the stock itself were packed out from the Starvation Canyon base camp. Springs with potable water were present at all the base camps, and were shared with mountain sheep, coyote, wolf, desert fox, mule deer and the everpresent burro. Off the jeep roads and the Telescope Peak trail, no persons were seen within the mapped area.

## Thesis Outline

The thesis has been divided into two sections which represent two basically different approaches to the determination of the intrusive history of the stock.

In the first section, a structural approach is used, and an intrusive history is worked out on the basis of the sequence of deformation of the country rock by the emplacement of the stock. The crux of this section is the construction of a detailed structure contour diagram on one of the stratigraphic contacts. With this as a basis, the displacements on the various faults associated with the stock

emplacement are determined, and the amount of deviation of the contoured contact from its original pre-stock position is estimated. Using this information, and by comparison of the structures associated with the stock's emplacement with structures associated with the emplacement of salt domes and salt diapirs, an intrusive history is worked out for the stock.

In the second portion of the thesis, a detailed intrusive history is worked out for the stock on the basis of detailed feldspar compositional variations obtained using the electron microprobe in combination with optical work. Since this is the first major petrologic study on an igneous body using the electron microprobe, this portion of the thesis is discussed in somewhat more detail than would be normal in future work.

After a brief general description of the stock, several phases of the stock are discussed in great detail, and crystallization sequences for each phase developed. On the basis of the probe work, the mechanisms by which the crystals adjusted to the various changes in physical conditions are outlined. The distribution of the various phases, textures, and derived crystallization sequences is then discussed, and an effort is made to estimate the distribution and composition of the fluid phase. Finally, after a discussion of the Or-Ab-An-Q-water system, the physical conditions of the stock magma at the various stages of crystallization are estimated and a summary intrusive history outlined.

## SEDIMENTARY ROCKS

### General Statement

The rocks in the vicinity of the Little Chief stock consist of a series of slightly-metamorphosed sedimentary rocks which can be correlated with formations present throughout the area to the east of the Panamints (Hazzard, 1937; Johnson, 1957; Stewart, oral communication, 1965). Starting with the oldest rocks, the formations present are: 1) basement of the Panamint Metamorphic Complex (Murphy, 1932; Lanphere et al, 1964; Albee and Lanphere, 1962); 2) The Pahrump Series, consisting of the Crystal Spring, Beck Spring and Kingston Peak Formations in this area (Albee and Lanphere, 1962); and 3) The Noonday, Johnnie, Stirling and Wood Canyon Formations. Major unconformities occur a) between the Pahrump Series and the metamorphic complex (Noble and Wright, 1954; Lanphere, 1962; Albee and Lanphere, 1962), and b) between the Pahrump Series and the Noonday Dolomite (Lanphere, 1962; Johnson, 1957; Noble and Wright, 1954). Rocks from the Noonday through Wood Canyon Formations are apparently conformable.

The lowest Olenellus zones (Lower Cambrian) occur within the upper Wood Canyon Formation (Hunt and Mabey, 1966; Hopper, 1947), so that in this area the rocks below the Wood Canyon Formation have been broken into 3 age groups. The Noonday-Johnnie-Stirling Formations are assigned a Precambrian(?) age; the Pahrump Series is assigned to the later Precambrian; and the metamorphic complex is assigned to the earlier Precambrian on a stratigraphic basis (Noble and Wright, 1954) and also on a radiometric basis as 1400-1800 m.y. ages (U-Pb) have been

obtained on it (Lanphere et al, 1964).

In the Wildrose area (Lanphere, 1962), rocks equivalent in age to the Pahrump Series have been metamorphosed in the 75-85 m.y. age interval to such a degree that it is difficult to distinguish between earlier and later Precambrian rocks. To the south, the distinction between earlier and later Precambrian rocks, based in part on degree of metamorphism, is clear, although all rocks (Lanphere et al, 1964) seem to have been affected by the Cretaceous metamorphism. Earlier workers (Hopper, 1947; Murphy, 1932; Johnson, 1957) used the degree of metamorphism as a major criteria for distinguishing between earlier and later Precambrian rocks, with the result that much of the rock termed earlier and later Precambrian is in fact equivalent to later Precambrian Pahrump Series rocks.

The Panamint Range, in the mapped area, may be thought of as a series of gently eastward dipping sedimentary formations, with the east slope of the range essentially a dip slope, and the west slope cutting down across the various formations. This simple pattern is perturbed by the intrusion of the Little Chief stock, which crops out mostly on the east slope of the range.

The stock itself, and its related rocks, is in intrusive contact with Noonday and Johnnie Formations over most of its area, except in the extreme northeast and extreme southwest corners of the stock, where upper Kingston Peak, and Kingston Peak and Beck Spring Formations, respectively, are intruded by the stock at the present exposure level. In terms of working out the structural relationships of the stock, most of the important deformation is confined to the

outcrop belts of the Johnnie and Noonday Formations; hence in the following section, major emphasis will be placed on descriptions and stratigraphic variations within these two formations. Descriptions of the Panamint Metamorphic Complex and the Crystal Spring and Beck Spring Formations are taken from various published and unpublished work by Albee and/or Lanphere, and Johnson (1957), as the outcrop extent of these rocks is minimal in the area mapped in detail.

## Earlier Precambrian Rocks

The rocks which lie unconformably below the Pahrump Series have been termed the Panamint Metamorphic Complex by Murphy (1932). Included are gneisses, schists, amphibolites, marbles and quartzites of both igneous and sedimentary origin. In the area between Pleasant and Happy Canyons, southwest of the mapped area, probable meta-igneous rocks occur which were called the World Beater Porphyry by Murphy (1932) and renamed the World Beater Complex by Albee (Lanphere et al, 1964).

The World Beater Complex, which makes up better than 90 percent of earlier Precambrian outcrop area in the Pleasant and Happy Canyon area, consists of two intimately intermingled units, an older foliated K-feldspar-quartz-plagioclase-biotite augen gneiss with quartz and K-feldspar augen, and a younger locally crosscutting porphyritic granite. The augen gneiss contains biotite-quartz schist inclusions, and both the gneiss and the granite are cut by small pegmatite bodies. (Lanphere et al, 1964). The few presumably metasedimentary rocks in this area consist of quartzitic gneiss, granulite, amphibolite and quartz-mica schist. In the Surprise Canyon area, the earlier Precambrian rocks consist of feldspar-quartz-muscovite gneisses and schists,

quartzites, amphibolites and marbles (Murphy, 1932).

Pb-U ages on zircons separates from the augen gneiss and the porphyritic granite of the World Beater Complex yield ages of approximately 1800 m.y. and 1350 m.y., respectively (Lanphere et al, 1964). Rb-Sr and K-Ar ages from muscovite from a pegmatite which cuts similar augen gneiss in the earlier Precambrian rocks of the Warm Spring area yield ages of about 1700 m.y. (Wasserburg, Wetherill and Wright, 1959). Zircons obtained from the gneiss, and from units thought to be metarhyolite or metadacites, from the same Warm Spring area, yield Pb-Pb ages of about 1800 m.y. (Silver, McKinney and Wright, 1961).

In the Wildrose area (Lanphere, 1962) the relationships between the earlier and later Precambrian rocks are obscured due to the superimposed later metamorphism of Cretaceous age. In this area, Lanphere has divided the rocks of the Panamint Metamorphic Complex into two groups; an older group made up of dominant micaceous quartzite with amphibolite and rare marbles, and a younger group of dominant marble, mica schists and rare amphibolites. The younger group is overlain unconformably by the Kingston Peak Formation. Both the Beck Spring and Crystal Spring Formations are not recognized, and Lanphere tentatively concluded that these formations were missing in the Wildrose area. Recent work, however, (Albee, oral communication, 1965), has suggested that the rocks which make up the younger metamorphic rocks in the Wildrose area may be equivalent to and continuous with the Beck Spring and Crystal Spring Formations in the Surprise Canyon area.

## Later Precambrian Rocks-The Pahrump Series

The type sections of the Pahrump Series are in the Kingston Range (Hewett, 1940) where it is made up of three formations; the Crystal Spring, Beck Spring and Kingston Peak Formations. These total 7000 feet in thickness. In the Panamint Range, a similar series of rocks about 4500 feet thick occur which show the same sequence of lithologies and which have been correlated with the three formations of the Pahrump Series (Johnson, 1957; Albee and Lanphere, 1962). These formations, along with the earlier Precambrian rocks, outcrop for the most part west of the main Panamint Range divide, on the western edge of the area mapped in detail.

The contact of the Pahrump Series with the underlying earlier Precambrian rocks is a major angular unconformity which truncates structural elements and mappable units of the earlier Precambrian rocks, and in the southern part of the area separates low grade (biotite zone) later Precambrian rocks from high grade earlier Precambrian rocks. Cobbles of earlier Precambrian rocks occur scattered throughout the Kingston Peak Formation of the Pahrump Series. The unconformity is best exposed in the upper reaches of Happy Canyon, in the southwest corner of the mapped area.

### Crystal Spring Formation

In the type section of the Crystal Spring Formation in the Kingston Range (Hewett, 1940), the formation is made up of 2000 feet of a variable interbedded sequence of shales, sandy shales, sandstones, quartzites, dolomites and rare limestones, and includes an aggregate of

300 feet of distinctive diabase sills scattered throughout the section. This formation makes up roughly the basal third of the Pahrump Series.

In the southwest corner of the mapped area, approximately 1000 to 1500 feet of Crystal Spring Formation rest unconformably on the earlier Precambrian rocks. It is characteristically highly variable in thickness and lithology, and is made up of laterally discontinuous interbedded quartzite, dolomite, quartzite conglomerate, argillite and arenite, with 50 to 600 feet of diabase sills included within the section. Locally, as on the west side of the domical World Beater Complex outcrop area in Happy and Pleasant Canyons, a thick basal cobble conglomerate with quartzite and dolomite clasts occurs, and the diabase sills are absent (Albee in Lanphere et al, 1964).

Murphy (1932) placed all rocks below his Marvel Dolomite in the Panamint Metamorphic Complex, and since it now appears that the Marvel is equivalent to the Beck Spring Formation, this implies that the Crystal Spring Formation is either absent in this area or is included in rocks of the metamorphic complex. Albee (1965, oral communication) reports that rocks equivalent to the Crystal Spring Formation are present throughout the Surprise Canyon area and probably also extend into the Wildrose area as part of the Panamint Metamorphic Complex. He also observes that the formation appears to change laterally in thickness and lithology over short distances a great deal in this region. This would be quite consistent with published work of other geologists of the Death Valley Region, as the formation is everywhere characterized by its variability. For instance, thicknesses reported for the Crystal Spring Formation are 2000 feet in the Kingston Range

type section with 300 feet of diabase, (Hewett, 1940), probably over 3000 feet in the Silurian Hills (Kupfer, 1954), 4300 feet with 1000 feet of diabase in the Alexander Hills (Wright, 1954), 1000 feet with no diabase in the Tecopa area (Mason, 1948), and 2300 feet including 200-600 feet of diabase in the Saratoga Hills (Wright, 1952). The formation is present in the Virgin Spring (Noble, 1949) and Warm Spring (Wright in Wasserberg et al, 1959) areas, but is not present in the Manly Peak quadrangle, directly southwest of the mapped area (Johnson, 1957). Judging from the large variations in thickness, and associated variations in lithology and amount of diabase, the extension of Crystal Spring equivalent rocks into the Surprise Canyon and Wildrose Canyon area would appear to be quite reasonable.

The Crystal Spring is exposed in the mapped area only in the extreme southwest corner, where it is locally exposed by uplift along some of the faults which appear to be related to the intrusion of the stock. It is extensively exposed on the west flank of the range, which is for the most part west of the mapped area.

Beck Spring Formation

In contrast to the Crystal Spring Formation, the Beck Spring Formation is characterized by its lack of variation in lithology and thickness. In the type section in the Kingston Range, it consists of 1100 to 1200 feet of 2 to 4 foot beds of massive light blue-gray dolomite, with minor interbedded shales and sandstones in the upper 200 feet. Its top and bottom are defined as the uppermost and lowermost dolomite beds, respectively, against the shales, sandstones, and conglomerates of either the Crystal Spring or Kingston Peak Formations.

The formation is 1200 feet thick in the Alexander Hills (Wright, 1954) and 1300 feet thick in the Saratoga Hills (Wright, 1952).

In the mapped area, the Beck Spring Formation consists of about 1200 feet of massive light-medium blue-gray dolomite or dolomitic limestone, with argillite, arenite and conglomerate beds in the upper quarter of the section. The dolomite of the lower three-quarters of the formation tends to interfinger with the dolomite and clastic sequence in the top quarter, and this in turn appears to lie unconformably below the Kingston Peak. Oolite beds occur throughout the massive dolomite sequence. The Beck Spring Formation is not present as the south and west sides of the World Beater Complex outcrop area to the southwest of the mapped area, and appears to be cut out by an unconformity at the base of the Kingston Peak (Albee in Lanphere et al, 1963). The basal Kingston Peak unit, which overlies the Beck Spring in the southwest corner of the mapped area can be traced continuously westward and southward until it lies directly on Crystal Spring lithologies. The Beck Spring Formation is also missing in the Warm Spring area to the southeast (Troxel, oral communication, 1966).

The name Marvel Dolomite was applied to this series of rocks in the Surprise Canyon area in 1932 by Murphy; well before the name Beck Spring Formation was applied by Hewett (1940) to similar dolomites in the Pahrump Series of the Kingston Range. However, the correlation of the Marvel with the Beck Spring was not realized until Johnson's work in 1957, when Kingston Peak and younger formations were described in the Manly Peak Quadrangle. During the period 1940 to 1957, Hewett's terminology has become the standard terminology for the Death Valley

Region, and for this reason the name Beck Spring is used in this region. This situation applied to Murphy's other formation names also.

As mentioned previously, the Beck Spring-Marvel Dolomite may extend north into the Wildrose area, where it was mapped (Ianphere, 1962) as part of a younger metamorphic complex.

Kingston Peak Formation

In the Panamint Range, the Kingston Peak Formation outcrops extensively on the western flanks of the range as a distinctive series of dark colored conglomeratic graywackes, argillites, and arenites. Murphy (1932) originally subdivided these rocks into five units, three of which are now thought to belong to the Kingston Peak Formation. These three consist of the older Surprise Member, the Sourdough Limestone, and the younger South Park Member, and all three have been mapped in the Manly Peak Quadrangle to the south (Johnson, 1957).

The type section of the Kingston Peak Formation (Hewett, 1940), located in the Kingston Range, can be subdivided into three roughly equal units; a lower shaly-sandstone unit with sporadic pebble zones, a middle coarse conglomerate unit, and an upper intermixed shaly-sandstone and conglomerate unit which contains graded beds and numerous other features related to a turbidite origin (Johnson, 1957; Troxel, 1966). At the type section, Hewett reports that the total thickness of the formation varies from 1000 to 2000 feet, but Troxel (1966) reports a total thickness of 6000 feet in the southern Death Valley Region. The thick upper unit is red colored, while the other

two units are black.

In the mapped area, the Kingston Peak Formation occurs only at the northeast and southwest corners of the stock, both areas that have been dragged upward by the intrusion of the stock. In the area to the northeast, in Hanaupah Canyon, the formation has been extensively metamorphosed and deformed by the dike swarm which passes through it. Here the South Park Member is dominantly dark gray argillite and arenite, with light gray quartzite and scattered zones of conglomerate and conglomeratic argillite; all thick bedded, all massive, and all weathering dark brown or red-brown. Clasts include dolomite, limestone, muscovite-rich quartzite, argillite, and quartz diorite or granodiorite gneiss. Other members here, and in the area in the southwest corner of the mapped area are so deformed and metamorphosed that further description will be taken from exposures just outside the mapped area.

The Surprise Member, in the Manly Peak Quadrangle to the south of the mapped area (Johnson, 1957), is dominantly dark gray conglomeratic graywacke or conglomeratic mudstone, with a few interbeds of graywacke or mudstone. The Sourdough Limestone Member is a distinctively coarsely laminated limestone with persistant dark and medium gray laminations spaced 3 to 30 mm apart. It is 0 to 170 feet thick and occurs essentially at the midpoint of the formation, making a convenient marker bed. The South Park Member is an interbedded series of gray quartzose sandstones, cobble conglomerate, conglomeratic mudstone, quartzite, and mudstone. The formation ranges in total thickness

from a few tens of feet on the south edge of the Manly Peak Quadrangle (Johnson, 1957) to 2700 feet at the north edge of the same quadrangle, and finally to roughly 2000-2350 feet in the Telescope Peak Quadrangle, at the southwest corner of the mapped area (Ianphere et al, 1964).

In the Manly Peak and Telescope Peak Quadrangles, the size distribution of the clasts is decidedly bimodal in the conglomeratic units, with size maxima which fall in the clay-silt, and pebble-cobble ranges. In most of the units, the percentage of clasts is about 10 percent, although rarely a few true conglomerates with greater than 50 percent clasts are present. This bimodal size distribution is present in all sections of the Kingston Peak Formation throughout the whole Death Valley region. Johnson (1957) feels that these distinctive conglomerates have a turbidite origin while Hewett (1940) feels that they were fanglomeritic material. Hazzard (1939) observed striated and facited pebbles in the conglomerates which he attributed to glacial processes. Troxel (1966), in a recent regional study of the formation, feels that the bulk of the formation has a turbidite origin, and to account for the presence of the striated clasts suggests that the deposit represents in part glacially derived sediments which were deposited along the shores of a marine basin and then redeposited further off-shore as turbidites.

Both the upper and lower contacts of the Kingston Peak Formation appear to be unconformable. The basal beds of the Surprise Member contain clasts of the Beck Spring Formation, while to the south and west of the mapped area (Albee in Ianphere et al, 1964) this basal

conglomerate rests progressively on the lower parts of the Beck Spring, on the Crystal Spring, and finally still further south on the earlier Precambrian basement. The upper contact of the Kingston Peak Formation with the Noonday Dolomite is a slight angular unconformity throughout the whole Death Valley region. In the Wildrose area just to the northwest of the mapped area, truncation of many of the mapped units in the Kingston Peak by the Noonday is readily apparent (Lanphere, 1962). Within the mapped area, basal conglomerates are locally present in the Noonday Dolomite which contain clasts which could have been derived from the underlying Kingston Peak Formation. Wright and Troxel (in press, 1966 ms.) report that the Noonday Dolomite, in the southern Death Valley region, progressively truncates the Kingston Peak, Beck Spring and Crystal Spring Formations in a northeastward direction until the Noonday Dolomite rests directly on earlier Precambrian rocks.

## Precambrian(?) Rocks

The Noonday Dolomite and the Johnnie Formation of Precambrian(?) age are present over most of the eastern slope of the central Panamint Range and make up 75 percent of the country rock in the mapped area. The formations can be correlated with the type section (Hazzard, 1937, p. 300). The distinctive cliff-forming Stirling Quartzite, also of Precambrian(?) age, lies conformably above the two formations, and an unconformity is present at their base below which the Kingston Peak Formation usually occurs. However, any units of the later Precambrian Pahrump Series, or the earlier Precambrian rocks can occur below the unconformity. The aggregate thickness of the Noonday Dolomite and Johnnie Formation is

3800 feet in the type section (Hazzard, 1937), 1100-2200 feet in the southern Death Valley area (Wright and Troxel, 1966), and 3600-4200 feet in the mapped area.

The type section of the Noonday Dolomite and the Johnnie Formation is in the Southern Nopah Range (Hazzard, 1937). Here the Noonday is some 1500 feet thick, and consists of light gray or yellow-gray, massive algal dolomite in 1-3 foot beds with a pronounced unconformity at the base. The upper 100 feet contains red-brown weathering sandy dolomite beds which contain gravel-, sand-, and silt-sized white quartz and red jasper grains in a dolomite matrix. These sandy beds are commonly crossbedded. The Johnnie Formation above the Noonday Dolomite in the type section is about 2550 feet thick, and consists of an interbedded series of dolomite, sandy dolomite, and quartzite which grades upward into a dominantly shaly section. Hazzard places the Johnnie-Noonday contact below the lowest quartzite (orthoquartzite) bed which interrupts the continuous sequence of massive dolomite and sandy dolomite of the Noonday Dolomite. This definition has been strictly followed by Johnson (1957) and by J. H. Stewart (1966).

The lower portion of the Johnnie is considered transitional from typical dolomite of the Noonday to typical Johnnie shale, siltstone, and quartzite. This contact between dolomite below and dolomite plus quartzite above is apparently of regional significance and can be used to define the Johnnie-Noonday contact from the type section to the Panamint Range (Stewart, 1966).

Hazzard (1937) refers to the entire 1500 feet of Noonday Dolomite in the type section as algal, but he presents no description

of the structures he terms algal. Several structures which have been termed algal have been noted in the Noonday or lower Johnnie in the mapped area.

The first are concentric thinly-laminated almost hemispherical 2-5 inch structures - reminiscent of a cross section of half a cabbage head. These have been seen in several dolomite beds including several in the Johnnie Formation. The second type, which had been termed algal-like by Wright, Troxel and Stewart (oral communication, 1965), consists of round tubes 2-6 inches long, with diameters of 1/3 - 1 inch. These invariably have a concentric structure with a thin rim of coarse calcite about a thick gray quartz core. The tubes are parallel and seem to lie perpendicular to the bedding. They tend to be spaced quite regularly at a distance of 6 inches to a foot throughout the rock, and invariably when well-developed pass completely through the bed in which they lie. Ellipsoidal or eye-like pods, with the same concentric calcite-quartz structure, 1/3 - 2 inches in maximum dimension, are seen throughout many of the massive dolomites of the mapped area. The relationships of the eyes to the tubes is not known, nor is the origin of the tubes known. The three structures will be referred to as algal-like tubes, or eyes, or heads - for the purposes of future discussion.

Noonday Dolomite

The Noonday Dolomite was first noted in the Panamint Range by Noble (1934) in the Warm Spring area, but it was not until Johnson's work in 1957 that the sections of carbonate on the western slopes of the Panamint Range were definitely shown to be equivalent to the Noonday Dolomite. Murphy (1932) subdivided the rocks which Johnson

has correlated with the Noonday Dolomite into three formations, the Sentinel Dolomite, Radcliffe Formation, and Redlands Dolomitic Limestone, and named rocks equivalent to the Johnnie Formation the Hanaupah Formation. While Hazzard's (1937) formational names have taken precedence in the Death Valley region, Murphy's three-fold division of what is now called Noonday Dolomite is still valid.

The Panamint Range Noonday section in the mapped area is best observed in the east or west sides of Telescope Peak, where the complete section is exposed in upper Hall or Jail Canyons, and in Hanaupah Canyon at the northeast corner of the stock. Because of accessibility problems the only complete section was measured in Hanaupah Canyon area. This section will be described in detail.

The lowest member of the Noonday in the Hanaupah Canyon measured section consists of a lower 100 feet of medium yellow-brown weathering medium gray, very siliceous limestone in 3 to 6 inch beds which tends to be thinly laminated in the upper 20 feet, and an upper 100 feet of massive light gray, yellow, or brown weathering gray or white dolomite with algal-like tubes and eyes throughout. This member corresponds to Murphy's Sentinel Dolomite and will henceforth be termed the Sentinel Member.

The middle 700 feet of the Noonday in Hanaupah Canyon consists of a varicolored, thinly laminated sequence of yellow-brown, brown, and gray weathering, grey, pink, green, or brown crystalline limestone in 0.1 to 0.5 inch lamellae, interlaminated with darker yellow-brown, brown or red-brown weathering, medium to dark gray-green or gray argillaceous limestone and argillite in 0.05 to 0.3 inch lamellae. The

percentage of argillite and the thickness of the argillite lamellae increase toward the base, so that the lower 140 feet of the middle member is entirely dark red-brown, dark gray-green or gray thinly-laminated to massive argillite with a local lensatic conglomerate beds, and the 100 feet above that is about 70 percent argillite. The conglomerate consists of argillite clasts in an argillitic matrix, and its conglomeratic nature is apparent only in weathered surfaces. A 50 foot laminated argillite, like that at the base, also occurs 80 feet from the top of the member. This member, including the basal argillite units is equivalent to Murphy's Radcliffe Formation, and is here termed the Radcliffe Member of the Noonday Dolomite. Both the upper and lower contacts of the Radcliffe Member are sharp.

The upper 500 feet of the Noonday Dolomite consists of massive light yellow-brown weathering, light gray dolomite with rarely less than 6 inch argillitic beds scattered throughout the upper 100 feet. The dolomite is essentially indistinguishable from the dolomite within the overlying Johnnie transitional member. Algal-like eyes occur scattered throughout the upper portions of the upper dolomite. This is equivalent to Murphy's Redlands Dolomitic Limestone and is henceforth referred to as the Redlands Member. In many parts of the area, this member becomes distinctly sandy, with varying percentage of fine-coarse sand, of pebble-sized quartz grains, and silt to medium sand-sized dolomite grains. In the Hanaupah Canyon area, these three members definitely occur below the lowest quartzite bed in the continuous dolomite sequence and hence are by definition within the Noonday Dolomite.

Plate 2 shows nine stratigraphic sections measured in various localities in the Telescope Peak and Manly Peak Quadrangles of the Panamint Range, and it can be seen from the figure that there are some lateral variations in the various members of the Noonday Dolomite.

The Sentinel Member is 425 feet thick in the Middle Park area and appears to thin in a northwestward direction. In the Wildrose area, Ianphere (1962) notes that Sentinel-type dolomite is present only in the south part of the area, and appears to pass northward into sandy and argillaceous limestones. Since lithologically these latter appear to belong to the Radcliffe Member, it appears that in this area the Sentinel Member grades both laterally and upward into the Radcliffe Member. There is no evidence of an unconformity between the two. A conglomeratic unit appears at the base of the sandy limestone north of the last distinctive Sentinel Member outcrop, with clasts of quartzite. Thin bedded Radcliffe-like limestones occur irregularly throughout several of the sections of the Sentinel Member. The Sentinel everywhere shows various algal-like tubes or eyes, with the best examples being found in some of Johnson's sections in the Middle Park area.

The Radcliffe Member contains the most variable lithologies of the three members. In the Manly Peak and Middle Park sections (Plate 2, section 9 and 3), the Radcliffe consists almost entirely of lamellar limestone with minor argillite, although the exposure is very poor in the Middle Park section due to faulting. The member appears simple in Murphy's Surprise Canyon section also, but this is due in large part to his sketchy descriptions. In other areas, the Radcliffe contains various percentages of argillite, quartzite and sandy limestone,

especially at the top and bottom of the member. It varies in thickness from 300 feet in the Manly Peak Quadrangle (Plate 2, section 2) to 800 feet in the Pleasant Canyon area. In all cases except the Wildrose area, the contacts of the Radcliffe Member with the Sentinel and Redlands Members are sharp and easily mappable. The Radcliffe locally contains penecontemporaneous conglomerate beds, and a few limestone beds in which 1-3 mm magnetite octahedra are scattered throughout.

The Redlands Member varies in thickness from 400 to 800 feet, and its chief lithologic variation consists of changing percentages of fine grained crystalline dolomite, carbonate silt-, or sand-sized grains, and quartz sand to conglomerate-sized grains. In some sections, as in Hanaupah Canyon (Plate 2, section 2) there is little or no visible clastic material, which in others, as in Johnson (section 4) and Pleasant Canyons (sections 6 and 7), very coarse quartz or carbonate sand is present and the beds are locally conglomeratic. The carbonate sand varies from silt to medium sand sizes, and is visible only on weathered surfaces as medium yellow-brown grains on a light yellow-brown dolomite background. The quartz sand, always well rounded, varies from fine sand to pebble size and shows up in fresh rock as clear grains and in weathered surfaces as dark red-brown grains on a light yellow-brown dolomite background. Crossbedding is common in both types of sand. The ratio of quartz grains to dolomite matrix varies from 0 quartz: 100 dolomite to 85 quartz: 15 dolomite in some of the coarse sands. This also makes the definition of the Noonday-Johnnie contact difficult at times, as it is very hard to distinguish the orthoquartzites from the dolomitic sandstones which occur in the

Redlands Member. The critical factor is whether the matrix is silica or carbonate. There is no question that the sandy dolomite of the Redlands Member is laterally equivalent to the massive dolomite of the Redlands, as numerous examples of continuous lateral gradation of sandy dolomite to dolomite have been observed in the mapped area.

Comparison of the various described sections of the Noonday Dolomite throughout the Death Valley region reveals some very important differences. As was noted above, the Noonday Dolomite can be subdivided on the basis of lithology into three members throughout most of the Panamint Range; the lower Sentinel Member algal dolomite, the middle Radcliffe Member thinly laminated limestone and argillite, and the upper Redlands Member massive sandy dolomite. In the areas to the east of Death Valley, a significantly different section is reported (Wright and Troxel, 1966 and unpub. ms.; J. H. Stewart, oral communication, 1965). Over most of that area, the Noonday Dolomite consists of two members, a lower massive algal dolomite like the Sentinel Member, and an upper massive sandy dolomite like the Redlands Member. This two-fold division holds true over all the area east of the southern part of Death Valley except along a northwest trending belt immediately to the east of Death Valley itself.

In this belt, which marks the outcrop of the Noonday Dolomite closest to the Panamint Range, the lower algal dolomite member is abruptly cut out by a southwestward thickening wedge of shale and graywacke which contains a basal conglomerate with numerous very large clasts of the algal dolomite. The sandy dolomite member is continuous through the belt in which the lower algal member is cut out unconformably,

so that in the westernmost sections exposed on the east side of Death Valley, the Noonday Dolomite consists of a lower clastic shale and graywacke member and an upper sandy dolomite member as before.

In the clastic wedge of the Ibex Hills, a very few thinly laminated limestone beds occur which are similar to the Radcliffe lithologies in the Panamint Range, and the shales are difficult to distinguish from the slightly more metamorphosed argillites in the Radcliffe Member. This suggests that the Radcliffe Member is the western equivalent of the clastic wedge facies. This would equate the Redlands Member with the upper sandy dolomite member to the east of Death Valley, and the Sentinel Member with the algal dolomite below the clastic wedge or sandy dolomite. This in turn suggests that the contact between the Radcliffe and Sentinel Members may be a disconformity in the southern part of the Panamint Range, and a gradational contact in the northern part as already noted.

Johnnie Formation

The Johnnie Formation in the Panamint Range has been subdivided into three members which are, starting at the base: a gradational member which consists of 300-600 feet of interbedded dolomite or sandy dolomite and quartzite, overlain by 120-300 feet of quartzite, which is overlain by 40-130 feet of massive dolomite at the top; a middle argillite member consisting of 600-900 feet of gray-green argillite with carbonate interbeds in the upper quarter; and an upper limy argillite member which consists of 600-1000 feet of ripple-marked, purple limy shale and limestone and/or sandstone. All three members can be mapped consistently throughout the Telescope Peak Quadrangle.

The most complete measured section of the Johnnie Formation in the mapped area is found in Hanaupah Canyon, and this is also one of the few places in the Panamint Range where an undisturbed section from the Kingston Peak to Stirling Formations may be seen. A detailed section is described below.

The basal unit of the gradational member is 550 feet thick and consists of 60-100 foot intervals of light yellow-brown or brown weathering, massive gray dolomite with some sandy dolomite containing quartz grains of silt- or fine-sand size, and rare limestone beds, alternating with 5-10 foot intervals of dark red-brown weathering, cross-bedded, coarse-grained gray orthoquartzite or dolomitic quartzite. The interval between the quartzite beds increases downward. Algal-like heads occur only in the uppermost dolomite beds of this unit.

The middle unit consists of 120 feet of dark red-brown weathering, brown, gray or blue-gray, 2-6 foot, cross-bedded quartzite beds and rare medium red-brown weathering, brown sandy dolomite. The member forms a distinctive dark band in outcrop and makes an excellent mapping horizon.

The upper unit of the gradational member is 130 feet thick and consists of less than 10 feet thick beds of light brown or yellow-brown weathering, medium gray or blue-gray dolomite, sandy dolomite, limestone, and sandy limestone. The quartz sandy beds are cross-bedded. One dark gray, thinly-laminated, limestone bed occurs 100 feet from the top of the member.

The argillite member is 1100 feet thick and is made up dominantly of gray-green weathering, gray, green or gray-green very thinly laminated micaceous argillite. In the basal 250 feet, 20 to 30

percent of the rock is dark yellow-brown weathering, gray or red-gray quartz-sandy, crystalline limestone and dolomite. The lower 300 feet of the argillite tends to weather red-brown rather than gray-green, and has scattered rusty spots after pyrite(?); its general appearance is suggestive of a rock of tuffaceous origin. This will be discussed in more detail later. In the upper 200 feet of the gray-green argillite member, numerous dark brown or medium red-brown weathering, medium-light red-gray crystalline limestone beds and dark gray aphanitic limestone beds are interbedded with the argillite in 0.1 - 0.4 inch laminations.

The limy argillite member is about 900 feet thick and consists dominantly of a ripple marked and flute-caste unit in which medium red-gray and rare green, gray-green and purple crystalline limestone lenses less than 0.8 inches thick or laminations less than 0.3 inches thick are interbedded with micaceous purple blue-gray, very thinly-laminated argillite beds less than 0.5 inches thick. The argillite beds are draped over the elongate limestone lenses, producing sections which look like typical aircraft wing cross-sections. There are also zones in which only the micaceous blue-gray argillite, strongly ripple-marked, occur.

In the top 200 feet, red-brown weathering, gray or light brown 1-8 inch quartzite beds occur and increase in abundance as the Stirling contact is approached. A discontinuous yellow-brown weathering 6-10 foot dolomite bed often occurs just below the Stirling contact. At a distance of 650 feet below the Stirling contact, a 50 foot penecontemporaneous conglomerate bed with slabby 0.5 feet by 2 feet maximum

pink crystalline limestone clasts in a medium-dark gray siliceous limestone matrix occurs. This is present throughout the Hanaupah Canyon area and is used locally as a marker bed as it forms a massive dark-brown weathering cliff in the otherwise slabby to platy, lighter-weathering section. The upper contact of the Johnnie Formation with the Stirling Formation is sharp and marks the abrupt break between the darker, finer-grained quartzites and argillites of the Johnnie and the very light-colored, coarser-grained quartzites of the Stirling Formation.

The type section of the Johnnie Formation occurs in the Nopah Range (Hazzard, 1937). The formation was originally named and described by Nolan (1929) in the Spring Range of Nevada, but since the section there is incomplete and bounded in part by faults, the section later described by Hazzard has become the working type section. J. H. Stewart has recently traced the regional variations of the Johnnie Formation to the east of Death Valley, and has subdivided the type section into several members. In the following section, a brief description of the type section will be given using Stewart's terminology and correlations (oral communication, 1966).

The basal 485 feet of the Johnnie Formation consists of an interbedded series of dominantly sandy dolomite with subordinate pebbly cross-bedded quartzite beds. This has been referred to as the "transitional member" by Stewart, and appears to correlate with the lower unit of the gradational member in the Panamint Range. The next 480 feet consists of massive fine- to medium-grained quartzite with a 45 foot thick dolomite bed occuring 200 feet from the base. It has

been termed the "quartzite member" by Stewart and appears to be equivalent to the middle quartzite unit of the gradational member.

Above this a section of 720 feet of interbedded light brown, fine-grained micaceous sandstone, dark brown shale, and minor quartzite occurs. An olive clayey dolomite bed, 10 feet thick, occurs 15 feet above the base of this 720 foot section, and Stewart places this dolomite and the 10 feet of shale below it in his "lower carbonate-bearing member," which he correlates with the dolomite unit in the upper part of the gradational member in the Panamint Range. The remaining 695 feet above this Stewart places in his "siltstone member," which appears to be equivalent to the lower part of the argillite member in the Panamint Range.

The next 500 feet, which Stewart terms the "upper carbonate-bearing member," consists of an interbedded series of brown cross-bedded quartzite, buff sandy dolomite and gray-green shaly sandstone, with quartzite predominating at the base and shaly sandstone at the top. This appears to correlate with the upper part of the argillite member in the mapped area.

The uppermost 365 feet of the Johnnie Formation in the type section consists of gray-green to maroon, cross-bedded, ripple-marked, micaceous shaly sandstone with sandy dolomite in the basal part. This part appears to be equivalent to the limy argillite member in the mapped area, and has been termed the "rainstorm member" by Stewart. A 10 foot thick oolite bed occurs 25 feet from the base.

The oolite bed noted above is apparently very widespread, and appears at the same relative stratigraphic position in all the various

measured sections between the Panamint Range and the type section in the Nopah Range some 60 miles to the east. (Wright and Troxel, 1966; Stewart, 1966, oral communication). It occurs in the lower part of Johnson Canyon, just at the edge of the mapped area, and it is apparently equivalent to the penecontemporaneous conglomerate noted in the detailed section from Hanaupah Canyon.

The basal 200-300 feet of the argillite member of the Johnnie Formation in the mapped area is characterized by rusty red-brown or yellow-brown weathering, cliff-forming beds which contain minute cubic cavities in the more argillitic portions which appear to be hematite after pyrite. Within this section, several distinctive light gray or blue-gray, massive, dense "argillite" beds which often have irregular close-spaced fractures filled with a dark brown material to produce a mosaic-textured rock. These break with an almost concoidal fracture, and produce fracture surfaces which in detail are quite hackly and irregular. Their general appearance is that of fine-grained tuffaceous sediments.

In the Pleasant Canyon and Happy Canyon area to the southwest of the mapped area, similar beds in the same stratigraphic position contain angular patches (<0.3mm) of white mica which have an overall form suggestive of feldspar crystals. Thin sections of these rocks, and also some from the mapped area, show that about 80 percent of the rock consists of a less than 0.01mm subparallel mesh of sericite grains with some minor feldspar and quartz, and the remaining 20 percent consists of rounded 0.1-0.2mm detrital quartz grains. Some sections of these rocks contain up to 95 percent sericite. By way of comparison, the

gray-green argillite which makes up the bulk of the section contains consistently 60-80 percent sericite plus some chlorite.

Pirrson (1915), in one of the few articles which deals in any way adequately with slightly altered felsic tuffaceous sediments, notes that many fine tuffs "...may be changed into minute scales of sericitic mica mingled with granules of quartz." His general description of some of the tuffaceous rocks is almost identical with the descriptions of some of the distinctive light-gray beds noted above, both in mineralogy, color, and mode of fracture and alteration. On this basis, it is felt that much of this lower 200-300 feet of the argillite member of the Johnnie Formation is tuffaceous in origin, and the distinctive light colored beds within this portion of the section were probably beds that originally contain the least material of non-volcanic origin.

Hazzard (1937, p. 304), in the type section, feels that the shaly beds in the middle part of the Johnnie Formation, which Stewart refers to as his "siltstone member," are in part of tuffaceous origin. These beds, as was noted above, are equivalent to the lower part of the argillite member which is thought to be of tuffaceous origin in the mapped area. Noble (1937, in Hazzard) also independently reached the same conclusion about the same beds in the type section.

Wright and Troxel (1966, p. 853) have also noted beds which they feel are of tuffaceous origin in the Johnnie formation, and they have correlated these beds throughout the area to the east of southern Death Valley. However, while the descriptions of the beds are the same as those in the mapped area which are referred to as tuffaceous

in origin, their stratigraphic position is quite different. They state that this shaly unit of tuffaceous origin "lies 20-400 feet stratigraphically below the oolite unit." This would place the tuffaceous beds in the upper parts of Stewart's "upper carbonate bearing member," which is equivalent to the uppermost parts of the argillite member in the mapped area. This is distinctly above the rocks which Hazzard refers to as tuffaceous, and is also above the suspected equivalent beds in the Johnnie Formation of the mapped area. In the mapped area, "tuffaceous appearing" beds were not noted below the oolite bed.

The lateral variations present in the Johnnie Formation in the southern Panamint range area are noted in Plate 2. The three members can be consistantly correlated from section to section, but minor variations occur within the members.

Variations within the limy argillite member are slight. On the east slope of the range, the small red-gray lenses which give the member its distinctive ripple-marked appearance are almost wholly of crystalline limestone, while on the west side of the range these same lenses are wholly quartzose and consist of fine to medium-grained quartz grains in a siliceous matrix. Carbonates are very rare to the west of the range divide.

The oolite bed near the base of the limy argillite member, which can be found extensively to the east of the Panamint Range, has a very erratic distribution in the area under discussion. In the lower Johnson Canyon-Six Spring Canyon area, the oolite is present as a 4 foot bed of thinly laminated dolomite with 0.5 to 2mm oolites. In the middle

Johnson Canyon area, on the southeast edge of the mapped area, the oolite is present as a distinctive penecontemporaneous conglomerate bed some 20 feet thick which contains slabby clasts of the thinly laminated oolite in a dark brown dolomitic matrix. In Hanaupah Canyon, at the same stratigraphic position, the non-oolitic penecontemporaneous conglomerate occurs, and mapping suggests that the two are equivalent.

Similar non-oolitic penecontemporaneous conglomerates have been reported (Albee, oral communication) in the Johnnie Formation of the Pleasant Canyon-Happy Canyon area to the southwest of the mapped area, but no normal oolitic dolomites have been reported from that area. Johnson (1937) notes neither oolite or penecontemporaneous conglomerate in this part of the Johnnie Formation in the Manly Peak Quadrangle. Hence it appears that the Panamint Range is at the western limit of the oolitic dolomite marker bed that is so common to the east of Death Valley.

Aside from the above minor variations, the limy argillite member of the Johnnie Formation is grossly unchanged throughout the southern Panamint range area. It ranges in thickness (Plate 2) from 800 feet to 1200 feet, and in weathered outcrop it forms a series of distinctive low irregular dark red or purple cliffs which can be traced for miles. Often, toward the base of the member, alternations of the scale of tens of feet between maroon and gray-green argillite are seen. These are especially prominant in upper Johnson Canyon and areas to the south.

The argillite member, the middle member of the Johnnie Formation,

forms slabby brown weathering slopes in which the exposures are poor and slumping widespread. The upper 200-300 feet of the member tends to have red-brown cliff formers because of the relatively higher percentage of dolomite beds there. These dolomite beds are laterally discontinuous and tend to irregularly pinch and swell. The member is 700 to 1200 feet thick, and tends to thicken toward the south and southwest and at the same time show an increase from silt to fine-medium quartz sand as its major constituent. Local pebble conglomerates occur. Slaty cleavage is weakly developed in the Hanaupah Canyon area, and the equivalent rocks in the Wildrose area to the northwest of the stock are phyllites and schists. The lower tuffaceous portion of the member appears the same throughout the range.

The contact between the argillite member and the underlying dolomite unit of the gradational member is taken at the top of the first massive dolomite bed, greater than 10 feet thick, below the tuffaceous beds. Thus chosen, the contact is very sharp and very continuous throughout the whole of the mapped area, and indeed the whole of the southern Panamint Range area. This contact is easily visible in the field, and structure contours have been drawn on it to aid in the determinations of the deformation associated with stock emplacement. In the section of structural geology, this gradational member-argillite member contact has been termed the dolomite-argillite contact.

The dolomite unit of the gradational member varies in thickness from 130 feet in Hanaupah Canyon to only 40 feet in the Johnson Canyon-Pleasant Canyon area to the south, and in general the unit tends to be pure dolomite to the north, and quartz sandy dolomite to the south.

The quartzite unit of the gradational member varies in thickness throughout the area from 120 feet to 300 feet, but is remarkably constant in lithology. It appears to thin by lateral addition of dolomite or sandy dolomite beds which soon dominate the immediate section and hence by definition are then put in the lower or upper units of the gradational member.

Variation within the lower unit of the gradational member almost exactly parallels the variation in the Redlands Member of the Noonday Dolomite immediately below. When the Redlands passes from dolomite to sandy dolomite, the lower unit of the gradational member does likewise. In general, this unit tends to thicken to the north at the expense of the Noonday Dolomite by the addition of new quartzite beds in the dominantly dolomite section. The highest percentage of quartzite in the lower unit occurs in the Hanaupah Canyon section, and to the south, as the percentage of quartz sand in the adjacent dolomite increases, the percentage of quartzite beds decreases.

Correlations of the Johnnie Formation with the section in the Wildrose area are uncertain. The limy argillite and argillite members of the Johnnie Formation appear to be at least in part present in the Wildrose section, as are the Sentinel and Radcliffe Members of the Noonday Dolomite. But much of the Redlands Member of the Noonday, and the gradational member of Johnnie appear to be missing in the measured sections (Lanphere, 1962; Stewart, 1965, personal communication). Whether this change is stratigraphic or due to faulting is not known, and solution of this problem must await further work in the Hall Canyon-Jail Canyon area to the northwest of the mapped area.

Correlation of the various Johnnie sections with the section measured by Johnson (1957) in the Manly Peak Quadrangle is also difficult due to the poor exposure in the latter section. Tentative correlations are shown in Plate 2.

Stirling Quartzite

The Stirling Quartzite outcrops only on the eastern edge of the mapped area, and for the most part, only the basal portion of the formation occurs. The formation will be described only briefly, as no sections were measured.

The contact between the Stirling and the Johnnie is abrupt and obvious, with massive white quartzite and conglomerate quartzite of the Stirling lying atop red-gray or red-brown weathering gray quartzite and argillite of the Johnnie Formation. The basal Stirling forms a massive continuous white cliff which can be easily seen on air photos and which can be easily mapped for great distances. Immediately below the Stirling, a 1-3 foot light yellow-brown weathering dolomite bed occurs which has great lateral extent and is seen at this position throughout most of the mapped area.

The lower 300-500 feet of the Stirling consists of quartzitic sandstone and conglomerate, with rose or smoky quartz clasts in a light gray or light brown siliceous matrix. Sandy and argillite lenses are common, and weather out in pockets. The unit is consistently cross-bedded, no matter the size of the clasts. Occasionally clasts of dark gray very fine grained hornfelsic-like rock are seen. Except for the lower 50-100 feet, the Stirling weathers a light-medium red-brown and forms massive discontinuous cliffs. About 400-600 feet above the base,

there is a distinctive sequence of 75 feet of thinly-laminated purple argillite or limy argillite followed by 50 feet of quartzite, another 50 feet of purple argillite, and finally another 100 feet of medium red-brown weathering quartzite similar to that below the argillite sequence. These argillites show up prominantly as twin very dark bands inset in the medium red-brown cliffs of quartzite, and form a very convenient marker horizon for mapping. Above this sequence is a thick section of light brown weathering quartzites. These are exposed on the high ridges in the lower Starvation Canyon area, east of the Telescope Peak Quadrangle. Since the higher portions of the Stirling and the Wood Canyon Formations do not occur within the mapped area, they will not be described here.

Johnson (1957) reports at least 1000 feet of Stirling formation in the Manly Peak Quadrangle, and Hopper (1947) reports 1200 feet in the Harrisburg Flat area.

## IGNEOUS ROCKS

### Little Chief Stock

The major igneous body within the mapped area is that of the composite Little Chief granite porphyry stock, a hypabyssal hornblende-biotite-granite porphyry which occupies some 15 square miles of area in the center of the mapped area.

The stock consists of two major intrusive phases, a north and a south phase, which have a roughly east-west contact in the vicinity of Starvation Canyon. The south phase is earlier than the north phase, as the latter is chilled against the former. The later north phase is in turn made up of two portions, an exterior portion, and a very slightly later interior portion. The exterior portion truncates a dike swarm in the Hanaupah Canyon area which formed when the magma of the stock's north phase was at some slightly deeper level. All contacts of the stock, in both the north and south phases, were intruded by dike rocks which formed a sheath around the stock. Remnants of an early igneous phase of the stock, emplaced at some level deeper than the present level of exposure of the stock, are found only as inclusions in the north and south phases of the stock.

Two important dike swarms related to the stock extend from the northeast and southeast parts of the stock, and areas of brecciated rock thought to be vents for the dike rocks that extended to the surface at the time of emplacement of the stock also occur.

At the present level of exposure, the stock is in intrusive contact with the Crystal Spring, Beck Spring, Kingston Peak, Noonday and Johnnie Formations, but of these four, the Noonday Dolomite is in contact with

the stock over 66 percent of the length of the contact and the rest of the contact is roughly equally subdivided among the remaining three formations. In several areas, the stock has a very thin buffer of Noonday Dolomite (or lower Johnnie dolomite-rich portion) between it and the argillaceous portions of the Johnnie Formation. This is accomplished by faulting parallel to the stock contact, or by dragging the dolomitic rocks up along the margins of the stock, thinning them in the process. This tendency of small intrusive bodies to surround themselves with envelopes of carbonate rock is also characteristic of the stocks in the Inyo and White Mountains (Sylvester, 1965, oral communication).

The stock can be subdivided into two major phases, a northern and southern intrusive phase. The northern phase consists of two portions, an interior hornblende-biotite granite with plagioclase and sanidine phenocrysts up to 10mm in size in an 0.5mm groundmass made up of roughly equal amounts of alkali feldspar and quartz ± plagioclase. Mafic mineral percentages commonly reach 9 percent. The outer portion of the north phase of the stock is a biotite ± hornblende granite with plagioclase and sanidine phenocrysts up to 7mm in size in an 0.4mm groundmass. The sanidine shows evidences of extreme replacement by sodic oligoclase. Near the contact with the wall rock, the grain size of the groundmass decreases to 0.1mm except in those areas where a leucocratic contact phase with less than 1 percent majic minerals is developed. The contact between the interior and exterior portions varies from sharp to transitional over 100 feet, indicating emplacement of the interior portion while the exterior part contained significant amounts of melt.

The southern phase of the stock is a hornblende-biotite granite with plagioclase and sanidine phenocrysts in the 1-5mm range set in a less than 0.5mm groundmass of alkali feldspar and quartz ± plagioclase. The mafic minerals consistently make up less than 6 percent of the rock. The contact between the northern and southern phase is always sharp and indicates that the northern phase is enough later than the southern phase for a contact chill zone to have formed in the northern phase.

Physical Details Along the Stock Contact

In the majority of locations, the dike-sheath aplitic or porphyritic aplitic rocks are interjected between the granite of the stock and the country rock. Dikelets of the dike-sheath rock are common in the country rock, and in most cases, are non-porphyrytic. In several cases, angular fragments of the wall rock, either the Noonday or Kingston Peak Formations, are found in the dike-sheath rocks. In a few cases, angular blocks, usually less than 1m in length, can be matched back to their probable starting place in the country rock. Large slabs, often up to 30m in length, are seen along the contact in positions such that the dike-sheath rock has almost surrounded them and appears to be in effect prying them away from the bulk of the country rock. This occurrence is very rare, and almost always involved the dolomite of the Noonday Dolomite. However, no large slabs of this sort were seen wholly within the stock--all retained some connection with the country rock.

In many locations, however, normal granite porphyry or contact phase granite are in direct contact with the country rock, and in these situations there is invariably a chill zone less than 0.3m thick

at the contact. In rare instances, apophyses of the granite extend out into the country rock for distances of up to 1000m from the contact. The largest of these, shown on the map at the northeast edge of the stock, is some 100m thick, but other apophyses are found which are less than 0.5m thick. While most of these apophyses are of normal granite of the stock, in a few instances, the material within the apophyses has an unusually high concentration of hornblende, which in terms of optical properties is very much like that in the normal stock granite. Commonly a flow banding of various concentrations of hornblende occurs in some apophyses, and hornblende selvedges occur around many of the inclusions of the Kingston Peak Formation which are caught up in the apophyses or in the dike-sheath or granite at the stock contacts.

In general, all the stock contacts are sharp, no matter which phase of the granite or the dike-like rocks is at the contact. The number of country rock inclusions found in the stock is very small, and except in rare instances is less than 1 percent of the rock.

Contact Metamorphic Rock

The contact metamorphism attributable to the stock is restricted to scarn-like or hornfelsic zones less than 1 foot thick, and usually less than 2 inches thick. Often, a single thin section spans the contact zone.

Against the argillitic rocks of the Kingston Peak Formation, hornfelsic zones up to 1 foot wide have been formed which consist of the assemblages (listed in decreasing order of abundance) hornblende-quartz-oligoclase-biotite-magnetite, diopside-quartz-oligoclase-biotite-magnetite, and biotite-epidote-quartz-magnetite, which appear roughly in

order going away from the stock. At the actual contact, and in inclusions of the Kingston Peak argillitic rocks in the stock, large concentrations of hornblende and biotite occur, and fringes of these two minerals grow out into the granite from the actual plane of the contact. In this region within 2 inches of the contact, one can see the diopside assemblage give way to the hornblende assemblages first by patches of separate hornblende grains, with common optical orientations, which appear in locally diopside-free patches in the diopside-rich areas, and which, going toward the contact, coalesce into equant hornblende crystals as the percentage of diopside decreases. Finally, in many cases, no diopside is left, and the hornblende assemblage occurs at the actual contact.

In some cases, the hornblende assemblage has not formed, and the diopside assemblage appears to be stable up to the contact. It is in areas like these that diopside crystals and reaction rims on the igneous hornblende are found in the granite adjacent to the stock contact. In general, the contact metamorphic and igneous hornblendes appear identical.

In other areas along the Kingston Peak contact, the assemblage quartz-biotite-cordierite-magnetite was noted.

In the area of the dike-swarm, stock junction at the northeast corner of the stock, the metamorphic effects due to the closely spaced dikes have extended the metamorphic aureol away from the stock for some distance. In this area, the Sourdough Limestone Member of the Kingston Peak Formation has developed assemblages of andradite-grossularite garnet and calcite with unidentified opaque minerals.

Rarely, calcite-opaque(?)-diopside assemblages are seen. The amount of garnet, easily visible in the field, appears to die out away from the nearest dike contact. It is suggested that metamorphism occurred in this region because of a combination of the heat provided by the dike swarm, which makes up 50 percent of the rock in many areas, and abundant volatiles associated with the dikes.

The contact zones with the Noonday Dolomite are seldom thicker than 3 inches, and consist for the most part of calc-silicate scarn against the carbonate rocks, and hornfels against the argillaceous rocks. At one locality, the following assemblages in well-defined bands are noted going from wall rock toward the contact. First, diopside with talc reaction rims-dolomite-phlogopite-serpentine (Chrysotile?), then phlogopite-diopside, then diopside with talc reaction rims-dolomite-quartz, and finally coarse diopside-dolomite with reaction rims against diopside only-quartz-oligoclase at the contact. Another scarn-like assemblage is a wollastonite-diopside-sphene assemblage in which coarse wollastonite crystals form patches with tabular rectangular shapes in a matrix of fine wollastonite. The mineral which had the tabular form was not seen. In this case, a talc(?) band occurs at the contact itself. The argillaceous rocks of the Noonday Dolomite have quartz-oligoclase-diopside-magnetite, and quartz-oligoclase-hornblende-biotite-magnetite assemblages similar to those of the Kingston Peak Formation.

## Age of the Stock

Several general lines of evidence suggest that the stock is Tertiary in age. In comparison with known Mesozoic intrusives in nearby areas, the textural features of the granite of the stock, the small amount of contact metamorphism, the style of deformation, and the shallow depth of

emplacement all tend to support a Tertiary age as opposed to a Mesozoic age. The country rock to the northwest of the stock has yielded radiometric ages which suggest that they were regionally metamorphosed in Upper Cretaceous time (Lanphere, 1962). The lack of evidence of metamorphism of the stock, relative to the chlorite to biotite-grade regional metamorphism of the immediately surrounding country rocks, suggests that the stock was emplaced after the time of regional metamorphism.

The stock itself cuts rocks of Precambrian(?) age or older, and near to the stock, faults associated with the emplacement of the stock, cut only Cambrian or older rocks. One fault which is thought to be associated with the emplacement of the stock, appears to extend well to the south of the mapped area, and at its southern end cuts andesitic volcanics of an unknown Tertiary age. Assuming only one stage of movement on the fault, this also supports a Tertiary age for the stock. However, on the east flank of the range, similarly oriented faults have cut tertiary volcanics but in this case the evidence is quite good that there were several periods of movement on these faults (Hunt and Mabey, 1966).

Recently (Stern, Newell and Hunt, 1966) radiometric ages were octained on some of the volcanic and shallow intrusive rocks on the east edge of the Panamint Range. A K-Ar age of 14 m.y. (K-feldspar) was obtained on a quartz monzonite which lies below, or to the east of, the basal fault of Hunt's Amargosa fault system, and 11 and 14 m.y. ages (biotite) were obtained on the augen gneiss which was intruded by the above quartz monzonite. Hunt and Mabey suggest that this quartz monzonite body is related to the Little Chief Stock. Zircons from the augen gneiss yielded 1820 m.y. (concordia) Pb-U ages with evidence of a later disturbance at roughly 240 m.y. In other areas of the

southern Panamint Range, 1700 m.y. (Wasserberg et al, 1959) K-Ar and Rb-Sr ages and 1800 m.y. (Lanphere et al, 1964) (Silver, McKinney and Wright, 1961) Pb-U ages were obtained on roughly similar earlier Precambrian rocks. The above data suggest that the biotite of the augen gneiss re-equilibrated at the time of the Upper Miocene igneous activity (Stern et al, 1966).

A 12 m.y. K-Ar (K-feldspar) age was also obtained on a rock described by Stern et al (1966) as a monzonite porphyry which was collected from a boulder at the mouth of Hanaupah Canyon. Since boulders of the Little Chief stock are common in that canyon, and to my knowledge no coarse igneous phases other than the stock are present upstream of the collection point, it is entirely possible that this boulder was indeed from the stock. It is not possible to make a petrographic comparison from the published information.

If, as indicated by Hunt and Mabey (1966), the shallow intrusives discussed above are related to the volcanic tuffs and sediments in that area, then this supports an Upper Miocene age for the stock, since the volcanics lie on an erosion surface which projects to a point roughly a mile above the stock, and petrographic work indicates a depth of emplacement of the stock of roughly the same amount. This would also agree with the tentative 12 m.y. age on the boulder cited above.

Stern et al (1966) have also determined 30±10 and 20±10 m.y. Pb-α ages on zircons from the quartz monzonite below the basal Amargosa fault, and from the monzonite porphyry boulder, respectively. In the light of the above upper Miocene ages, coupled with evidence of xenocrystic zircon of possible Precambrian age in these rocks, the

authors feel that the Pb-$\alpha$ ages are too high.

On the basis of the above discussion, the age of the Little Chief stock is thought to be Upper Miocene.

Soda Minette Sill-Johnnie Formation

In the Hanaupah Canyon area, a 50-150 foot lamprophyre sill occurs just below the top of the argillite member. The sill has contacts which are irregular in detail but in general are parallel to bedding. Sediments at the upper and lower contacts are highly indurated, and the sediments adjacent to the contact have been extremely plastically deformed in many area. In a few areas, above the sill, portions of the argillite have been converted to pods of breccia in which shattered angular purple hornfelsed argillite clasts occur in a white chalky matrix. The best developed breccia trends perpendicular to the upper dike margin and extends about 25 feet into the argillite as a zone 2-4 feet wide well through the hornfelsed zone into the unaltered argillites and carbonates. When it reaches the sill, it flattens out into a pod against the sill, parallel to the sill contact. It is suggested that this breccia is due to steam explosions associated with the intrusion of the sill into a series of wet sediments. The sill is deformed in the same way as the rest of the Johnnie Formation by the faults mapped in the area, so that it was at least emplaced before most of the faulting.

The sill may be properly termed a soda minette. It shows a typical lamprophyric or panidiomorphic texture, made up of subhedral to euhedral feldspar crystals and euhedral biotite and hornblende crystals, all in the 0.5-5mm size range. The rock is highly altered,

so that any estimate of the original mineralogy is only approximate. An estimate of the original mineralogy includes; a) 40-60 percent sodic orthoclase, now finely patch perthitic with roughly 60 percent K-phase and 40 percent Na-phase as estimated from a stained thin section, with a 2V of about 65 degrees. It is highly saussuritized and fractured, with fracture fillings of calcite; b) 15-25 percent pleochroic medium-dark brown biotite, in stumpy plates of about 0.5-4mm in size, and c) 5-15 percent ferrohastingsitic hornblende, in typical hornblende prisms 0.5-2mm in size. It shows the following pleochroic formula: Alpha = medium yellow-brown, Beta = deep blue green, Gamma = light to medium yellow or yellow-brown, and has a negative 2V of less than 15 degrees. d) about 5 percent sphene in 0.5-1mm euhedral, often skeletal crystals. e) about 2 percent plagioclase. f) about 2 percent apatite and opaques. The opaque is probably a Ti-rich magnetite.

A light yellow-brown pleochroic biotite also is present which occurs as an alteration product of both the brown biotite and the hornblende, and also occurs in 0.1-2.0mm laths scattered throughout the thin sections along grain boundaries. It comprises 10-25 percent of some slides, and may have been formed as a very late crystallization product or hydrothermal alteration product.

Most of the ferrohastingsite has been altered to the later yellow-brown biotite, chlorite, and riebeckite. The riebeckite forms parallel intergrowths with the yellow-brown biotite in some cases, and in other cases forms radial bundles of fibers which cross-cut yellow-brown biotite, feldspar and brown biotite, so that it

appears to be later than most of these minerals. The brown biotite is flecked and spotted with dark brown-black patches which appear to be leucoxene(?). The brown biotite is often rimmed by the light yellow-brown biotite.

Both biotites, and possibly some riebeckite, have altered to radial or fibrous bundles of chlorite. In some slides, only relict patches of the brown biotite and the ferrohastingsite are left, and most of the mafic minerals consist of yellow-brown biotite, sphene, chlorite, leucoxene and magnetite. Rarely, zeolite minerals fill interstitial positions, and large calcite crystals and calcite fracture fillings are common. In some cases, the sill is 15 percent calcite.

The late alteration to chlorite may be associated with the chlorite grade regional metamorphism of the surrounding Johnnie Formation while the previous alteration to biotite and riebeckite occured at the time the sill intruded the wet sediments.

Diorite or andesite dike swarms occur throughout the area to the southwest of the mapped area (Albee, oral communication), and similar dikes of Triassic(?) age have been mapped by Johnson (1957) in the Manly Peak Quadrangle still further to the southwest. Dikes of this type have not been noted in the mapped area.

Andesite dikes of Tertiary age within the mapped area intrude the Little Chief stock, and similar dikes and plugs are exposed extensively to the east of the mapped area (Hunt and Mabey, 1966).

Regional Metamorphism

Throughout the eastern part of the mapped region, the rocks of the Kingston Peak, Noonday and Johnnie Formations are metamorphosed to roughly chlorite grade or equivalent assemblages. To the west, biotite grade assemblages appear, and higher grade assemblages are reported by Ianphere (1962) still further to the west. Thus it appears that the stock was emplaced in an area in which the metamorphic grade is gradually increasing to the westward.

The Kingston Peak Formation, in the areas away from the stock contact, consists of argillite with the assemblage clastic quartz-calcite-epidote-chlorite-opaque. In the conglomeratic graywacke, reaction rims of talc occur around the carbonate clasts against the sandy quartz-feldspar-epidote-chlorite-opaque assemblage of the matrix.

To the northwest, Ianphere (1962) reports dominantly quartz-biotite-muscovite-chlorite-opaque assemblages, indicating a slight increase in grade to the northwest. No Kingston Peak is exposed in the mapped area between the stock and Ianphere's area. Garnet, chloritoid, staurolite, and cordierite are present in the Kingston Peak to the southwest of the mapped area (Ianphere et al, 1964).

The massive dolomite and limestone beds of the Noonday Dolomite, for the most part, consist of slightly recrystallized calcite or dolomite-rounded quartz-minor epidote-opaque-phlogopite assemblages. The Radcliffe Member limestone consist of calcite-albite-minor epidote, while the argillaceous beds have muscovite-chlorite bearing assemblages

very similar to those of the Johnnie Formation argillites. Tremolite rosettes occur in the Redlands Member (Albee, oral communication, 1966). Similar assemblages, with the addition of biotite in the argillaceous beds, are reported by Lanphere to the northwest.

The Johnnie Formation, to the east of the stock, consists of argillaceous, or locally phyllitic, muscovite-quartz-chlorite-opaque ± calcite ± albite rocks for the most part. The dolomite beds in the lower part of the formation have the same assemblages as the massive Noonday Dolomite noted above. In a few of the dolomite beds, small eyes, less than 2 inches wide, of calcite with phlogopite rims occur. The only significant feldspar in the Johnnie occurs in the suspected tuffaceous beds toward the base of the formation, or in the matrix of the penecontemporaneous conglomerates in the upper part of the formation.

To the northwest and west of the stock, the typical assemblage observed was muscovite-quartz-biotite-chlorite-opaque±epidote±calcite in the argillaceous rocks. In this region, the rocks are consistently phyllitic. In one specimen, taken only 1000 feet from the stock contact, the assemblage muscovite-biotite-andalusite-quartz-opaque occurs, and traces of andalusite in chlorite-poor argillite in the Bennett Peak area are observed.

Similar quartz-muscovite-chlorite-opaque±biotite assemblages are noted by Lanphere to the northwest, and one quartz-andalusite-muscovite-biotite-opaque assemblage is noted by him some 2.5 miles northwest of the stock. Cordierite and andalusite bearing assemblages

are reported to the southwest of the mapped area (Lanphere et al, 1964).

# STRUCTURAL GEOLOGY

## Distribution of Rock Types

In a gross sense, the whole Panamint Range may be considered a single fault block which has been tilted gently to the east, and in which the strike of the Cambrian and later Precambrian sediments is slightly to the northwest of the trend of the range, so that going both to the north and to the east, progressively younger strata are exposed. The eastern slope of the range, especially that portion just to the east of the range divide, may be thought of as a dip slope. Further to the east the topographic slope decreases and the dip of the sediments becomes greater than the ground slope. The western slope of the range cuts across the eastward dipping sediments, and hence progressively older beds are exposed to the west.

The regional dip of the later Precambrian and Cambrian strata is consistently 10 to 20 degrees to the east. This regional dip is well shown in two east-west cross sections through the mapped area, section A-A', just to the north of the stock, and section L-L', just to the south of the stock: Both are shown in Plate 3. In section A-A' the blocks between the north-south striking, westward dipping faults which intersect the section at right angles, have each been rotated toward the east, so that the eastward dip of the beds within each fault block is in general steeper than the regional dip averaged over the numerous fault blocks. In section L-L', there appears to have been no such rotation of the various fault-bounded blocks. In general, the regional dip appears to be somewhat greater to the north of the stock than to the south of it.

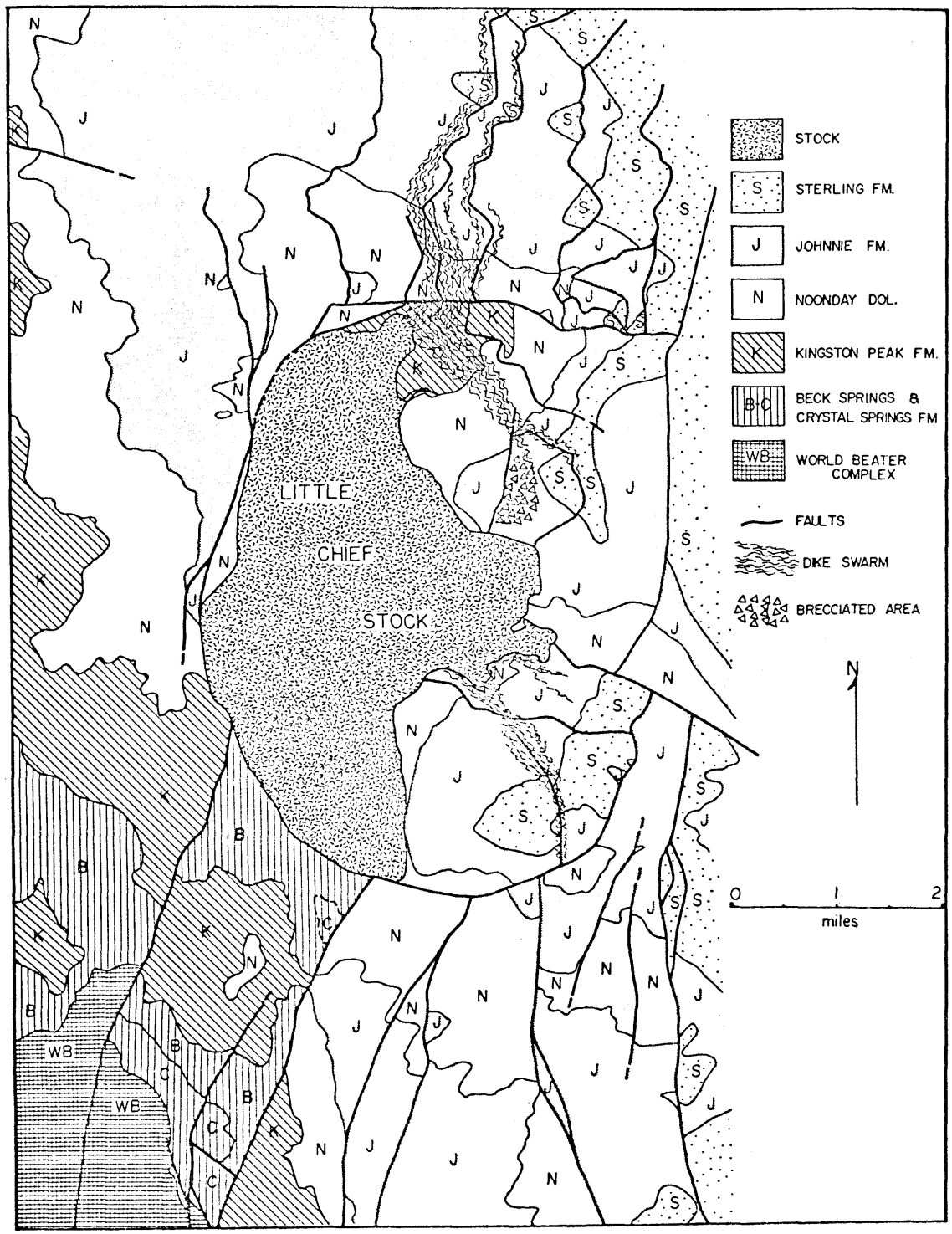


Fig. 2. Simplified geologic map of the Little Chief stock area. Portions along north edge taken from Hunt and Mabey(1966), portions to southwest from Albee(written comm.).

This eastward regional dip is shown in Fig. 2, a very simplified geologic map of the area around the Little Chief Stock (see also Plate 1). The oldest rock units-the World Beater Complex, and the Beck Spring, Crystal Spring, and Kingston Peak Formations of the Pahrump Series crop out in general to the west and southwest of the stock on the west side of the range divide as a roughly north-south belt. The younger units-the Noonday Dolomite, and the Johnnie and Stirling Formations-crop out extensively along the range divide and to the east of the divide.

## Form of the Little Chief Stock

Because of the excellent exposure and high relief in the mapped area, very good control is available on the attitude of the stock contact over its whole extent. The stock contact ranges in altitude from roughly 10,400 feet to 4000 feet in a distance of three miles, and crosses several 3000 foot ridges. Hence, there is adequate control on the stock contact along most short segments for vertical distances of 3000 feet or more.

Figure 3 shows the form of the stock by means of structure contours drawn on the contact. Note that the solid lines refer to the portions of the contact which dip away from the stock, and the dashed lines refer to the portions which dip toward the stock. Contact attitudes were obtained through direct measurements, through graphic solutions on mapped segments of the contact, and through the combined use of air-photographs and topographic maps to make general estimates of the attitudes.

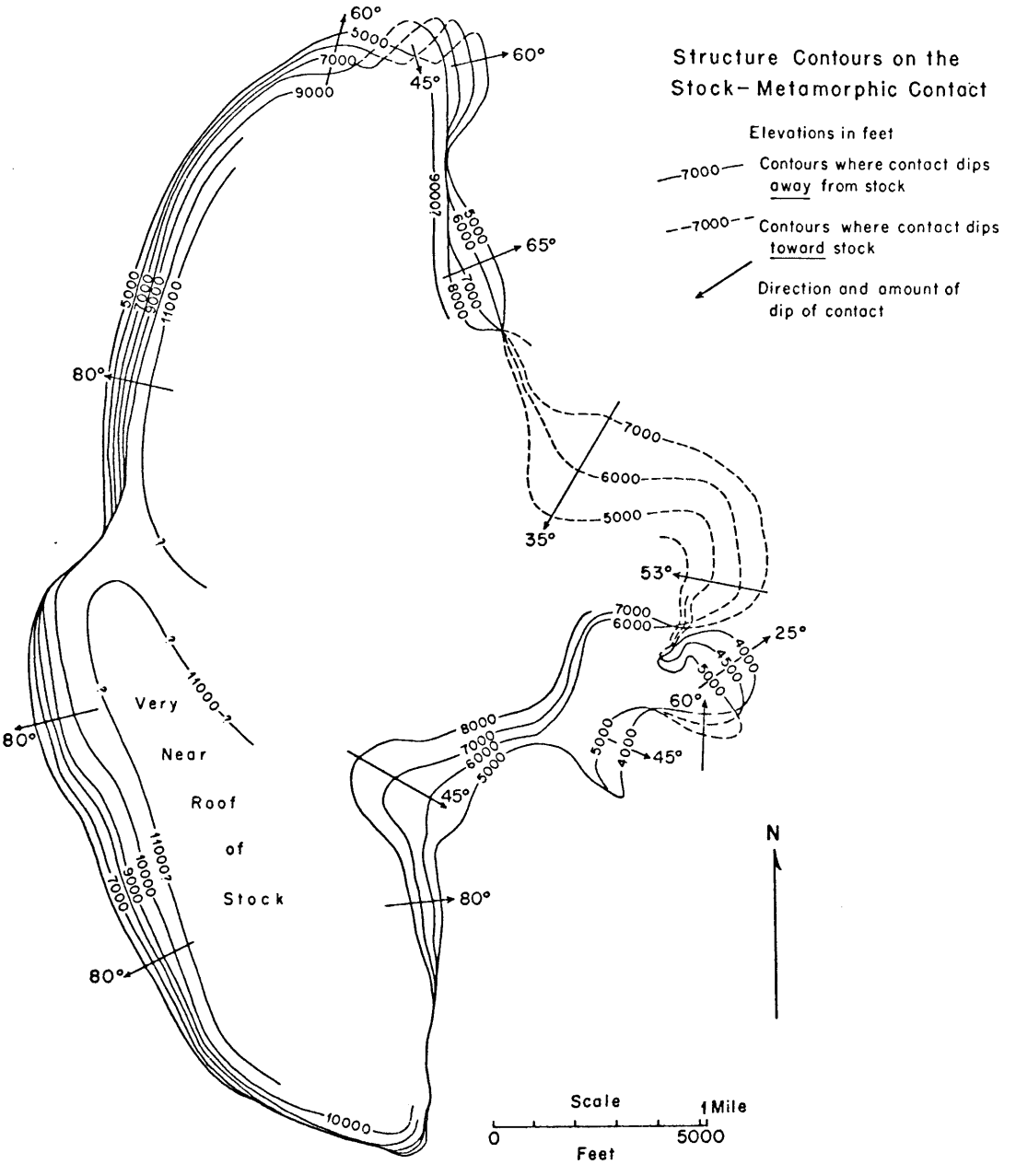


Fig. 3. Structure contours on the stock contact.

In general, Fig. 3 shows that the overall form of the stock is simple, and that the stock contacts dip outward at very steep angles. Thus dips of vertical to 80 degrees outward predominate along the entire portion of the contact from the southeast corner through the western side to the northwestern side. In the north and northeastern edges of the stock, the contact for the most part dips outward at angles of 60 to 65 degrees with the exception of a small portion that dips inward at an angle of 45 degrees. It is only along the east-central margin of the stock that the contact becomes complex.

Roughly 60 percent of the stock contact is vertical or outward dipping at angles of 80 degrees or greater, 12 percent of the contact dips outward at angles of roughly 60 degrees, 12 percent of the contact dips outward at angles of 45 degrees or less, and 16 percent of the contact dips inward at angles of 35 to 55 degrees. All the shallow outward dips, and all the inward dips except for the small area mentioned above, are found in the east-central extension of the stock.

Cross sections through the various parts of the mapped area are shown together in Plate 3, and the individual section lines are located in Plate 1 and 4. In some sections, information has been projected onto the sections from various distances up to 1000 feet in a direction perpendicular to the section. In these cases, the amount and direction of projection has been noted.

Sections which cross the vertical or steeply-outward dipping portions of the stock contact, (K-K', M-M', J-J', D-D', and C-C'-C") illustrate that the stock contact clearly crosscuts the country rock.

Very near the actual contact the sedimentary rocks are either abruptly folded, or dragged upward, as in section D-D', or a fault occurs, as in section C-C' or D-D'. In this latter case, the fault is essentially parallel to the stock contact and usually less than 1000 feet horizontally from the contact, and the block between the fault and the stock has been moved upward with the stock.

In several of these sections, such as K-K', J-J', and C-C', the probable elevation of the roof of the stock has been shown. This has been located on the basis of the distribution of contact phases in the stock, and other textural features within the stock which indicate proximity to the stock contact as described in Part II. In general the roof of the stock occurs at an elevation of roughly 10,500 feet and is fairly flat. Hence, the sedimentary units are probably concordant with the stock contact in the roof portion of the stock.

Cross sections in Plate 3 which pass through the eastern extension of the stock in the Starvation Canyon area are sections E-E', F-F', G-G' and H-H'. For descriptive purposes, this portion of the contact, which is complex and irregular, has been divided into two parts. The northern part, as shown in Fig. 3 and section E-E', dips inward at angles of roughly 35 and 53 degrees, and represents a significant increase in the width of the stock at higher elevations. This portion was formed by the north phase of the stock. The southern part, which was formed by the south phase of the stock, consists of a flat shelf-like extension of the stock which makes up the part of the stock east of the 6000 foot contour in Fig. 3. To the west, at

elevations of 6000 feet or greater, the stock contact again appears to become vertical or steeply outward dipping, as is common along most of the stock's contact. The placement of the 6000 foot contour and the location of the shelf-like area is based on the distribution of roof-pendants, contact sheath rocks, and contact phases of the stock in that area.

The shelf-like portion east of the 6000 foot contour is bounded on its south side by a vertical contact, and on the east and northeast sides by shallowly outward dipping contacts. The distribution of faulting associated with the stock just to the east of this shelf-like area indicates that the stock does not extend to the east, at depth, for any great distance as a major intrusive body.

It is significant that the shelf-like expansion of the stock is along the contact between the Noonday Dolomite and the overlying Johnnie argillaceous rocks, since as noted before most of the stock contact is very near, but below, this contact. Indeed, the only area of the stock which clearly crosscuts the Johnnie argillaceous rocks is in the overhanging area just to the north.

The dips of the stock contact at the surface indicate that it is essentially a vertical plug, with steep, and sometimes overhanging contacts. The most likely feeder area for the stock is an east-west band that passes through the widest part of the stock in the Starvation Canyon area, essentially along the contact between the north and south phases of the stock. This is also along the westward extension of an east-west striking vertical tear fault which extends from the east side of the stock to the east edge of the range. Fragments of

the earlier igneous phase are concentrated along this zone, and later zones of alteration occur here also. This suggests the possibility that the stock changes from an elongate north-south mass to a very much narrower elongate east-west body at depth. Whether this takes place through the formation of a flat floor, or by a gradual necking downward is not known.

## Deformation of the Country Rock

In this section the emphasis is on the structural relationship of the stock to the surrounding sediments. An attempt will be made to determine in what way the emplacement of the stock disturbed the sedimentary rocks, and whether the mode of deformation can be made to fit any logical pattern relative to the emplacement of stocks in general.

The structure of an area can be particularly well illustrated and understood from the three-dimensional distribution of one well-defined sedimentary horizon, but this requires good topographic control and rock exposure. In the area around the stock the contact between the gradational member and the argillite member of the Johnnie Formation is an excellent marker horizon. It marks the break between the pastel green or gray argillites of the Johnnie above, and a dominantly white dolomitic section below which includes the lower Johnnie member and all of the Noonday Dolomite. It is made even more conspicuous by the tendency of the thick dolomite beds to form massive white cliffs. In Fig. 2, this contact is just above the Johnnie-Noonday contact, but at the scale of the figure the two contacts appear as the same line. The extensive outcrop of this

contact around the stock is clearly shown.

The topographic relief over the mapped area is 8000 feet, and 7000 feet of this change takes place in a horizontal distance of 3 miles, from Telescope Peak to the floor of Hanaupah Canyon. The local relief over any given ridge, aside from the main range divide, is usually 2000-3000 feet in a horizontal distance of a mile or less. Hence, three dimensional control on the contact is excellent.

Structure contours on the contact noted above, which will henceforth be referred to as the contoured contact, are shown in Fig. 4. Contours are labelled in thousands of feet, and drawn every 500 feet. All contours over the stock are dashed, as they have been projected in from outside the stock contact.

The general eastward dip of the strata can be seen in the figure, as well as the high area over the stock itself. It is evident that the stock has domed the sediments to some degree, although it appears that doming does not extend very far from the stock itself. The contoured surface dips more steeply in the areas adjacent to the stock as a function of the degree of doming. The 13,000 feet contour in the extreme southwest corner of the figure indicates the location of the edge of the World Beater Dome.

Faulting

The distribution of the important faults in the mapped area is shown in Plate 4 (also Fig. 4). The stock outline is shown by the row of circles, and the contact between the north and south phases of the stock is shown by the dotted line. The faults are shown by the various line-, dash-, and dot-symbols. In most cases, the throw of the various faults, as determined from the contoured surface

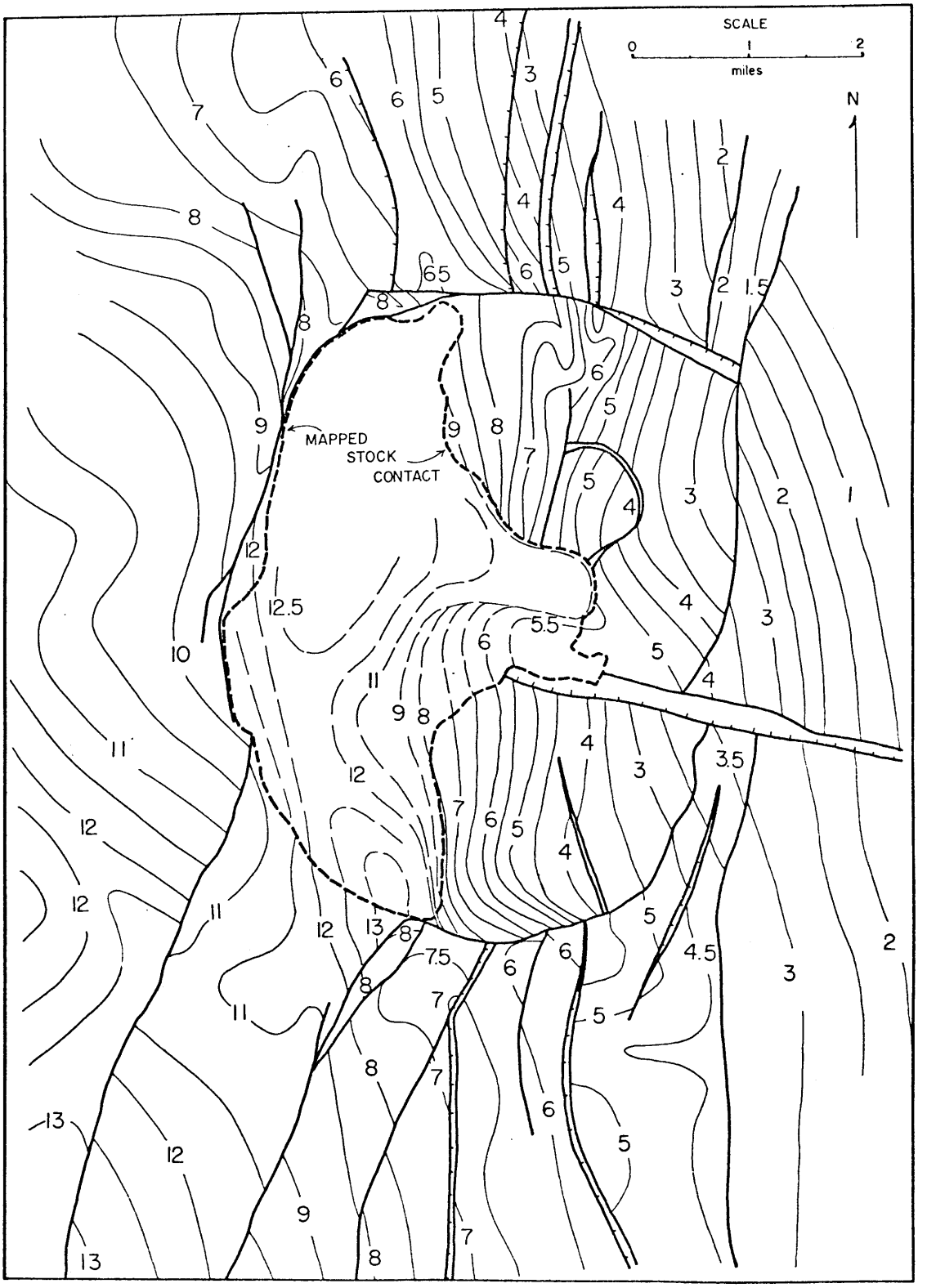


Fig. 4. Structure contours on the contact between the gradational and argillite members of the Johnnie Formation. Stock outline dashed, faults in heavy solid lines, contours in light solid lines. Elevation shown in thousands of feet.

of Fig. 4, is shown in thousands of feet and is always placed on the upthrown side of the fault. The "X" indicates the upthrown side of faults which have displacements of less than 500 feet in a vertical sense.

For purposes of discussion, the faults shown in Plate 4 will be subdivided into four major groups. The most obvious fault system in the mapped area is the ring fault shown by the solid line in the figure, which completely surrounds the stock. Most of the faults in the area have north-south trends and are truncated by the ring fault. These faults can be subdivided into three groups. In the north, the short-dash symbol indicates a westward dipping system of normal faults with west-side down motion along which the major dike swarm associated with the stock was intruded. In the south, two systems of vertical, west-side-up, faults are indicated by the two dot-one dash and four dot-one dash symbols, which trend roughly north-northeast and north-northwest, respectively.

The ring fault is very well exposed throughout its whole extent. In general it is vertical and the interior portion has risen relative to the surrounding rocks in such a way that maximum displacements are on the western side and a hinge line of no vertical motion occurs near the east side, giving the interior block the form of a trapdoor which opens to the west. This fault will henceforth be referred to as the trapdoor fault.

At the north edge of the trapdoor, the trapdoor fault dips 75 degrees south. Along this edge, displacement of the trapdoor

ranges from 0 at the northeast corner to 2000 feet up at the northwest corner, and both drag folds and graphical solutions of fault movement indicate that the interior moved vertically upward with a slight eastward component.

The western part of the trapdoor fault shows east-side-up displacements of 2000-3000 feet. Along much of the western side of the trapdoor, the edge of the trapdoor and the edge of the stock coincide. The magma apparently intruded upward, using the trapdoor fault plane as its western boundary.

On the south side, the displacements of the trapdoor increase from 0 at B to 5000 feet up at the southwest corner. To the east of B, from B to the southeast corner of the trapdoor, the displacements increase to 1500 feet upward with the south side up: That is, the trapdoor portion dropped down relative to the surrounding rocks.

Extending roughly in a straight line from B to the northeast corner of the trapdoor, there is a line of no relative vertical motion which acted as a pivot for the westward opening trapdoor. The small portion of the trapdoor to the east of this line actually moved downward relative to the surrounding rocks.

On the southeast side of the trapdoor, the simple trapdoor concept breaks down in that a portion of the rocks outside the "ideal" trapdoor were lifted up with the trapdoor itself. The two faults which define the extension of the trapdoor are the Stone Corral and World Beater faults. To the north of point D, the throw on the Stone Corral fault increases from 1500 feet to 5000 feet at the edge of the trapdoor. On the World Beater fault, the west-side-up motion decreases

to zero north of point C, and still further north, the fault has east-side-up displacements, on the trapdoor side, of 1000 feet or so. It thus appears that the obvious effects of the trapdoor forming stage were confined to the area to the north and east of a line from C to D.

The east side of the trapdoor has been offset by an east-west fault in the Starvation Canyon area. This fault, which will be referred to as the tear fault, offsets the hinge line of the trapdoor, but does not cut the stock. In fact, the exterior portion of the stock's north phase has extended itself to the east along the fault plane. Thus, while the tear fault post-dates the formation of the trapdoor, it predates the emplacement of the exterior portion of the north phase of the stock.

Near the trapdoor, the tear fault dips roughly 70 degrees north. A graphical solution of the movementon the tear fault indicates that the north side moved roughly 2000 feet vertically and 1000 feet to the west, relative to the south side. Further to the east, the apparent vertical motion appears to reverse itself so that roughly 2 miles east of the stock, the south side of the fault has moved relatively upward. The fault therefore has a scissors-like motion.

The tear fault appears to extend to the eastern range front as a zone of highly brecciated rock, and is the same fault as the tear fault which Hunt and Mabey (1966) refers to as truncating the Burro Trail thrust and other faults related to his Amargosa Thrust Fault system.

Plate 4 shows that the west-side-down displacements on the trapdoor fault just north or south of the tear fault are quite different. The displacements are consistently larger to the south of the tear fault, and the change in the magnitude of the displacements takes place very abruptly across the tear fault. This fact, combined with the north-side-up motion of the tear fault may indicate that at the same time that movement was taking place on the tear fault, renewed movement was occuring on the portion of the trapdoor to the north of the tear fault. Thus, on a portion of the trapdoor fault in which the west side moved down as the main trapdoor formed, the sense of movement was reversed and the west side later moved up when the tear fault formed. This sort of motion is consistent with the later intrusion of the north phase of the stock, which is thought to be the cause of the tear fault.

The attitude of the faults to the north of the trapdoor (short dashed lines, Plate 1) is roughly N15°E, 45-60°W. The major dike swarm associated with the stock was intruded along this fault system before the trapdoor was formed. Both the dike swarm and the fault system have been offset by the movement of the trapdoor fault. The apparent vertical motion on most of these faults is west-side-down with throws of 500 feet or less.

This fault system appears to extend some 6 miles to the northeast, where it merges with the north-south striking faults, with similar westward dips, which Hunt and Mabey (1966) consider as part of their Amorgosa Thrust Complex. This fault complex extends along the eastern foothills of the Panamint Range from the tear fault in Starvation Canyon some 32 miles to the north to Tucki Mountain, and

Hunt feels that it is related to the Armorgosa thrust system in tne Black Range to tne east of Death Valley. Botn Noble (personal communication in Hunt and Mabey, 1966) and Hunt and Mabey (1966) feel that the low-angle faults in the Panamint Range foothills are related to the various rhyolitic-felsitic volcanics which are intruded along the faults, and Hunt in turn relates these volcanics to the Little Chief Stock, and suggests that the stock itself was emplaced along the basal fault of this system of low angle faults.

The majority of the low-angle faults are confined to the eastern footnills of the range. Hunt's mapping indicates that the only two areas in which low-angle, westward-dipping faults are commonly present in tne nigher parts of the range to the west are in those areas in which there are large Tertiary intrusives; namely the Little Chief stock and the granite at Skidoo, an elongate intrusive body some 9 miles north of the Little Chief stock. This supports the contention that the low angle faults are related to the emplacement of the stocks.

The faults south of the trapdoor, which are shown by the two dot-dash symbols in Plate 4 consistently show west-side-up apparent vertical displacements, and in general, the fault planes have dips that are within 15 degrees of vertical. The apparent vertical displacements are roughly 500-1500 feet. The eastern set strikes roughly N15$^{o}$W while the western set is oriented N20$^{o}$E. Both of these fault systems are truncated by the south side of the trapdoor and none of these faults has been correlated with any of the faults within the trapdoor.

The fault systems to the south of the stock are continuous for distances of up to 10 miles south of the stock. The relative displacements on the World Beater and Stone Corral faults, south of points C and D, are constant with west-side-up motions of 1000 feet and 1500 feet, respectively. Graphical solutions of fault movement indicated that the west side of the former fault has a slight northward component.

The Porter Mine fault extends some 10 miles south of the stock to Butte Valley (Albee, oral communication, 1965), and the west-side-up displacement is 500-1000 feet over the whole distance. To the south of Butte Valley, Johnson (1957) has inferred a fault on strike with the Porter Mine fault which has a similar sense of displacement. This fault offsets a series of Tertiary andesitic volcanics. If this fault and the Porter Mine fault are the same, then this suggests that the displacement on the Porter Mine fault occured after the volcanics were deposited. If the Porter Mine fault is related to the emplacement of the stock, then, assuming faulting at one time only, this in turn suggests that the stock was emplaced after the andesitic volcanics were formed. This must be balanced against the possibility that there have been several periods of movement on this fault, as Hunt has suggested for some faults in the eastern foothills of the range.

The eastern set of vertical normal faults (dash-four dot symbol, Plate 4) which occur to the south of the trapdoor and which end against the south side of the trapdoor, also extend well to the south and have consistent west-side-up displacements for the entire distance. The easternmost of this set of faults in the mapped area ends against

the tear fault in Starvation Canyon. No offset portion could be found. Faults with similar orientation and sense of displacement are mapped by Hunt and Mabey (1966) in the area to the east of the mapped area, and their maps show these faults as consistently offsetting the westward dipping faults which occur only to the north of the stock in the mapped area. Indeed, the area east of the stock appears to be a transitional zone, with the westward dipping faults dominating to the north, and the younger vertical faults dominating to the south. The above relationships indicate that at least the eastern system of faults south of the trapdoor are younger than the westward dipping faults found to the north of the stock, but are older than the tear fault in Starvation Canyon. The same is probably true of the western system of faults.

The faults within the trapdoor are few in number. The westward dipping fault which meets the north side of the trapdoor at A is clearly an offset part of the fault system to the north of the trapdoor. The fact that its dip is less than the dips of the faults to the north of the stock is consistent with its having been rotated to the east with trapdoor movement.

The most interesting fault within the trapdoor is that at point F. This fault strikes roughly north-south, and dips 20°W. To the north of point F, the fault motion is such that the west side has moved relatively up, or to the northeast, making that portion a true thrust fault. To the south of point F, the west side has moved relatively downward, and the fault is a low angle fault. The overall motion appears to have been a clockwise rotation of the upper plate

with dominant movement toward the northeast. This fault, which will be termed the thrust fault, was truncated by a short vertical normal fault on its west side.

Doming

It is readily apparent from Fig. 4 that extensive doming of the sediments has occured around the stock, with the main axis of doming coinciding with the north-south axis of the main part of the stock. Because of the tentative nature of the contours in Fig. 4 over the stock, closure produced by the doming can only be roughly estimated as 2500 feet at the south end of the stock. However, the actual amount of doming is greater due to the eastward regional dip of the sediments in this area.

It is also apparent that, for all practical purposes, the doming is wholly confined within the trapdoor fault, except at the southwest edge. The configuration of the contoured surface within the trapdoor, even allowing for the eastward rotation of the trapdoor, cannot be matched across any of the edges of the trapdoor. For instance, at the point where the simple trapdoor meets the Stone Corral fault, the dome within the trapdoor cannot be matched by a similar dome to the south, outside the trapdoor.

This strongly indicates that doming and trapdoor formation were simultaneous, since if doming had preceeded the time of trapdoor formation there should be some evidence of doming centered on the stock in the area outside the trapdoor.

In order to obtain a better idea of the amount of deformation relative to the pre-stock configuration of the dolomite-argillite

contact, an attempt has been made to show the amount of deviation of the contoured surface at present from its original position. A very simplified estimate of the pre-stock contact configuration was made, using the overall regional trend of the bedding in the range and the elevations of the contoured contact at present in the areas away from the stock which appeared to be the least deformed. The very simple surface was then subtracted from Fig. 4 to obtain a rough estimate of the degree of deviation of the present surface from this estimated original surface.

The result is shown in Fig. 5. The amount of deviation has been noted in thousands of feet, and the spacing of the lining in the various areas reflects the degree of deviation. Once again, the major axis of doming is seen to be directly over the axis of the stock, where the contact in question has been domed upward by roughly 4000 feet from its original position. The pronounced depressed area, in the southeast corner of the trapdoor, is also readily apparent, and its abrupt truncation by the tear fault shown. The area of considerably less deviation immediately to the north of the tear fault may represent the renewed later upward intrusion of the stock's north phase to the present level of emplacement. The extension of the north phase of the stock to the east is indicated by the slightly positive area against the north side of the tear fault which extends across the edge of the trapdoor. The high area in the southwest extension of the trapdoor is also apparent.

The very prominant extension of the highly deviated area to the east, in the central part of the trapdoor reflects the estimated lifting of a small portion of the contoured contact above the overhanging portion

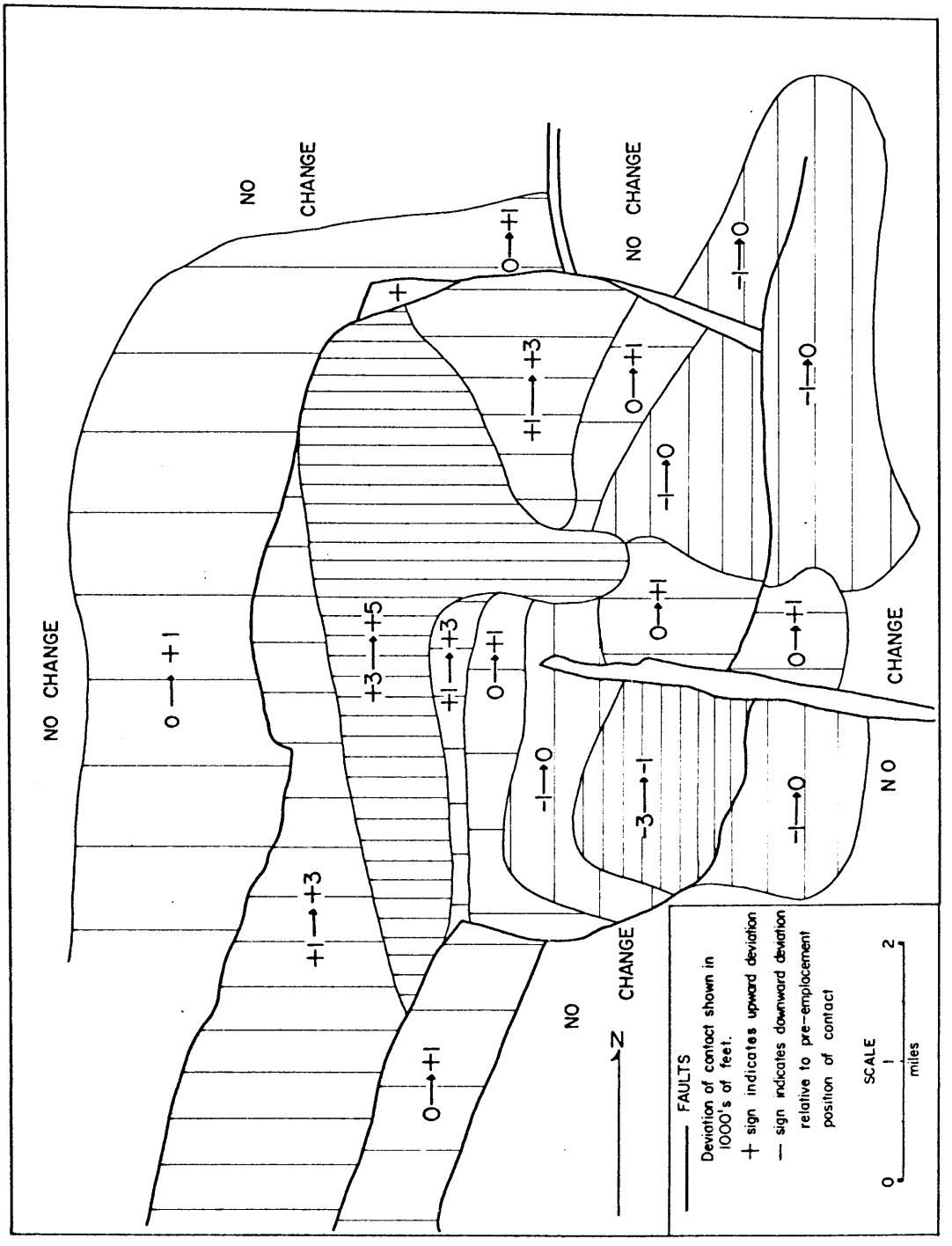


Fig. 5. Generalized deviation of the contact of the gradational and argillite members of the Johnnie Formation from its original position by emplacement of the stock.

of the stock.

Outside the trapdoor itself, there has been relatively little change in the contoured surface. Just outside the northwestern and western edges of the trapdoor, there is an area of slight positive deviation. This is matched, just outside the eastern edge of the trapdoor, by a slightly negative area-with the exception of the small positive area related to the tear fault and eastward extension of the stock. The combination of the positive area to the west with the negative area to the east indicates that this change in the contoured surface outside the trapdoor occurred at the time the trapdoor was formed, since it accurately reflects the movement of the trapdoor itself. It was probably caused by the drag effects of the trapdoor during its movement.

Considering the argillite-dolomite contact just outside the trapdoor itself, it is apparent that in several locations, the rocks outside the trapdoor have been dragged upward as the trapdoor moved upward. Such features show up in the contoured surface just outside the trapdoor fault, as, for instance, along the northwest side by the 9000 foot and 7500 foot contours, along the northeast side by the 3500-4000 foot contour, and along the south side by the 6000 foot and 7500 foot contours. Some of the larger folds which show up in the contoured surface at various distances outside the trapdoor are probably also related to the formation of the trapdoor. Thus the northward plunging-anticline due north of the northwest corner of the trapdoor appears to be related to the normal fault to the south, which in turn seems to be related to the trapdoor itself.

If the majority of the doming took place during the time of trapdoor formation, then the pre-trapdoor configuration of the dolomite-argillite contact must have been fairly simple, and should have approximated the regional eastward dip of the sediments. Assuming the various north-south striking faults outside the trapdoor have formed at the time of intrusion of the stock, then very few major faults cut this pre-trapdoor surface. It was only at the time that the stock initially moved relatively close to its present position that this surface was disturbed and the north-south striking faults formed.

Two cross sections through Fig. 5 are shown in Fig. 6. Both sections are oriented perpendicular to the regional strike of the dolomite-argillite contact, and hence both are approximately east-west sections. Section 2 crosses the south part of the stock, south of the tear fault, and section 1 crosses the north part of the stock, just to the north of the flap-like area lifted by the overhanging portion of the stock. In both sections, the original pre-stock contoured surface, and the deformed post-stock surface are shown by the light and dark solid lines, respectively. The estimated outline of the stock is shown by the light dashed lines, and the edges of the trapdoor are shown by the heavy, steeply dipping lines. Note that in both sections the vertical scale is equal to the horizontal scale.

In both cases, the doming of the dolomite-argillite contact over the stock is very well shown, and the restriction of the area of most extreme doming to the position of the stock is obvious. Once again, it

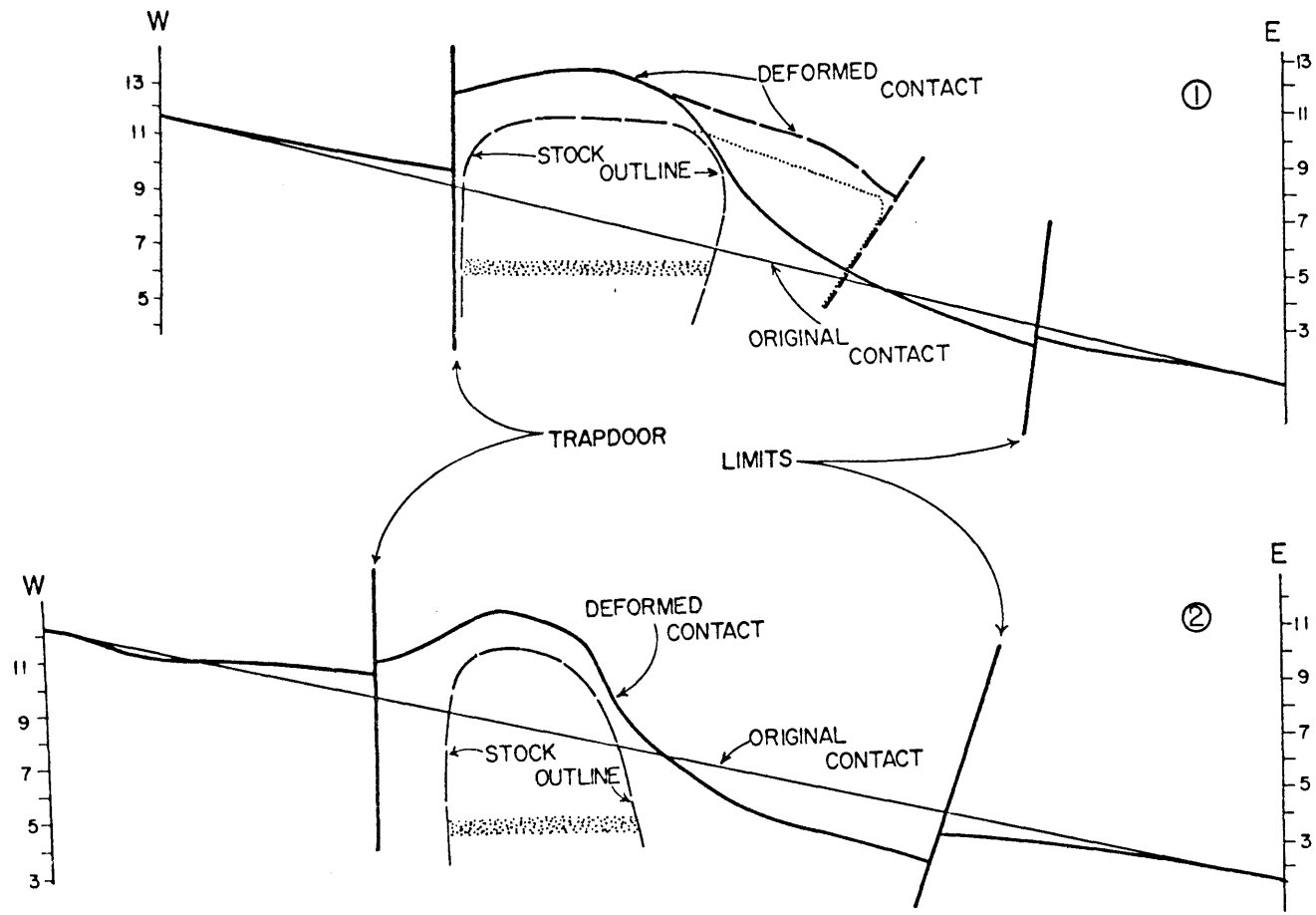


Fig. 6. East-west cross sections through the deviation surface of Fig. 5. Elevations shown in thousands of feet. Light line shows original position of contact, heavy line shows same contact after doming and trapdoor formation. Area of stock above broad bands accounted for by room created on deformation of contact.

must be noted that the post-stock position of the contact directly over the stock has been estimated, although in both cases control on the contact is good at the edges of the stock.

In section 1, the dotted portion of the stock outline, and the dolomite-argillite contact shown by the dark dashed line, represent a cross section that passes through the overhanging portion of the stock, immediately to the south of section 1. In this case, the contacts have been projected onto section 1 from less than 1000 feet to the south. This serves to illustrate the prying up, as it were, of a flap of the dolomite-argillite contact in that area of the stock that has extended itself to the east out over the country rock.

Both these cross sections indicate that the original length of the rocks above the stock has been extended. In numerous instances near the stock, the beds have been observed to thin as they are turned upward along the stock contact. This is especially true of the dolomitic units, which dominate the rocks immediately adjacent to the stock. Thinning adjacent to the stock is especially well shown in cross section K-K' (Plate 3) at the east side of the stock. Here a two-fold thinning of several massive dolomite beds can be observed as they approach the stock. In this case, the overlying argillaceous beds of the Johnnie Formation also show evidence of thinning. Immediately to the southwest of the stock, oolitic carbonate beds of the Beck Spring Formation have stretched oolites which suggest, in that area, an elongation of the beds by a factor of two or so.

Thus it appears that the dominantly carbonaceous sediments have deformed by stretching and thinning in a "plastic" manner, and in

this way they have accounted for the absolute lengthening of the beds required by the emplacement of the stock. It is probably true that the beds have undergone considerable disruption over the roof of the stock, in the area now removed by erosion, and in this case some of the required lengthening of the beds can be accounted for by normal faulting.

Time Relations Between Faulting, Doming and Stock Emplacement

The time of formation of the trapdoor is clearly later than the emplacement of the dike swarm in Hanaupah Canyon, but the tear fault in Starvation Canyon, which offsets the trapdoor fault, is itself older than the emplacement of the exterior portion of the north phase of the stock. Thus the time of trapdoor formation is bracketed by the earlier emplacement of the dike swarm, and the later simultaneous formation of the tear fault and emplacement of the stock's north phase exterior portion to near its present level.

The fact that the magma reached the fault plane which forms the western and southern side of the trapdoor suggests that trapdoor formation was simultaneous with emplacement of the stock to, or almost to, the present level of emplacement. There is no evidence of shearing along these contacts which would indicate trapdoor movement after emplacement of the stock.

The exterior portion of the north phase of the stock truncates the dike swarm at the northeast corner of the stock. The existence of mineral textures indicating high volatile concentrations in the part of the stock nearest the truncated dike swarm suggests that this portion of the stock, at the present level of erosion, is not

very far vertically above the point at which the dike swarm was released from the then deeper magme chamber.

The general form of the trapdoor indicates that both the north and south intrusive phases of the stock were involved in its formation. However, the sense of movement on the tear fault is such that it could have been formed by the emplacement of the north phase of the stock, and then immediately intruded by the stock to give the eastward extension of the stock along the tear fault place. This fact, along with the truncation of the dike swarm by the north phase, the reversed motion on the east side of the trapdoor, and the distribution of volatiles in the stock, suggests that while the north phase was involved in the trapdoor formation, it reached its present level after the bulk of the trapdoor had been formed.

This suggests the following relationships between the faults in the area, and the formation of the trapdoor. The first faults formed were the westward-dipping normal faults now present to the north of the stock. These were probably formed by stretching over a magma chamber located some depth below the present erosion level, and were almost immediately intruded by the dike swarm. Upward movement of the stock magma then caused trapdoor formation and doming. At this time, the south phase was at its present position, while the north phase was at a slight distance below the present erosion surface.

The north-south striking, vertical faults present to the south and east of the stock may have been formed at this time. However, similar faults are present to the west of the mapped area (Albee, oral communication, 1965), and therefore, these faults probably

predate the time of stock emplacement. Renewed movement occurred on the portions of these faults nearest to the trapdoor at the time of stock emplacement, and renewed movement may have occurred further south on these faults at this time.

After the original trapdoor was formed, the north phase of the stock then moved up to its present position along a zone of weakness reflected by the east-west tear fault. The upward motion of the stock renewed movement on the tear fault, reversed the movement on the east side of the trapdoor north of the tear fault, and truncated the dike swarm. Thus, the north phase essentially broke the trapdoor into two halves, and lifted the north half still further above its original level.

The form of the stock (see Fig. 3), while elongate in a north-south direction, does not appear to be controlled by any of the visible systems of faults seen in the mapped area.

The feeder of the stock appears to have been an elongate east-west dike under the stock in the Starvation Canyon area along the zone of weakness coincident with the tear fault.

The Room Problem

Figure 6 may be used to illustrate the relationship of the volume of the stock relative to the volume created for the stock through doming and faulting. In both sections, the lower limit of the approximate area of the stock in cross section that is accounted for by the deviation of the contoured surface from its original position is shown by the broad horizontal bands.

Thus in sections 1 and 2, the area of the stock above the broad dotted band is accounted for by the deformation of the exposed country rocks. Consideration of the volume of the stock indicates that all the stock above approximately the 4000 foot elevation plane can be accounted for by the volume created by the deviated surface. This result agrees with the results gotten in the cross sections.

The steep contact dips of the stock suggest that the stock extends downward below an elevation of 4000 feet. The presence of the east-west feeder zone in Starvation Canyon suggests that the stock necks downward from the shape seen at the surface to the narrow zone in Starvation Canyon, and the suggested depth for this downward necking is less than 6000 feet below the present level of exposure. Thus the room problem remains at depth, although only to a slight degree.

Two other mechanisms by which the stock may make room for itself arethrough assimilation, or by stoping of large blocks which then sink into the magma chamber. There is some evidence that some large slabs of Noonday Dolomite were in the process of being pried away from the magma chamber walls at the present level of erosion, but no wholly enclosed clocks were seen. Similarly, there is evidence that assimilation has occurred. However, neither of these processes appears to be volumetrically significant and to be able to account for large volumes of displaced country rock.

It may be possible that the unaccounted-for volume of the stock may have been formed by lateral shouldering aside of the country rock through the processes of shortening by folding and stacking by thrusting. However, there is no evidence of these processes at the present level of exposure.

Relationship of Structures Associated With Stock Emplacement to Structures Associated With Salt Domes

It is very informative to compare the deformation associated with the stock with the very well-known deformation associated with salt domes and salt diapirs. Because of the similarity of form and emplacement mechanism with small, shallow, igneous intrusive bodies, certain structural features associated with salt intrusives should at least roughly correspond to the deformation around igneous bodies.

The driving force behind salt diapir movement is the density difference between the salt and the overlying rock , and this is basically the same as in the case of igneous intrusives. A density difference which amounts to roughly 0.3-0.2g/cc in the case of salt domes, is also easily attainable in the case of granitic magmas. The density of a homogeneously hydrated rhyolitic obsidian with roughly 6 percent $H_2O$ by weight is 2.30g/cc (Shaw, 1965), and this is probably a good estimate of the magma density of the Little Chief stock due to its high water content. Allowing for the percentage of phenocrysts, the effective density of the stock magma was roughly 2.45g/cc at the time of emplacement.

The estimated density of the country rock near the present level of emplacement of the stock is roughly 2.70-2.85g/cc, yielding a density contrast with the stock magma of roughly 0.3-0.4. This, coupled with the much lower viscosity expected from the granite magma relative to crystalline salt, should be more than ample to provide a driving force for upward movement of the magma.

Some characteristics associated with salt domes that are important in the present analogy are as follows (Murray, 1966; Trushein, 1960). In general, the diapiric salt bodies tend to dome up the overlying sediments, and produce domes which have diameters roughly 3 times the diameters of the salt masses involved, although many have no domes at all. Stretching of the sediments over the roof of the salt body yields a complex of normal faults which can take several forms. If the salt mass is perfectly round in plan, the faults tend to be radial. If the salt mass is elongate, then the fault pattern in plan will tend to have faults with one dominant strike, and that parallel to the axis of elongation of the dome. In cross section, the ideal salt dome has two sets of opposing normal faults in the overlying sediments which tend to converge on the highest point of the salt body. The dips of the faults are in the range of 45-60 degrees (Wallace, 1944). Several cross sections through typical salt domes or diapirs are shown in Fig. 7.

The sediments adjacent to the dome tend to be dragged upward with it and often thinned. True reverse faults are commonly present only adjacent to those portions of the salt mass which actually overhang the surrounding sediments. A ring-like, or moat-like marginal syncline is present around most salt domes and diapirs.

Model studies tend to duplicate the above observations, and the relationship of the shape of the salt body in plan to the faults in the overlying sediments is very well shown in many of the model studies (Parker and McDowell, 1955). Currie (1956) noted, on the basis of model studies, that the faults over the salt mass tend to steepen upward, and Nettleton (1934) observed in models that the salt

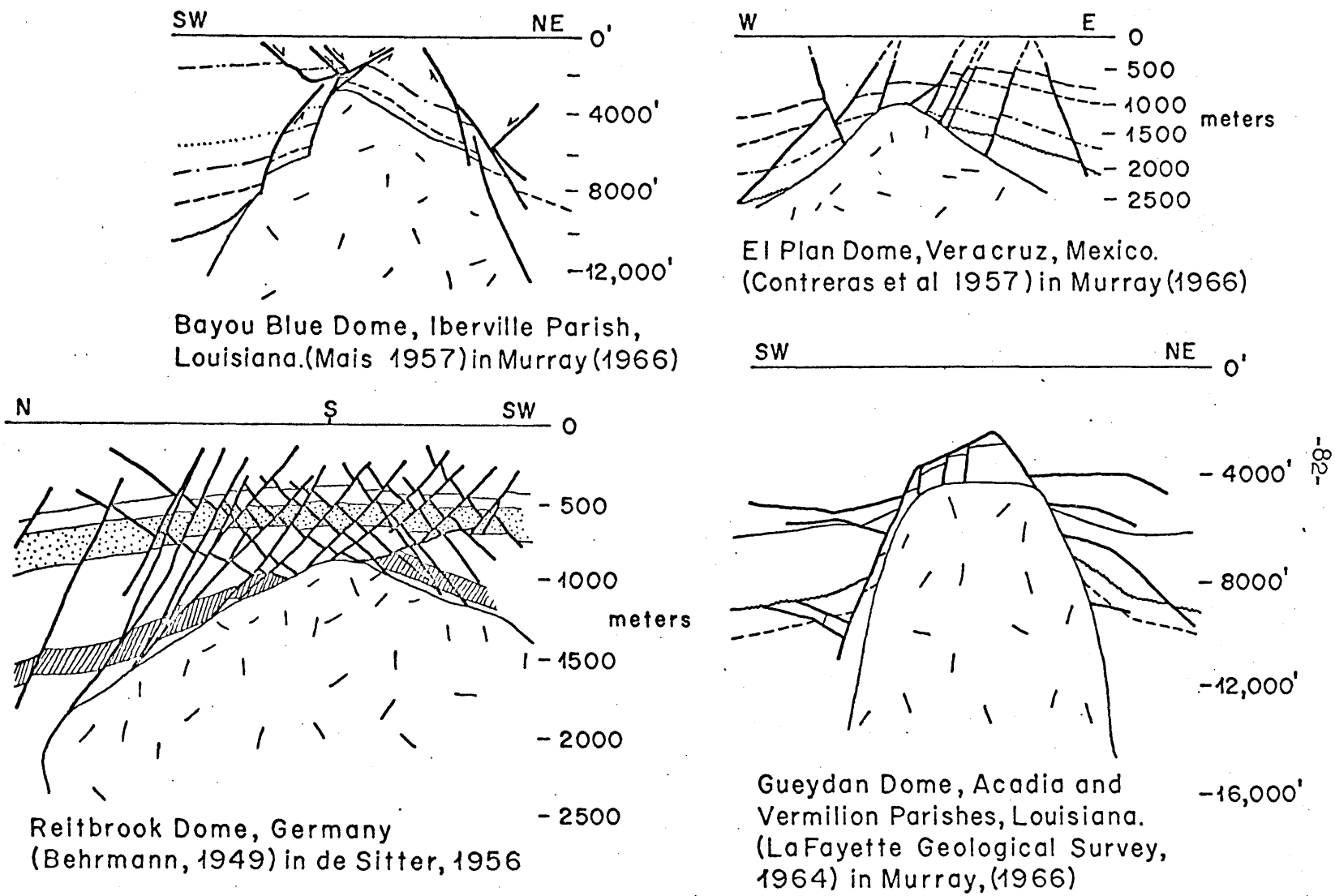


Fig. 7. Cross sections showing deformation associated with four typical salt domes.

mass could actually lift its roof as a discrete block.

The cross sections in Fig. 7 illustrate many of these features, with variations. In the Bayou Blue dome, the sediment directly above the dome has been lifted upward, and the opposing set of normal faults has developed above and to the southwest of the lifted block. The El Plan and Reitbrook domes show the opposing set of normal faults very well, and in both cases, one member of the paired fault sets has dominated the deformation over the salt dome. In both sections, the fault set that dips to the left on the figure is dominant. In the El Plan dome, one member of the pair is almost completely missing, while in the case of the Reitbrook dome, the dominant set consistently offsets the subordinant set, although both sets are present. These faults in cross section center on and interject the highest parts of the salt dome. The Gueydan dome again illustrates the lifting of the roof of the salt plug, and in this case, shows very little tendency to form the normal fault sets over the dome.

Comparison of these structures with structures related to the stock indicates some striking parallels. First, the trapdoor related to the stock is exemplified by the lifted portions of roof in some of the salt domes. The chief difference is that the trapdoor extends much further away from the stock to the east, while the lifted blocks over the salt bodies tend to be restricted to the area directly above the salt bodies. This difference may be due to the fact that the metamorphic rocks around the stock pose much greater strengths than the semi-consolidated unmetamorphosed sediments adjacent to the salt domes, and hence can transmit stress to the extent of allowing the trapdoor to

act as a relatively simple block.

No marginal syncline has been observed around the stock, but none should be expected using the salt dome analogy since the marginal synclines related to the salt domes have been caused for the most part (Nettleton, 1955) by lateral flow in the normal salt bed which supplies the salt for growth of the salt dome. This tends to thin the supplying salt bed and hence cause a peripheral sink. Since the granitic magma has probably not undergone this lateral accretionary process, no rim syncline should form. The small thrust fault within the trapdoor is immediately adjacent to that portion of the stock which overhangs the country rock, and is directly comparable with similar thrusts formed next to the overhanding portions of salt domes.

Thus far, the structures discussed have related to the stock at or just below its present level of emplacement. However, the north-south striking faults which the trapdoor truncates are thought to have developed when the stock was at some deeper level. These faults should then be analogous to the various faults which form over the top of the salt diapirs.

The faults to the north of the stock, with westward dips of 45-60 degrees, could well represent one pair of the two sets of normal faults that are normally found above salt domes, and in this case, as in some of the domes, one set only is present. The fact that the faults strike north-south can be related to the fact that the stock itself is elongate in plan and would hence favor one dominant strike direction. If one were to extend these westward dipping faults downward,

and require them to roughly intersect the top of a magma chamber directly below the present one, the top of the magma chamber would have to be roughly 4000-6000 feet below the present level of outcrop.

Comparison With Hunt's Conclusions

On the basis of reconnaissance mapping near the stock, Hunt and Mabey (1966) stated that the form of the Little Chief stock (Murphy, 1932), which he refers to as the "granite at Hanaupah Canyon," is "wedge shaped, the form to which the names sphenolith (Burckhardt, 1906) and harpolith (Cloos, 1921) have been applied." In cross section, he shows the granite as being floored, with upper contacts on both the east and west sides that dip away from the granite at angles of roughly 25 degrees.

An east-west cross section through the granite drawn by Hunt and Mabey (1966, Fig. 90, p. A122) is shown in Fig. 8, section A. The shallowly westward dipping series of low angle faults in the eastern part of the section belong to Hunt's Armorgosa thrust system, a series of north-south striking low angle faults which he feels are related to the similar Armorgosa thrusting in the Black Range to the east of Death Valley. The main fault of this system, labelled as the Armorgosa thrust in the figure, is felt by Hunt to define the entire floor of the stock, and he feels that this fault extends completely under the granite and intersects the ground surface west of the range divide. In the figure, the main break has been extended as the dotted line in the western part of the section through T and on to the extended ground surface shown by the dashed lines. This portion of the section has been

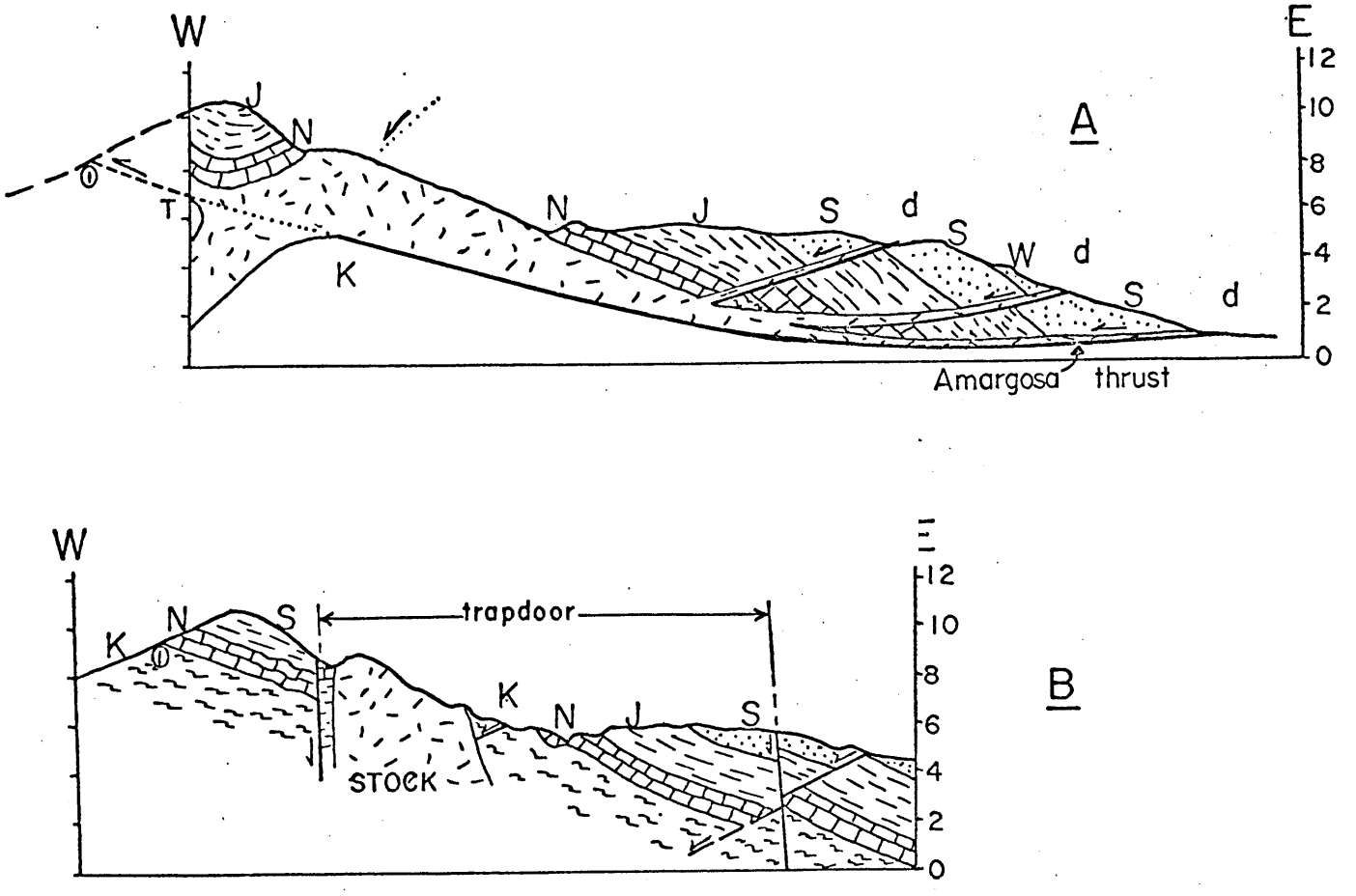


Fig. 8. Comparison of east-west cross sections through the stock by Hunt(Hunt and Mabey, 1966) and by the writer. Section A from Hunt and Mabey(1966), slightly modified. Section B from work of writer. See text for detailed explanation. W=Wood Canyon Formation, S=Stirling Quartzite, J=Johnnie Formation, N=Noonday Dolomite, K=Kingston Peak Formation, d=dike rocks. Horizontal scale equal to vertical scale.

added to Hunt's Fig. 90 from his Fig. 108 (p. A139).

Hunt feels that the granite was intruded along the main thrust plane from a source under its western side, and extends well to the east and appears at the ground surface along the eastern edge of the range.

Section B of Fig. K is a similar east-west cross section through the northern part of the stock which is based on the detailed mapping done by the author in the area around the stock. It is approximately the same as section C of Plate 3. It shows that the stock is considerably narrower than shown by Hunt, and that both contacts of the stock are relatively steeply dipping. As was previously noted in the discussion on the form of the stock, approximately 60 percent of the stock's contact is within 15 degrees of being vertical. Only a small part of the stock's contact dips shallowly outward, and the overall form of the stock is of a sharply cross cutting igneous body with steep contacts. There is no evidence of a major extension of the stock to the east. Hence the stock is by no means wedge shaped.

No evidence has been found of thrusting immediately to the west of the divide, in the area of the number 1 in section B. Indeed, there is no convincing evidence that the westward dipping low angle faults which Hunt shows on the east side of the range change to eastward dipping low angle faults, as would be required by Hunt's cross section. In fact, westward dipping faults present in the mapped area to the north of the stock, which belong to the same set of faults as Hunt's Amorgosa thrust system, tend to dip more steeply to the west as one goes toward the west. By analogy with diapiric-salt dome

structures, these faults most probably developed above the stock when it was present at some slightly deeper level, and hence were related to the emplacement of the stock.

Hunt and Mabey (1966) have postulated that the stock was the source of some of the dikes and plugs which occur in Hunt's Amargosa Thrust system on the east flank of the range, and they show the stock in cross section to extend along the postulated fault system (Fig. 8) from its present position to the east side of the range. As was noted previously, the form of the stock does not support the concept of a large conformable igneous body, but rather suggest that the stock is a diapir-like body with only a small area of possible eastward extension in the Starvation Canyon area. The westward extension of the fault system also was not found in the present mapping.

However, along the trace of the westernmost major low-angle fault of Hunt's Amargosa Fault system, which he terms the Burro Trail fault, just to the north of the tear fault which defines the southern end of the fault system, a small plug of porphyritic rhyolite was found which contains sanidine and plagioclase phenocrysts that are clearly related to the phenocrysts of the stock. Alteration has obscured many of the textural relationships, but it appears that the magma which produced this plug was separated from the main stock magma at the beginning of the groundmass crystallization stage in the stock, after the time that the stock's roof was fractured and the normal faults over the magma chamber were formed.

The fact that this plug is at the nearest point along the Burro Trail fault to the stock, at the portion of the stock which shows the small eastward extension in Starvation Canyon, indicates that some stock

magma at least found its way well to the east. However, the majority of the nearby igneous bodies along the Burro Trail fault belong to the dacitic-andesitic rocks and are not directly related to the stock. Thus while the major eastward extension of the stock postulated by Hunt does not appear to exist, some magma directly derived from stock magma was able to move this far to the east of the stock-a distance of some 4 miles. It is significant that this plug occurs directly to the east of the east-west feeder zone postulated for the Little Chief stock, and also occurs very close to the east-west striking tear fault zone which also lines up with the feeder zone. This supports the concept of a major "zone of weakness" occurring at this point which allowed the stock to move up to its present position, the tear fault to form, and the magma which formed the plug to move laterally eastward.

Still further to the east, on the east side of the fault that Hunt feels is the basal fault of his Amargosa fault system, a quartz monzonite body is exposed which, according to Hunt, represents the major eastward extension of the stock. This intrusive cuts only earlier Precambrian augen gneiss of the lower, or eastward, plate of the basal fault, and does not reach the fault itself. It consists of a subgraphic intergrowth of alkali feldspar and quartz, with oligoclase laths and scattered biotite flakes. While compositionally it is similar to the Little Chief stock, texturally it is quite different, and can only be compared to the volumetrically minor contact phases of the stock. If the small plug noted above can preserve the characteristic feldspar textures of the stock, it is not apparent why the much larger quartz monzonite did not also preserve these textures if it were

directly connected to the stock. On this basis, and also because of its greater distance from the stock, it is felt that there is no direct connection of this body with the main Little Chief stock.

In the light of the discussion of the relationships of the faults in the country rock to the emplacement of the main stock, another possibility is suggested. This eastern quartz monzonite body could be an entirely separate intrusive body which was emplaced at roughly the same period as the Little Chief stock and possibly the granite at Skidoo to the north. This being true, then the common westward dipping low angle faults, which Hunt places in his Amargosa fault system, could rather be due to deformation of the country rocks associated with emplacement of the various granitic bodies just mentioned. They would then be analogous to the similarly oriented "roof stretching" faults to the north of the Little Chief stock. Based on Hunt's mapping, as was observed before, the distribution of these westward dipping faults suggests a relationship to the igneous bodies in the Panamint Range.

In the mapped area, and especially along the lower flanks of the Panamint Range east of the mapped area, minor amounts of volcanic rocks are found. On the basis of the work of Hunt and Mabey (1966) and on reconnaissance mapping and petrology by the author, the volcanics may be described as follows.

The dominant rock types are andesites and dacites which contain phenocrysts of plagioclase compositionally zoned from sodic bytownite to the dominant calcic oligoclase, and microphenocrysts of biotite or oxybiotite, hornblende, magnetite, augite or diopside, all set in a

matrix which ranges from a cryptocrystalline to a felted mass of plagioclase with interstitial alkali feldspar and quartz. Rarely, embayed quartz phenocrysts occur, but in several cases inclusions of quartzite are found in the rocks and the embayed quartz may be related to these rather than being a true igneous mineral. The volcanics occur as dikes, sills and small plugs. Their emplacement appears to have been controlled by the north-south striking, westward dipping faults which are related to the emplacement of the stock and which Hunt places in his Amargosa thrust system. Rocks of this group cut the stock, and hence are clearly later in age than the stock.

Some of the above contain feldspars which are so altered that it is very difficult to identify them optically, but probe work suggests that in the majority of cases the feldspar is albitized oligoclase and therefore these rocks probably also are related to the dacitic-andesitic rocks.

On the lowest slopes of the range, various volcanic breccias, tuffs, tuffaceous sediments, perlitic domes and rare welded tuffs occur which compositionally appear to be related to the above rocks. These were deposited on a relatively smooth erosion surface which, if extended to the west, would pass roughly a mile above the top of the stock (Hunt and Mabey, 1966). Since petrologic work on the stock has indicated that it was emplaced roughly 7500 feet below the ground surface, this suggests that the above erosion surface, and the ground surface above the stock at the time of emplacement, could be the same. The volcanics have been tilted to the east from their presumed original

position by 15-20 degrees (Hunt and Mabey, 1966).

Probe work on the dacitic-andesitic rocks indicates that the plagioclases crystallized at significantly lower water pressures throughout most of their crystallization history than did the plagioclases of the stock, and the zoning indicates quite a different sequence of events during that crystallization history. On this basis, the andesitic and dacitic rocks were not derived from the stock magma directly. It is possible that these rocks represent magma that was untimately derived from the same source as the stock magma, but which underwent a considerable degree of contamination to produce the more basic compositions.

## Summary Structural History

Before summarizing the structural intrusive history of the stock, it would be well to preview some of the results of the detailed petrologic studies in the latter part of the thesis. Based on the feldspar phase relationships, the stock at the present level of exposures is estimated to have been at a total pressure of 0.7Kb., or a depth of roughly 7500 feet below the surface. The coexisting feldspar phenocrysts crystallized at pressures of roughly 1.3 and 2.0Kb., or at depths of roughly 13,000 and 20,000 feet, respectively. The assimilation stage, noted briefly above in the discussion of the room problem, occurred immediately after this coexisting feldspar stage, and extensive devolatilization of the system occurred in the interval between the assimilation stage, and groundmass formation at the present exposure level.

Based on the structural evidence, the westward dipping faults to the north of the stock, and the dike swarm, formed roughly 5000 feet below the present outcrop level. Combining this with the above data, fracturing and dike formation took place when the stock magma was roughly 12,000 feet below the surface at the time of emplacement of the stock.

On the basis of the preceding discussion, the following outline of the structural emplacement history of the stock may be given.

The first effect of the stock's magma on the development of structures in the mapped area was to form the roughly north-south striking set of westward dipping normal faults that are now found to the north of the stock. These faults formed as a result of the stretching of the sediments over the top of the magma chamber, and at this point, the magma was roughly 12,000 feet below the surface. This event occurred shortly after the period of coexisting feldspar development in the magma, which took place at a depth of 13,000 to 20,000 feet for various parts of the stock. Immediately before the faults were formed, but after the coexisting feldspar stage, the contaminated early igneous phase had developed and the magma had undergone a stage of assimilation of carbonate-rich rocks. This most probably occurred in the basal members of the Pahrump Series, immediately above the dominantly granitic earlier Precambrian basement rocks, at a depth of 12,000 feet or less.

The dike swarm was then formed, using the tension faults over the roof of the magma chamber as a means of exit, and the devolatilization

of the magma and further upward magma movement was initiated. While the magma moved upward, extensive reaction of the feldspars took place in the volitile-rich environment.

The first portion of the stock to reach its present level was the southern phase of the stock, which along with the northern phase formed the trapdoor and domed the sediments over the top of the magma chamber. At this point, the northern phase was just below its present level of outcrop. The sediments adjacent to the stock were dragged upward and simultaneously thinned, and much of the doming related to the stock emplacement occurred at this time. Renewed movement took place on the faults south of the stock.

The northern phase then moved up to its present level, truncating the dike swarm, forming the thrust fault, and finally forming the tear fault and reversing the sense of motion along the east side of the trapdoor north of the tear fault. At this point, the bulk of the stock was approximately 7500 feet below the ground surface.

The magma can reliably be located in two positions, one 12,000 - 13,000 feet below the ground surface, and the other 7500 feet below the ground surface. The latter is now represented as the stock at the present level of erosion. The source of the stock appears to be an east-west zone directly below the contact of the present north and south phases of the stock, in Starvation Canyon. This suggests that the stock necks downward in form, and changes from an elongate north-west body at the present levels to a very thin elongate east-west feeder body at depth.

The presence of inclusions of only the early igneous phase of the stock, and their distribution, indicates that as the magma passed through this feeder, the only rock it was in contact with was the early igneous phase of the stock. This phase is probably the outer contaminated margin of a magma chamber at a depth of roughly 12,000 feet and probably was formed when the magma first reached this level. Eventually the roof was fractured, forming the westward dipping faults and the dike swarm as the magma moved upward.

The granite seen at the present level of erosion was probably part of the magma that was present in the center of this deeper magma chamber. This magma broke through the contaminated contact phase which made the roof of the magma chamber, incorporated numerous inclusions, and moved upward to the present erosion level through the east-west feeder zone. This requires that the form of the stock mapped be such that it changes from the north-south to the east-west elongation at some level shallower than 12,000 feet below the original ground surface, or roughly 5000 feet below the present ground surface.

# II. PETROLOGY AND PETROGENESIS

## INTRODUCTION

The following portion of the thesis is devoted to the petrology and petrogenesis of the Little Chief stock and associated rocks. Emphasis is placed on the variations in composition within individual feldspar phenocrysts, using microprobe chemical analyses, and a correlation of these compositions with textures in various parts of the stock. These data are then used to reconstruct in as much detail as possible the crystallization history of the stock, the mechanisms by which certain textures were produced, and the physical conditions that prevailed during the crystallization sequence.

A general outline of the way in which this study was carried out is given in the following paragraph. Initially, the area was mapped in some detail with emphasis on structural relationships of the stock, and variations within the stock itself. Numerous samples were collected from the various mapped phases of the stock, (see Fig. 9) and these were examined in thin section in order to work out the general petrology of the stock. Then, on the basis of this extensive optical work, samples were picked that were representative of each of the various features in the stock that were critical to a determination of its intrusive history. These samples were then investigated in detail with the microprobe.

In effect, the sampling procedure was a method whereby an igneous body as large as the stock could be effective reduced to a small number of samples that could, with the time available, be investigated using the microprobe. This is necessary because the microprobe is an instrument with which it is only possible to investigate an exceedingly small area, and hence much effort must be put forth to bridge the gap between miles and microns. With regard to the igneous petrology of large intrusive masses, this problem of scale is the most serious drawback of the microprobe.

In the light of the problems just discussed, the major section of the thesis on the petrography and petrology of the stock has been

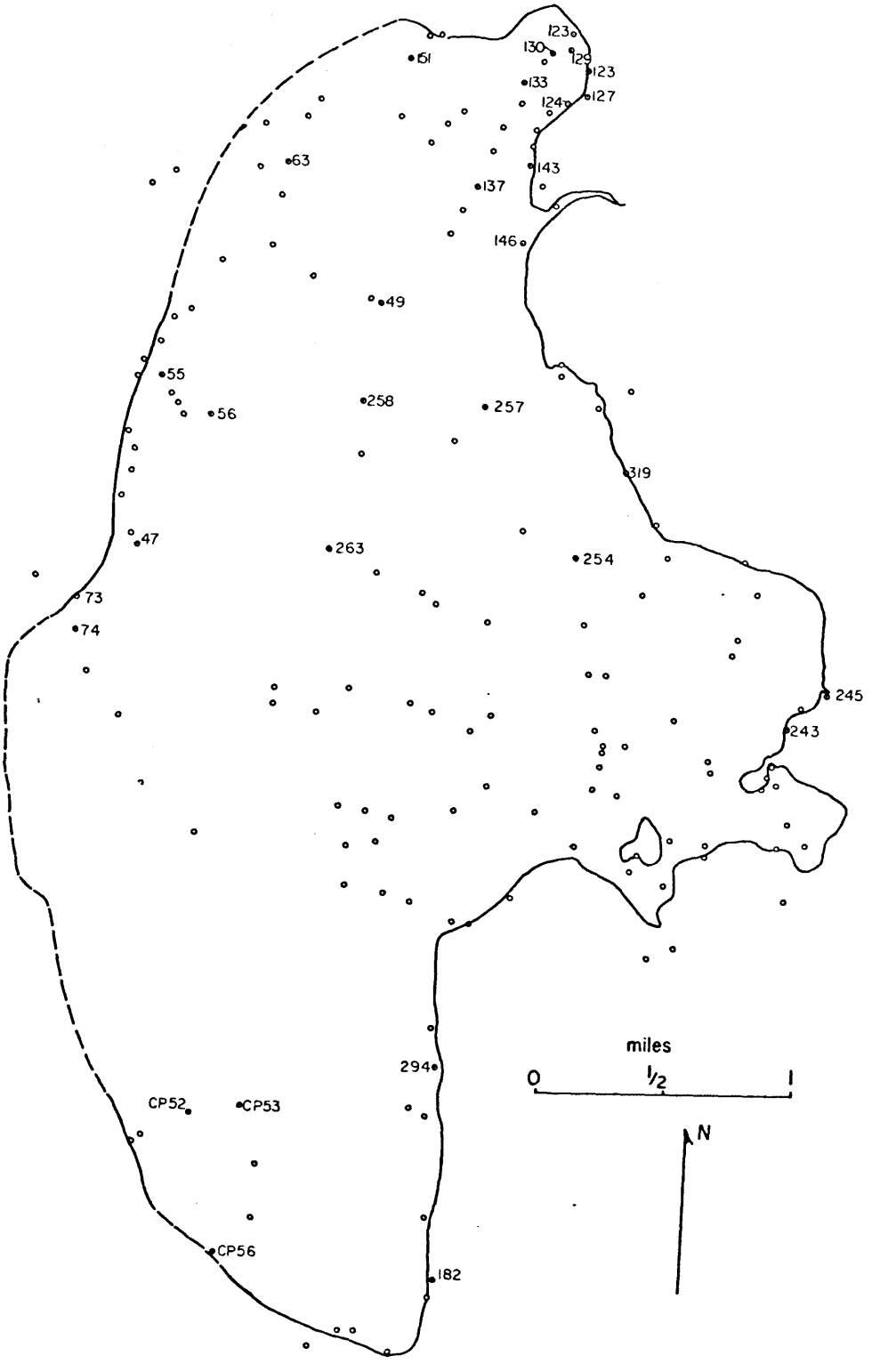


Fig. 9. Location of samples collected from stock. Samples referred to in text are numbered.

arranged in the following way. After a brief introduction in which the general petrography of the various portions of the stock is discussed, several specimens will be discussed in great detail, and their features correlated with microprobe analysis. Each specimen was picked as being representative of a certain area, or feature, in the stock, and hence while the discussions that follow will constantly refer to one specimen, it is to be understood that a larger feature is being referred to. After the various specimens of the stock and dike rocks have been described in detail, an attempt will be made to discuss the variations, in the light of optical studies, that occur relative to the reference specimens. Finally, the petrogenesis of the stock and its associated features will be discussed.

Throughout the section on the detailed description of the various reference specimens, numerous compositions will be noted, either in the text or graphically or both. Each of these compositions is the result of many probe analyses of a specific feature or area, and hence represents a true chemical analysis. As a rule, as for instance in the case where many individual lamellae of a perthitic feldspar were chemically analysed with the probe, each stated or graphed composition is effectively the averaged result of a great many chemical analyses of a given feature. This is, in effect, a new concept in petrology, since previously one chemical analysis required considerable effort in terms of time and money. The probe is, by contrast, capable of producing incredible amounts of accurate chemical information. Thus the problem of chemical analysis of minerals is completely inverted. With the probe, the problem becomes one of assimilating, correlating, and generally making sense out of very large amounts of accurate data. Because of this fact, much reliance has been placed on graphical presentations which average many probe scans on many grains. It becomes a necessary evil, as it were, that all compositions reported in a study like this must have undergone considerable sifting and averaging before they are in a form that can be assimilated by anyone who wishes to benefit from the work.

Several actual data scans are shown in Appendix B, and the

methods of averaging and compiling the data are briefly outlined.

## PETROLOGY OF THE LITTLE CHIEF STOCK

The intrusive Little Chief hornblende-biotite granite porphyry stock may be divided on the basis of field work into two intrusive phases. (Plate 1) The northern intrusive phase occupies the northern two-thirds of the stock from Starvation Canyon to Hanaupah Canyon, an area of some 8 square miles, and may in turn be subdivided into an exterior portion and an interior portion. The southern intrusive phase of the stock, which crops out in southern Starvation Canyon over an area of some 4 square miles, is clearly earlier than the northern phase. Two granite porphry dike swarms, a major one in the Hanaupah Canyon area and a minor one in the Starvation Canyon area, are related to the stock. The stock, along 75 per cent of its contacts, is surrounded by a sheath of granite porphyry dike-like rock which separates the stock granite from the wall rock.

The major intrusive phases of the stock consist of 2-10 mm phenocrysts of sanidine and plagioclase in an 0.1-0.8 mm groundmass consisting of quartz, alkali feldspar and some plagioclase. Minor minerals include hornblende, biotite, magnetite, sphene and apatite. The phenocrysts make up 30-50 per cent by volume of the granite.

The plagioclase phenocrysts are always grossly normally zoned, and usually show three broad zones in normal succession with minor abrupt irregularities in zoning at the outer edges of the phenocrysts. They contain interior calcic cores which show evidence of embayment. While the calcic cores are albite-twinned, the outer sodic zones are untwinned so that optical compositional determination is made very difficult.

Plagioclase commonly forms glomeroporphyritic aggregates which are associated with hornblende and biotite crystals. Again the more calcic cores show evidence of embayment.

The sanidine phenocrysts vary in texture throughout the stock, and a brief outline of the varous textures will be given below. In the simplest case, clear rounded sanidine cores are rimmed by wide,

clear sodic plagioclase rims. These, along with the plagioclase phenocrysts, commonly have very thin outer alkali feldspar rims. This type of sanidine phenocryst is typical of the interior portion of the north phase.

In many areas of the stock, the outer portions of the sanidine are rimmed by cloudy, quartz-bearing sodic plagioclase. In other areas, this cloudy, quartz-bearing plagioclase appears to have extensively replaced the sanidine, almost completely in some cases, and the sanidine itself is patch perthitic. All gradations are observed between the two types just described. The former type is characteristic of the south phase of the stock, while the latter is characteristic of the exterior portion of the north phase.

The sanidine megaphenocrysts commonly show regular oscillatory zoning, and on their outer edges, show the same types of textures observed in the sanidine phenocrysts of the rock in question.

The groundmass consists of quartz and alkali feldspar, and variable amounts of plagioclase, along with the minor minerals. Quartz usually makes up 30-45 per cent of the groundmass, and in most cases the remainder is dominantly alkali feldspar. The most common groundmass texture is a typical granitoid texture, but in much of the southern phase of the stock, and near the outer contact of the northern phase, aplitic textures are observed. In the contact phase rocks and volatile-rich areas, the groundmass becomes distinctly micropegmatitic with vermicular to graphic quartz-alkali feldspar intergrowths. In these areas, radial quartz-alkali feldspar intergrowths typical of granophyric rocks are noted, and the groundmass tends to be coarser.

Vugs are lined with euhedral quartz and albite-rimmed sanidine, and in the intercrystal areas, or in some cases the entire vug, a filler of cristobalite has formed.

In gross aspect, the southern phase of the stock is a uniform medium gray color, with very little variation even when contacts are approached. The sanidine and plagioclase phenocrysts have a restricted size range, from 2 to 5 mm, and tend to be very evenly distributed throughout any given hand specimen. The few megaphenocrysts that do

occur range in size up to 15 mm and usually consist of a single alkali feldspar phenocrysts which may or may not have thin outer plagioclase rims, depending on the type of textures present in the normal phenocrysts of that particular specimen. Plagioclase aggregates may reach 10 mm in maximum dimension on rare occasions. The plagioclase, either as rims or phenocrysts, stands out as white material against the smoky gray translucent sanidine or the gray groundmass. The mafic crystals are small, usually less than 1 mm in size.

The northern phase of the stock, in gross aspect, is much more variable than the southern phase, and can be itself subdivided into two portions on the basis of hand specimen examination. The interior portion of the northern phase is white to very light gray in color and consists of phenocrysts which range in size from less than 2 mm to 10 mm set in a very light gray groundmass. The white color of the rock is mainly due to the presence of wide plagioclase rims and numerous plagioclase phenocrysts. Megaphenocrysts consisting of plagioclase aggregates and single sanidine crystals are as large as 20 mm and are quite numerous in this portion of the northern phase of the stock. The sanidine tends to be an opaque white or light gray color, much lighter in color than that of the southern phase of the stock. The mafic minerals make up 7-10 per cent of the rock and are as large as 6 mm. Of the mafic minerals, hornblende is always the coarsest and makes up almost half of the mafic minerals, while biotite, magnetite and sphene, in that order, make up the rest of the mafic minerals.

The exterior portion of the northern phase of the stock appears very similar to the bulk of the southern phase on hand specimen examination, with a few significant differences. The color ranges from light to medium pinkish-gray, while the southern phase has no hint of pinkish color. The phenocrysts are generally less than 7 mm in size, and range downwards to 1 mm or less. Rare megaphenocrysts up to 15 mm are seen. The mafic minerals make up less than 5 per cent of the rock and are always less than 1 mm in size.

Along some areas of the contact of the northern phase of the stock with the wall rock, a contact phase occurs which grades into normal granite porphyry. The major change in the contact phase is a general coarsening of the groundmass until it no longer can be differentiated from the phenocrysts, coupled with extensive development of very coarse lamellar perthite in the alkali feldspar crystals.

The contact between the interior and exterior portions of the north phase of the stock indicates that the interior portion was intruded into the exterior portion while both portions had significant amounts of melt present, as no chilling effects were noted, and the contact ranges from sharp to transitional over a distance of 100 feet. The groundmass is identical in the two portions across the contact. This supports the concept of the "effective" immiscibility of two viscous crystal-rich silicate magma pulses, which allowed only slight amounts of mixing along the contact between the pulses.

The contact between the north and south phases of the stock, where it is not completely obliterated by a zone of intense alteration, is sharp, and the northern phase has chilled against the southern phase, indicating a relatively long time gap between the intrusive phases.

The dike rocks, and the dike sheath rocks, are very similar in appearance and consist of dense, very fine-grained white or light gray rocks, with spherulites and regular gray laminations similar to the flow banding in the dike rocks, in which scattered white alkali feldspar phenocrysts occur. Most of the dike sheath rocks are later than the granite, but in a few cases, the dike sheath rocks are transitional into the normal granites. Similarly, the dike rocks are cut by the dike sheath rocks in some cases, and grade into them in other cases.

Vugs are scattered throughout all the phases of the stock, but they are seldom over 5 mm in size and usually make up less than 2 per cent by volume of the rock. However, in the northeastern portion of the north phase of the stock, an area with 10-15 volume per cent vugs, and associated pegmatitic pods, aplitic and

graphic-textured areas, and very coarsely perthitic alkali feldspar, is found, immediately adjacent to the major dike swarm in Hanaupah Canyon.

## Resorbtion-Rimming Sequence-Specimen DV56

The first specimen to be described in detail, DV56 is representative of the interior portion of the north phase of the stock. It was collected near the western edge of the north phase of the stock, as shown in Fig. 9. The relationships among the feldspars is simple, as the rock contains zoned plagioclase phenocrysts and sanidine phenocrysts which have clear oligoclase rims. Very thin alkali feldspar rims occur on both the plagioclase and oligoclase rimmed sanidine phenocrysts. The groundmass consists of a microgranitic mosaic of less than 0.5 mm grains of alkali feldspar and quartz, with hornblende and biotite microphenocrysts and smaller crystals of magnetite, sphene and apatite. The mode and simple calculated norm of the rock, and the groundmass, are listed in Appendix A.

### Plagioclase Phenocrysts

The plagioclase phenocrysts of DV56 range in size from 1 to 10 mm, and as a rule the smaller phenocrysts tend to be euhedral while the larger ones are subhedral, with rounded corners and smooth edges. The plagioclase is invariably zoned, with calcic cores which have well developed albite twinning, intermediate-plagioclase zones, and outer sodic zones. The albite twinning dies out in the intermediate plagioclase zones, and is rarely present in the more sodic outer plagioclase. The calcic plagioclase cores are often slightly altered to a fine-grained micaceous mineral.

Figure 10b shows the results of microprobe scans of the plagioclase phenocrysts of DV56; it is a composite diagram using data scans from six different phenocrysts. This diagram will be discussed in some detail in order to develop some of the terminology that will be used throughout the thesis, since the features seen in the plagioclase phenocrysts here are the same as those seen in all other

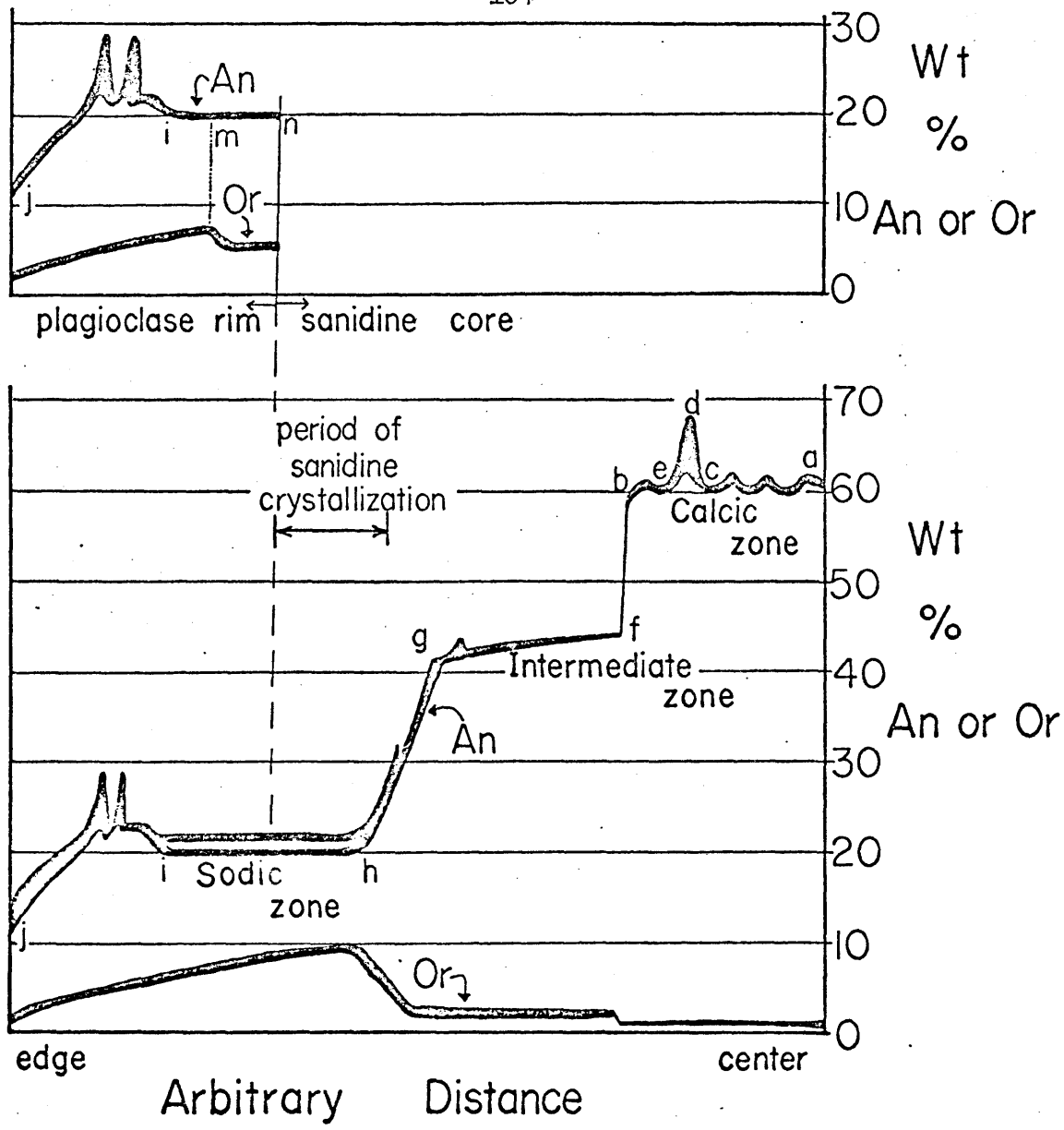


Fig. 10. Composite plagioclase probe scans across plagioclase rims on sanidine phenocrysts(upper profile), and across plagioclase phenocrysts(lower profile), in weight percent Or and An. DV56.

specimens in the stock.

The overall pattern in Fig. 10b is one of three broad zones, the calcic, intermediate, and sodic or oligoclase zones, which are progressively more Ab-rich toward the outer parts of the phenocrysts. The breaks or gaps in zoning between these broad zones differ, and this specimen shows the two common types observed throughout the stock. One is very abrupt (b to f), while the other is transitional (g to h) so that plagioclase of compositions between those of the intermediate and sodic zones is found. This latter type is very informative regarding the mechanismswhich were responsible for the breaks in zoning.

The calcic zones commonly show oscillatory zoning, as noted in Fig. 10b (a to b), while the intermediate (f to g) and sodic (h to j) zones have very little variation in percentage within the broad zones. In many cases, especially in the sodic zones of the plagioclase phenocrysts, however, strong oscillations in zoning occur. For purposes of illustration, the strong oscillation in the calcic zone will be used. Here, the plagioclase composition abruptly increases in percentage from the general composition of the broad zone (c) to a high percentage (d) and then just as rapidly decreases to the general composition of the calcic zone (e). To avoid confusion with the normal magmatic oscillatory zoning, which has a much lower variation in An percentage these large oscillations will be termed reversals, and this term will be taken to include both the increase and decrease in An percentage. The most prominant, well developed and continuous reversals in most cases are those located in the outer parts of the sodic zone.

The sodic zone, when necessary, will be divided into two sections. The broad inner portion (h to i) will be referred to as the stable oligoclase portion because of the lack of variation in An percentage, while the outer portion will be referred to as the unstable oligoclase portion due to the large variations in An percentage. The outer reversals, such as the two shown in Fig. 10b, always occur on this outer portion of the oligoclase or sodic zone.

The thickness of the lines in Fig. 10b roughly represents the amount of scatter in the data that was averaged to give the composite scan shown; thus the greater thickness near j indicates greater variability than, for instance, the intermediate zone compositions between f and g in the figure. Finally, an arbitrary distance scale has been used because of the problem of orientation of the phenocrysts. The zone widths shown are based on optical study and hence are all relatively correct except for the outer unstable oligoclase portion, which has intentionally been slightly extended to show the details better.

A summary of the compositions of the plagioclase phenocryst zones from DV56 is as follows: (see Fig. 11) the calcic zone of the core of the phenocrysts oscillates regularly in composition between $Or_{1.5}Ab_{38-39}An_{59-60}$ and $Or_{1.5}Ab_{35-36}An_{62-63}$, and contains one large reversal near the outer edge of the zone which reaches $Or_1Ab_{31}An_{68}$ in composition. The intermediate zone is simple, and shows slight normal zoning. Its composition is $Or_{2-2.5}Ab_{54-57}An_{41-44}$, and in some cases, very small reversals are noted at the outer edge of the zone or in the transitional region to the sodic zone.

The sodic zone, in the stable portion, zones steadily from $Or_{9.5}$ to $Or_{6.5}$ in all grains analyzed, while two An percentages occur; $An_{19-21}$ and $An_{22-24}$. The latter of the two An percentages is the more common and is the same as the oligoclase rim compositions. In the unstable oligoclase region, while the Or percentage steadily decreases from $Or_{6.5}$ to $Or_2$, the An percentage increases from $An_{19-21}$ in most cases to $An_{23-24}$ and then rapidly drops off to $An_{11-12}$. This is best illustrated in Fig. 11, which shows the same compositional data plotted in the Or-Ab-An system. The reversals in the unstable oligoclase portion are especially prominant and commonly occur in pairs.

Rimmed Sanidine Phenocrysts

The rimmed sanidine phenocrysts range in size from 4 to 10 mm and are euhedral to subhedral in shape. The clear very faintly albite-twinned oligoclase rims are 0.5 to 1 mm in width, and are

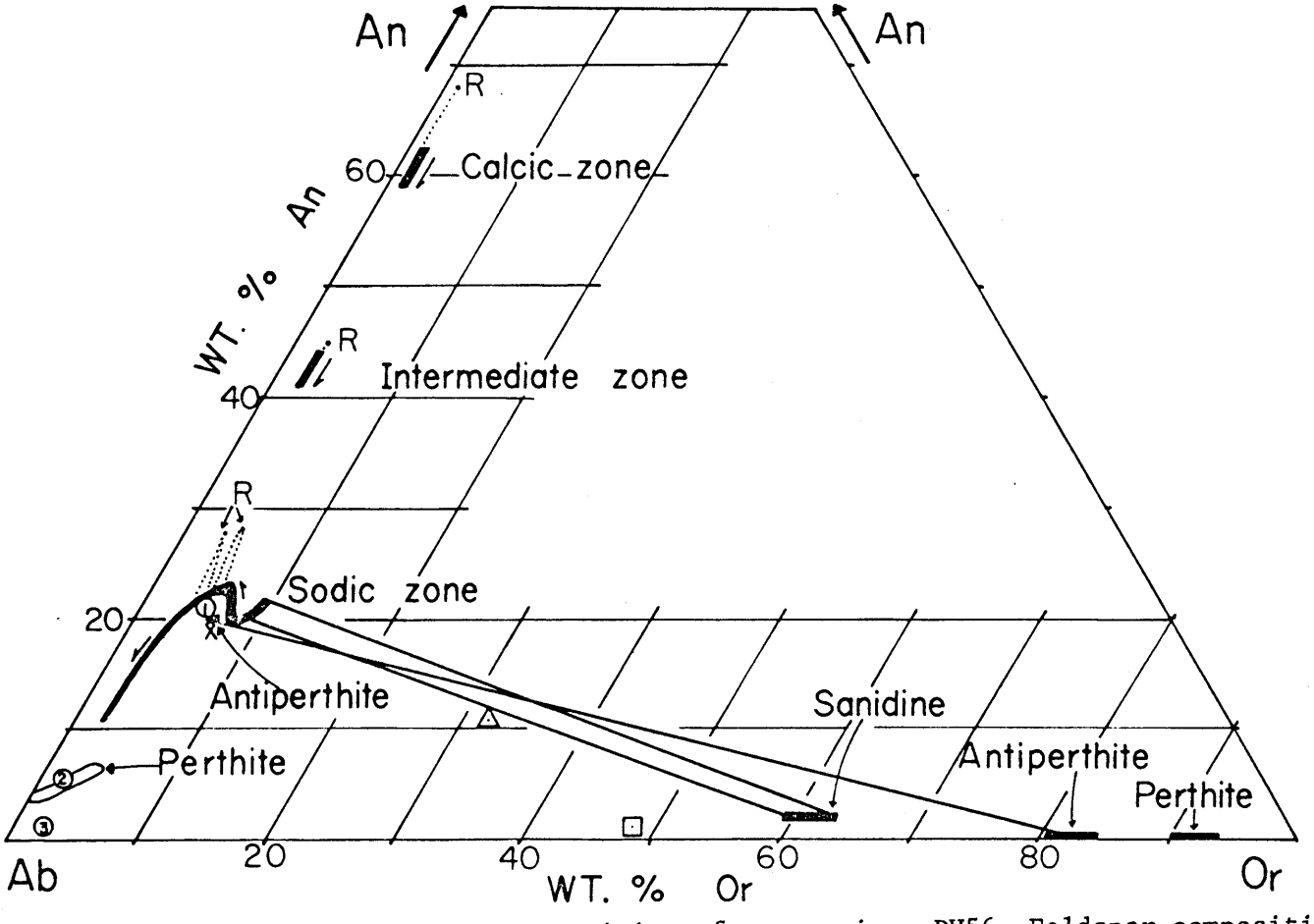


Fig. 11. Summary diagram of feldspar compositions from specimen DV56. Feldspar compositions shown by solid or open areas. Tie lines connecting coexisting sanidine and plagioclase, or coexisting antiperthite phases, shown by heavy solid lines. R=most calcic composition on reversals. Arrows show compositional change in direction of outer edge of phenocrysts. Triangle=calculated bulk rock composition. Square=calculated groundmass composition. All compositions in weight percent. Circled numbers indicate peristerite compositions.

present on almost all the sanidine phenocrysts. The rims tend to be thickest at the ends of the slightly elongate phenocrysts. A typical rimmed sanidine phenocryst is shown in Fig. 12a.

While the outer edge of the phenocrysts, defined by the oligoclase rim, is usually euhedral, the sanidine core-oligoclase rim contact tends to be quite irregular in detail, and in overall shape to be rounded and anhedral. The gross form of the core is much like that of the outer phenocryst outline except that the sharp corners are rounded off and the contact made much more irregular.

Figure 10a shows the results of microprobe scans across the oligoclase rims of three such phenocrysts. The reversals at the outer edge of the rim were present in all phenocrysts examined, and are visible continuously around the entire phenocryst. In most cases two reversals were noted, but in a few cases only one reversal was present.

The An percentage of the stable portion of the oligoclase rim- from i to n in Fig. 10a- is exactly the same as that in the majority of the plagioclase phenocrysts; namely, $An_{19-21}$. In fact, in the outer one-third to two-thirds of the rims, the Or percentage is also as expected for the outer part of the stable oligoclase zone. But in the inner one-third to two-thirds of the oligoclase rims, the Or percentage is relatively low and is in the range $Or_{5-7}$. The composition of the unstable portion of the oligoclase rim is exactly the same as that same portion on the plagioclase phenocrysts. Thus it appears that, except for the inner portion of the oligoclase rims, the oligoclase rim compositions duplicate the oligoclase zone compositions on the plagioclase phenocrysts, and both were formed in the same manner at the same time.

In all cases minute optically oriented patches of K-feldspar, less than 50 microns in maximum dimension, occur in association with the relatively Or-poor oligoclase of the inner portion of the rims. The composition of this K-feldspar is $Or_{80-85}Ab_{15-20}An_{<0.3}$, and it makes up, by volume, roughly 2 per cent of the inner, Or-poor portion of the rim in which it occurs. In the light of the similarity in

composition of the rest of the rims and the sodic plagioclase zones, it is likely that the Or percentage of this inner portion of the rims was once higher, and has been decreased due to the concentration of the Or-component in an antiperthitic K-phase which now makes up the K-feldspar patches. A rough calculation as to the amount of the K-feldspar expected by starting with oligoclase with 8-9 percent Or and ending with oligoclase with 5-7 percent, (X, Fig. 11) Or, yields roughly 2 per cent which is the amount of K-feldspar actually observed.

The sanidine cores are clear and, relative to most other areas in the stock, have a minimum amount of clouded or turbid areas within the feldspar. The approximately 15 per cent of the sanidine that is clouded tends to concentrate in several areas: along the contact plane of the carlsbad twins, around inclusions in the sanidine core, along fractures, and at parts of the outermost edges of the sanidine core. Under high magnification, these clouded areas appear as minute, hairlike, brown-stained aggregates in parallel orientation, and probe analysis indicates that it consists of an exceedingly fine-grained lamellar perthitic intergrowth in which the individual perthitic lamellae are seldom greater than 2 microns in width.

The sanidine cores, in this specimen, are unzoned, and consist of alkali feldspar of composition $Or_{60-64}Ab_{35-39}An_{1-1.5}$. In detail, small areas differ in composition slightly more than the analytic error. Thus one 100 micron scan may have values ranging from $Or_{61-63}$, while another similar scan may range from $Or_{62-64}$. There is no logical pattern to these variations, but the fact that all sanidines that were X-rayed indicate strong cryptoperthitic intergrowths are present may indicate that this variation is related to perthite formation.

The sanidine phenocrysts show three types of "included" plagioclase. The first are true inclusions of albite-twinned plagioclase grains with euhedral shapes, sharp boundries, and an orientation within the sanidine core such that the long direction is commonly parallel to the nearest edge of the phenocryst. The

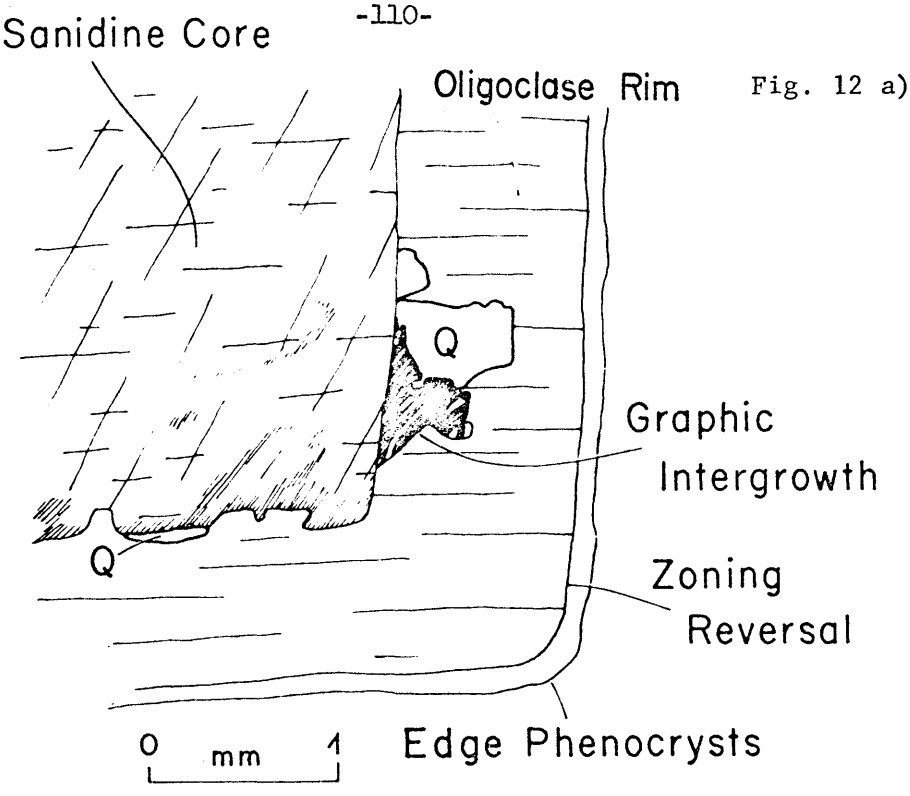


Fig. 12 a)

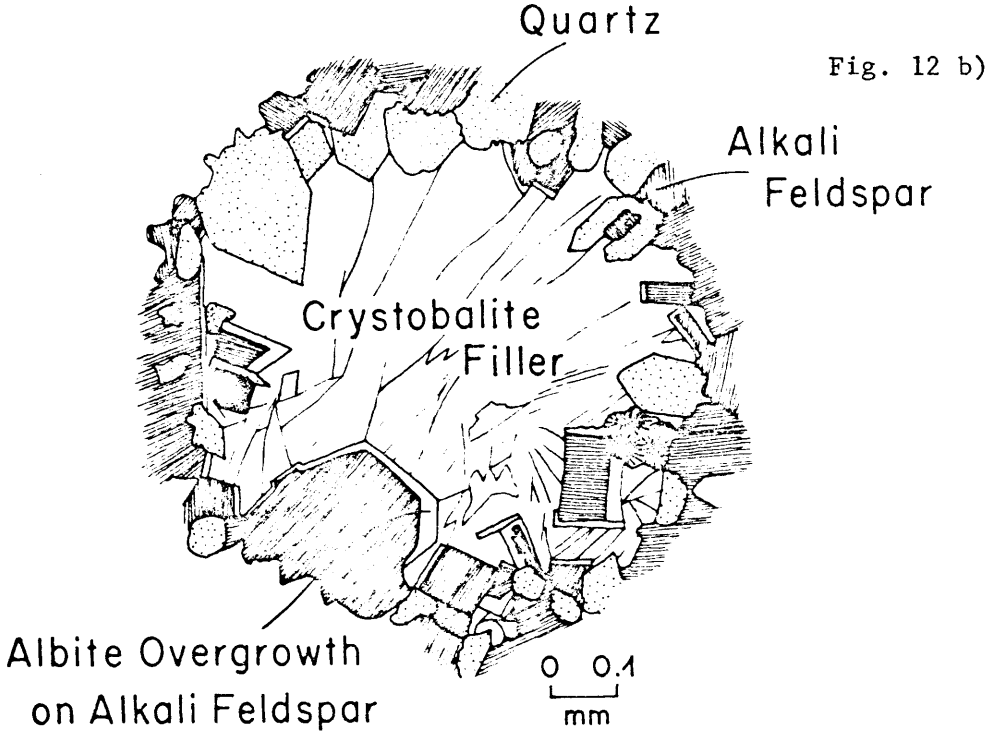


Fig. 12 b)

Fig. 12. a) Sketch showing replacement of oligoclase rim by graphic groundmass quartz and alkali feldspar.
b) Sketch of filled vug. Sanidine-shaded, quartz-speckled, cristobalite-jagged pattern, albite overgrowths-clear. Vug from specimen DV49.

composition of these grains is consistently $Or_{5-6}Ab_{74-75}An_{20-21}$. They are located anywhere within the sanidine core, and can occur well away from any other areas of "included" plagioclase. These are felt to be true inclusions of plagioclase crystals incorporated within the rapidly growing sanidine crystals.

The second type of plagioclase that occurs within the sanidine has the same composition as the above, but it is invariably of much more irregular shape, has in detail a much more irregular contact with the sanidine, is present only in the outer portion of the sanidine core, and is oriented in such a way that the weakly developed twinning is parallel to that present in the plagioclase rim. Indeed, in some cases, these patches are continuous with the rim plagioclase. These patches are probably due to resorption of the outer portions of the sanidine core. This is supported by the rounded shape of the sanidine core and its irregular contact in detail with the plagioclase rim, as noted above.

Finally, the third type of plagioclase "inclusion" in the sanidine core takes the form of very small (less than 100 microns) irregularly shaped, untwinned patches with very diffuse boundries and which are invariably surrounded by clouded sanidine. The composition of these patches is $Or_{0.5-1}Ab_{94-95}An_{4-5.5}$. Their form and composition suggests a patch perthite development. One patch of this type, on examination with the probe, was found to be completely ringed by a 20 micron thick band of feldspar of composition $Or_{90-94}Ab_{6-10}An_{0.2}$ --probably the corresponding K-phase of the patch perthitic albite.

In summary, there are three identifiable plagioclase phases associated with the sanidine phenocrysts--an included oligoclase, an oligoclase which crystallized after sieve-textured resorption features were formed in the outer edges of the sanidine phenocrysts, and an albitic patch perthitic phase. The timing of the first two is relatively well fixed, and the suggested timing of the patch perthitic phase will become clear in the discussions of later specimens with different plagioclase rimming relationships.

Quartz Distribution

The composition of the groundmass feldspars is shown in Fig. 11 by the square. This groundmass composition is roughly that of all the specimens examined in the main portion of the stock. This feldspar, as was noted before, is almost always perthitic and feldspar compositions were obtained using the moving spot technique to obtain bulk grain compositions. The very thin alkali rims on all the phenocrysts have the same composition as the groundmass alkali feldspar.

The distribution of quartz in specimen DV56 indicates that it began to crystallize late in the crystallization sequence. Quartz crystallized as a definite part of the groundmass, and apparently did not crystallize before this time. All quartz grains or aggregates of grains which occur within the phenocrysts, as for instance along rim-core contacts, or along grain boundaries in glomeroporphyritic aggregates, appear to have been formed at the same time as the groundmass and hence represent replacement or filling of cavities in the phenocrysts due to resorption. Fig. 12a shows a sketch of a particularly informative relationship. Here a quartz grain and an associated patch of graphically intergrown quartz and feldspar, occur wholly within the oligoclase rim in a sanidine phenocryst, along the rim-core contact. The presence of the graphic intergrowth, which occurs only in the groundmass stage of crystallization, suggest that this quartz and graphic patch formed by replacement at the time of groundmass crystallization.

Many of the sanidine phenocrysts contain very small, worm-like quartz blebs which tend to concentrate in imperfections within the sanidine core, such as along fractures or along the carlsbad twin composition plane. In a majority of cases seen, these quartz blebs are intimately associated with small patches of perthite, and in some cases with subgraphic K-phase-quartz intergrowths.

Vugs

The drusy cavities which occur in specimen DV56 tend to be small, usually with a maximum dimension of less than 2 mm. The mineralogy in thin section of the vugs is the same as in other specimens and hence this description will serve as a general description of the vugs of the stock. Fig. 12b shows a sketch of a vug. The bladed, carlsbad twinned sanidine phenocrysts, which may or may not be visibly perthite, have a very thin rim of almost pure albite along parts of the edges adjacent to the cavity. The ends of the blades are commonly corroded. The quartz crystals which extend into the vugs range from euhedral to slightly rounded in the portion within the void. Both the sanidine and the quartz grains are continuous with typical anhedral groundmass grains away from the vug. Cristobalite occurs as a filler, either filling in the void areas between the euhedral sanidine blades, or filling in the whole cavity. It always shows a very irregular, jagged extinction, and has a 2V ranging from 0 to 25°. Compositionally, the sanidine of the cavities is the same as the groundmass feldspar.

Summary of Crystallization Sequence

Based on the textural relationships of the feldspars along with the compositional data obtained with the probe, the general crystallization sequence of the feldspars in specimen DV56 is as follows. (refer to Fig. 11) Initially, plagioclase of labradoritic composition began to crystallize and formed regular oscillatory zoning throughout its history. Near the end of the period of labradorite crystallization, a distinct reversal was formed, and immediately after this event, an abrupt change in conditions occured and the labradorite was briefly resorbed by the melt. Andesine then crystallized, and formed a zone around the labradorite cores, with a small reversal at the outer edge. Again conditions changed such that the andesine was resorbed.

Immediately after the period of andesine resorption, both sanidine and oligoclase crystallized. The sanidine then went out of equilibrium, was briefly embayed in a few cases, and then was immediately rimmed by oligoclase. Throughout this whole period oligoclase crystallized in a stable manner on the plagioclase phenocrysts. This period of stable oligoclase crystallization was followed by a period of unstable oligoclase crystallization, during which time the Or percentage of the oligoclase steadily decreased while the An percentage initially increased and then rapidly decreased to sodic oligoclase compositions. Major reversals were formed during this time. Finally, conditions changed abruptly, and the alkali feldspar of the thin rims and groundmass crystallized with quartz.

## Patch Perthite Replacement Sequence-- Specimen DV151

The next specimen to be discussed in detail is specimen DV151, located on the north edge of the stock. (Fig. 9) It is representative of both the outer portions of the north phase of the stock, and in terms of feldspar textures is similar to the textures seen throughout all the southern phase of the stock. It consists of alkali feldspar and plagioclase phenocrysts with microphenocrysts of biotite set in a groundmass of quartz, perthitic alkali feldspar, biotite, magnetite, and sphene. The alkali feldspar phenocrysts range in size from 1 to 8 mm and consist of stumpy subhedral laths that grossly preserve a typical sanidine morphology, but tend to have slightly rounded corners. Carlsbad twins are common.

The plagioclase phenocrysts consist of more elongate laths in the size range of 0.5 to 5 mm, and tend to form into glomeroporphyroblasts which reach 15 mm in size. The groundmass, which makes up 65 per cent volume of the rock, has a normal granitoid texture except for occasional large quartz patches, and ranges in grain size from 0.2-0.5 mm. The modal volume percentage of biotite, magnetite and sphene is 5 per cent, and the rock contains 0.5-1 per cent drusy cavities.

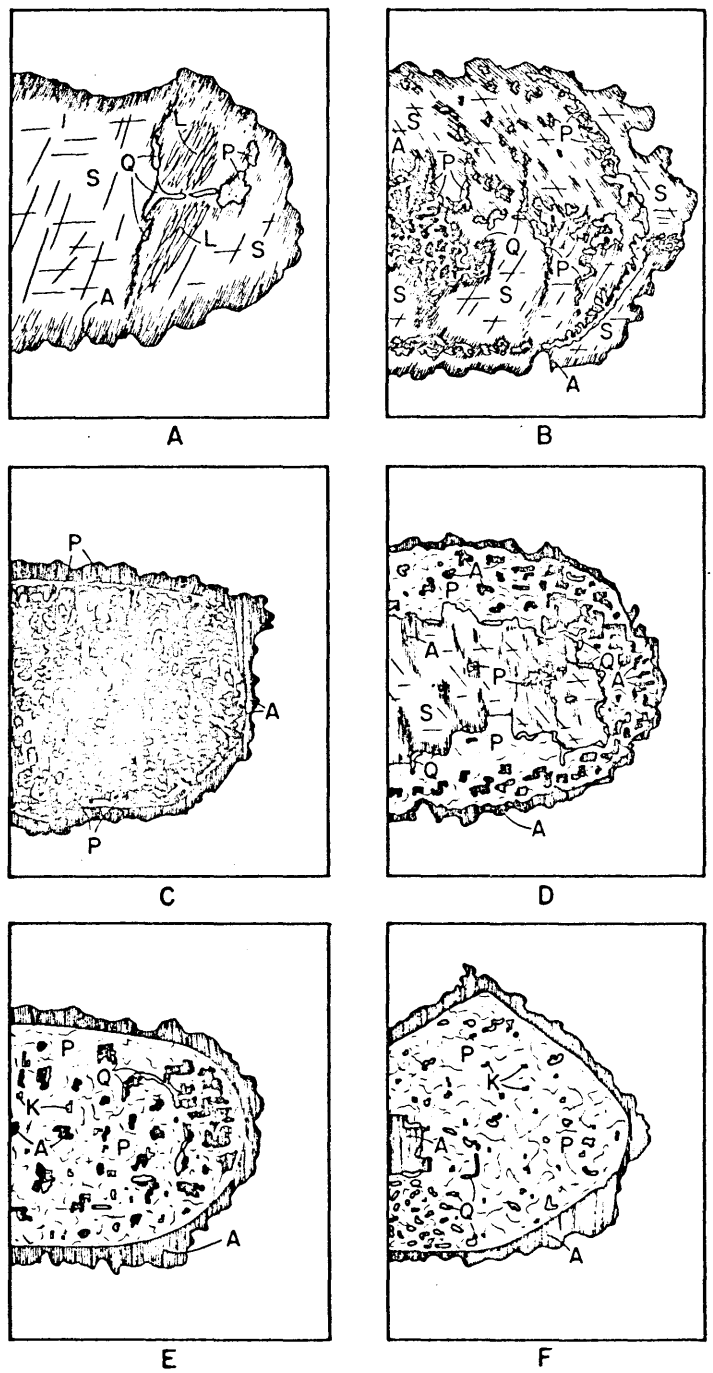


Fig. 13. Sequence of sketches showing different stages in the replacement of the sanidine phenocrysts from specimen DV151. S=sanidine, Q=quartz, L=lamellar perthite, P=sodic plagioclase and patch perthite, A=very finely perthitic alkali feldspar, K=K-rich phase.

Sanidine Phenocrysts

The most important, and striking, difference between this specimen and the one previously described is the internal texture of the alkali feldspar phenocrysts. No clear oligoclase rims exist, and the alkali feldspar phenocrysts consists of various proportions of sanidine, very fine perthite with the same bulk composition as the sanidine, two types of K-rich feldspar, and two types of albite-oligoclase--all intimately associated and intermixed to create very complex textures on various scales. In fact, the proportions of these various phases change in such a manner that, speaking in terms of bulk phenocryst compositions, there is a complete transition in compositions from the sanidine of roughly $Or_{50}Ab_{50}$ composition to albite-oligoclase of composition in the range $Ab_{92\text{-}85}An_{8\text{-}15}$.

This range in bulk composition is interpreted as being due to the progressive replacement of sanidine by sodic plagioclase. To illustrate this replacement series, six typical alkali feldspar phenocryst textures have been illustrated in Fig. 13, and this figure will be used as a basis for the following textural and compositional descriptions.

Figures 13a and 13b show the initial stages of the replacement sequence. Here, the phenocryst is dominantly sanidine(S), but various parts have been changed to the a very finely lamellar ($\ll$ 1 micron) perthite, shown by the shading. (A). This perthite, which has a bulk composition essentially the same as that of the adjacent sanidine, will be referred to as the cloudy perthite because of its appearance in thin section. Irregular, rounded patches of quartz blebs (Q) and sodic plagioclase patches (P) are associated with, and surrounded by, this cloudy perthite.

As the degree of replacement progresses, the amount of sodic plagioclase patches (P) increases, as shown in Fig. 13b. Note that the plagioclase patches tend to concentrate in a band roughly 0.3 mm inside the outer edge of the phenocryst. When detailed scans are made, a K-rich phase is found which is invariably adjacent to, and often

surrounds, the plagioclase patches. In these initial stages of replacement, however, this K-rich material is seldom greater than 5 microns in width and is very difficult to see optically.

The sanidine itself is compositionally zoned, with a range in composition from $Or_{65}Ab_{34}An_{0.5-1}$ at the center continuously to $Or_{45}Ab_{53}An_{2}$ at the outermost edges. Rarely, large oscillations in the zoning occur superimposed on the normal zoning which appear to change the Ab percentage by roughly 5-10 percent. These oscillations tend to concentrate in the outer third of the phenocrysts, and in several instances, can be shown to have been preferentially replaced by the plagioclase patches and associated K-rich phase, forming the band as noted above.

Occasionally, coarse lamellar perthite (L) is developed in the sanidine, as shown in Fig. 13a. The compositions of the two phases are $Or_{90-95}Ab_{5-10}An_{0.5}$ and $Or_{0.2}Ab_{95-100}An_{0-5}$ (1). Arguements will be made later that this relatively pure perthite is later than most of the textural features in the alkali feldspar phenocrysts.

The intermediate stages of the replacement sequence are shown in Fig. 13c and d. In the case of 13c, there is no sanidine left, and the phenocryst consists of sodic plagioclase patches (P) in cloudy perthite (A). Again, note the concentration of the plagioclase patches in the outer portion of the phenocryst. Fig. 13d illustrates a very commonly occurring texture in which almost the entire outer portion of the phenocryst, inside the outermost thin alkali "rim," has been replaced by the sodic plagioclase, leaving relict rectangular patches of cloudy perthite scattered throughout. The variation in the percentage of the cloudy perthite relict patches shown in the figure is quite common. The quartz blebs tend to concentrate at the edge of the interior relict sanidine core, forming almost a complete ring around the core in many cases.

In the intermediate stages of the replacement sequence, the size of the K-rich phase has increased to a maximum of 50 microns (0.05 mm), and is scattered throughout the sodic plagioclase.

The final stages of the replacement sequence are shown in Fig. 13e and f. By this time, no sanidine is left, and the percentage of

rectangular cloudy perthite patches (A) is small. The K-rich phase (K) ranges in size up to 100 microns (0.1 mm) and is shown in the two sketches as the small clear rectangular patches. Quartz blebs (Q) are scattered throughout the sodic plagioclase, and in some instances, as shown in Fig. 13e, have geometries which suggest that they once were located at the edge of a relict sanidine core that has since been removed. In the extreme case, there is no cloudy perthite left, and the phenocryst, inside the outermost alkali "rim," consists entirely of the sodic plagioclase with scattered patches of K-rich phase and quartz blebs. Commonly, however, there is a small core of cloudy perthite remaining, as shown in Fig. 13f.

It is to be emphasized that all gradations exist between phenocrysts that are essentially unreplaced, like 13a, and phenocrysts that are entirely replaced, like 13f. Moreover, all these textures are present in a single thin section or rock specimen. The sanidine progressively gives way to increasing amounts of the sodic plagioclase.

Replacement Mechanism

The observed range in bulk compositions could have been produced by two mechanisms. The favored mechanism is the progressive replacement of sanidine by plagioclase. However, another mechanism which must be considered is that the range in bulk compositions is original, and is due to phenocrysts which had compositions ranging from sanidine to albite-oligoclase.

The replacement mechanism is favored, firstly, because of the irregular distribution of the sanidine within the phenocrysts, and, in the initial stages at least, the textures illustrated in Fig 13b, c, and d, which support the replacement mechanism. Phenocrysts were seen in which unaltered sanidine occurred in both the outer and inner portions, while other parts of the phenocryst were wholly sodic plagiolcase, cloudy perthite and K-rich phase. In no case did the outer composition of the sanidine exceed $Ab_{55}$ in composition. In cases like these, it is clear that the sanidine made up the whole phenocryst, and no anorthoclase was present.

Secondly, there are two distinct feldspar phenocrysts morphologies, one of elongate laths of the plagioclase phenocrysts with calcic cores, reversals and so on just like the normal magmatic plagioclase of DV56, and the other with the stumpy laths of sanidine and the textures of Fig. 13. The overall shape of all the feldspar phenocrysts of the above replacement sequence is most similar to that of the "unreplaced" sanidine phenocrysts. No form characteristic of the plagioclase phenocrysts were seen in feldspars of this suggested replacement sequence.

The sodic plagioclase of replacement origin has a very distinctive appearance. It has a characteristically mottled extinction and contains or is intimately associated with K-rich phase patches and quartz blebs. Occasionally, very finely-lamellar albite twinning is observed. All the magmatic sodic plagiolcase of the outer zones of the plagioclase phenocrysts, which has roughly the same composition as the replacement plagioclase, is clear, rarely coarsely albite-twinned, and lacks both the K-rich phases and the quartz blebs.

Finally, if indeed Or-rich albitic plagioclases or anorthoclases did exist, by analogy with other reported occurences, the sodic plagioclase of the plagioclase phenocrysts should increase in Or percentage and grade into anorthoclase at the same time that the sanidine zones toward more Ab-rich compositions. However, this has not been observed, and in fact, as in specimen DV56, the plagioclase zones to more Or-poor compositions with no suggestion of antiperthitic textures.

In many of the sanidine or alkali feldspar phenocrysts, rim-like outer bands of plagioclase occur, and several typical examples are shown in Fig. 14. The position of the band is the same as the position of the sodic plagioclase patch concentrations in the outer portions of the phenocrysts, and in a few cases, this band has been observed to pass into these plagioclase patch concentrations. In other cases, the band is abruptly terminated by sanidine and cloudy perthite, and as a general rule, the band tends to pinch and swell.

As shown in Fig. 14, the plagioclase band can occur on

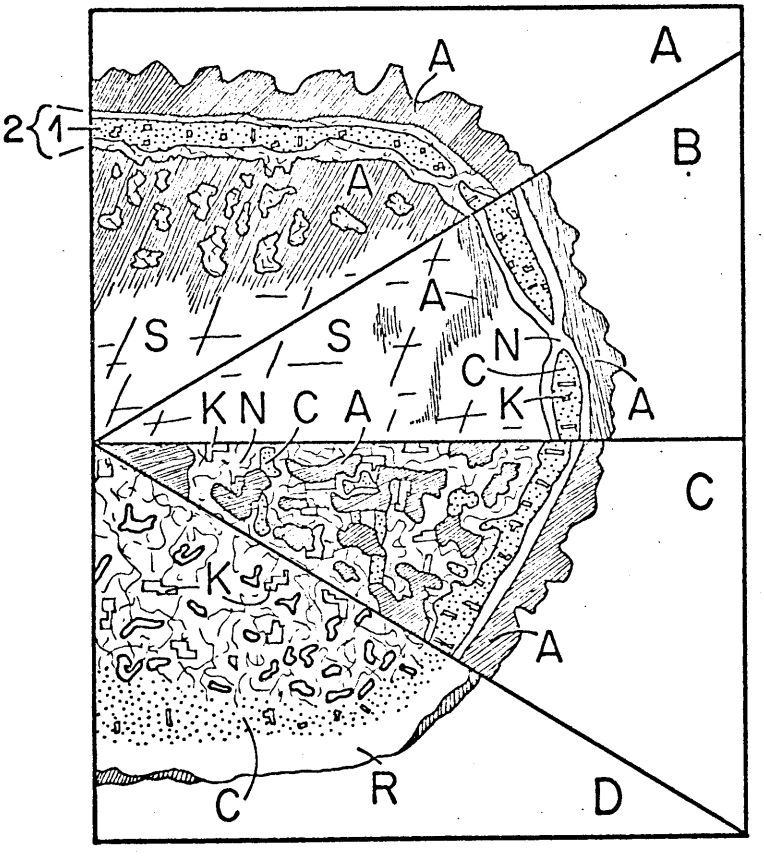


Fig. 14. Four sketches(A, B, C, &D) of the rim-like outer bands of sodic plagioclase in some of the sanidine phenocrysts of specimen DV151. S=sanidine, A=very finely perthitic alkali feldspar, K=K-rich phase, N=more sodic plagioclase($An_{6-10}$), C=more calcic plagioclase ($An_{11-13}$), R=clear outer plagioclase rim.

phenocrysts of any of the stages of the replacement sequence. In a few instances, a clear plagioclase rim (R) occurs outside this band, as shown in Fig. 14d.

The plagioclase band, under crossed nicols, shows evidence of having a slightly more calcic plagioclase (C) in its central portion, and invariably contains elongate K-rich (K) patches which tend to be oriented roughly perpendicular to the margin of the phenocryst. In Fig. 14, this more calcic plagioclase (C) is outlined by the light lines and has been stippled lightly. Probe studies indicate that the composition of this more calcic plagioclase, which occupies most of the band, is $Or_{1-3}Ab_{85-87}An_{11-13}$. If one examines the composition of the plagioclase which occurs in the completely replaced phenocrysts, such as 13e and f, or 14d, one finds that it is uniformly of the same composition as the more calcic plagioclase of the bands noted above, throughout the entire phenocryst.

However probe work on the plagioclase patches which occur in the initial stages of the replacement sequence consistently indicate a composition of $Or_{1-3}Ab_{88-92}An_{6-10}$. This is also the composition of the more sodic plagioclase (N) adjacent to the more calcic plagioclase of the bands, and this slight difference in An percentage accounts for the difference in extinction noted above. Hence, somewhere in the replacement sequence, the plagioclase that originally appears to have partially replaced the sanidine is itself replaced by a more calcic plagioclase.

Fig. 14c shows the $An_{6-10}$ to $An_{11-13}$ change taking place. This phenocryst had an optical orientation such that the extinction difference could be easily seen. It shows that there occur patches of the more calcic plagioclase (C) wholly within the more sodic plagioclase (N) as shown by the small stippled patches in the interior of the phenocryst. K-rich phase (K) patches also occur in the interior and these both appear to have an elongation that is roughly parallel to the (001) cleavage. It is not parallel to the (081) plane found in peristerites. The distribution of these patches of $An_{11-13}$ plagioclase in the $An_{6-10}$ plagioclase suggest progressive replacement of the latter

by the former. This change appears to take place in the intermediate stage of the overall replacement sequence.

The larger K-rich patches associated in the plagioclase replacement, in the interior of the phenocrysts, and the smaller K-rich patches in the more calcic plagioclase of the band, both have compositions in the range $Or_{86-90}Ab_{9-13}An_{0.5}$. The size and orientation differences of these two types of K-rich patches, as shown in Fig. 14c, are so consistant that the location of the band can be seen in Fig. 14d, a wholly replaced phenocryst, even though the entire phenocryst is of the more calcic plagioclase (N) and the extinction difference no longer exists between the two plagioclases. This location has been stippled in the figure.

If the bulk composition of the more calcic $An_{11-13}$ plagioclase (C) portion of the bands in the outer parts of the phenocrysts, or the bulk composition of the wholly replaced phenocrysts is obtained by point counting, one gets a composition of $Or_{4-5}Ab_{82-85}An_{11-13}$. This composition is exactly that of the outermost zone on the plagioclase phenocrysts of this specimen, and suggests that the $An_{11-13}$ bands formed at the time that the outer plagioclase zone was crystallizing. The suggestion is also supported by the formation of these bands on the outer portions of the alkali feldspar phenocrysts, and the tendency of the bands, in the most completely replaced phenocrysts, to appear more like the true magmatic sodic plagioclase zones. This tendency is emphasized in the phenocrysts of Fig. 14d, as here, the stippled area of the band, with its cloudy feldspar and characteristic K-rich phase, is in turn rimmed by a clear outer zone (R) with exactly the appearance and composition of the sodic zones on the plagioclase phenocrysts. The K-rich phase of the band would then have originated by antiperthitic exsolution.

The thin outermost perthitic alkali feldspar rims, which occur on both plagioclase and alkali feldspar phenocrysts and which are shown in Fig. 13c-f and in Fig. 14a-d, are thought to have crystallized directly from the melt. In many cases, the rim alkali feldspar is continuous with groundmass grains, and often the orientation of the rim,

or parts of the rim, is different from the orientation of the sanidine or cloudy perthite of the core of the phenocrysts.

Plagioclase Phenocrysts

The plagioclase phenocrysts can be summarized as follows. (See Fig. 15) The calcic core has a composition of $Or_{1.5}Ab_{46-50}An_{48-52}$ and is slightly embayed, with the direction of embayment preferentially parallel to the albite twin composition plane. The composition of the next, narrow rim, which conforms to the outline of the calcic core, is $Or_3Ab_{60-64}An_{33-38}$. It contains reversals which range in composition up to $An_{42}$ or so. There is then a very abrupt change to an outer thin zone of plagioclase of composition $Or_{4-5}Ab_{73-76}An_{19-22}$, which contains reversals in composition up to $An_{27}$. In its outermost portions, this appears to change continuously in composition to that of the $An_{11-13}$ plagioclase of the alkali feldspar phenocrysts. However, in some phenocrysts, there is no outer $An_{19-22}$ zone, and the composition changes abruptly from $An_{34-40}$ to $An_{11-13}$. Optical study indicates that this latter type of zonation predominates.

The sanidine, like that in DV56, appears to have coexisted with the $An_{20}$ or so plagioclase. The correlation of the $An_{11-13}$ zone on the plagioclase phenocrysts with the late plagioclase of the replacement sequence then brackets the time of reaction of the sanidine as being after sanidine crystallized but for the most part before the most sodic plagioclase crystallized. Sanidine reaction clearly took place before the groundmass crystallized.

Crystallization and Replacement Sequence

In the light of the above, the following tentative crystallization sequence of the feldspars is suggested, and plotted in Fig. 15. Crystallization began with the $An_{48-52}$ plagioclase cores. This was then resorbed slightly, and rimmed by plagioclase of $An_{33-38}$ composition. Reversals were formed at this time. Next, plagioclase of composition $An_{19-22}$ crystallized simultaneously with the sanidine. As the sanidine

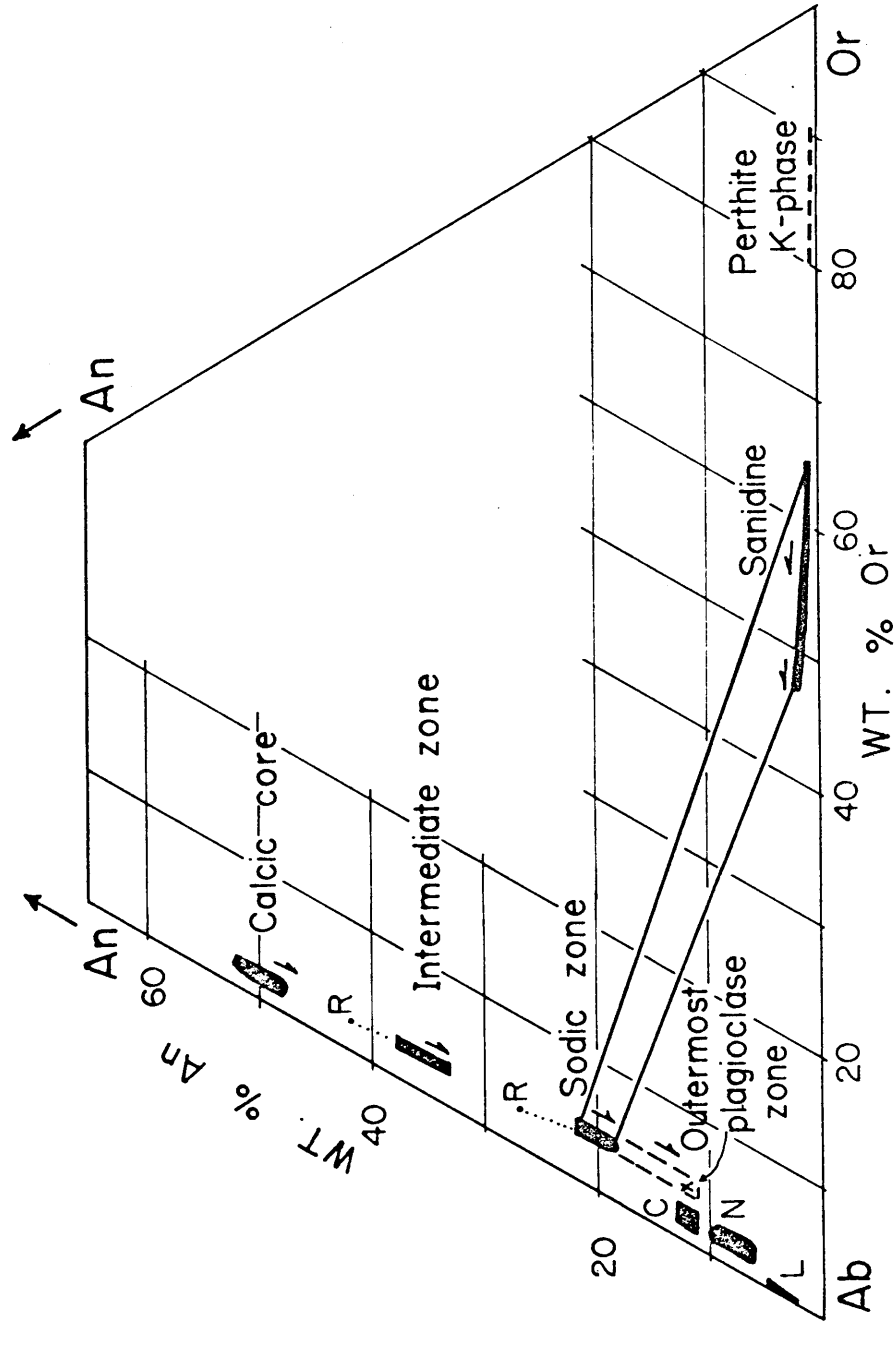


Fig. 15. Summary diagram of feldspar compositions(weight percent) from specimen DV151. Tie lines connect coexisting feldspars. R=reversal composition. See text for detailed explanation.

zoned from $Or_{65}$ to $Or_{45}$, the plagioclase apparently zoned from $An_{22}$ to $An_{19}$ or so. This is shown by the tie lines in Figure 15. But by the time the plagioclase composition in equilibrium with the melt started to decrease below $An_{19}$ and toward $An_{12}$, the sanidine was out of equilibrium with the melt and the replacement process started. Locally, some of the $An_{19-22}$ plagioclase may have been resorbed.

The following model of the replacement sequence is suggested. Instead of being rimmed by the sodic plagioclase, as in DV56, the sanidine was replaced by a complex mechanism. The initial response of the sanidine, was to form the cloudy perthite, and then, as evidenced by the close association of the plagioclase patches and the K-rich phase, to exsolve into a patch perthite with phases of composition $Or_{85-90}Ab_{9-13}An_{0.5}$ and $Or_{1-3}Ab_{88-92}An_{6-10}$ (N). There is in detail little evidence that initially the $An_{6-10}$ plagioclase directly replaced the sanidine--apparently the patch perthite formed first.

The general concentration of the patch perthite in the outer portions of the alkali feldspar phenocrysts reflects the zonation of the phenocrysts toward more Ab-rich sanidine in the outer edges. In this specimen, the most sodic sanidine observed was $Ab_{55}$. The crest of the solvus in the alakli feldspar system is roughly at $Ab_{65}$, and the observations has been made by numerous workers that alkali feldspars in the region $Ab_{50-70}$ tend to unmix very easily relative to other compositions. Hence, initial patch perthite formation would occur in the outermost, more sodic, portions of the sanidine phenocrysts preferentially. The interiors of the phenocrysts, on the other hand, would tend to resist patch perthite formation due to their relatively more potassic compositions. This is supported by the observations already noted.

As replacement progressed, it is suggested that the K-rich phase of the patch perthite was then preferentially replaced by the sodic plagioclase. The growth in size of the K-rich patches represents a coalescence of the existing smaller K-phase regions as time progressed. The end result of this would be the wholly replaced phenocrysts which contain approximately 3-4 percent by volume of the K-rich phase.

Somewhere in the middle of this sequence, plagioclase of

composition $Or_{1-3}Ab_{85-87}An_{11-13}$ appears to have begun to replace the first plagioclase of composition $Or_{1-3}Ab_{88-92}An_{6-10}$. This probably occurred when the $An_{11-13}$ play first started crystallizing from the melt onto plagioclase phenocrysts. Hence in the outer portion of the phenocrysts, the plagioclase that had originally replaced the K-rich phases exsolved from the patch perthite, was in turn replaced by a slightly more calcic plagioclase. In the phenocrysts at the end stages of the replacement process, as those in Fig. 13e and f, or 14d, all the more sodic plagioclase was replaced, and the entire phenocryst became essentially the $An_{11-13}$ plagioclase. In a few instances, $An_{11-13}$ rims crystallized on the phenocrysts directly from the melt (Fig. 14d).

The K-rich phase in the "rims" of Fig. 14 is due to anti-perthitic exsolution of an original plagioclase of composition exactly similar to that on the plagioclase phenocrysts. Hence the second replacement plagioclase probably originally had 4-5 per cent Or in solution in it. This suggests, then, a limiting case for the removal of the K-rich phase of former sanidine phenocrysts. The K-rich phase would be removed, or replaced by the plagioclase, until it was present in the plagioclase in such per cent as to make the bulk composition of the plagioclase of the interior the same as that of the outer zones on the plagioclase phenocrysts, i.e., $Or_{4-5}$. Hence, while the K-rich phase of the calcic plagioclase "rims" may have originated via true antiperthitic exsolution, the K-rich phase of the interior of the phenocryst could have just as well been relict from the patch perthite exsolution stage at the beginning of the replacement sequence.

This sequence was followed by quenching of the system and crystallization of the outer alkali rims and the groundmass.

If this suggested sequence is valid, here is a situation where perthite formation occurred before the bulk of the system had crystallized--in this case, when the system was only 35 per cent crystalline. It is also a case where patch perthite formation is an integral part of the replacement process by which sanidine is converted into sodic plagioclase. The compositions of the sanidines in this specimen are in the range which has been observed to form perthites most readily in

in the laboratory.

If this replacement model is correct, then it seems likely that the total energy required to form the patch perthite, replace the K-rich phase with the sodic plagioclase, and change the composition of the plagioclase slightly was less than that required to replace the sanidine directly with the $An_{11-13}$ plagioclase. Also, the formation of the perthite --either the fine cloudy perthite or the patch perthite--tends to form discontinuities within the phenocryst and therefore make access to the interior that much easier during the later replacement stages.

It appears that the sanidine could exsolve, for the most part at this time, only to a Na-phase which contained 6-10 per cent An. Hence the secondary plagioclase replacement process was necessary. However, there is some evidence from one alkali feldspar phenocryst that the perthitic plagioclase patches that formed in the most interior parts of the sanidine phenocrysts are more An rich than those in the exterior portion of the phenocryst. Fig. 16 shows a sketch of this phenocryst on which the probe-determined patch perthite compositions have been plotted. While the data are rather scanty, it does suggest that the more potassic sanidine of the interior initially exsolved to a more calcic plagioclase in the $An_{11-13}$ range, while the more sodic sanidine of the exterior exsolved to a more sodic plagioclase in the $An_{6-10}$ range. This would agree with the expected tie lines, and also allow some of the $An_{11-13}$ plagioclase to be of perthitic origin.

No quartz phenocrysts occur in DV151, and it appears that, as in DV56, the quartz did not start to crystallize until groundmass crystallization started. Occasionally one sees large quartz crystals, up to 4 mm in length, in the groundmass which have a grain size range of 0.2 to 0.5 mm. These are exceedingly lobate, as shown in Fig. 17, and contain all the other minerals of the groundmass in the elongate areas that penetrate into the quartz grain. Its extremely irregular shape, and the distribution of features like these within the stock, which will be discussed more fully later, suggests that it is due to late growth in the groundmass crystallization stage which enveloped and replaced some of the

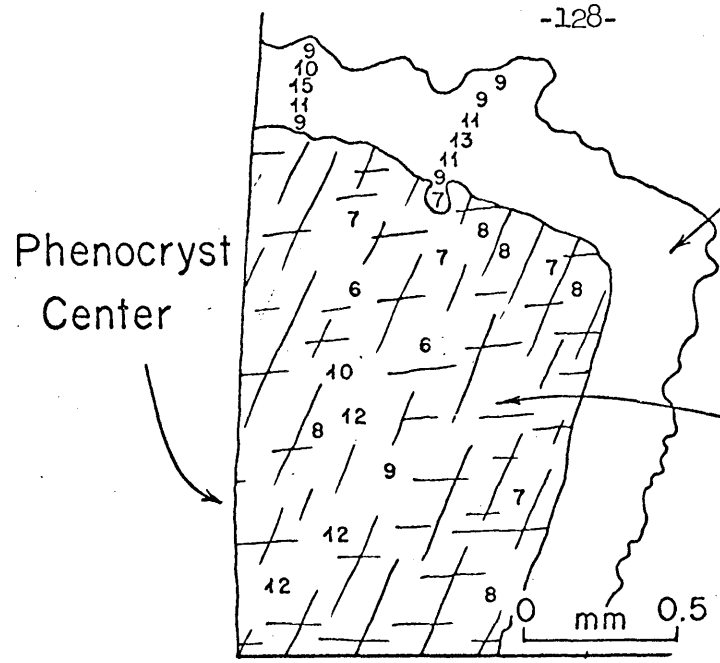


Fig. 16. Distribution and composition(weight percent) of patch perthite and rim plagioclase in sanidine phenocryst.

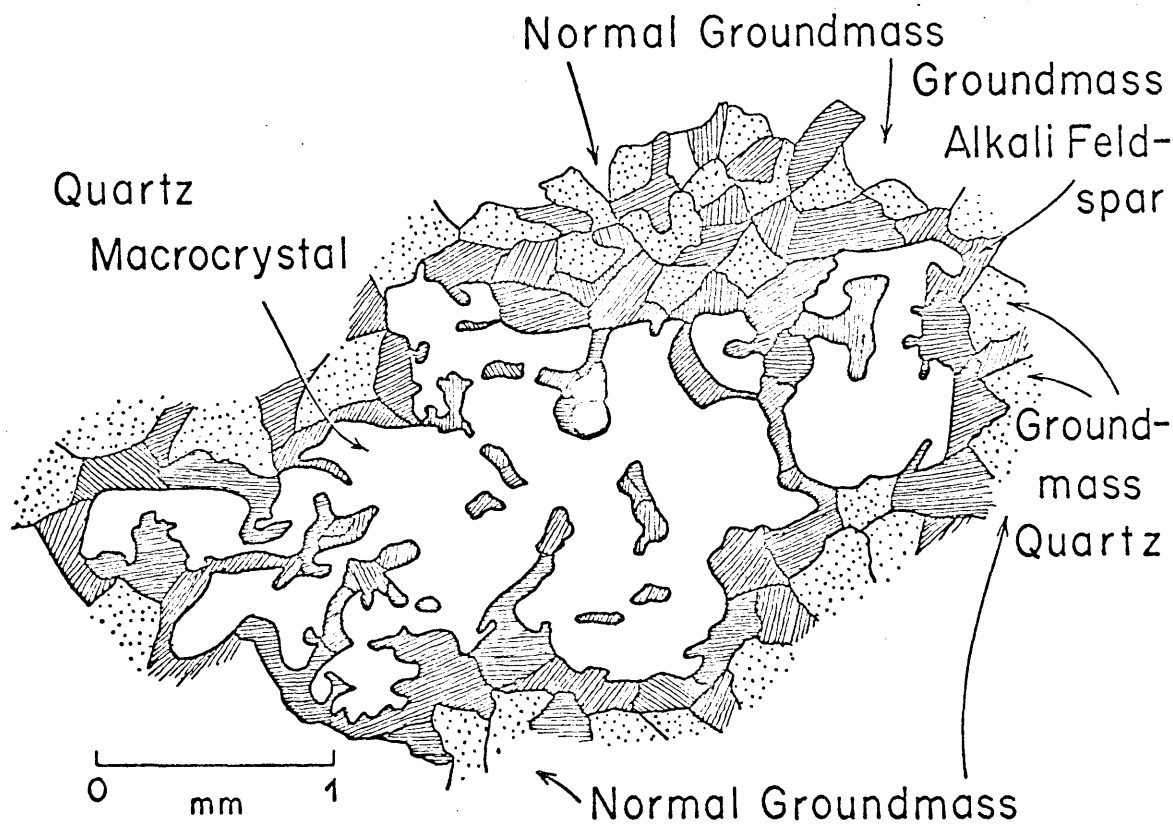


Fig. 17. Quartz macrocryst in groundmass of specimen DV151.

surrounding groundmass feldspar.

The origin of the quartz blebs in the various phenocrysts is thought to be dominantly due to a late stage replacement process which occurred at the time that quartz was in equilibrium with the melt. The much greater percentage of the quartz blebs in the wholly replaced phenocrysts, and the common association of the cloudy perthite and the plagioclase patches with the quartz blebs, would then reflect the greater ease of accessibility of the Si to the interior of the phenocrysts due to the great number of crystal imperfections created during the replacement process. This would also explain the very irregular distribution of the quartz blebs in some of the phenocrysts (see Fig. 13f), and the restriction of the quartz blebs in the unreplaced sanidine phenocrysts to obvious crystal discontinuities. However, if this is true, quartz was replacing the feldspar at least before the time when the quartz outlines were formed around some of the relict sanidine cores in the late and intermediate stages of the replacement sequence. This is required because of the cases where these outlines are preserved after the sanidine core has been removed, as it is not obvious that the quartz blebs would have taken such a form had they been later.

## Description of Other Representative Specimens

The two specimens just discussed are representative of the crystallization sequences seen throughout the stock. The details of the plagioclase normal steplike zoning, the reversals, the coexistence of two feldspars and the removal from equilibrium of the sanidine are common to all the rest of the specimens from the stock. In a sense, the two represent end members of a series, with DV56 at one end, where the sanidine was rimmed by oligoclase with little or no replacement of the sanidine, and DV151 at the other end, where the sanidine was extensively replaced by albite-oligoclase through a patch perthite replacement process. In all cases, when the sanidine did coexist with a plagioclase, the composition of that plagioclase was invariably oligoclase near $An_{20}$ in composition.

The following section will consist of very brief discussions of several other specimens on which both probe and optical work was done. The emphasis will be on differences from either the DV56 or DV151 results.

Direct Replacement Sequence-Specimen DV74

Specimen DV74 is located (Fig. 1) in the extreme northwest corner of the earlier southern phase of the stock, very near to the roof of this portion of the stock. Its textures are typical of most of the textures seen in the bulk of the southern phase, except that the groundmass is slightly finer grained. It consists of 1 to 5 mm sanidine and plagioclase phenocrysts in an 0.1-0.3 mm quartz-alkali feldspar-plagioclase groundmass which makes up 77 per cent of the rock. The minor and accessory minerals consist of biotite, hornblende, magnetite, and sphene, which total less than 8 per cent of the rock by volume. The mode and calculated norm are listed in Appendix A.

In general terms, this specimen shows many of the replacement features typical of DV151, and a whole sequence of replacement textures occurs ranging from essentially untouched sanidine to wholly replaced alkali feldspar. There are slight differences in the style of replacement, however.

Figure 18a, b, and c shows some typical alkali feldspar phenocrysts. There is very little of the patch perthite that was so common in DV151, and extensive areas of the cloudy perthite are rare. The sanidine is preserved up to the very last stages of replacement, and is never completely changed to the patch perthite and cloudy perthite combination. Hence, as shown in the figure, the phenocrysts consist of sanidine, slightly clouded at the very outer edges, with rims of the mottled, quartz-bleb filled replacement plagioclase of various widths. Again, the quartz blebs tend to concentrate at the sanidine core-plagioclase replacement rim contact. In Fig. 18c, the quartz blebs appear to outline the former edge of the core which has been further embayed to produce the later indentation on the right-hand side of the figure. In a few cases, wholly replaced phenocrysts are seen, with

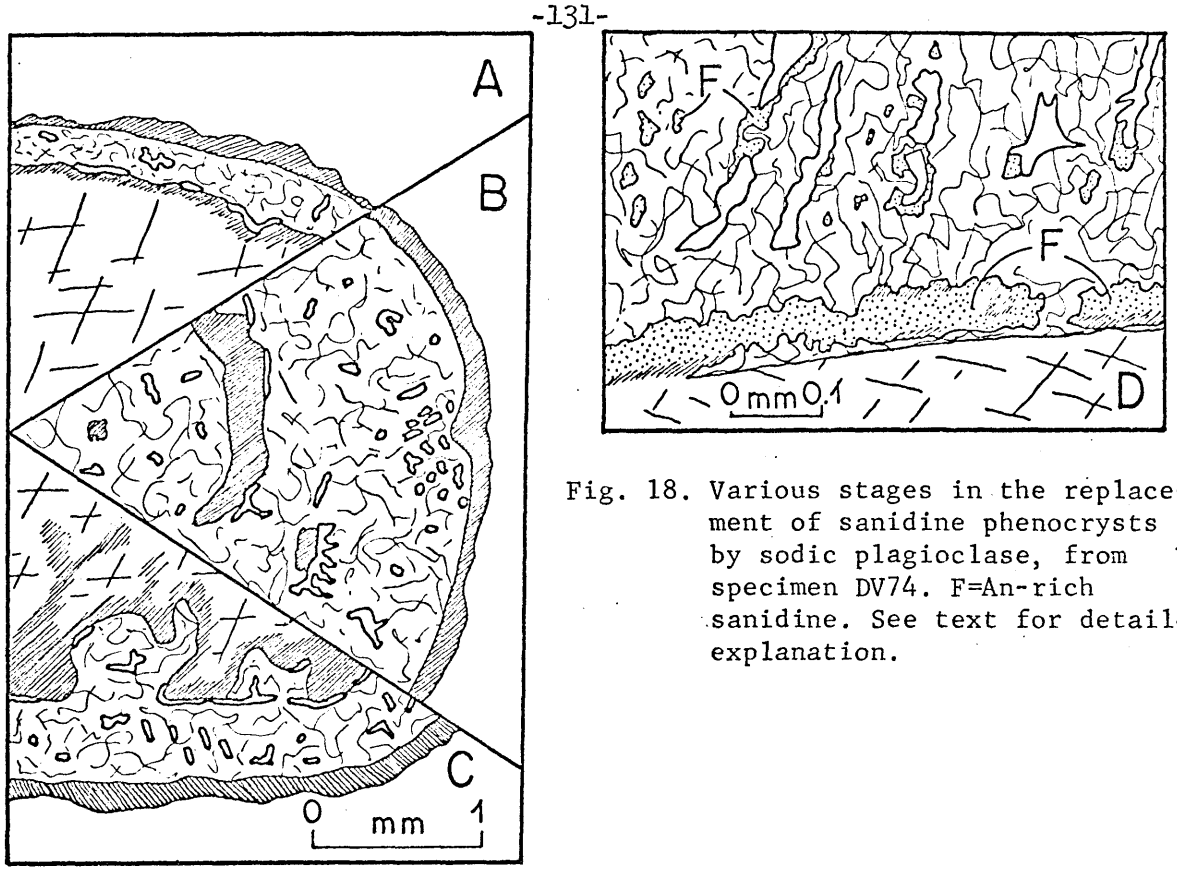


Fig. 18. Various stages in the replacement of sanidine phenocrysts by sodic plagioclase, from specimen DV74. F=An-rich sanidine. See text for detailed explanation.

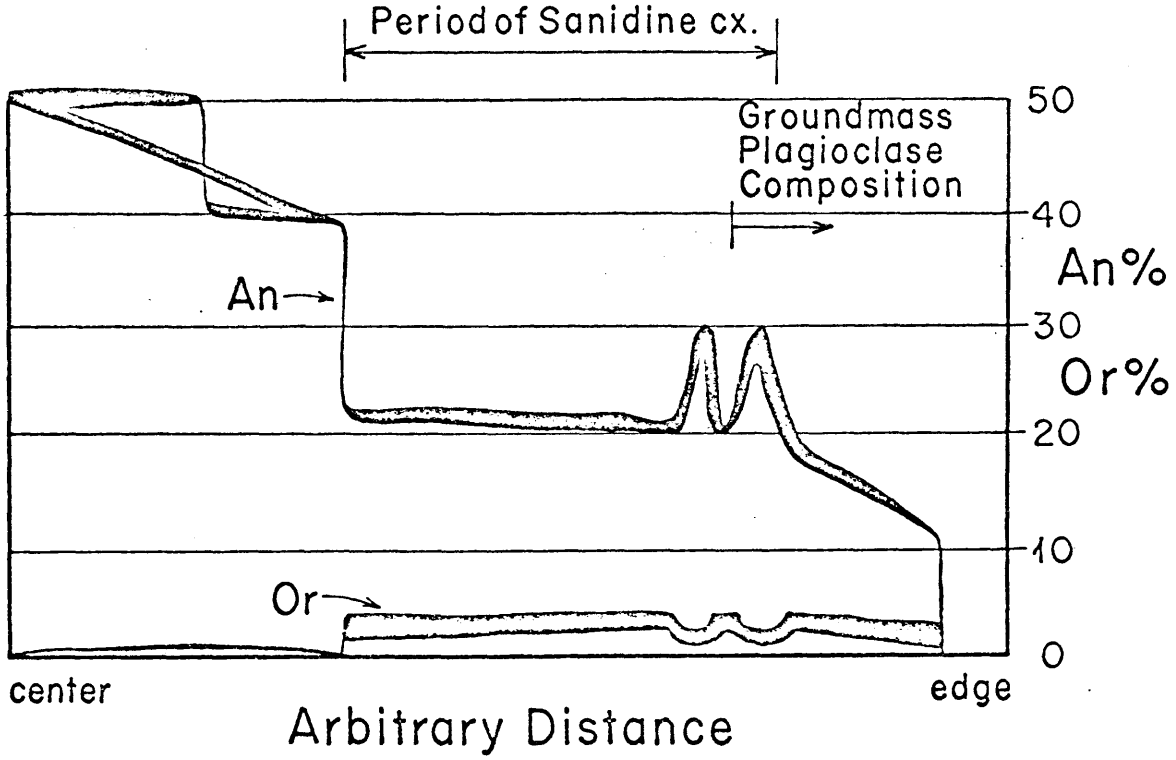


Fig. 19. Composite plagioclase probe scans, specimen DV74, across plagioclase phenocrysts. Or and An percentage in weight percent.

relict islands of either sanidine or cloudy perthite rarely seen, as in Fig. 18b.

In this specimen, the initial and intermediate stages of the replacement sequence, which had widespread development of cloudy perthite and replacement patch perthite and extensive areas of relict cloudy perthite patches in the replacement plagioclase, are effectively telescoped so that the change from sanidine to replacement plagioclase is texturally much more abrupt. It appears that here the sanidine was directly replaced by the sodic plagioclase without the intervening patch perthite replacement stage.

The composition of the sanidine (Fig. 20) ranges from $Or_{57}Ab_{42}An_1$ in the center of the phenocrysts to $Or_{40}Ab_{58}An_2$ at the outer edge. The composition of the plagioclase replacement rims, and the very rare patch perthite, is in the range $Or_{0.5\text{-}3}Ab_{82\text{-}86}An_{11\text{-}16}$ with a few areas having Or percentages as high as $Or_{5\text{-}6}$. In a few rare instances, an An-rich alkali feldspar of composition $Or_{30\text{-}33}Ab_{62\text{-}64}An_{4\text{-}5}$ occurs as patches in the replacement plagioclase or as patches along the core-rim contact, as shown by the stippled areas (F) in Fig. 18d.

The plagioclase phenocrysts are similar to those of the two specimens previously described. They consist of calcic cores with compositions ranging from $Or_{0.5\text{-}1}Ab_{49}An_{50}$ to $Or_{0.5\text{-}1}Ab_{59}An_{40}$ either continuously or with an abrupt step omitting the intermediate $An_{42\text{-}48}$ compositions. This core is embayed and corroded, and surrounded in turn by a broad zone of composition $Or_{2\text{-}4}Ab_{74\text{-}78}An_{19\text{-}23}$. This outer zone often has one to three reversals superimposed on it that range in composition up to $An_{30}$, and in one case, one very prominant reversal was noted with compositions reaching $An_{40}$. Outside the reversals, which tend to concentrate at the outer edge of the $An_{20}$ zone, the composition drops off steadily and continuously to compositions typical of the plagioclase replacement rims.

The number of inclusions of calcic plagioclase phenocrysts within sanidine phenocrysts is unusually large in this specimen, allowing the timing of the initial appearance of the sanidine to be fixed more accurately. As a rule, the larger the sanidine phenocrysts, the

more calcic the last plagioclase to crystallize before armoring by the sanidine. In all cases, sanidine is post the $An_{\sim 23}$ calcic core crystallization, and apparently started to crystallize along with the $An_{19-23}$ plagioclase. In one case, in a very small phenocrysts of sanidine, the sanidine armored the plagioclase after at least some of the reversals on the $An_{19-23}$ plagioclase zones had formed, but in these cases it is rather hard to decide whether to call the grain a sanidine phenocryst or a plagioclase phenocryst with a thick sanidine rim. Hence sanidine probably coexisted with the plagioclase until the plagioclase reached compositions of $An_{16}$ or so.

The groundmass of this specimen is unlike that of either DV56 or DV151. in one important respect. Approximately one-third of the equant alkali feldspar crystals of the groundmass contain zoned plagioclase cores. Probe work indicates that these groundmass plagioclase grains, later rimmed by the alkali feldspar, exactly duplicate compositionally the outer portions of the normal plagioclase phenocrysts. They appear to have started to crystallize just before the outermost reversal was formed on the plagioclase phenocrysts in the $An_{19-23}$ zone, as indicated on Fig. 19. Occasionally the cores of the groundmass alkali feldspars show evidence of replacement.

Comparison of the groundmass and phenocryst compositions indicates the following crystallization sequence. (refer to Fig. 20) First, crystallization of the calcic plagioclase cores. Then, after a period of resorption of the calcic plagioclase, sanidine ($Or_{57}$) and plagioclase ($An_{23}$) crystallized simultaneously. They continued to crystallize together until the sanidine reached compositions near $Or_{40}$ and the plagioclase reached compositions of $An_{16}$ or so. The sanidine may have zoned to compositions of $Or_{30-35}$ rapidly in the very last stages of crystallization. During the time that the sanidine was crystallizing, reversals formed on the plagioclase with compositions up to $An_{30}$ in most cases. The evidence indicates that the second generation or groundmass feldspars had started to crystallize before the reversals on the plagioclase phenocrysts had been formed, and hence were crystallizing along with the outer parts of the phenocrysts. Thus,

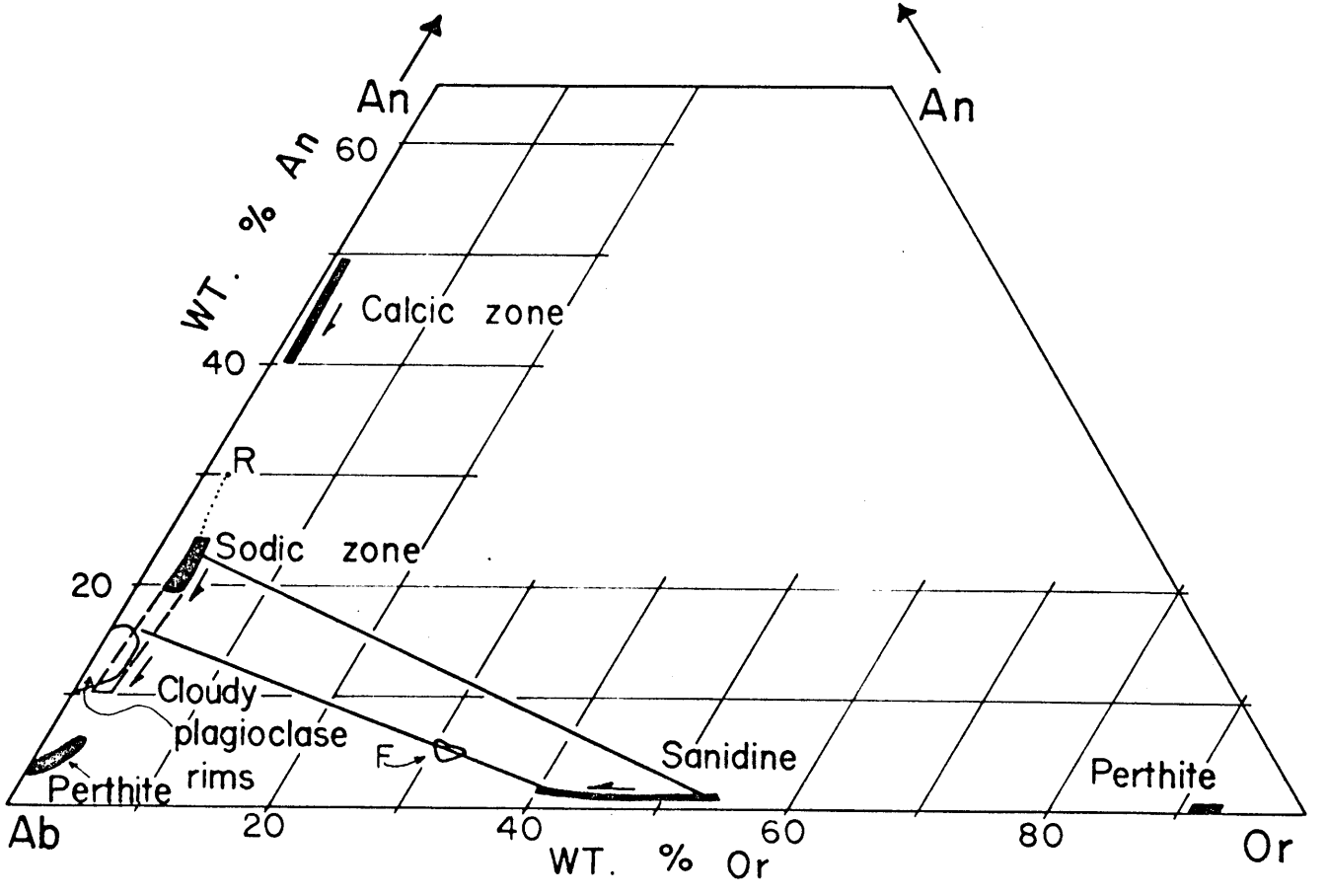


Fig. 20. Summary diagram of feldspar compositions from specimen DV74. Tie lines connect coexisting feldspars. R=reversal composition. F=An-rich sanidine. All compositions in weight percent.

at this point, both sanidine phenocrysts and rare microcrystals, and plagioclase phenocrysts and numerous microcrystals were crystallizing. By the time the plagioclase composition became less than $An_{16}$, both the sanidine phenocrysts and microcrystals were being replaced by the $An_{11-16}$ plagioclase. Finally, as in all the other specimens in the stock, everything was rimmed by alkali feldspar and the bulk of the sanidine and groundmass quartz crystallized.

The initiation of the second generation plagioclase (and perhaps alkali feldspar) at roughly the time of the reversals on the oligoclase zones of the phenocrysts, during which time the sanidine was still crystallizing, suggests that the event which caused the groundmass formation started at this point in the crystallization sequence.

Megaphenocrysts-Specimen DV294

Another specimen from the southern phase of the stock, DV294, has textural features in the alkali feldspars that are exactly like those noted in DV74. The sanidine, which ranged in composition from $Or_{54}Ab_{45}An_1$ in the center to $Or_{35}Ab_{63}An_2$ at the outer edge, coexisted with a plagioclase of the approximate composition $Or_5Ab_{75}An_{20}$. However, one very unusual feature of this specimen is the presence of a euhedral magaphenocryst, with dimensions of 12 by 16 mm. It consists of a cloudy, albite-pericline twinned plagioclase core with dimensions of 10 by 7 mm, surrounded by a clear sanidine rim about 6 mm wide.

The composition of the sanidine rim of the megaphenocryst is in the range $Or_{40-50}Ab_{47-57}An_3$, hence it is consistantly more An rich than the normal sanidine. The plagioclase of the megaphenocryst has a composition of $Or_{4-6}Ab_{74-77}An_{19-21}$, essentially the same as the normal plagioclase phenocrysts.

The presence of normal magmatic oligoclase laths as oriented inclusions in both the sanidine rim or the oligoclase core of the megaphenocryst, suggest that the megaphenocryst grew at the same time as the coexisting feldspars. This is also supported by the fact that the outer edges of the sanidine of the megaphenocryst are replaced in the same manner as the normal sanidine phenocrysts, and in places the

groundmass appears to have used the megaphenocryst as a substrate during initial crystallization.

The reason for the rapid growth of the megaphenocryst is not known. There is little evidence of growth associated with a vapor phase, although it is possible that the accelerated growth was due to a high water concentration in the melt even though no separate vapor phase formed. The High An percentage of the sanidine could be due to its rapid growth. This megaphenocryst is one of the few seen which contains both sanidine and oligoclase--the majority consist of only sanidine.

Oscillatory Zoning in Sanidine Phenocrysts-Specimen DV129G

Several interesting features are noted in specimen DV129G. This sample, located in the extreme northeast corner of the north phase of the stock, is essentially a duplicate of DV151 in terms of the replacement sequence of the sanidine phenocrysts. However, in this specimen, oscillatory zoning was noted in the sanidine phenocrysts.

The sanidine ranges in composition from $Or_{62}Ab_{37}An_1$ to $Or_{40}Ab_{57}An_3$, with different phenocrysts having different parts of that range and no phenocryst indicating whether the interior parts are more or less sodic than the exterior parts. In several of the phenocrysts, 0.1 mm bands alternate in composition between $Or_{42-46}$ and $Or_{52-58}$. This is shown in the scan of Fig. 21. The oscillations are continuous optically around the entire unreplaced parts of the respective phenocrysts, and minor features such as truncation of older oscillations by younger oscillations are commonly noted. An excellent example of a zoned phenocryst is shown in Fig. 22, taken from specimen DV146.

In DV129G, one also sees, as in DV151, the two plagioclase compositions involved in the replacement sequence ($An_{6-10}$ and $An_{11-16}$) in the same situations. However, in this sample, as the An percentage of the replacement rim plagioclase increases the Or percentage also increases until, in some of the $An_{11-16}$ rims, compositions with as much as 7 per cent Or are reached. In one phenocryst that was examined, in which the sanidine is almost wholly replaced and is restricted to a

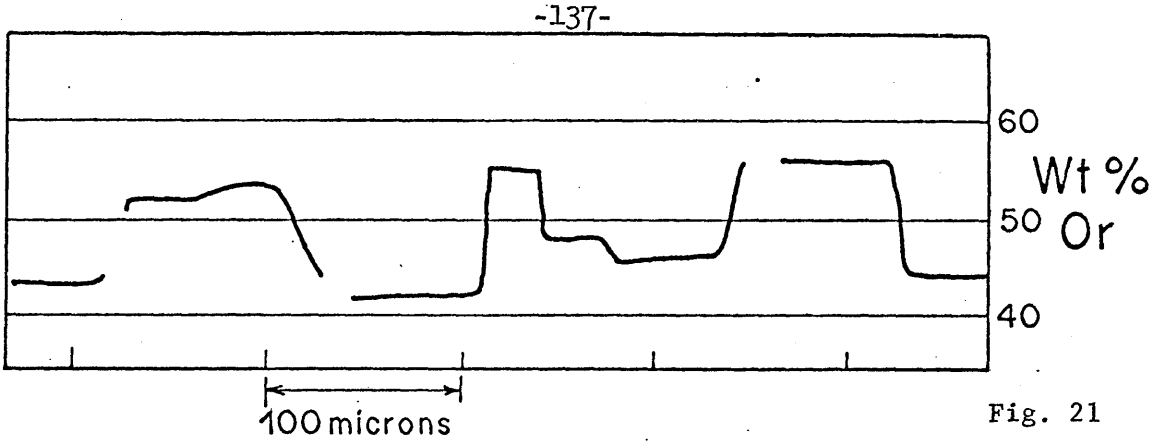


Fig. 21

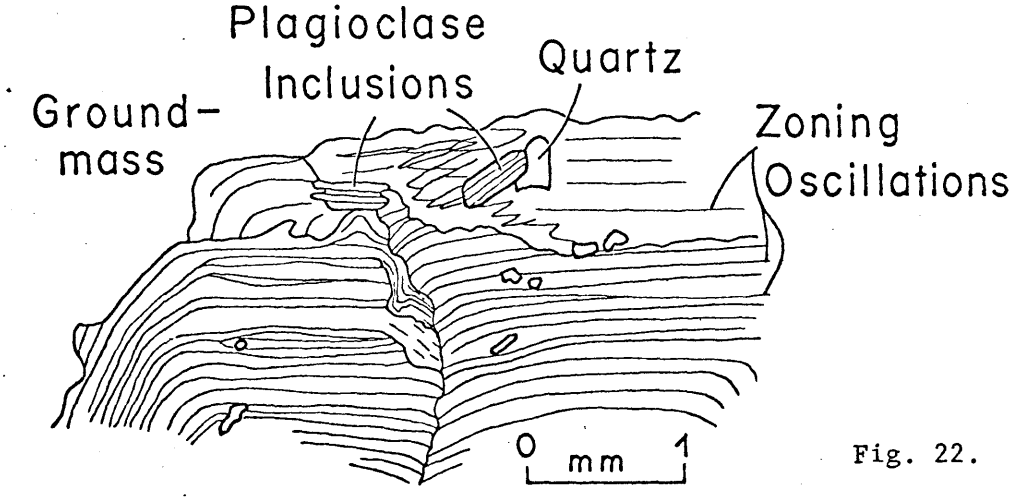


Fig. 22.

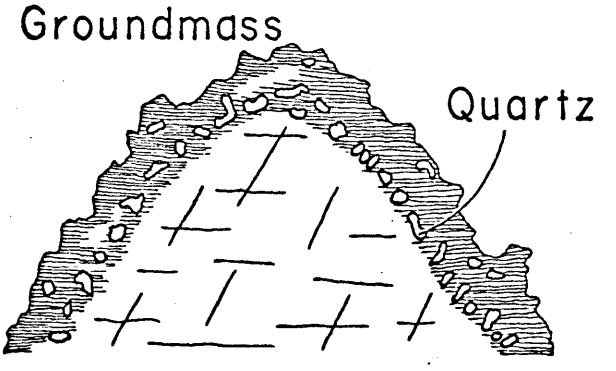


Fig. 23.

Fig. 21. Probe scan across oscillatory zoned sanidine phenocryst, specimen DV129G.

Fig. 22. Sketch of oscillatory zoning in sanidine phenocryst of Fig.21.

Fig. 23. Sketch showing concentration of quartz belbs in outer edge of sanidine phenocrysts, specimen DV129G.

relict patch in the center of the phenocryst, the composition of the plagioclase nearest the outer edge of the phenocrysts reaches compositions of $Or_{10}Ab_{77}An_{13}$, while the interior portion has a more normal composition. Unfortunately, no plagioclase phenocrysts could be run in this specimen due to their alteration, so that the Or percentage of the normal sodic plagioclase is not known. It is possible that the magmatic plagioclase could have zoned to this composition.

A final point of interest in DV129G is shown in Fig. 23. Quartz blebs, in many of the unreplaced sanidine phenocrysts, tend to line up in a band just inside the outer edge of the phenocryst. Similar bands of quartz blebs are seen next to the inner edge of the thin alkali rims on the plagioclase phenocrysts. This feature is interpreted as being due to the simultaneous crystallization of quartz and alkali feldspar at the time of alkali rim formation and groundmass crystallization.

Contact Phase Granite-Specimen DV128A

The next variant of the stock to be discussed is that represented by specimen DV128A. The chief characteristic of this sample is the almost complete lack of replacement of the sanidine. The groundmass is relatively coarse, --in the 0.2 to 1 mm range--and makes up 68 per cent of the rock. The phenocrysts are all anhedral and fall with a grainsize range of 2 to 5 mm, and plagioclase in phenocryst form is very rare and makes up less than 2 per cent of the rock by volume, making this rock one of the least calcic in terms of bulk compositions of all the stock specimens.

The sanidine phenocrysts range in composition from $Or_{50}Ab_{49}An_1$ to $Or_{40}Ab_{59}An_1$, and there is some hint that sanidine as sodic as $Ab_{35}$ exists in the rock. It is exceedingly difficult to determine the bulk composition of the sanidine in most of the phenocrysts, however, as a coarse lamellar perthite is characteristically developed which usually is present throughout the entire phenocryst. The Na-rich phase of the perthite tends to concentrate in the outer portion of the phenocrysts, and on occasion, is so abundant that a perthite rim forms. This is illustrated in the sketch of Fig. 24. The width of the individual

lamellae ranges from 0.01 to 0.1 mm, and the lamellae tend to pinch and swell. This perthite is identical to the lamellar type perthite noted in DV151 (Fig. 13a), and like that perthite is thought to have developed late in the history of the stock.

The composition of the lamellar perthite, as shown on Fig. 25 consists of a sodium phase of composition $Or_{0-1}Ab_{97-100}An_{1-2}$ and a potassium phase of composition $Or_{92-96}Ab_{4-7}An_{<0.5}$.

The composition of the plagioclase phenocrysts is shown in the composite probe scans of Fig. 25 and in Fig. 26. The calcic cores have a composition of $Or_1Ab_{58-60}An_{39-41}$, and there is some indication that a few of the calcic cores of the plagioclase phenocryst themselves have a rare central core with a composition of $Or_3Ab_{71}An_{26}$. Other specimens examined optically have suggested the presence of this inner sodic core also, but in terms of percentages, it accounts for less than 2 per cent of the plagioclase in the samples.

Outside the calcic core, the composition changes rapidly from roughly $An_{40}$ to a broad sodic plagioclase rim. The distribution of phases in this rim is such that, as shown in Fig. 25, its' composition changes from $Or_{5-6}Ab_{73-75}An_{20-21}$ at the innermost edge, to $Or_{4-5}Ab_{71-73}An_{23-24}$ in the central portion, and finally to $Or_{5-6}Ab_{75-77}An_{18-19}$ just before the reversal at the outer edge of the sodic zone which reaches compositions of $An_{30}$ or so. The outermost edges of the plagioclase zone continuously to $Or_1Ab_{84}An_{15}$, but no more sodic plagioclase was reached. The lack of both the $An_{11-15}$ plagioclase on the plagioclase phenocrysts, and the total lack of replacement features, supports the suggestion in the discussion of specimen DV74 that replacement of the sanidine did not take place until the plagioclase in equilibrium with the melt reached compositions of $An_{<16}$.

Contact Phase Granite-Volatile Rich Areas

The extreme northeast corner of the northern phase of the stock has many features which indicate that the magma was saturated in the volatile components to the extent that a separate fluid phase was formed. It contains numerous very large drusy cavities, and numerous pegmatitic

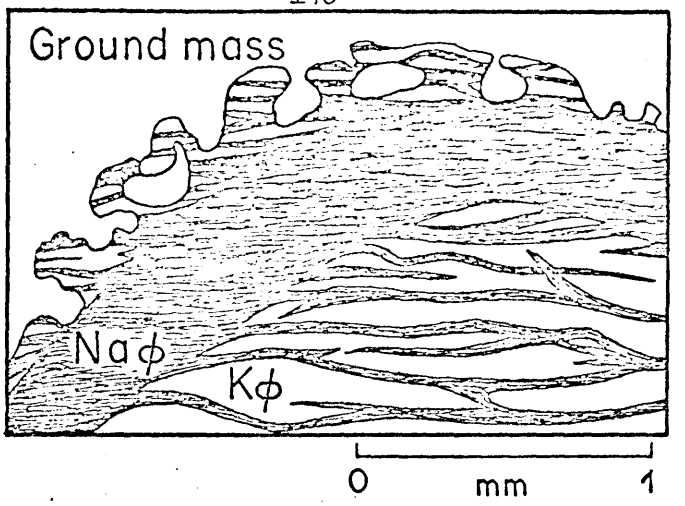


Fig. 24. Sketch showing concentration of lamellar perthite in rim position of sanidine phenocryst, specimen DV128A.

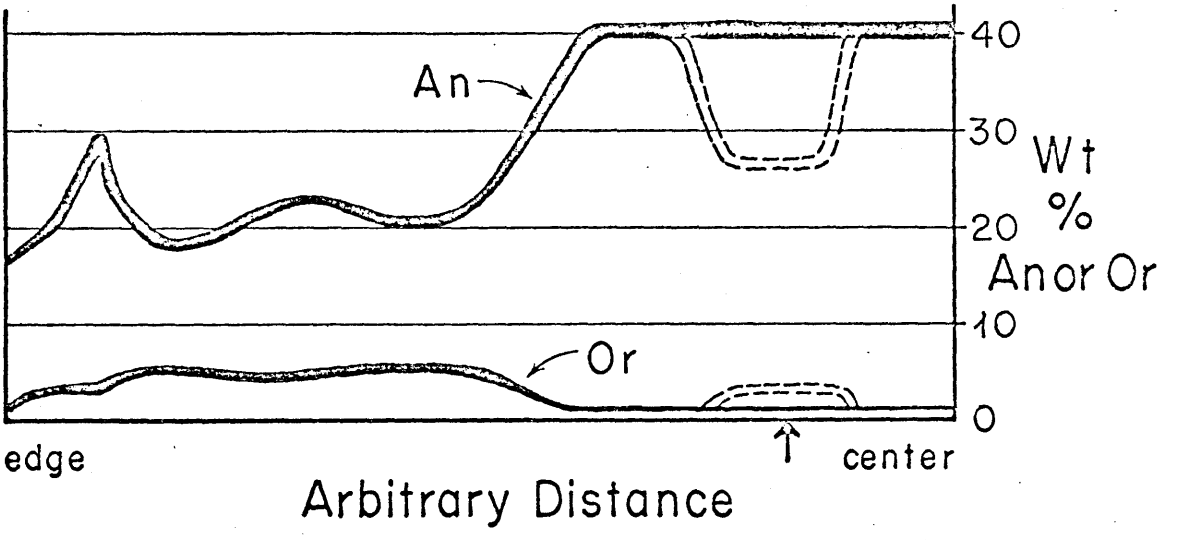


Fig. 25. Composite plagioclase probe scans across plagioclase phenocrysts, specimen DV128A. Or and An in weight percent.

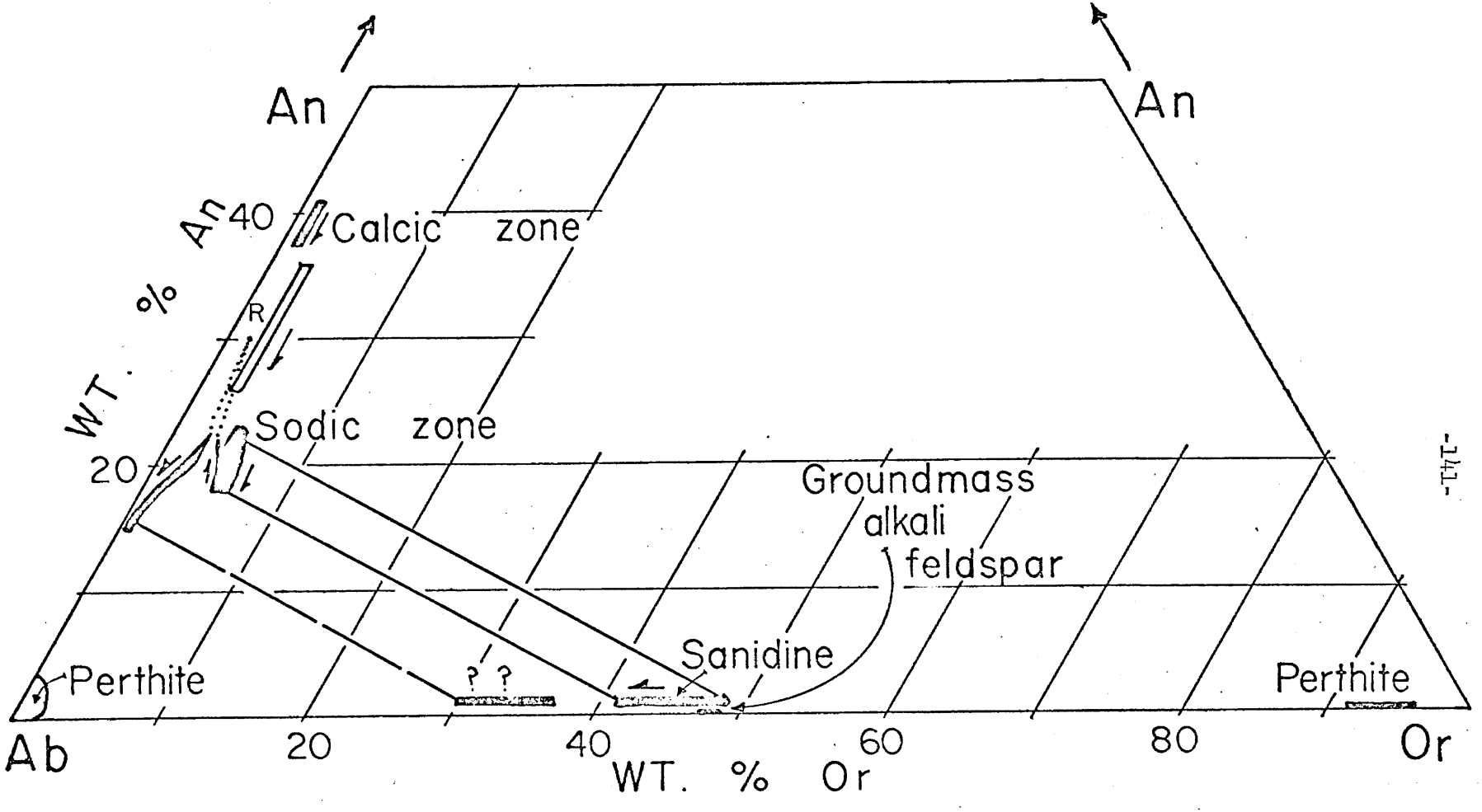


Fig. 26. Summary diagram of feldspar compositions(weight percent) from specimen DV128A. Tie lines connect coexisting feldspars. R=reversal composition

pods, as well as aplitic and granophyric textures.

The pegmatitic patches, which take the form of slightly flattened ellipsoids, range in size from several cm to a maximum of 5 m and consist of coarsely-perthitic alkali feldspar and quartz in crystals up to 10 cm in length. No vugs or drusy cavities have been found within these pods. The pods tend to allign themselves so that their planes of maximum flattening are parallel and essentially vertical.

DV127 is a typical example of one of the pegmatitic pods. It contains 0.5 to 2 cm blades of coarsely perthitic alkali feldspar and irregular shaped intergrown 0.1-2 cm quartz crystals which seem to be highly strained under crossed nicols. The feldspar blades are often rimmed by a zone of graphic textured quartz and alkali feldspar which has quartz rods up to 1 mm in length. The graphic rods tend to grow radially outward from the adjacent alkali perthite grain. The interblade areas consist of this graphic material or wormy intergrown quartz-alkali feldspar areas.

The bulk composition of the alkali feldspar (see Fig. 30,A) blades is $Or_{46-48}Ab_{54-52}An_{0}$. The compositions of the perthite phases are $Or_{1-5}Ab_{95-99}An_{0}$ and $Or_{84-87}Ab_{13-16}An_{0}$. (Fig. 30,A')

Closely associated with the pegmatitic pods are drusy cavities which are as large as 5 cm. As opposed to the normal smaller spherical cavities of the bulk of the stock, the cavities in this area are generally ellipsoidal in shape with maximum: minimum axis ratios from 2:1 to 4:1. There is no evidence of extreme flattening of the cavities anywhere in the stock. The crystals, as noted before, consist of euhedral sanidine, quartz and magnetite with very rare cristobalite.

In several planar bands 5 to 30 m across, which are vertical and essentially perpendicular to the nearest contact of the stock, the vugs make as much as 25 per cent by volume of the rock. The ellipsoidal cavities tend to be parallel to the orientation of the band in which they are located. Throughout this northeast area of the stock, the percentage of cavities is consistently 10-15 per cent by volume, as opposed to less than 2 per cent in most of the rest of the stock.

The drusy cavities and the pegmatitic pods are never in contact with each other, and as a general rule, bands rich in pegmatitic pods are poor in drusy cavities. Hence in outcrop, roughly 20 m wide bands rich in drusy cavities tend to alternate with roughly 20 m wide bands rich in pegmatitic pods.

As one approaches the extreme northeast contact of the stock, near stations 124 and 123, the normal granite porphyry of the outer portions of the northern phase of the stock fades into the area rich in drusy cavities and pegmatitic pods. The porphyry itself at first becomes less porphyrytic as the groundmass increases in size until the distinction between groundmass and phenocryst is impossible to make. Areas of aplitic, microgranitic and micrographic granite become more numerous, until, near the contact, no normal granite porphyry is left. The composition of the single feldspar of the micrographic or micropegmatitic areas is the same as that of the alkali perthite of the pegmatitic pods, as is shown on Fig 30(B'), and the perthitic phases are similar in composition also (B''). Rarely, ragged sanidine phenocrysts are found in the aplitic or microgranitic portions, with compositions as shown on Fig. 30(B). The perthite of the phenocrysts is very coarse, and ranges in type from lamellae perthite to perthite in which the lamellar have become so disaggregated that the perthitic phases form an aplitic texture made up of individual grains of the two phases. In this latter case, when the groundmass is also aplitic, it is often very difficult to see the phenocrysts in plane light in thin section.

All of the above rock types are cut by aplite dikes which range from 0.3 to 2 m in width and which have sharp, straight contacts. The grainsize is very consistantly 0.3-0.6 mm and consists of perthitic alkali feldspar and quartz in equant grains. The composition of the feldspars, shown in Fig. 30(C), is very similar to that in the pegmatitic feldspars.

The granite of both phases of the stock differs in several ways adjacent to the contact. In some cases, normal granite porphyry is found immediately adjacent to the country rock. In other cases, the

groundmass grainsize tends to increase as noted before, until essentially no groundmass as such exists. At the same time, the percentage of phenocrysts increases, for the most part due to growth of what would have been groundmass alkali feldspar onto the phenocrysts instead of forming discrete groundmass grains. The percentage of plagioclase phenocrysts drastically decreases to the point that commonly none are present in a thin section, and only rare grains in hand specimen. In many cases, the percentage of graphic textures in the groundmass position increases radically. In specimen DV319A, fully 25 per cent of the rock consists of graphic or vermicular alkali feldspar and quartz intergrowths. In this case, the graphic quartz growth is clearly later than the phenocrysts, as it has grown through many of them from centers at phenocryst contacts.

The contact phases of the stock granite may also tend to be like specimen DV128A, already discussed, in that the sanidine is essentially unreplaced, and shows none of the rimming features so common in the bulk of the stock. The coarse lamellar perthite is very well developed, and features like that shown in Fig. 24 are common. The compositions of the phases of this type of perthite tend to approach the pure endmembers, Ab and Or, as noted before.

## Inclusions within the Stock

More than 95 percent of the inclusions in the stock consist of rounded fragments of an earlier igneous phase of the stock. These are found scattered throughout the stock and for the bulk of the stock, make up less than 2 per cent of the rock in any given outcrop area. However, in several areas of the stock, zones occur in which these inclusions make up 50 percent or more of the stock. These zones, which occur in both phases of the stock, are shown in Fig. 28 by the circles. Note that the zones essentially concentrate in an east west band across the central portion of the stock, near the contact between the north and south phases of the stock, in the Starvation Canyon area.

In appearance, the inclusions are a light to medium gray-green very fine grained rounded fragments, 1 to 40 cm in diameter, which

usually contain less than 10 per cent white feldspar phenocrysts up to 7 mm in size. No flow banding is apparent. Thin section studies indicate that the groundmass is made up of 40 to 75 per cent by volume of 0.2 to 1 mm plagioclase laths with length to width ratios of 3:1 to 6:1 which are either rimmed by alkali feldspar, or which form a felted network in which interstitial alkali feldspar and quartz grains occur. The alkali feldspar is always less than 0.5 mm in size, usually perthitic, and texturally is later than the plagioclase, as is the quartz. The plagioclase is usually albite and carlsbad twinned, and is strongly zoned with very calcic interiors and very sodic outer zones.

The phenocrysts, in some of the inclusions, are exactly like those seen in the rest of the stock. They consist of clear to cloudy sanidine cores with cloudy plagioclase and quartz-bleb rims. Texturally, they are similar to the DV74 or DV151 types and show the same replacement features. A few have alkali rims which appear to be continuous with the groundmass alkali feldspar. In all cases, they are phenocrysts and not porphyroblasts. In a few cases, magmatic zoned plagioclase phenocrysts like those of the rest of the stock are also found.

In other inclusions, however, the phenocrysts are characteristically equant, euhedral cloudy plagioclase phenocrysts with numerous fine quartz blebs. They are much more altered than the cloudy plagioclase phenocrysts of the rest of the stock, and in almost all cases show a very fine albite twinning which is not typical of the cloudy plagioclase phenocrysts of the stock. The mottled texture on extinction is also much more extreme than in the cloudy plagioclases. In a few rare instances, irregular patches of clear, coarsely albite-twinned, more calcic plagioclase are found in the interior of these cloudy plagioclase phenocrysts, and the texture is such that it appears that the more-sodic cloudy plagioclase is replacing the clearer more-calcic plagioclase.

All of these cloudy plagioclase phenocrysts, without exception, have a very thin outer clear calcic plagioclase rim which rapidly zones to very sodic compositions at the outermost edges of the phenocrysts.

Crystallization Sequence of Early Igneous Phase

The compositions of the feldspars of the inclusions are shown in Fig. 27 as determined with the probe. The gross similarity of these compositions with those of the various samples from the stock is apparent. From the probe work, and thin section study of other inclusions of the early igneous phase, the following crystallization sequence has been determined.

The first stages of crystallization in this early igneous phase of the stock appear to be exactly the same as those in the bulk of the stock, that is, crystallization of calcic plagioclase of composition about $An_{60}$, then crystallization of intermediate plagioclase of composition $An_{40}$ (area A Fig. 27), and finally crystallization simultaneously of sanidine and $An_{20}$ plagioclase. (About area D, Fig. 27). At this point, however, differences begin to appear.

The cloudy plagioclase phenocrysts of the early igneous phase have compositions in the range shown by B of Fig. 27. This range is consistantly more calcic than that of the normal sodic plagioclase, near $An_{20}$ in composition, of the rest of the stock, and it appears from textural evidence that the cloudy plagioclase replaced both this normal clear sodic plagioclase and parts of the intermediate plagioclase.

This replacement stage, not seen in the rest of the stock, was followed by the abrupt crystallization of the clear calcic $An_{55}$ plagioclase zones, of composition C in Fig. 27, which occur on the cloudy plagioclase phenocrysts. At the same time, the cores of the groundmass plagioclase laths formed, as shown by their exactly similar compositions.

This stage was followed by the crystallization, on both the plagioclase phenocrysts and the groundmass plagioclase laths, of sodic plagioclase of composition $An_{23-19}$ (area D, Fig. 27) which zoned to very sodic, albitic, compositions as shown by Area E in the figure.

In a few rare cases, in the gap between the $An_{55}$ calcic rims and the $An_{23}$ or less outer sodic zones, zones of compositions $An_{40}$ and $An_{33}$ occur, but these are very thin and seldom continuous.

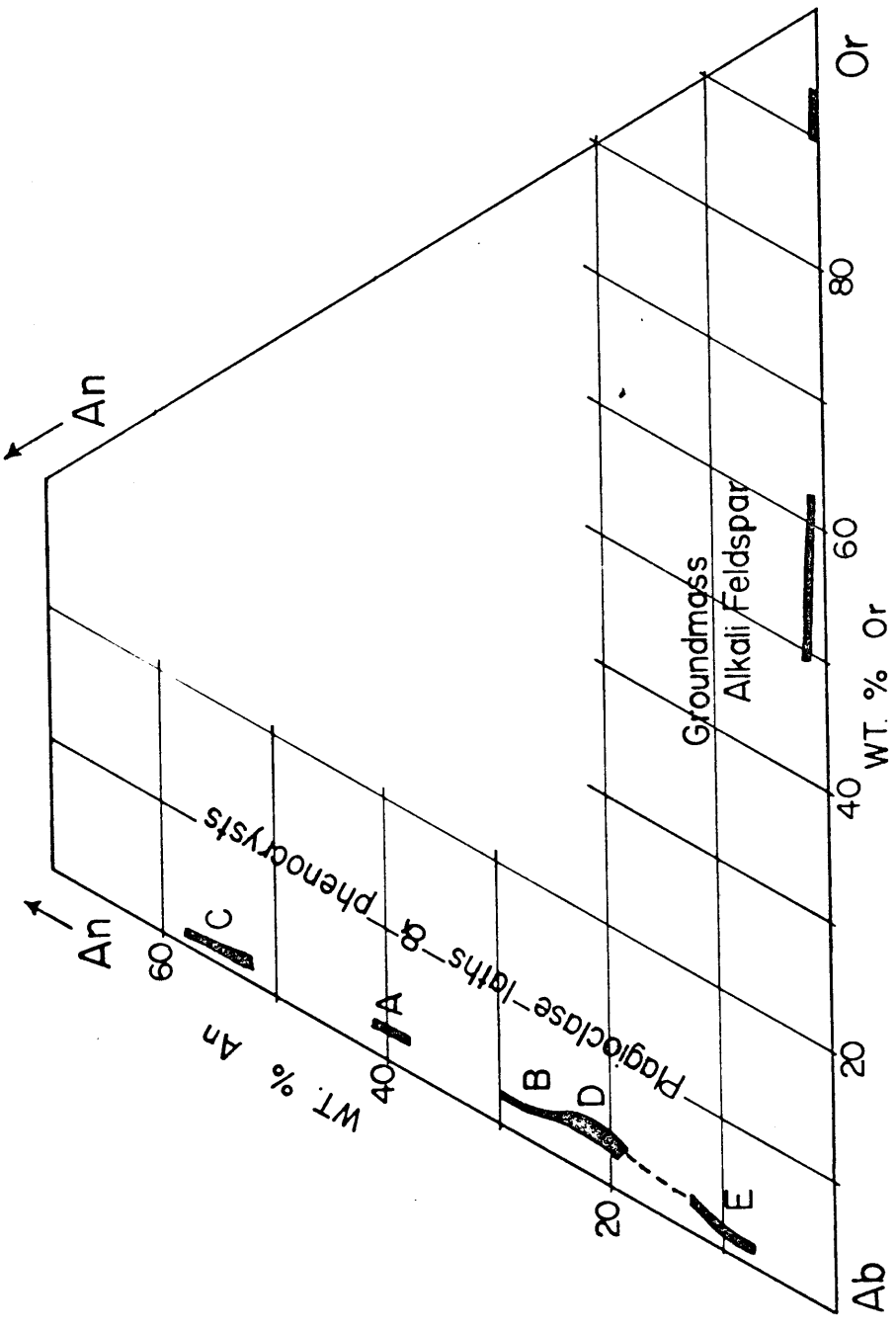


Fig. 27. Summary diagram of feldspar compositions (weight percent) from various early igneous phase specimens. See text for detailed explanation.

Crystallization of the outermost albitic plagioclase was followed by crystallization of alkali feldspar and quartz to complete crystallization of the groundmass. The composition of the alkali feldspar, as shown in Fig. 27 is slightly more Or-rich than the composition of the groundmass feldspars in the bulk of the stock, and the range in composition is also larger. This alkali feldspar then developed a fine patchy perthite which has a K-rich phase of composition $Or_{90-94}Ab_{6-10}An_0$--a very pure perthitic phase. In most cases, the Na-rich phase is too small to analyze with the probe.

The chief differences between the early igneous phase and the rest of the stock are the presence of the $An_{27}$(B) cloudy plagioclase replacement of earlier more sodic plagioclase (D), and the presence, magnitude and composition of the calcic rims and groundmass plagioclase laths (C). By analogy with the plagioclase phenocrysts of the rest of the stock, the rim is similar to the reversals in composition in the outer parts of the sodic plagioclase zones of the stock plagioclases. However, it is consistantly broader and more calcic in composition, and appears to be timed with the widespread nucleation of the plagioclase of the groundmass at the beginning of the groundmass crystallization stage.

Minor Minerals of Early Igneous Phase

The minor minerals of the early igneous phase of the stock consist of hornblende, biotite, magnetite, diopside, sphene, apatite, and secondary chlorite. The volume percentage of these minerals is consistently about 20-25 per cent, much higher than in the bulk of the stock. In terms of the origin of the feldspar textures discussed above, the relationships among these minerals is very informative.

In any given specimen of the early igneous phase, the chief mafic minerals are hornblende, biotite, diopside and magnetite. In some specimens, only hornblende, biotite and magnetite occur. In other specimens, however, the hornblende is consistently rimmed by diopside, similar to that described in the mafic minerals of parts of the stock.

As a rule, there are two distinct generations of mafic minerals, a microphenocryst stage with crystals up to 1 mm in size, and a groundmass stage in which all crystals are below 0.3 mm in size. In the hornblende, biotite, and magnetite bearing rocks, all three mafic minerals have a groundmass generation of similar appearance. In the cases where the hornblende microphenocrysts are rimmed by diopside, however, the second generation consists of diopside, biotite and magnetite. As a rule, the sphene is concentrated in the groundmass crystallization stage.

The high mafic percentages, and the diopside-after-hornblende sequence, both strongly suggest the addition of assimilated Ca,Mg-rich material, probably impure carbonate rock from the country rock. In support of this, assemblages of minerals in the thin contact metamorphic zone around the stock contain for the most part hornblende and diopside, as do inclusions of the same rocks within the stock.

Crystallization History of Early Igneous Phase

The following sequence of events for the early igneous phase is suggested (Fig. 27). The initial crystallization was essentially that of the rest of the stock as already outlined, with calcic, then intermediate plagioclase (A) crystallization, followed by sodic plagioclase (D) and sanidine. However, sometime late in the two-feldspar crystallization period, significant amounts of carbonate-rich material were assimilated by the stock. This initially caused the replacement of the sodic plagioclase by the slightly more calcic plagioclase (B), and at the start of groundmass crystallization, the formation of the $An_{55}$ rims and groundmass plagioclase lath cores (C).

The mechanism of initiation of groundmass crystallization could have been via rapid depressuring of the system, or it could be in part related to the rapid assimilation of large amounts of wall rock material. In this regard, the sudden drop from the $An_{55}$ plagioclase of both the rims and groundmass plagioclase laths, to sodic $An_{23}$ or less compositions is difficult to understand, since if large amounts of dolomitic material were added to the system, the bulk composition should

be permanently changed and the system would then ideally finish crystallizing with much more calcic plagioclases than actually observed.

After the calcic plagioclase crystallization, it appears that the system rapidly changed back to what would be considered to be an almost normal composition for the stock at approximately this stage of crystallization. This suggests that there was significant addition of normal granite to the more calcic phases near the contacts of this earlier igneous mass. The abruptness of the composition change would be a direct reflection of the abruptness with which the normal granitic material was added. The simplest model would be that of an assimilation produced contact phase which is rapidly intermixed with unchanged interior parts of the same igneous body.

In this respect, the differences in the inclusions of the early igneous phase are informative. Those with the best developed calcic rims and calcic plagioclase laths have the least normal phenocrysts and groundmass alkali feldspar and quartz. Those with the poorest developed calcic rims, and the smallest calcic cores in the plagioclase laths, have the most normal alkali feldspar and plagioclase phenocrysts and have the largest amounts of groundmass alkali feldspar and quartz. Indeed, in one of the inclusions, no calcic cores and rims were detected at all, and, except for the percentage of phenocrysts, this specimen would be identical to DV74, with sodic plagioclase cores in the groundmass alkali feldspar. In one case, an inclusion similar to this latter case was found which had, in turn, an inclusion of its own which showed well developed calcic plagioclase lath cores and calcic rims. Hence it appears that all gradations are present between relatively normal stock granite, and the most calcic of the early igneous phase rocks. This is compatible with the normal granite, then assimilation, then further addition of normal granite sequence postulated above, with the variations produced by the degree of initial assimilation and the amount of later mixing of granitic material.

Other types of inclusions are rare within the stock, and consist mainly of fragments of the wall rock of various types. These will be described in the section on minor minerals to follow.

## Minor Minerals

The common minor minerals in the stock include hornblende, biotite, magnetite, sphene and apatite. In most cases, all these minerals are present in a given specimen, and their total volume percentage is 10 per cent or less. The most mafic-rich phase is the interior portion of the north phase of the stock, in which the percentage is consistently above 7 per cent. In some of the contact phases, the percentages of mafic minerals is consistently less than 2 per cent.

The minor minerals range in size from 0.2 to 5 mm in longest dimension, and therefore can be considered as microphenocrysts in many cases. Of the four common minerals--hornblende, biotite, magnetite and sphene--only magnetite is commonly anhedral. It forms irregular shaped grains scattered throughout the groundmass which are seldom greater than 1 mm in size.

The hornblende, of the common igneous variety, occurs as euhedral elongate prisms which show no preferred orientation within the bulk of the stock. They range in size from 0.2 to 5 mm, and are the coarsest-grained of the mafic minerals. The pleochroic formula is generally $\alpha$ = light green or yellow green, $\beta$ = green or yellow green, and $\gamma$ = light to medium green or brownish green. The 2V, as measured on the universal stage, is 72 to 76°, and $\gamma$:c is 12 to 13°. This suggests an Fe/Fe + Mg + Mn ratio of about 0.5.

Biotite occurs as plates which range in form from euhedral to ragged and irregular, and is strongly pleochroic, with colors ranging from light brown or yellow-brown to dark brown or red-brown. It tends to be of slightly smaller size than the associated hornblende. The biotite occurs in one of three situations--as scattered individual grains, as grains associated with hornblende and magnetite in aggregates in the ground mass, and as grains associated with hornblende and biotite in plagioclase glomeroporphyritic aggregates.

Sphene occurs as euhedral crystals, 0.1 to 0.6 mm in size, which are often skeletal in form. In many of the specimens studied, very small, euhedral grains of apatite are present as a replacement product of sodic plagioclase and alkali feldspar.

The crystallization sequence of the mafic minerals is very difficult to determine due to the tendency of these minerals to form separately and not be found as inclusions in the feldspar phenocrysts. However, a few such inclusions make the following generalizations possible.

Biotite, hornblende and magnetite started to crystallize together roughly at the time that the andesine zones were crystallizing in the plagioclase phenocrysts, and there is some suggestions that of the three, magnetite was the first to form as it is consistently found as inclusions in both biotite and hornblende. Sphene was slightly later than the above minerals, and apparently began to crystallize during the later stages of andesine crystallization. Apatite texturally is late and appears both as inclusions in the last hornblende and biotite to form, and as a replacement produce of the oligoclase phenocrysts and groundmass feldspars.

As a rule, over 95 per cent of the mafic minerals occur wholly within the groundmass. In the rocks which have the very obvious, large, crystals of biotite and hornblende, there appears to have been at least two periods of growth. All the biotite and hornblende found as inclusions in the sodic plagioclases occurs as very small grains, some 10 per cent of the size of the large crystals in the groundmass. This observation is so common that it appears that the mafic minerals crystallized very slowly at first, but after the time of oligoclase crystallization, crystallization was very rapid, giving rise to the large crystals of biotite, hornblende and possibly magnetite.

## Hornblende and Related Minerals

The pleochroic green to brownish-green hornblende, characteristic of all the various phases of the stock, often contains a core made up of an aggregate of normal biotite grains which in many cases is physically connected with the groundmass. Indeed, numerous hornblende crystals are almost skeletal and have "cores" of groundmass quartz and alkali feldspar. The biotite, which is definitely later than the hornblende in all cases, apparently has replaced a preexisting

mafic mineral which formerly occupied the cores of the hornblende crystals and which in other cases has been resorbed entirely. The morphology of the better preserved cores suggest the original mineral was a pyroxene.

In one specimen collected in place in the southern phase of the stock, augitic pyroxene cores occur in two hornblende crystals, and similar occurrences were found in a float boulder in Surprise Canyon. In all cases the augite is in the form of an aggregate of crystals. Optical study indicates that it is indeed a true augite, relatively rich in Mg and Ca but not quite enough to be called a diopside or diopsidic augite. This appears to be the original mineral which formerly occupied the cores in the other hornblende crystals so common in the stock.

In the bulk of the stock, biotite consistently replaced hornblende, and in a few instances biotite forms aggregate rims around the hornblende crystals.

In ten specimens from both phases of the stock, undoubted reaction rims of pyroxene occur on the hornblende crystals, and a few pyroxene pseudomorphs after hornblende were also noted. In all cases the pyroxene rims are thin and do not make up a significant percentage of the mafic minerals. Optical study indicates that the pryoxene is a true diopside, and hence it is definitely more Mg-rich than the augite cores noted above. Rarely, the diopside appears to be altering to biotite.

The majority of the late diopside bearing specimens are located relatively close to the stock contacts, and three of the specimens are within 1 m of a stock contact in which a diopside-bearing scarn zone occurs. The distribution of the late diopside suggests that the assimilation of dolomitic wall rocks could have added the required Mg and Ca.

There are almost no discreet inclusions within the stock which can be traced back to a dolomitic wall rock origin. In the contact areas noted above, the scarn material seems to disaggregate immediately into separate crystals, which may account for this fact. There are

numerous less than 1 cm irregular clots of minerals throughout the stock which consist of hornblende and biotite with some sodic plagioclase, magnetite and sphene, and it is entirely possible that these represent inclusions of Ca-Mg rich material. The hornblende and biotite are similar to the same minerals in the stock, and also are the same as these same minerals in contact hornfelsic rock in relatively carbonate-rich zones of the Kingston Peak Formation. It appears that these clots, which apparently formed at the time the later sanidine and sodic plagioclase was forming in the stock, are the result of the assimilation of relatively calcareous wall rock. Their uniform distribution throughout the stock indicates that this period of assimilation took place at a deeper level.

Studies of the compositions of pyroxenes in various acidic differentiating systems indicate that the pyroxene tends to become less Mg, more Fe-rich in the later stages of differentiation, and this is borne out by the recently determined liquidus diagram of the pyroxene quadrilateral (Yoder, Tilley and Schairer, 1963, p. 85). Hence in the simplest case, in the stock, the later pyroxene should be more Fe-rich. The fact that it is more Mg-rich strengthens the assimilation hypothesis.

Biotite

Biotite, ranging in pleochroism from light to dark brown to red-brown, is present in all specimens of the stock. In a few cases, in the southern phase of the stock, there are two generations of biotite--the relatively coarse biotite up to 1 mm in size which grew in the late phenocryst stages, and a fine grained less than 0.2 mm generation of biotite entirely restricted to the groundmass. The later, finer-grained biotite is consistently less pleochroic, reaching only medium brown colors, and appears to have slightly lower refractive indices than the earlier phase of the biotite.

The difference in optical properties of the two generations of biotite indicates that the later groundmass biotite has a higher Mg/Mg+Fe ratio than the earlier biotite. This observation is reinforced by a few of the larger biotite crystals which have distinctly less

pleochroic edges with lower indices which also appear to be of a more Mg-rich biotite.

The appearance of a later Mg-rich biotite is compatible with the assimilation of dolomitic material suggested by the diopside rims on the hornblende crystals noted above. However, it is possible that the later Mg-rich biotite could be due to $P_{O_2}$ effects. According to the work of Wones and Eugster (1965), as the water pressure on the biotite-magnetite-sanidine assembledge decreases, the Mg/Mg+Fe ratio of the biotite could increase if the temperature of the system remained relatively constant. This mechanism would favor the formation of a more Mg-rich biotite in the groundmass on depressuring of the system, and would fit the general intrusive history of the stock.

The above $P_{O_2}$ model would be favored if the $P_{O_2}$ remained relatively high in the late stages of groundmass crystallization, since this would allow more Mg-rich biotites to form also. In support of this, it is noted in a few of the volatile rich specimens that the magnetite has in part altered to hematite, and some of the biotite, at the outer edges, appears to have altered to magnetite (or hematite).

Thus, both the assimilation process, and plausible $P_{O_2}$ variations in the biotite-magnetite-sanidine system, could produce late Mg-rich biotite, and at this point, it is not known which process is the dominant one. It would seem likely that the $P_{O_2}$ based process could dominate the volatile-rich fringes of the stock and dike rocks, at the present erosion level, as observed, while the assimilation process could dominate the less volatile-rich areas.

Throughout much of the interior of the northern phase of the stock, the biotite, and commonly the hornblende, grains have altered to chlorite on their outer margins. In some places, whole biotite grains have been replaced by chlorite. This reaction appears to have occurred after crystallization of the groundmass of the stock, as small, less than 0.05 mm radial clusters of chlorite are found in patches in the feldspars of the rock also. The restriction of the chlorite alteration to the interior portion of the stock suggests that this is, in effect,

a retrograde reaction which occurred in the relatively slower cooling interior parts of the stock.

A summary of the crystallization sequence of the minor minerals indicates the following. Initially, augite and probably magnetite crystallized along with the labradoritic plagioclase. By the time that the andesine was crystallizing, the augite was out of equilibrium and was rimmed by hornblende which coexisted with both biotite and magnetite. About the time that oligoclase and sanidine were forming, sphene was also crystallizing, yielding four coexisting minor minerals.

The mafic minerals biotite, hornblende and possibly magnetite existed as small crystals which were growing very slowly until the last of the sanidine and oligoclase was crystallizing. However, about the time that the reversals on the oligoclase were being formed, the mafic minerals started to grow very rapidly, yielding very large crystals of hornblende, biotite and magnetite. Apatite appeared at this point as discreet crystals in the melt and as a replacement product of the sodic plagioclase.

Apparently immediately after the period of rapid mafic mineral growth, at roughly the later stages of the sanidine replacement stage when the very sodic plagioclase was crystallizing, the hornblende was rimmed by diopside, apparently due to the assimilation of dolomitic material. This particular feature occurred immediately before the groundmass crystallization stage, but the common occurrence of clots of hornblende, biotite, magnetite and oligoclase or more sodic plagioclase suggests that the assimilation of basic rock had probably been occurring at least as far back in the crystallization sequence as the time of the reversals on the oligoclase grains.

At the time of depressuring of the system, when the groundmass rapidly formed, the stable minor minerals were apparently biotite, magnetite, apatite and sphene. In the southern phase of the stock a second generation of more Mg-rich biotite formed in the groundmass, and in other areas of the stock, a more Mg-rich biotite apparently crystallized on preexisting less Mg-rich biotite crystals. In a very few instances, the diopside rims were altered to biotite, and everywhere in

the stock, the preexisting hornblende was altered in various degrees to biotite. The second generation biotite could have been caused by the depressuring effect on the $P_{O_2}$ equilibria, or by the assimilated material.

After the bulk of the groundmass had crystallized, in the marginal volatile-rich areas of the stock magnetite reacted to hematite and biotite reacted to magnetite or hematite, indicating high $P_{O_2}$ at this late stage. In the immediate vicinity of vuggy cavities, oxybiotite was formed around the edges of the biotite crystals. Similar reactions took place in the dike rocks. In the interior of the stock, where cooling was relatively slower, retrograde chlorite formed from biotite and hornblende.

## Distribution of Textures Within Stock

### Distribution of Phenocryst Replacement Textures

The thin sections of the various specimens collected from the stock were used to determine the dominant form of replacement texture in the sanidine phenocrysts relative to the several specimens described in detail in the previous sections. The simplified classification used was as follows: If the thin sections showed a dominance of clear plagioclase rims with oscillatory zoning reversals on clear sanidine cores, with some unrimmed sanidine or cloudy plagioclase phenocrysts of probable replacement origin, they were referred to DV56--a resorption-rimming sequence. If the thin sections showed a dominance of clear sanidine cores surrounded by distinct cloudy plagioclase plus quartz bleb rims, outer alkali rims, occasional cloudy perthite in the sanidine, and common single cloudy plagioclase phenocrysts, they were referred to DV74--a direct replacement sequence. Thin sections showing a predominance of cloudy alkali feldspar, patch perthite, concentrations of patch perthite in the "rim" position, dominately cloudy plagioclase phenocrysts with or without relict alkali feldspar patches, and common alkali rims were referred to DV151--a patch perthite replacement sequence. Finally, slides showing no replacement of the sanidine, no plagioclase rims, a very coarse groundmass, and a predominance of coarse lamellar

perthite were referred to DV128--an unreplaced sequence.

Many slides were transitional between types, and as a general rule, the DV56 resorption-rimming type graded into the DV74 direct replacement type by an increase in the number of grains with features typical of DV74. The DV128 unreplaced type graded into either the DV151 or DV74 types, and the latter two were often mixed indiscriminantly with no particular pattern considering these two alone.

The distribution of the replacement types is shown in Fig. 28. The two intrusive phases of the stock will be considered separately.

The northern phase of the stock shows the greater variation in replacement textures, as shown in the figure. The area with the horizontal ruling shows the extent of the DV56 resorption-rimming type sequence. Invariably associated with the dominant clear sanidine cores and plagioclase rims of the alkali feldspar phenocrysts in these slides are variable amounts of feldspars which show the DV74 type distinct cloudy plagioclase replacement rims. As a rule, the percentage of these grains increases outward toward the edge of the area until this textural type dominates. Hence, the outer edge of the resorption-rimming dominant area is transitional and the contact as marked is only approximate. However, in all cases where there is adequate control, it appears that this texture is no longer dominant by the time the outer relatively sharp contact of the interior light colored portion of the stock is reached. In all cases, there is a buffer zone of DV151 and/or DV74 dominant textures around the core of the DV56 resorption-rimming type sequence.

The areas of the northern phase of the stock in which the dominant textures of the alkali feldspars are of various combinations of the DV151 and DV74 types is shown by the unlined areas on Fig. 28. Within this area in general, the DV151 type appears to be slightly more common and may tend to concentrate in the outer portions of the area. All combinations between various amounts of phenocrysts showing either the direct replacement or patch perthite replacement sequences are found, and indeed, many of the phenocrysts themselves cannot be classed as one or the other, but are transitional grains. Hence it appears that

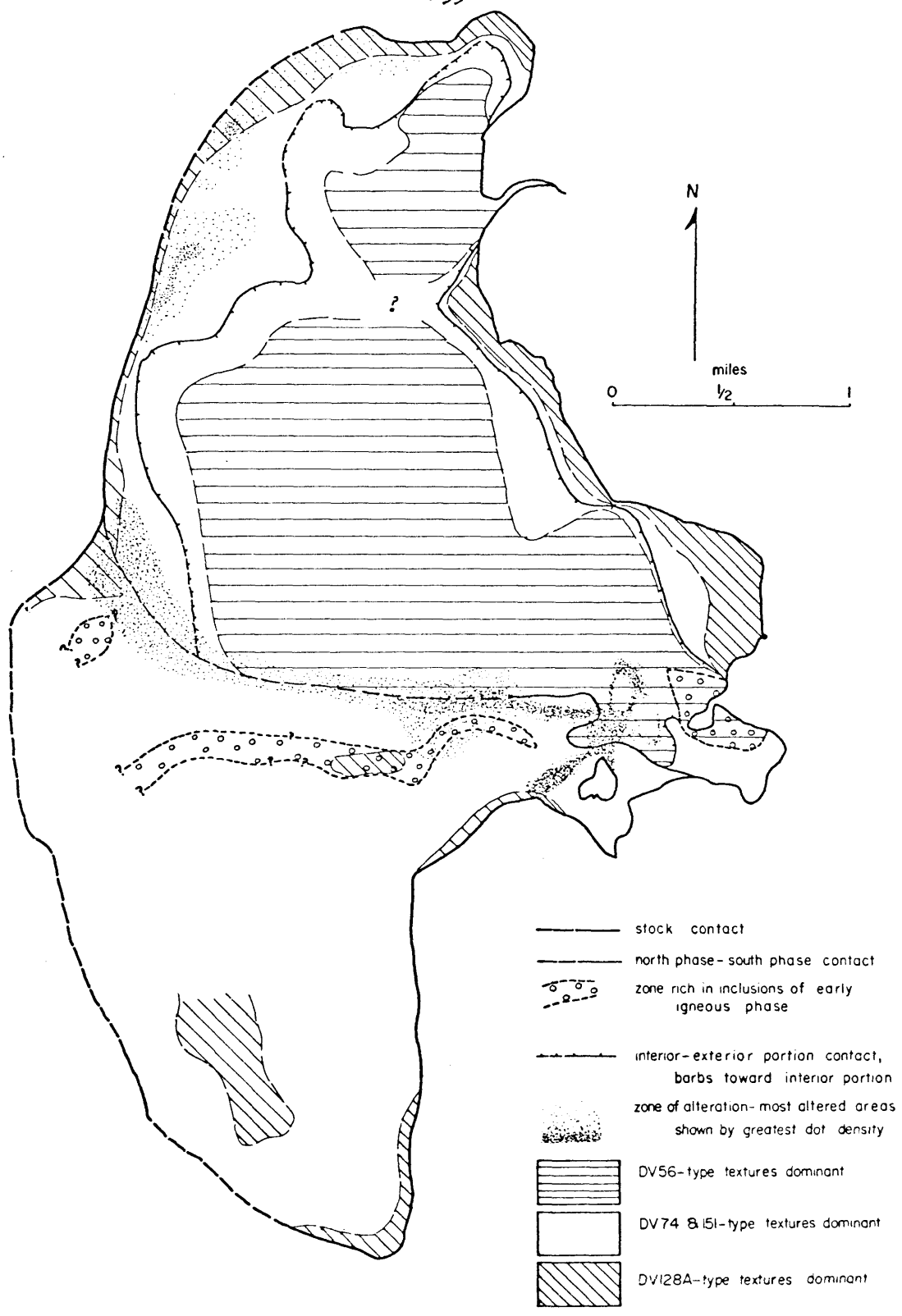


Fig. 28. Map showing distribution of replacement textures in stock.

these two processes took place under closely similar conditions, allowing the intergradations to occur as commonly as they do.

Note that the textures on either side of the exterior-interior portion contact in the northern phase of the stock are indistinguishable, again reinforcing the suggestion that the two portions were intruded within a very short time period.

The diagonally ruled areas around the margins are those areas in which the DV128 unreplaced type alkali feldspars are found. Again the contact is transitional, and these textures gradually pass into rocks dominated by the direct replacement or patch perthite replacement textures. In effect, the appearance of the dominant DV128 type area is due to a gradual increase in the percentage of unreplaced phenocrysts until they dominate the phenocrysts. At the same time, and apparently over a much shorter distance, the percentage of magmatic plagioclase phenocrysts decreases to zero so that in most of the area in which the unreplaced alkali feldspars occur, no plagioclase phenocrysts are found at all, and the rock consists of alkali feldspar and quartz. The percentage of mafic minerals also decreases markedly in these alkali-rich rocks, and in most cases, they contain less than 2 per cent by volume of biotite, hornblende, magnetite, sphene and apatite.

In essence, two types of gradations exist which must be differentiated. In one case, all possible combinations may be seen between the "end-member" textures within the phenocrysts, as for instance all variations between the direct and patch perthite replacement sequences. This implies that, since these intermediate textures could exist, they also existed on a gradation between the physical conditions that produced these textures.

In the other case, and on a much larger scale, gradations occur between large areas dominated by phenocrysts having one of the replacement sequences and areas dominated by phenocrysts showing another sequence. In this case, it often appears that the phenocrysts of one type have been physically intermixed with the phenocrysts of another type, suggesting that mixing between discreet magma pulses at their contacts may have taken place on intrusion.

The southern phase of the stock is considerably simpler than the northern phase. The bulk of the southern phase, shown as unruled in Fig. 28, consists of alkali feldspar phenocrysts of the DV74 direct replacement type with some phenocrysts showing the DV151 patch-perthite replacement type, and, as before, a few grains showing transitional type textures. However, the DV74 type is clearly the dominant type, in contrast to the unruled area of the northern phase of the stock. The sanidine cores tend to have a minimal development of cloudy perthite. Only along the highest parts of the southern phase does the DV151 type become significant. This region is felt to be quite near the roof of the stock.

Again, these textures tend to grade outward into a DV128 type unreplaced sanidine rock, as in the northern phase, by an increase in the number of unaltered sanidine phenocrysts and a decrease in the number of plagioclase phenocrysts. The area in which the DV128 unreplaced texture dominates is shown on Fig. 28 by the NW rules lines.

The DV128 type rocks of the northern phase are characterized by an abundance of lamellar perthite. The DV128 rocks of the southern phase, however, are essentially completely lacking in lamellar perthite, especially in the southern part of the southern phase. The alkali feldspars are thus the most unaltered and unreplaced anywhere in the stock. However, their external form is not euhedral, but subhedral with rounded off corners. There is no evidence of resorbtion, and it appears that the sanidine grew in this form from the melt. The composition of these feldspars is roughly that of the sanidine phenocrysts of specimen 182D, namely $Or_{41}Ab_{58}An_{1}$. In some of the more northern areas of the southern phase in which the DV128 texture dominates, small amounts of lamellar perthite are present, but never in amounts as great as those in the similar rocks of the northern phase.

The distribution of the rocks in which the DV128 unreplaced textures dominate is unique in the southern phase of the stock in that, while it occurs dominantly along the contact, it also occurs in two areas in the center of the stock as shown in Fig. 28. These areas are topographically high suggesting proximity to the roof of the stock.

A roughly similar feature is noted in the northern phase of the stock, where the contact of the light colored coarse and dark colored fine portions, and the contact of the DV56 texture dominated area, also tend to cross the stock in an area away from the contact. Again, this occurs on a major ridge which crosses the stock, suggesting proximity to the stock roof, although in the northern phase the actual roof contact may be slightly higher above the present topographic surface than in the southern phase.

Distribution of Groundmass Textures

The groundmass of the southern phase of the stock has an aplitic texture throughout almost the whole of the southern phase. As a rule, the interior portions of the southern phase has a groundmass which falls in the size range of 0.3-0.5 mm. As the contact is approached, the grainsize in general decreases to roughly 0.15 mm or less except in those areas characterized by DV128 type textures where the groundmass percentage markedly decreases as the grainsize coarsens.

Thus the local coarsening associated with the DV128 textures is superimposed on a more general decrease in groundmass grainsize as the contact is approached. In this respect, it is interesting to note that all the samples collected in the northwest corner of the southern phase of the stock have groundmasses very close to 0.1 mm in size. These samples are all located on the Panamint Range divide, above 9600' elevation, suggesting proximity to the roof of the stock. This is the same ridge which contains the area of DV128 unreplaced textures within the stock in its southern portion, as noted on Fig. 28. Thus, both grainsize variations and textural variations tend to support the suggestion that the roof of the stock was relatively close to the present elevation of the ridges in the southern phase of the stock--probably within a 1000' feet or so judging by the widths of the various zones in question along the present stock contacts. These near-contact areas, either actual or suggested, also contain rare pegmatitic patches and vermicular quartz-alkali feldspar patches in the groundmass, both features common to rocks in the northern phase of the stock very near

the contact.

The groundmass grainsize and textural distribution in the northern phase of the stock is roughly analogous to that in the southern phase. The normal texture of the interior of the northern phase is a granitoid texture which tends to change as the contact is approached. In general, as the western contact is approached, the groundmass texture becomes more aplitic and the grainsize decreases from the 0.3-0.5 mm size range of the interior to grainsizes of less than 0.2 mm toward the contact. Once again, in those areas which contain the DV128 phenocryst textures, the groundmass locally coarsens. As a rule, the percentage of plagioclase in the groundmass decrease to almost zero as the contact is approached.

Going from the interior toward the eastern contact, the granitoid texture persists and the grainsize again in general decreases to the 0.2-0.1 mm size range, with the exception of the unreplaced phenocryst bearing rocks as noted elsewhere. However, a major difference between the eastern and western contacts of the northern phase of the stock is in the amount and distribution of pegmatitic pods, and vermicular and graphic quartz-alkali feldspar intergrowths.

Aside from the northeast corner of the stock, the eastern and southern margins of the northern phase of the stock are relatively rich in the above features. The presence of the lamellar perthite is also more widespread in these areas, and it tends to be significantly coarser than in other areas in the stock.

The pegmatitic pods and quartz-feldspar intergrowths so common near the eastern stock contacts are also found along some of the highest ridges transecting the northern phase of the stock, including the ridge already noted in the discussion of the distribution of the replacement textures (Fig. 28). This again supports the suggestion that the roof of the stock was not very far above the present ridge tops in the outcrop area of the stock.

The large irregular quartz crystals that were briefly noted in the last parts of the discussion of specific samples, are more common in the rocks nearest the contact of the stock. This is true of both

the northern and southern phases of the stock. As the amount of pegmatitic pods and quartz-feldspar intergrowths increases, the amount of these irregular quartz crystals also increases.

Origin of the Groundmass Features

The presence of very high percentages of extremely large vugs in the northern phase of the stock, plus the observation that the great majority of the rocks in the stock contain from 0.5 to 2 per cent by volume of vugs, indicates that, at least in the stage of groundmass crystallization, the effective fluid pressure was equal to the total or lithostatic pressure, allowing a separate fluid phase to form. The extreme fluid concentration in the northeastern corner of the stock, and the fact that the dike swarm meets the stock in that area, both suggest that this concentration of volatile material is due to fracturing of the roof rocks and rapid volatile release. An obvious analogy is the sudden opening of a pop bottle, allowing the gas bubbles to concentrate at the point of pressure release.

The dike swarm observed to the northeast of the stock is clearly older than the granite of the north phase of the stock, which contains the numercus vugs and other features, and the time gap is large enough that chilling of the later granite occurred against the earlier dike swarm. Hence, it was not possible to trace a vug-rich band or zone of the granite into a dike rock which travels some distance from the stock contact. Nonetheless, the orientation of the vug-rich zones into bands or zones with vertical dips which are essentially perpendicular to the contact nearby indicates that these vug-rich zones could indeed be due to a pressure release effect like the one postulated. Considering the position of the vuggy-rich area, at an elevation of roughly 6000 feet, it is quite conceivable that a possible dike-stock intersection, or at least a fracture-stock contact, could have been present above the present outcrop area in a part of the stock now removed by erosion. The proximity of the supposed stock roof to the present ridge tops, however, indicates that this intersection was not very far above the present erosion level. Basically, what is required

is some sort of opening to a lower total pressure area to allow the volatile concentration and escape.

The timing of the pressure release is thought to be coincident with the time of groundmass crystallization and alkali rim formation. A sudden release of fluid pressure could cause the apparent sudden nucleation of alkali feldspar (and quartz in some cases) on the preexisting alkali feldspar or plagioclase phenocrysts. At this point, the rate of crystallization would then be effectively controlled by the rate of heat loss to the exterior. That this rate of heat loss was relatively large is attested to by the fine grain size of the groundmass even in the most interior parts of the stock. Relatively more rapid cooling in the exterior parts would then produce the general decrease in groundmass size toward the outside of the stock.

The fewest, and thinnest, alkali rims are observed in the interior portions of the stock, and most of the area of the light colored coarse portion of the north phase of the stock has no alkali rims except at the outer edges. This is compatible with the cooling model proposed in that the less rapid cooling of the interior portion would inhibit rim formation.

The chief active component of the fluid phase was most probably water, as has been noted before in numerous cases. The effects of water pressure on the "granite" system, under conditions where the water pressure is equal to the total pressure, are now relatively well known. However, other components are quite likely in the fluid phase--for instance Cl, F, P, and $NH_3$--as these have been observed in fumerolic situations, or as fluid inclusions. Recent experiment work by Von Platen (1965) and Wyllie and Tuttle (1961, 1964) has dealt with the changes introduced in the Ab-Or-Q system by these components.

Apatite is ubiquitous as an accessory mineral in all the rocks of the stock and the refrective indices and birefringence indicate that it is dominantly fluorapatite. Hence the melt, at relative late stages when apatite crystallized, contained both P and F, but probably very little Cl. Both F and Cl could occur in the hornblende and biotite also.

In terms of the minerals found in the drusy cavities within the stock, no minerals indicative of the above components are found. This is also true of the vugs in the rocks of the dike swarm.

However, in the vugs within the rocks of the dike swarm, calcite is commonly found, and while the textural relations are not conclusive, it is felt that calcite crystallization was associated with the vapor phase within the vugs. Thin reaction zones, usually less than 2 inches thick, are found at the stock contacts with wall rock calcsilicate minerals indicative of decarbonation of the carbonate country rock. Within the area of the dike swarm nearest to the stock, formation of calcsilicate minerals is widespread throughout the carbonate rocks of the Sourdough Limestone Member of the Kingston Peak Formation. Finally, the stock is essentially completely enveloped by carbonate rocks, mostly dolomitic. Hence, significant amounts of $CO_2$ were probably present in the vapor phase, especially in the dike rocks.

This observation is bolstered by the presence of reaction relationships between diopsitic augite and hornblende, which, as discussed more fully in the section on the major accessory minerals, suggest that some assimilation of carbonate material did occur. Any assimilation of this sort would contribute carbonate to the system. Hence, aside from water, the chief component of the vapor or fluid phase was probably $CO_2$.

Studies by Wyllie and Tuttle (1959) indicate that, under fluid pressure=total pressure conditions, $CO_2$ is for all practical purposes an inert component. That is, at a given total pressure made up of x partial pressure of water, and y partial pressure of $CO_2$, the granitic melt behaves as if it were crystallizing under an effective fluid pressure=x, with some slight increase in liquidus temperatures due to the effect of the larger real total pressure by the amount y of $CO_2$. Hence $CO_2$ appears not to significantly effect the melting relationships as does water, and thus in working with the feldspar-quartz experimentally determined feldspar-quartz systems, $CO_2$ can be neglected in most cases. However, with regard to the mechanism of fracturing and pressure release in the stock, $CO_2$ cannot be neglected and, in fact,

may be an exceedingly important factor in the type of mechanism postulated.

One method by which the stock roof could be fractured is by the vapor pressure in the system building up to values greater than the load pressure. The presence of $CO_2$ as well as water in the vapor phase makes this process more likely, especially in the light of the high volatile concentrations necessary to form the vug-rich areas of the stock. Since the stock at its present position was relatively shallow in depth below the earth's surface, the vapor pressure would not have to build up to very high values before fracturing of the rocks over the stock could take place.

However, the possibility must be considered that fracturing of the roof was caused by upward emplacement of the magma body, so that at the time of fracturing the fluid pressure need not have been equal to the load pressure.

Features which seem to be closely associated with large amounts of volatile components in the groundmass include the vugs, the large irregular quartz crystals, pegmatitic pods, graphic or vermicular quartz-alkali feldspar intergrowths, and very coarse lamellar perthite. These all tend to concentrate in the areas with the largest and most numerous vugs and hence are especially common in the northeast corner of the stock. This direct relationship, plus the common occurrence of some of these textures in pegmatites known to be rich in volatile components, indicates that in this situation, these features are also due to variations in the volatile content of the system.

The features listed are distributed in roughly the following ways. The most common features are the irregular quartz crystals and the small vugs, both of which are present in all but the most interior parts of the northern phase of the stock. The next most common texture is the quartz-feldspar intergrowths, which are present in various localities around the edge of both phases of the stock. The coarse lamellar perthite is somewhat more restricted, but is also found in the contact areas of the stock, especially along the eastern side. The least extensive, but most spectacular, are the larger pegmatitic

pods and patches, and the large vugs, both of which are commonly found only in the extreme northeast corner of the stock. Smaller micropegmatitic patches are found throughout much of the stock, but are most common close to the stock contacts. Finally, porphyroblast-like megaphenocrysts, usually sanidine, are found throughout the stock.

All the features but the last appear to be closely related to the time of groundmass crystallization, and all appear to have been related to the volatile content. The distributions above suggest that the first response of the groundmass, during crystallization, to high volatile concentration was to form the irregular quartz crystals. This was not vapor phase crystallization as such, but rather an accelerated crystallization rate due to the presence of the volatile components. Whether a separate vapor phase existed at this time is not known.

The next step in the tentative sequence would be the formation of the quartz-feldspar intergrowths. At the same time, pegmatitic pods of smaller size could form as an extension of the earlier quartz crystal growth. Hence, rocks exist which contain the intergrowths and the quartz crystals, or the intergrowths and the smaller pegmatitic pods. In the latter case, the amount of intergrowth material is much larger. The last to form, in the areas of highest vilatile concentration would be the large pegmatitic pods and widespread graphic textures common in the northeast corner of the stock.

The distribution of the coarse lamellar perthite suggests that it too is related to the volatile concentration of the system, and is probably late in the above tentative sequence.

This picture would then suggest higher volatile concentrations in the exterior parts of the stock, since in all cases, the features attributed to crystallization catalyzed by volatile content are found near the margins of the stock. The textural relationships of the intergrowth textures suggests that this was a late feature in the groundmass crystallization, so that the percentage of melt present at this time would have been relatively small and a vapor phase as such probably existed.

The time of formation of the megaphenocrysts of alkali feldspar was significantly earlier than the above features. Thin section study indicates that these formed at the same time as the last of the sanidine phenocrysts formed, before the period of replacement and while plagioclase was also crystallizing from the melt. It is tempting to attribute the megaphenocrysts to accelerated growth due to increased volatile concentrations at the later stages of crystallization. This would also be compatible with the model proposed previously in which the stock roof was fractured by the build up of volatile pressure. The more common occurrences of the megaphenocrysts in the northern phase of the stock would be related to the more common occurrence of features indicative of high volatile content in that phase of the stock.

Detailed zoning and compositional features in specimens DV56 and DV151, from the time of removal of sanidine from equilibrium with the melt, to the sudden quenching of the system and formation of the groundmass, would be compatible with a slow build up of fluid pressure in the system leading to the roof fracturing stage.

Alteration Zone

One of the more obvious features of the stock in the field, and on air photographs, is a broad band of red-brown and yellow-brown altered granite which essentially follows the southern and western boundries of the northern phase of the stock. This is shown in Fig. 28 as the stippled area, and the two intensities of stippling indicate the degree of alteration of the granite. The zone is 100 to 1000 feet wide, and the contacts vary from very sharp to broad transitional zones. It is invariably associated with contact dike sheath rocks which themselves have been altered.

In the areas of most intense alteration, the rock is essentially a semi-consolidated aggregate of yellow-brown feldspar crystals and quartz crystals which will crumble quite easily. In the slightly less altered areas, where thin sections could be cut, the rock consists of cloudy brown-stained alkali feldspar, translucent to opaque in many cases, in which the cleavages, fractures and cracks stand out as white

lines and form an almost brick-wall texture. The plagioclase is invariably sericitized, and the mafic minerals completely altered to hematite or hydrous Fe-oxides. In a few cases, hornblende which had altered to biotite, was in turn altered to sericite, so that sericite pseudomorphs after hornblende occur. Aside from the hematite, the only optically identifiable mineral in the alteration zone is sericite. No unusual ore minerals were found.

In the less altered areas, only the groundmass alkali feldspar, and the outer portions of the sanidine phenocrysts, are altered, and the plagioclase and mafic minerals are only slightly altered. In many cases, alteration is confined to the groundmass, and in the least altered areas within the alteration zone itself, alteration occurs only along fractures and joints in the rock. Fractures or joints with alteration zones are also present scattered throughout the stock, especially the volatile-rich northeastern portion of the northern phase of the stock.

The cause of the alteration is probably hydrothermal fluids which were localized along the outer margins of part of the north phase of the stock. The alteration may have occurred immediately after the emplacement of the dike sheath rocks, and the fluid may represent expelled volatiles from deeper portions of the stock which also supplied the later dike sheath rocks.

## Dike Rocks Associated with Stock

There are essentially two major dike swarms which cut the country rocks for various distances from the stock. The larger of the dike swarms intersects the stock in the Hanaupah Canyon area, at the northeast corner of the stock. This swarm is clearly earlier than the normal granite porphyry of the north phase of the stock, as the complex of porphyry dikes of the swarm are consistently cut by both the granite stock and apophyses of the granite into the country rock. The granite has thin chilled margins against the rocks of the dike swarm. Finally, in this same area, dike-sheath rocks cut both of the above and hence are last in the intrusive sequence. However, in the nearby vug and

pegmatitic pod-rich areas described previously, these same dike-sheath rocks are transitional into the stock granite.

In the Starvation Canyon area, the smaller of the two dikes swarms extends to the northeastern corner of the southern phase of the stock. Here, the dike-sheath rocks are clearly directly connected to the dike rocks of the swarm, so that it appears that they acted as feeders of the swarm. In this area, the dike-sheath rocks are always later than the granite of the stock. This relationship of a connection between the dike-sheath rocks and the dike rocks in the country rocks is seen in several single porphyry dikes in the country rock adjacent to the southern phase of the stock.

Dike Sheath

Along approximately 80 per cent of the contacts of the stock, a thin sheath of very fine-grained dike-like rock, 1 - 50 m thick, is interjected between the granite porphyry of the stock, and the country rock.

The relationships between the stock granite and the dike sheath rock are complex. In the majority of cases, the dike sheath rocks appear later than the granite, as they are chilled against the granite or rarely have bleached the adjacent granite. In cases like these, the adjacent granite may be either normal porphyry, or the groundmass-and plagioclase-poor contact phase of the granite described above. In other localities, however, the contact phase of the granite is clearly transitional into the rocks of the dike sheath. The transition between the two takes place, going from the sheath rock to the granite of the stock, by the appearance of small pods and bands of phenocrysts like those in the stock. These increase in size and number until the transition is complete, and no fine-grained dike-like material remains. Transition takes place over distances of 1 - 20 m. There seems to be no logical pattern to the stock-dike sheath age relationships.

In appearance, the contact phase rocks are typically very fine-

grained, white rocks with scattered, barely visible phenocryst and occasional pods and lenses of coarser material. The percentage of phenocrysts seldom exceeds 15 per cent by volume, and in many cases there are no phenocrysts.

The bulk of the contact sheath rocks consists of equigranular quartz and perthitic alkali feldspar crystals, ranging in size from 0.05 to 0.3 mm, with a uniform aplitic texture. The alkali feldspars are usually finely perthitic, and have compositions in the range $Or_{43-48}$ $Ab_{52-57}An_{0}$, as shown in Fig. 30 (D). In a few cases, the feldspars are very coarsely perthitic, and as shown in Fig. 29, often reach the point where the two phases have completely separated into different grains. Compositions of this type of completely exsolved feldspar are shown in Fig. 30 (D). In Fig. 29, some of the feldspar grains are wholly K-rich phase, others wholly the Na-rich phase, and the rest very coarse perthite. In one specimen all the feldspar, both in the aplitic groundmass and in the phenocrysts, had the compositions of the K-rich phase shown in Fig. 30, so that the rock consisted of only K-rich feldspar and quartz. Specimens like this, or of the completely exsolved type, are found along the overhanging portion of the contact of the southern phase of the stock, in the Starvation Canyon area, where the stock has a very thin contact sheath and is in contact with carbonate wall rock. It is not an area characterized by an abundance of lamellar perthite, pegmatitic pods, graphic textures and vugs. Just to the south, these same dike sheath rocks pass outward into dike rocks in the country rock.

The phenocrysts which occur in the dike sheath rocks are invariably alkali feldspar, and show almost all of the textures seen in the phenocrysts of the bulk of the stock. The predominant phenocrysts are those which are unreplaced and which have the coarse lamellar-type perthite. In a few instances, the phenocrysts are highly fractured and form fragments rather than whole crystals. The compositions of most of the phenocrysts are in the range of the compositions observed for the alkali feldspar phenocrysts in the rest of the stock, with the exception noted above. If any unusual alkali feldspar phenocryst compositions occur, they are always in the same short portion of the contact which

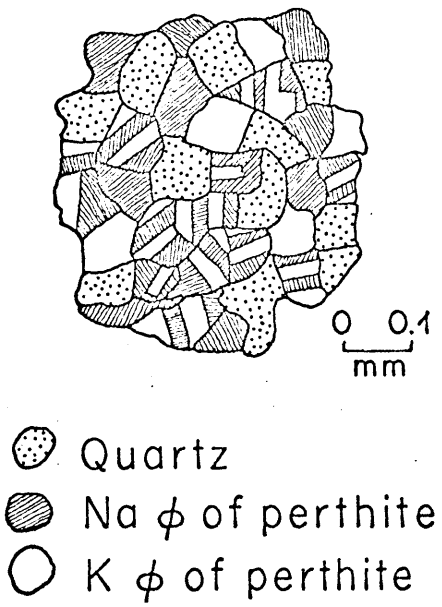


Fig. 29. Sketch of completely exsolved alkali feldspar in groundmass of contact sheath specimen.

contains the completely exsolved feldspars.

Specimen DV182D contains clear, equant, euhedral sanidine phenocrysts, completely unresorbed or replaced, which have compositions of $Or_{41}Ab_{58}An_1$. These are full of wormy 0.05 X 0.2 mm muscovite grains which appear to be altering from the sanidine. In some cases, the phenocrysts reach 75 per cent muscovite, but most of the phenocrysts have less than 30 per cent muscovite. No other phases, such as highly aluminous phases,were seen, and it appears that the reaction was sanidine + water yields muscovite + quartz + excess $K^+$. This particular rock contains fringes of graphically intergrown quartz and feldspar on the edges of the phenocrysts which grew at the time of groundmass crystallization--hence, there is the possibility that a fluid phase was present, or at least the volatile content was relatively high.

Several of the contact sheath rocks examined in thin section contain small, rounded, resorbed microphenocrysts of quartz. While these may have crystallized from the melt, there is a good possibility that they are xenocrysts. In one of the specimens examined, numerous inclusions of quartzite were found. The quartzite was made up of rounded quartz crystals of the same size as the phenocrysts in some of the other dike sheath rocks, and in this particular slide, some of the quartzite fragments had disaggregated and yielded single grains of quartz which, if seen elsewhere, would be indistinguishable from quartz phenocrysts. The scarcity of quartz phenocrysts throughout the stock suggest that indeed most of the quartz grains seen in several of the contact sheath specimens are xenocrysts.

## Dike Swarm Rocks

### Distribution

There are several large concentrations of porphyry dikes, all of which are found on the eastern side of the stock. (see Fig. 2) The major swarm of dikes occurs at the northeast corner of the stock in Hanaupah Canyon, and other smaller dike swarms occur in the Starvation Canyon area east of the stock.

The major dike swarm is approximately one-half mile wide in outcrop width at its widest point, and it extends for almost two miles to the south and more than four miles to the north, away from the stock. The widest point of the dike swarm is in the area closest to the northeast corner of the stock, where the dikes constitute almost 25 per cent of the outcrop width, for an aggregate thickness of 500 to 600 feet of porphyry dike material. The overall width of the dike swarm, and the density of dikes within the swarm, both decrease to the north and to the south, away from the northeast corner of the stock.

The major dike swarm dies out gradually to the north and at a point three miles north of the stock consists of less than four individual dikes which continue northward for another mile. To the south, however, the major swarm ends much more abruptly in a quarter square mile area of brecciated rock which occurs wholly within the upper Johnnie Formation. Here angular, broken fragments of dominantly Stirling Quartzite, Johnnie argillite, and possibly rare Noonday (?) dolomite occurs in a less than 0.1 mm matrix of microgranitic quartz and feldspar with rare broken alkali feldspar phenocrysts like those in the stock scattered throughout. This represents an explosion breccia related to volatile escape associated with the dike swarm emplacement which has been pervasively infiltrated by typical dike rock. The Stirling fragments are at least 500 feet down from their position over this vent area, and the questionable Noonday fragments are at least 800 feet up from their expected position.

The gross attitude of the individual dikes within the swarm is roughly north-south with 30 to 60 degree westward dips. In detail, however, the strike and dip of the dikes vary considerably and the dikes merge and separate at various low angles, so that viewed from a distance the whole presents the general appearance of an anastomosing stream. Dike junctions suggest that most of the dikes were emplaced at essentially the same time. At the fringes of the swarm, many of the thinner dikes turn and become parallel to the sedimentary bedding.

The majority of dikes are 15 to 30 feet thick, but thicknesses vary from 1 to 75 feet in very short distances. Dikes less than 20

feet thick end abruptly and pick up again within 100 feet on strike. The dikes follow a preexisting set of faults which trend north-south, dip 45-60° west, and consistently show apparent normal displacement with less than 500 feet dip slip motion.

The second major area of dike concentration is in Starvation Canyon. This small dike swarm, which is continuous with the contact sheath rocks in that area, extends roughly three miles southeast from the shelf-like extension of the stock at the bottom of Starvation Canyon. Near the stock, the swarm consists of one vertical 300 feet thick dike which breaks up into a subparallel swarm 500 to 100 feet wide at a distance of 1000 feet from the stock. Like the other dike swarm, this one also follows a preexisting fault which was vertical and had roughly 200 feet of dip-slip motion.

Other dikes, all less than 50 feet thick, and pods of dike rock up to 400 by 800 feet in size, occur scattered throughout the wall rock within a mile or so of the stock contact. The pods appear to have acted as feeders for the nearby dikes. One such pod, on the range divide west of the stock, is associated with an area of brecciated rock and may represent another vent. In general the number of dikes increases as the stock is approached.

All the dikes, whether single or in swarms, weather dark red-brown and stand out as cliff-forming bands across the much lighter Noonday Dolomite. When viewed from a distance, the close-packed subparallel dikes of the swarms suggest sedimentary bedding, so regular is their appearance.

## Petrography of the Dike Rocks

The general appearance of the dikes, both in hand specimen and in thin section, is remarkably similar. In hand specimen, the dikes are cream, white or light gray, and for the most part show two textural features of interest. The first is a strong lamination of alternating white and light gray laminae from 0.5 to 30 mm thick. The second feature is the occurrence of very fine, 0.1 to 1.0 mm, spherulites, some of which show concentric structure which tends to stand out on

Fig. 30. Summary diagram of feldspar compositions(weight percent) from various minor phases of the stock.

A=Alkali feldspar from pegmatitic pods, with associated perthitic phases(A'). Specimen DV127.

B=Sanidine phenocrysts in micropegmatite or micrographic areas, with groundmass feldspar(B'), and associated perthitic phases(B''). Specimen DV124A.

C=Alkali feldspar from aplite dikes in stock, specimen DV129A.

D=Alkali feldspar compositions from aplitic dike sheath rocks; with associated perthitic phases(D') from completely exsolved alkali feldspar.



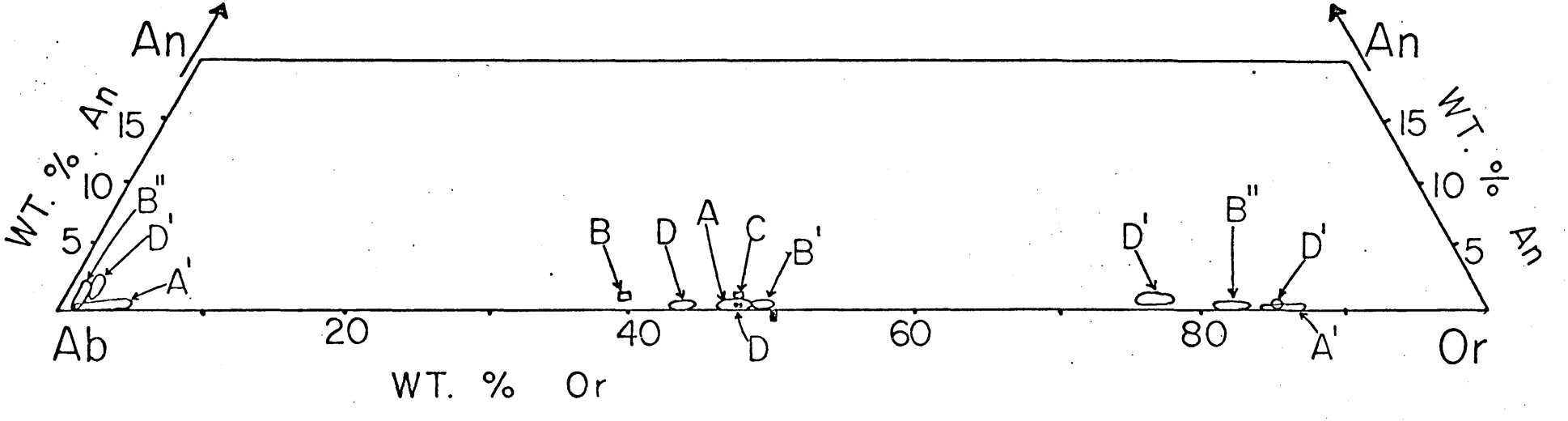

weathered surfaces and which give the rock a definitely oolitic appearance. These are present in over 75 per cent of the dikes seen. Phenocrysts of feldspar, and rarely quartz, are scattered throughout both types of laminae. In a few cases, dikes which show the spherulites are massive and show no laminations.

Where present, the laminations are parallel to the dike contacts and appear to define a flow banding. These laminations are regular and continue for great distances within the dikes. However, in some parts of the dikes which are very thick, or in pods of dike rock of large size in the country rock, the laminations tend to be contorted and often assume roughly spherical geometries on the scale of 5 to 30 feet. Even within these contorted areas, however, the laminations remain regularly spaced. In some cases, where laminated rock passes into non-laminated rock, the transition takes place by a gradual fading out of the visible laminations. Where this occurs, the dike thins at the same time.

As a general rule, the percentage of visible phenocrysts in the dikes ranges from 5 to 15 per cent. These consists almost entirely of chalky white, euhedral, 0.5 to 3 mm alkali feldspars which often show carlsbad twinning. In only two dikes, in widely scattered localities, were rounded 1 to 4 mm quartz grains observed, and these are probably xenocrysts. The phenocrysts are evenly scattered throughout the dikes, and show no tendency to concentrate in selected laminae.

In the roughly 25 per cent of the dikes which do not show laminations and spherulites, there are no visible phenocrysts, and the rock becomes a dense, massive white to light gray rock which tends to fracture irregularly. These phenocryst-free dikes tend to be less than 15 feet thick.

## Petrology of the Dike Rocks

The most common type of porphyry dike is the thinly laminated spherulitic variety. In thin section, these consist of 0.1 to 1 mm diameter spherulites set in brown-stained matrix.

The spherulites consist of less than 0.02 mm aggregate of alkali feldspar grains with rare albite and quartz. The central part is often heavily brown-stained and has a characteristic rectangular regularly spaced fracture pattern, so that the spherulites may have a dark core with a surrounding clear ring. The outer edge of the spherulite is defined by a sharp line separating the clear spherulite aggregate from the distinctly-coarser, brown-stained matrix material.

The matrix consists of microgranitic albite, quartz and rare alkali feld grains which often pass gradually into areas of coarser micropegmatitic texture. These latter areas are located the furtherest from the spherulites. The grain size changes from 0.05 mm next to the spherulites to 0.5 mm in the micropegmatitic areas, and at the same time the degree of staining decreases so that the latter areas are often unstained. The micropegmatite feldspars tend to grow radially outward from the nearest spherulite, and often vugs are present at the points furtherest from the spherulites.

The medium-dark gray bands appear to have been formed by a coalescing of spherulites. All gradations exist between very faint bands made up of slightly higher concentrations of spherulites relative to the surrounding material, and bands made up completely of very fine-grained spherulites. In some cases, where the cores of the spherulites tend to be strongly brown-stained, islands of this brown-stained material are scattered throughout the very fine grained aggregates of the darker bands.

The phenocrysts in better than 95 per cent of the dikes observed consist of euhedral to very slightly-rounded, cloudy, alkali feldspar phenocrysts with various degrees of perthite development. They range in size from 0.5 to 3 mm and are generally carlsbad twinned. Each phenocryst is invariably surrounded by a ring, roughly 0.1 to 1 mm thick, of a clear, very fine-grained crystalline aggregate like that in the spherulites. Occasionally, brown-stained areas occur in the rings which have the characteristic cross fractures typical of the brown cores of many of the spherulites. The sequence outside the rings is exactly like that around the spherulites.

This three-fold textural subdivision--into phenocrysts, fine-grained spherulite and phenocryst ring aggregates, and coarser-grained matrix and associated vugs--holds true for the majority of the dike rocks studied. There are variations on the above scheme which related mainly to the make-up of the spherulites, and these will be described below.

In some specimens, the spherulites are sensibly larger, up to 4 mm in diameter, and consist of radial sheaths of feldspar growing outward from the center of the spherulite. The matrix in these dikes is of the normal type. However, in one specimen with the larger radial-type spherulites, the matrix is divided into two parts. The portion next to the spherulites is made up of 0.1-2 mm crystals of feldspar and quartz, and the portions farthest from the spherulites, in the "vug" position, are made up of 0.5-2 mm strained blades of quartz growing perpendicular to the sharp contact with the first portion. In this case, there is no stained material and no size gradation in the matrix away from the spherulites.

This lack of grain size gradation is present in one other specimen, which has a great number of 0.1-0.2 mm spherulites of the aggregate type in a matrix of 0.05-0.2 mm quartz and feldspar. In some areas of this specimen, the spherulites consist of clear, single feldspar crystals which preserve the round shape of the spherulites and which have outer edges which preserve in great detail the irregular, crinulated margin of the normal aggregate spherulites against the matrix. The textural relations suggest that the single-crystal spherulites were formed from the aggregate-type spherulites. In this specimen also, there are no rings of aggregate material around the phenocrysts.

One or two dikes, strongly banded, were observed to be without spherulitic structures. In these rocks the dark gray bands are composed of the same very fine-grained aggregate of crystals that is characteristic of the spherulites in other rocks. No brown-stained spherulite cores were noted in these bands. The feldspars in the coarser-grained, lighter bands occur in roughly radial aggregates of a

pseudospherulitic nature. The contact between layers is very sharp. Hence, even in spherulite-free rocks, the division into the very fine-grained aggregate material and the coarser matrix material holds true.

The non-banded, non-spherulitic, dense white massive dikes consist of phenocrysts very much like those described above, set in a groundmass which is made up of a jig-saw puzzle-like aggregate of quartz and feldspar, in the 0.05 to 0.2 mm size range, with occasional ragged clusters of radial feldspar crystals up to 0.5 mm in size which are only suggestive of spherulitic structures.

Accessory Minerals

Very few minerals other than quartz and feldspar are found in the dike rocks. The most common accessory is magnetite, which occurs with two habits. In the first, magnetite occurs as small, euhedral grains which are scattered throughout the rock in a random manner, so that it is as likely to appear within spherulites as within the matrix. In this case, the magnetite makes up less than 1 per cent by volume of the rock. The second habit, magnetite occurs as very irregular, ragged patches up to 1 mm in size which are restricted to the matrix micropegmatite and vuggy areas. With this type of magnetite, its volume percentage in the rock may be as high as 4 per cent. The euhedral variety occurs in the vug and micropegmatite-poor dike rocks, while the ragged variety occurs in the vug and micropegmatite-rich rocks.

The magnetite of the vuggy dike rocks is intimately associated with hematite. Often, the smaller vugs are filled with hematite, and in cases like these, the magnetite has altered to hematite wholly or at least in part. If both magnetite and hematite occur, the hematite occurs in the position nearer to the vug than the magnetite. In a few slides, magnetite of the euhedral type is altered to hematite, yielding small crystals of hematite after magnetite.

Rarely, highly altered, deep-red-brown biotite occurs in scattered grains. Where the biotite occurs away from the vug-micropegmatite areas, it is clearer and much less altered, but adjacent to vugs

or micropegmetitic areas, it is very clouded and red-brown colored and appears to be altering to hematite. The percentage of hematite in some vuggy dike rocks is as great as 8 per cent, and much of this may have resulted from the alteration of biotite. Rarely, biotite aggregates pseudomorphous after hornblende were noted.

Many vugs are lined with calcite, and rarely epidote, quartz and magnetite-altering-to-hematite are all three present in or adjacent to vugs. Where this latter occurs, there are invariably magnetite-epidote-quartz scarn in the adjacent carbonates of the country rocks.

Composition of the Dike Feldspars

The composition of the feldspars in the various dike rocks examined in detail is remarkably consistent from sample to sample. The three-fold subdivision into phenocrysts, spherulites and bands around phenocrysts, and matrix material appears to have considerable compositional significance.

Feldspar phenocryst compositions fall into three rough groups. The first consists of feldspars which have exsolved to various degrees, but which contain considerable amounts of unexsolved alkali feldspar. The perthite occurs as irregular elongate patches, commonly blunt-ended, with the sodium phase very clear and albite twinned, and the potassium phase very cloudy and commonly quite brown-stained. The distribution of perthite has no regular pattern--that is, it is not concentrated near the edges of the phenocrysts, or in zones within the phenocrysts that might reflect a fundamental chemical variation within the phenocrysts. In brecciated phenocrysts, the perthite does tend to concentrate along fractures.

The composition of the K phase is generally $Or_{95}Ab_5An_0$, although phases in some grains have compositions of roughly $Or_{93}Ab_7An_0$. The Na-phase composition is $Or_2Ab_{97}An_1$. By using a large moving spot on the microprobe, a bulk composition of approximately $Or_{75}Ab_{24.5}An_{0.5}$ was obtained, in agreement with the estimated ratio of K-phase to Na-phase.

The second group of feldspars consists of feldspars which are

completely exsolved. In overall form they are exactly like the preceding phenocrysts, but internally they range from brown, cloudy, very finely-intergrown microperthite or submicroscopic perthite to phenocrysts that are made up of two completely separate exsolved phases with no interpenetration whatsoever. In this latter case, the phenocryst is made up of a granoblastic aggregate of 0.05 to 0.1 mm feldspar grains, with the two phases distributed in an apparently random manner. The K-phase composition is roughly $Or_{87}Ab_{13}An_0$, and the Na-phase composition is roughly $Or_1Ab_{95}An_4$.

The phenocrysts of the last group, while they are indistinguishable in hand specimen from the other groups, are made up entirely of Na-phase of composition $Or_{1-3}Ab_{97-98}An_{0-1}$. There are no patches of alkali feldspar or K-phase, as determined from probe, thin section and staining work. The albite twinning of the phenocrysts is irregular in that the twin lamellae extend for short distance only, and tend to pinch out rather than ending abruptly. There appears to be a gradation between the last two phenocryst groups, brought about by a progressive replacement of the K-phase of the perthite by Na-phase, until pure albite phenocrysts result. Phenocrysts in intermediate stages of the replacement process are common.

The composition of the very fine-grained aggregates, whether in spherulites, in bands about phenocrysts, or in the dark gray bands, is uniformly K-feldspar rich, as indicated by staining and probe studies. The probe feldspar composition is approximately $Or_{92-95}Ab_{5-8}An_0$. Feldspar totals, especially in the brown cloudy areas, tend to be low, and this is felt to be due to the presence of a clay-like alteration product of the feldspar. Where the aggregates are clear, the totals approach 100 per cent.

In one specimen studied, minor amounts of a Na-phase with a composition of roughly $Or_5Ab_{95}$ were noted in the spherulites, and low probe totals suggest the presence of roughly 50 per cent quartz in these same spherulites. This same specimen contains some orthoclase in the matrix; unlike the normal matrix.

The texture of the spherulites apparently has no affect on

the composition of the feldspar, as both the fine grained aggregate spherulites and the larger spherulites with the radial feldspar clusters appear to be made up only of quite pure K-feldspar, and minor quartz.

The matrix has a very simple mineralogy also, and is made up of quartz plus albite with a probe composition of $Or_{1-2}Ab_{95-98}An_{0-4}$. The feldspar crystals which grow out into the vugs have visible albite twinning, but all the other albite is untwinned, cloudy, and often has rather variable extinction.

The volume percentage of quartz in the matrix ranges from 40 to 70 per cent by visual estimate, and the remainder is albite. No point counting was done due to the fine grain size of much of the matrix material.

In summary, the feldspar compositions are as follows. All spherulites, whether of the very fine-grained aggregate or radial feldspar crystals or single feldspar grains, all aggregate rings around the phenocrysts, and all fine-grained aggregate material of the dark bands, consist only of very pure K-feldspar, in the range $Or_{85-95}Ab_{5-15}An_{0}$. All matrix feldspar, whether in microgranities or micrographic or vuggy areas, consists of very pure albite, in the range $Or_{0-3}Ab_{95-100}An_{0.2}$. The phenocrysts, all alkali feldspar, consist of all gradations from partially perthitic grains with patches of relict alkali feldspar, through completely perthitic grains which are in fact themselves aggregates of pure K-feldspar and albite, to grains which are entirely made up of pure albite. Thus, as in the replacement sequences seen in the stock, the alkali feldspar exsolved and then the K-feldspar phase was progressively replaced to yield a sodic plagioclase.

## Origin of the Structures in the Dikes

The presence of spherulities in the dike rocks strongly suggests that these rocks were once glassy and that the spherulites are due to devitrification. Many of the spherulites observed are very similar to those seen in glassy volcanic rocks (Ross and Smith, 1961) of acidic composition, and similar textures are commonly produced in

various ceramic processes. Similar laminations, caused by concentrations of spherulities, are also observed in glassy acidic rocks.

That acidic rocks with the same compositions as the dike rocks can form glass under natural conditions is well known, and indeed many ceramic glass-formers have very similar compositions. Typical ceramic glass-formers have viscosities at the melting temperatures which are very similar to those expected in silicate melts of dike-like compositions (Shaw, 1965, see below). Basically, however, glass formation is a cooling rate phenomenon and requires that the material in question be cooled at a fast enough rate that nucleation cannot take place and glass will form. The thinness of the dikes, and their shallow emplacement, would quite conceivably allow these conditions to take place.

The lamination in the dike rocks has a geometry that strongly suggests that it was formed by some sort of flow process in the initial melt. Calculations and experiments by Shaw (1963, 1965) indicate that the viscosities of crystal-free melts in the Or-Ab-Q-$H_2O$ system, which is essentially the same compositional system as the dike rocks, fall in the range of $10^{+5}$ to $^{+7}$ poises. The presence of crystals or vapor phase bubbles both tend to increase the viscosity, so that the above viscosities are minimal for the dike rocks.

With the above viscosities, it would be very difficult to obtain turbulant flow with most reasonable flow velocities (Spry, 1953; Shaw, 1965), except perhaps near orifices or stock-dike junctures. Thus, in such dikes laminar flow would be expected in all cases, and would be compatible with the flow lamination observed.

Banding in glassy acidic volcanic rocks is often made up of varying concentrations of minute crystallites, which consist of microscopically almost unresolvable beads or lines of beads or small crack-like features. These may be minute crystals (microlites) or true cracks or concentrations of impurities. Darker bands are the result of higher concentrations of these crystallites, while lighter bands are devoid of these features. Other glassy volcanics show flow lines (Harker, 1954), which consist of aligned crack-like features which also tend to concentrate in bands.

Observations in glass technology have emphasized the importance of material in the glasses which could act as nucleii for spherulite formation, and indeed, several types of ceramic glazes are made by controlling the number of foreign particles which act as spherulite substrates. Special mention is made of spherulitic structures initiating along cracks within the glass.

In the dike rocks in question, certain features suggest spherulite formation along fractures in the original glass. Often straight dark bands of spherulites, very similar to the dark laminations, are noted which cross the normal flow-lamination and which invariably have a fracture along the centerline of the band. In a few instances, these fractures have passed through phenocrysts. These appear to be original through-going fractures which have localized the spherulites in the glass.

In the light of the above, it is suggested that the dike rocks were originally glassy and contained flow banding made up of concentrations of crystallites due to lamellar flow of the original magma. Immediately after emplacement, in the presence of a vapor phase, devitrification initiated using these various impurities as substrates. Due to the large degree of undercooling of the glass, nucleation rates were high but growth rates very slow (Swift, 1947; Yee and Andrews, 1956; Winkler, 1947, 1949) so that aggregates of very small crystals were formed on devitrification. Any substrate material was used-hence not only crystallites, but also phenocrysts and fractures in the rocks were used effectively. This led to the spherulites and fine aggregage bands around the phenocrysts.

The rapid formation of the spherulites of effectively anhydrous minerals may have resulted in concentration of the volatile material in the interspherulite, or matrix, areas, and this plus the evolution of heat on devitrification could have been enough to locally decrease the degree of undercooling and cause devitrification in the matrix areas with higher growth rates and lower nucleation rates, resulting in progressively larger crystals. In the vuggy areas, true vapor phase crystallization occurred, resulting in the micropegmatitic patches and

drusy cavities.

The above model accounts for the distribution of the textures in the dike rocks quite well. However, it does not account for the compositional distribution of phases. In many glassy volcanics of similar composition, devitrification results in intimate intergrowths of feldspar and christobalite (Ross and Smith, 1961), and the restriction of K-feldspar, and quartz and albite into separate parts of the rocks are not noted. Similarly, while nucleation rate studies indicate that different minerals have measurably different growth rates, it is noted that the maximum growth rates of all the minerals occurs at the same temperature (Swift, 1947). Thus in the dike rocks, aggregates of several minerals should occur in the spherulites and the K-feldspar-albite separation should not occur via simple devritrification.

If, as is indicated, the rocks were saturated with a vapor phase, it is possible that the original compositional distribution due to simple devitrification was strongly modified by vapor phase transport.

Origin of Dike Rock Feldspar Compositions

Recent work on the solubilities of feldspars in fluid phases can be summarized as follows. Orville (1963) found that, at a water pressure of 2000 bars, in the system Ab-Or-Water, invariant assemblages consisting of albite, orthoclase, and a vapor phase coexisted at equilibrium at a given temperature. At this temperature, the vapor phase contained in solution approximately a 4:1 ratio of albite: orthoclase, decreasing with increased temperature. Hence, at higher temperatures orthoclase would be dissolved and albite precipitated, and the reverse would take place at lower temperatures. Thus the concentration gradients set up would be a function of the ratios of ab:or in the vapor and the temperature gradients that existed, as long as two feldspars coexisted. This model was verified by a laboratory study in which alkali transfer along a temperature gradient was demonstrated under these conditions (Orville, 1963).

Burnham (1962, lecture at CIT), determined the approximate

solubilities of albite, orthoclase and quartz in a vapor phase at various pressures and temperatures, and found that the solubilities increased with water pressure and temperature, and that at lower water pressures quartz was the most soluble, albite the next, and orthoclase the least soluble. At higher water pressures, about 10Kb, albite was slightly more soluble that quartz, and both were much more soluble than orthoclase.

The presence of two feldspars plus vapor in the dike rocks indicates that Orville's model could be applicable if the temperature gradients were present. The addition of $SiO_2$ as a component is matched by quartz as a phase, and hence the phase rule remains satisfied. If the previous devritrification model is valid, the coarser-grained, vapor-rich matrix areas might in general be hotter than the spherulites, causing vapor transport to take place.

According to Orville's model, K-feldspar would tend to crystallize in the cooler spherulites, while albite would crystallize in the warmer matrix areas. The high solubility of quartz, and its common association with albite, indicates that it acted similar to albite and hence crystallized in the high temperature areas. The crystallization of albite and quartz in the vugs is also compatible with their higher solubility in the vapor phase, according to Burnham's data, and in fact similar albite-quartz association has been noted in all the vugs in the stock itself.

In the case of the one dike in which the matrix itself is subdivided into a quartz,plus albite region, and a quartz region next to the vug position, it appears that the vapor phase model has gone one step further, and has started to separate the albite and quartz. Such a zonal sequence is also seen in naturally occurring pegmatites. This is compatible with Burnham's data in that the quartz was shown to have a higher solubility in the vapor phase than either of the feldspars at lower temperatures. This particular specimen was collected from the major dike swarm near the stock, and hence relative to the other dikes, would have been expected to cool at a slower rate, allowing this later quartz-albite separation to occur at lower temperatures. It is from

the same region in which the dike contact-metamorphism occurs in the Sourdough Limestone Member of the Kingston Peak Formation.

Thus the dike crystallization is the result of the complex interaction of vapor phase equilibria and devitrification phenomenon, with a water-charged fluid phase acting both as a transport medium and as a catalytic medium to speed devitrification.

There seems to be little relationship between the observed devitrification-vapor phase compositions and textures, and the type of alkali feldspar phenocrysts in the rock. Thus in specimens with exactly the same type of spherulites and matrix features, the phenocrysts can range from alkali feldspar to albite. This suggests that the processes of perthite formation and albitization of the phenocrysts took place before the devitrification-vapor phase sequence. Nonetheless, the albitization process may well have involved a vapor phase and vapor transport, since compositionally the perthite phases of the phenocrysts are the same as the spherulite-matrix feldspar compositions.

Dikes within Stock

A very few dike-like bodies of granitic rock with phenocrysts of alkali feldspar, plagioclase, and mafic minerals in a very fine-grained intimately-intergrown quartz-feldspar groundmass, are scattered throughout the northern phase of the stock. They range from 1-10 feet in thickness, are vertical in dip, and extend laterally for distances of over 200 feet in all cases. They are entirely restricted to the interior portion of the north phase of the stock, and no connection was observed between these dikes and other types of dikes which are related to the stock. They also cut the late aplite dikes.

The dikes under discussion show chilled margins against the normal granite porphyry of the stock, and rarely, minor dikelets are observed which extend out into the stock porphyry for short distances. Angular inclusions of the stock porphyry are seen within the dikes in positions which indicate that they have been rotated from their apparent starting position. Flow banding, always parallel to the dike contacts, is common and takes the form of streaks of various shades of

gray in the groundmass or bands with different size distributions and concentrations of phenocrysts. In some places, lensatic concentrations of phenocrysts are observed, which are parallel to the flow banding.

The percentage of phenocrysts is roughly 15 to 25 per cent by volume of the rock, so that the rock appears as a very fine-grained, gray rock with white feldspar phenocrysts scattered throughout it. The phenocrysts range from 0.1 to 15 mm in size, and are often broken and fractured into various irregular angular shapes. The groundmass is less than 0.02 mm in size.

In terms of the textures that have been previously described, the feldspars in these late dikes, specimens 55B, 130B and 130C, tend to be intermediate between specimens DV56 and DV151. Here, the sequence of crystallization and reaction is such that the sanidine coexisted with a slightly more sodic plagioclase, $Or_{4-5}Ab_{75-78}An_{17-20}$ (Fig. 31,A) than was observed in DV56. Sanidine phenocrysts are seen which have a "rim" of the replacement type plagioclase, with its mottled extinction and numerous quartz blebs, which is in turn surrounded by another rim of clear, albite-twinned, quartz-free plagioclase of the same composition, which appears to have crystallized directly from the melt. The composition of these plagioclase rims is $Or_{3.5-5}Ab_{78-81}An_{15-17}$ (Fig. 31,A'), which is the same as the composition of the outermost parts of the sodic zones of the plagioclase phenocrysts.

Hence, the later crystallization sequence would be: crystallization of the sanidine and plagioclase A of Fig. 31, then as the plagioclase zoned from A to A', reaction and replacement of the sanidine in the outer parts of the phenocrysts by the mechanisms previously outlined, and finally crystallization of plagioclase A' on both the plagioclase and alkali feldspar phenocrysts. The replacement of the sanidine in these dikes is slight compared to either DV151 or DV74, and it appears that the replacement stage was rather short in this case.

In many of the sanidine phenocrysts, especially the smaller ones, cloudy perthite is extensively developed. However, patch perthite is very rare. Most of these have the normal sanidine compositions

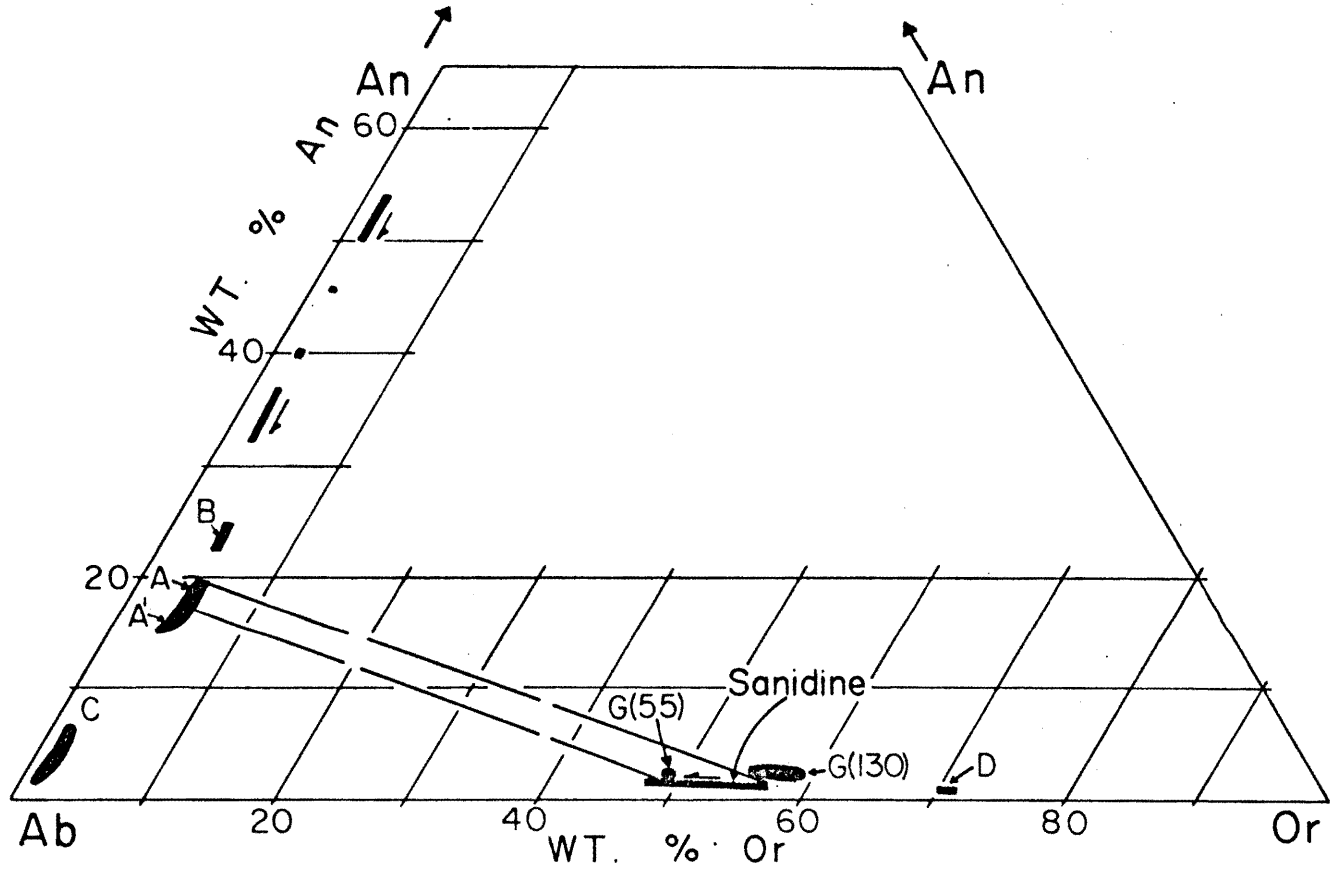


Fig. 31. Summary diagram of feldspar compositions(weight percent) from specimens DV55B and DV130B and 130C, dikes in interior portion of north phase of stock. Tie lines connect coexisting feldspars. G=groundmass feldspar composition. See text for detailed explanation.

(Fig. 31), but in a very few cases, some of the sanidine phenocrysts appear to have become completely albitized, and have compositions in the area C of Fig. 31. This type of replacement is very similar to that seen in many of the prophyry dikes of the dike swarms associated with the stock, which has been discussed further in the section on the porphyry dike rocks. In a few rare instances, very small alkali feldspar microphenocrysts with abnormally potassic compositions were noted (Fig. 3, area D). They also have an appearance like the albitized phenocrysts.

Fig. 32 shows composite plagioclase scans for specimens DV55B and DV130B,C. The zoning is more complex than that noted in many of the other specimens, but still shows the same general pattern of progressively more sodic rims. Reversals are rare. There is some indication in some of the phenocrysts that a relatively more sodic core exists as was noted in some of the plagioclase phenocrysts of DV128A. The sodic core composition is shown in Fig. 31 by area B. Groundmass compositions, analysed by moving spot scans, are also shown in Fig. 31 as areas G. Relative to most of the specimens analysed, the groundmass of DV130 is more Or-rich.

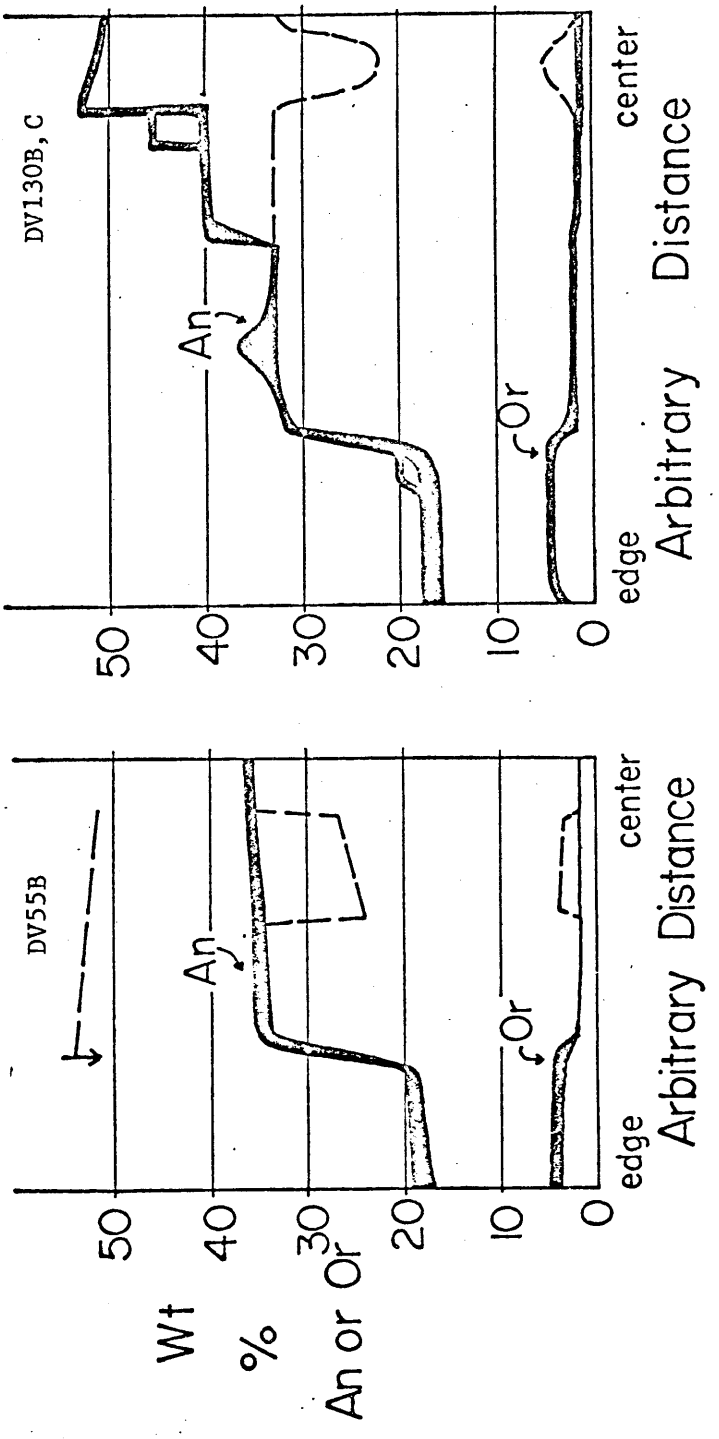


Fig. 32. Composite plagioclase probe scans across plagioclase phenocrysts, specimens DV55B and DV130B,C. Or and An percentage in weight percent. Dashed scans show rare phenocrysts with sodic core.

# PETROGENESIS

## The Ab-Or-An-Q-$H_2O$ System

The crystallization sequence in granitic rocks may be described in terms of the Ab-Or-An-Q tetrahedron at various water pressures. Since granites are, relatively speaking, "wet" systems, the variation of $P_{H_2O}$ is an important and vital one. Obviously, the more closely the composition of the rocks being described approaches the compositions which are present in the tetrahedron, the more meaningful is the comparison between the experimentally derived phase systems and natural rocks. In the case of the Little Chief stock, Ab plus Or plus An plus Q make up 90 to 95 percent by volume of the rock - hence this rock is ideally suited to be treated in the granite tetrahedron. Henceforth, in this section, the mafic minerals will be neglected.

However, in order to treat the crystallization sequence with any accuracy, the variations within the granite tetrahedron must be known in some detail. This next section will be devoted to a brief discussion of the phase systems which are most readily usable; namely, the Ab-Or-Q and Ab-Or-An systems at various water pressures. The sources of information include the experimentally determined phase diagrams, and compositional data on coexisting feldspar plus melt, or two feldspars plus melt, from naturally occurring rocks. In this section, water pressure only will be considered, and the effect of other volatiles neglected.

### Experimental Data

The best known system related to the granite tetrahedron is the

Ab-Or-Q system at various water pressures. In all cases, $P_{H_2O} = P_{total}$ in the experimental systems. Figure 33 shows the location of the various field boundaries of this system at various water pressures (Tuttle and Bowen, 1958; Luth et al, 1964). The quartz-feldspar boundary, which migrates toward the Ab-Or sideline with increasing pressure as shown, is a cotectic, and represents the intersection of the quartz-feldspar cotectic surface of the tetrahedron with the Ab-Or-Q face. The two-feldspar boundary is, for this An-free system, a minimum trough at water pressures less than about 2.2Kb, a cotectic at water pressures greater than 4.3Kb, and part cotectic-part minimum trough at pressures in between. The points at which the boundary changes from a minimum trough to a cotectic line are noted for the various pressures (3, 3.5, 4, 4.3Kb). The variation of this intersection is due to the combined effects of the addition of $SiO_2$ and the pressure variation on the solvus-solidus intersection.

It can be seen that the eutectic or minimum on the quartz-feldspar boundary consistently has a lower Ab/Or ratio than the minimum or eutectic on the Ab-Or sideline at the same water pressure.

Recent work by Von Platen (1965) has given some indication of the changes produced in the Or-Ab-Q system, at 2Kb in this case, by the addition of various amounts of An. Basically, the method was to melt an obsidian with a known bulk composition, then cool it to the point where a melt formed in equilibrium with alkali feldspar, plagioclase, quartz, and vapor and then to determine the bulk composition of the melt by finding the amounts and compositions of the coexisting mineral phases and subtracting them from the bulk composition. Unfortunately,

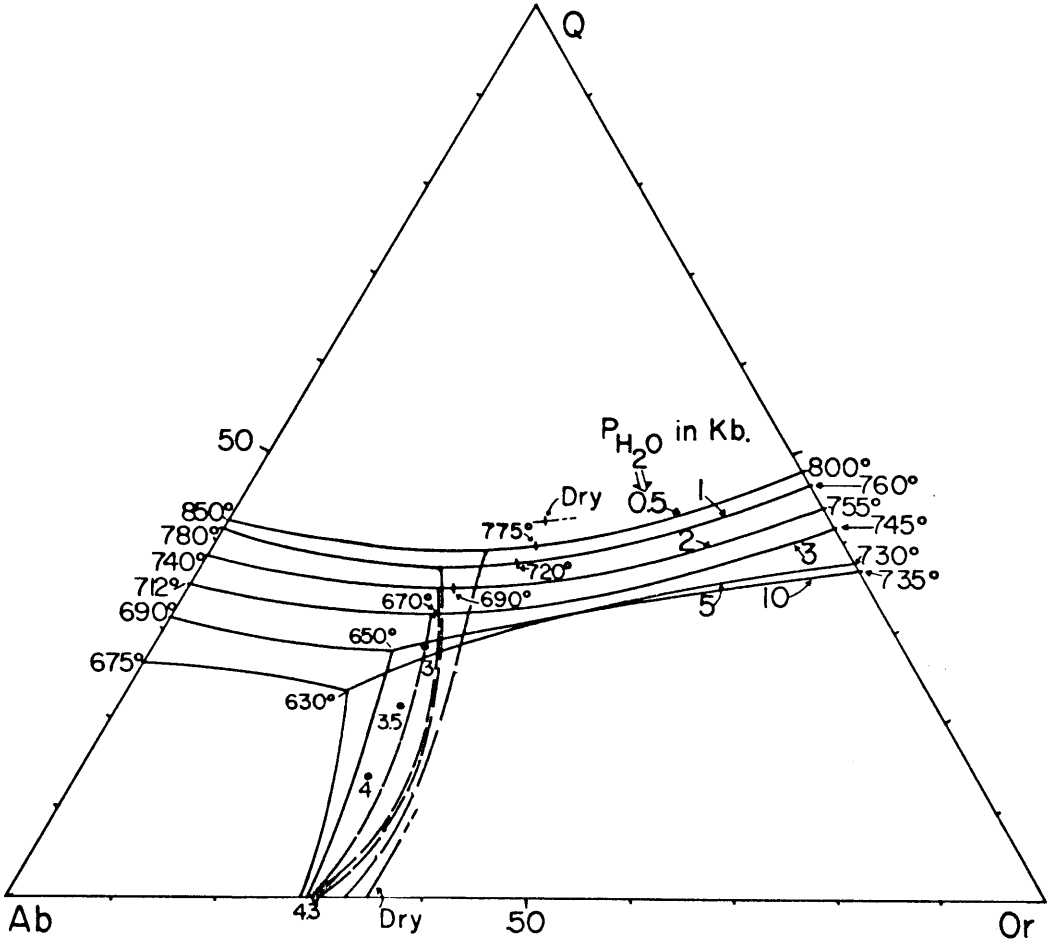


Fig. 33. Or-Ab-Q system, showing feldspar and quartz boundries at various water(=total) pressures. Water pressure shown in Kb., temperatures in °C. shown for ternary minimum or eutectic, Q-Ab eutectic, and Q-Or eutectic. Diagram in weight percent. Numbers 3, 3.5, 4 and 4.3 refer to estimated pressure in Kb. at which feldspar boundry changes from eutectic to minimum trough at the composition shown.

emphasis was on the Ab-Or-Q ratio of the melt, and the An percentage was seldom determined. However, a few eutectic melts were determined, and these are plotted in Fig. 34.

The apparent shift of the quartz-feldspar cotectic toward the quartz corner with increasing An percent is shown by the generalized set of cotectic lines, as estimated from the data. The three more quartz-rich points in the Or-Ab-Q system represent melts in which the vapor phase is nearly pure water, or an aqueous $NH_3$ solution which acts just like water. The lower two points represent eutectics melts in which the vapor phase initially contained 0.5m HCl or HF solutions. The square shows the minimum on the quartz-feldspar boundary in the 2Kb Or-Ab-Q system with pure water and no An added, as in Fig. 33.

The experimental work on the Or-Ab-An system at various water pressures is much less extensive. Figure 34 shows the experimental results thus far available. The heavy solid curve is the feldspar cotectic determined by Yoder et al (1956) at a total pressure of 5Kb $H_2O$. The light dashed curve is the suggested cotectic for the dry system (Franco and Schairer, 1951). However, due to the extreme sluggishness of reactions in the dry system, plus the complexities produced by the presence of leucite, this latter cotectic is probably not very dependable.

In the Or-Ab-Ab system of Fig. 34, the heavy dashed curve is the tentative cotectic constructed from Von Platen's data. This is essentially an estimate of the quartz-saturated feldspar cotectic; the line along which two feldspars and quartz, plus melt and vapor, coexist. Again, the three most An-rich points are for the systems with $H_2O$ or $NH_3 + H_2O$ as the volatile phase at a total vapor pressure of 2Kb. The

Fig. 34.

Or-Ab-Q system. Shift of quartz-feldspar boundry due to addition of An to the system, as estimated from the data of Von Platen(1965). An percentage shown on right. Circles show melt compositions in equilibrium with two feldspars + quartz + a vapor phase containing $H_2O$(two points nearest boundary for 4% An), or $H_2O$ + $NH_3$(point nearest boundary for 5% An). Other points represent melts as above with a vapor phase containing $H_2O$ and either HF or HCl. Square shows eutectic in system with no An. All points at fluid pressure of 2000 bars. Triangle represents Von Platen's starting material.

Or-Ab-An system. Solid line-feldspar boundary at water pressure of 5000bars (Yoder et al, 1956). Light dashed line-feldspar boundary under dry conditions. Heavy dashed line-estimated feldspar boundary from data of Von Platen(1965). Circles show compositions of melts in equilibrium with two feldspars + quartz + a vapor phase containing $H_2O$ and $NH_3$(points nearest heavy dashed line) or $H_2O$ and HF or HCl(other circles). Triangle represents Von Platen's starting material. All data from Von Platen at 2000 bars fluid pressure.

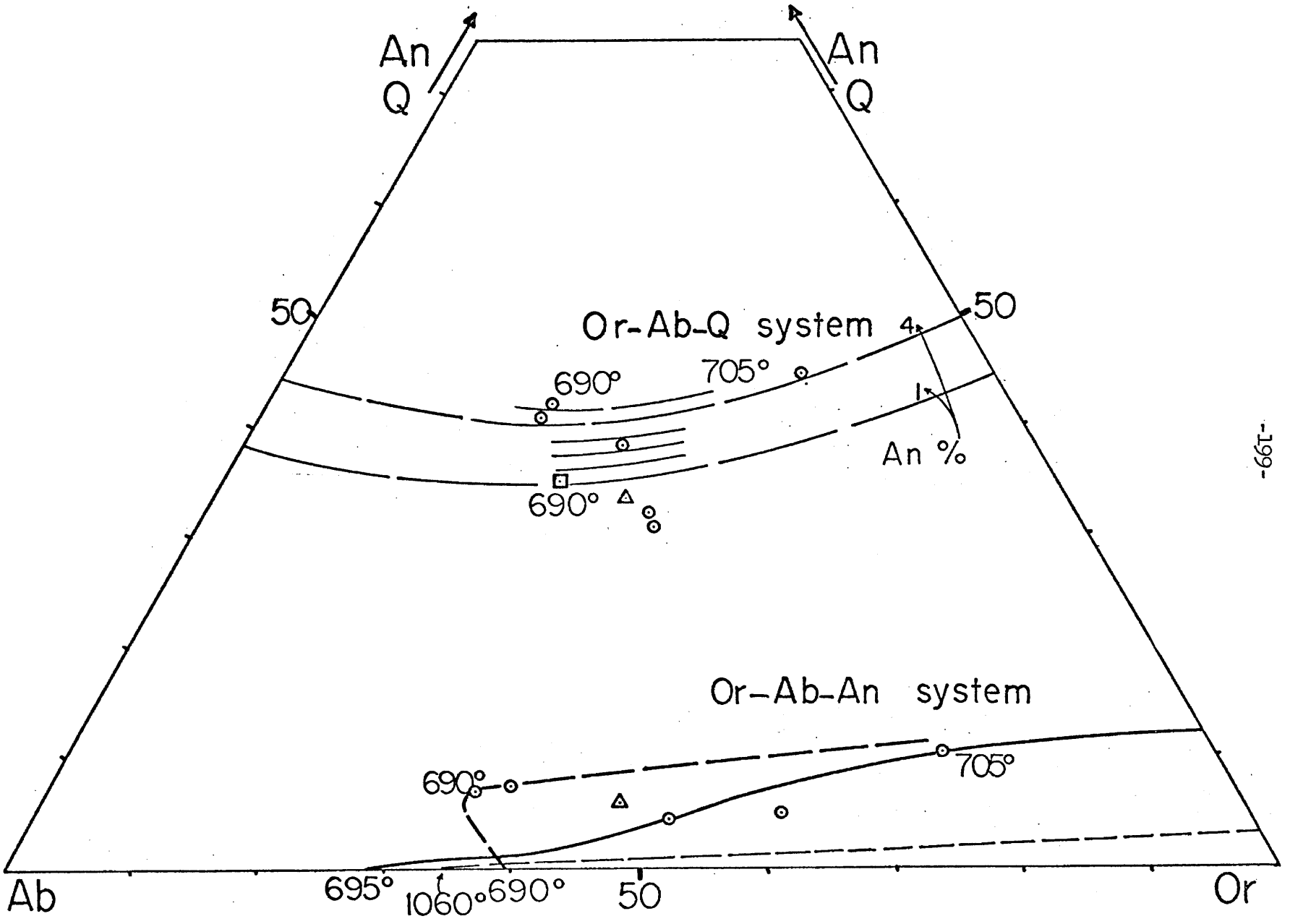
An
Q
An
Q
50
50
Or-Ab-Q system
4
1
690°
705°
An %
690°
Or-Ab-An system
690°
705°
Ab
695°
1060°
690°
50
Or

two An-poor points are for the same total pressure, but with HCl or HF as part of the vapor phase.

There are two important points to be noted about this latter quartz-saturated cotectic. First, the cotectic in the Or-Ab-An system is constrained to double back on itself due to the high Or percentage of the minimum melt in the quartz-saturated An-free system (compare Fig. 33). Hence, further complexities would be introduced into the area of transition from a cotectic to a minimum trough (Stewart and Roseboom, 1962).

At lower water pressures, in the quartz-saturated system, the minimum on the Or-Ab sideline shifts still further toward the Or corner, and it is possible that at lower water pressures the doubling back in the cotectic trend will be even more extreme.

A second important point is that, if Von Platen's data are reasonably reliable, eutectic melts can exist in a region of the Or-Ab-An system in which previous experimental work had led various workers to suggest the absence of such melts.

Comparison of the lowering of the melting points of An and Or by the addition of quartz suggests that, in the Or-An system, the addition of quartz to the system will shift the Or-An eutectic toward the An corner. Hence, in Fig. 34, the 2Kb quartz-free cotectic should lie below, or toward the Or-Ab sideline, relative to the 2Kb quartz saturated cotectic. The simplest suggestion is to place the quartz-free cotectic at this pressure just below the 5Kb cotectic, as has been done by Stewart (1959). This assumes, however, that the dry cotectic has some validity.

Hence, using this simple model, for a constant water pressure, the addition of quartz to the Or-Ab-An system will tend to move the cotectic away from the Or-Ab sideline and, in the Ab-rich region, cause the progressive development of a doubling back in the cotectic curve. The maximum doubling-back would be developed at quartz-saturation. Similarly, at a constant quartz content, an increase in water pressure would tend to move the cotectic away from the Or-Ab sideline. Hence, the 5Kb quartz-saturated cotectic curve could lie still further from the Or-Ab sideline of Fig. 34 than the 2Kb cotectic gotten using Von Platen's data, but it is probable that the doubling-back would be less pronounced due to the high Ab percentage of the quartz-saturated eutectic in the An-free system.

In order to obtain further information on the location of the cotectic curves in the Or-Ab-An-$H_2O$ system, we must turn to data on natural feldspars.

However, before this is done, the following assumptions regarding water pressure and total pressure will be made. All experimental systems have operated under conditions of $P_{fluid} = P_{total}$. In the usual case, $P_{fluid} = P_{H_2O}$, as was true of the previously discussed diagrams. According to the work of Wyllie and Tuttle, $P_{CO_2}$ can be neglected.

In natural systems, this will be carried one step further. If, as would be likely in many situations, $P_{fluid}$ is not equal to $P_{total}$, it will be assumed that the granites can be treated as if they crystallized in a system in which $P_{fluid} = P_{total}$ for the amount of water actually held in solution in the melt. For instance, if a melt contains 3 weight percent $H_2O$, according to the work of Tuttle and Bowen (1958, p. 58)

this amount of water would saturate the melt at roughly 0.5kB. If the system were actually crystallizing at 1Kb, it will be assumed that the granite can be relatively accurately treated in the 0.5Kb $P_{H_2O} = P_{total}$ system, slightly modified by the 0.5Kb increase to the total pressure. Since the total pressure effect is small in terms of the geometry of the phase diagram, its effect will be neglected.

Natural Feldspar-Groundmass Data

The best source of information on natural systems comes from the few available analyses of groundmass or glass in porphyritic rocks which contain two feldspars and quartz as phenocrysts. The simplest assumption in these cases is that the groundmass material truly represents the melt that was in equilibrium with the phenocrysts just before the groundmass crystallization period began; that is, just before extrusion in most cases. This assumes that crystal sorting, addition of xenocrysts, and so on, is not important. This also assumes, in the case of the volcanic rocks, that little or no reaction took place between the crystals and melt on the way to the surface. While this latter may be roughly true, in detail the common occurrence of strongly embayed quartz and feldspar phenocrysts casts doubt on this assumption. However, as a working model, equilibrium between melt and phenocrysts will be assumed.

Figure 35 shows the available reliable data in an Or-Ab-An plot. Three cotectic lines are shown, two of which are the 5Kb quartz-free boundary (dark solid line) and the estimated 2Kb quartz-saturated boundary from Fig. 34 (dashed line). The third is that estimated from the bulk, groundmass and feldspar compositions of natural trachytic rocks by Tuttle and Bowen (1958, p. 132) (light solid line). This line

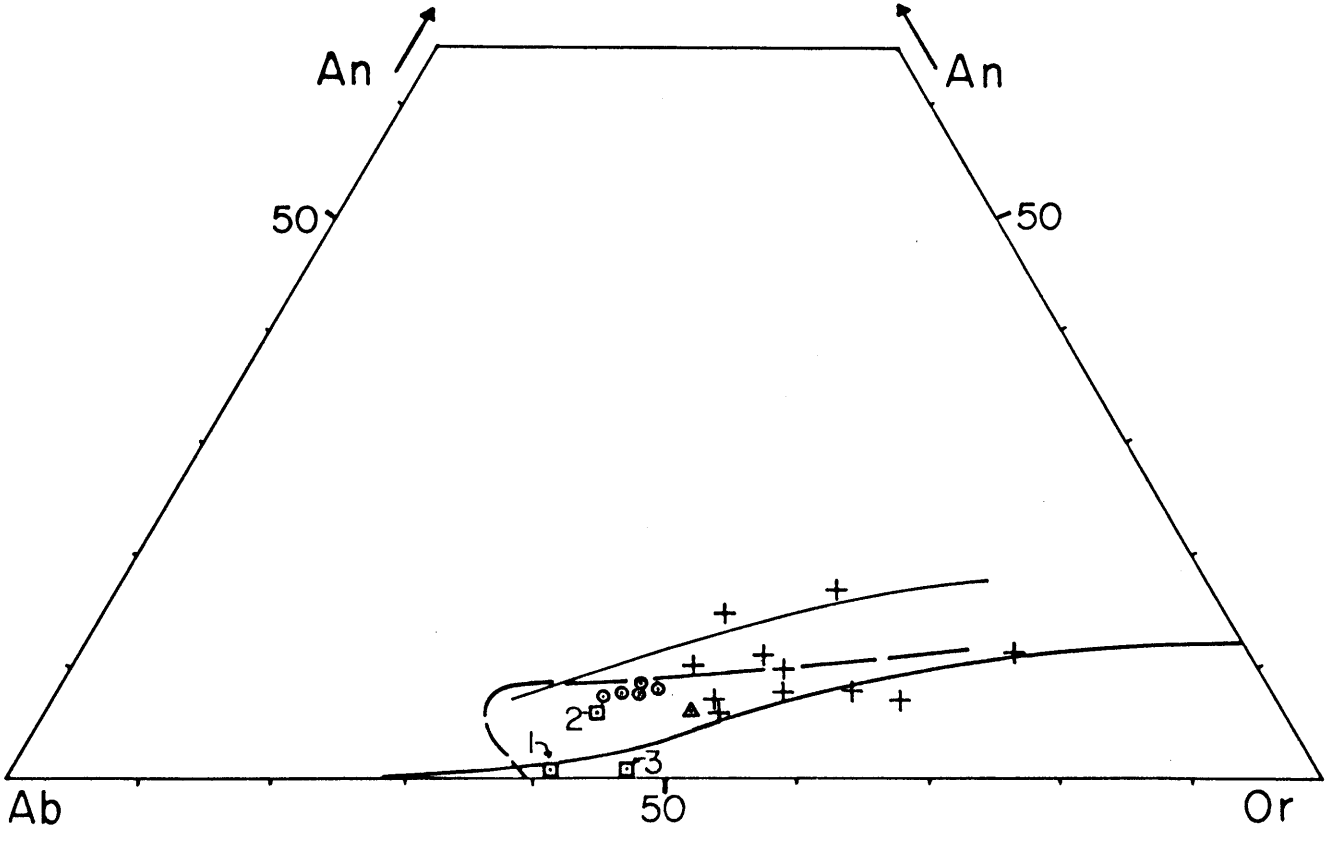


Fig. 35. Composition of naturally occurring melts in equilibrium with two feldspars. Solid line-feldspar boundary at 5000 bars water pressure(Yoder et al, 1956). Dashed line-quartz-saturated feldspar boundary at 2000 bars water pressure from data of Von Platen(see Fig. 34.). Light solid line-feldspar boundary estimated from trachytic rocks(Tuttle and Bowen, 1958). Plus sign-melts from Tertiary ignimbrites(Scott, 1965). Circles-melts from Tertiary ignimbrite(Ewart, 1965). Triangle-melt from San Juan rhyolite flow(Larsen et al, 1937, 1938)(Larsen and Cross, 1956). Squares-melts from Tertiary acid glasses(Carmichael, 1960, 1963). All data in weight percent.

roughly represents a low water pressure quartz-free boundary, and hence in the experimental systems should be closest to the "dry" feldspar boundary. That it is not is obvious, and at this point, the reason for the discrepancy is not known.

Plus signs represent calculated groundmass-melt compositions of quartz-plagioclase-alkali feldspar bearing welded tuffs from the Grant Range of Nevada (Scott, 1965). The large scatter of the points is due in large part to the fact that the glassy groundmass is hydrous and has been altered by late stage or hydrothermal processes. Since these groundmass compositions were computed from the bulk analyses of the variously altered rocks, these points can only represent approximations of the melt compositions. Nonetheless, the general distribution of the points suggests that a quartz-saturated boundary curve could be located through this area, somewhat above the 5Kb curve.

The circles in Fig. 35 are groundmass analyses, both calculated and directly analysed, of various rocks from a welded tuff from New Zealand (Ewart, 1965). In this case, the samples were obtained using drill holes through the cooling unit analyzed, and the rocks show minimal amounts of post-crystallization alteration effects. Hence, these points are regarded as quite accurate representations of the melt compositions in equilibrium with quartz and two feldspars. The analyses in this case include glassy material, devitrified material, and non-devitrified pumice inclusions within the above.

The similarity of the compositions indicates that a melt existed at the location of the five points in Fig. 35. Ewart, using the phase data in the Or-Ab-Q system of Fig. 33, obtained water pressures of 0.75 to 1Kb, making no allowance for the An percentage. If, using Fig. 34,

the water pressure is estimated using Von Platen's data to allow for the An percentage values of roughly just higher than 3Kb are gotten. In the light of the coexisting feldspars, and the data in the Or-Ab-An system, this seems slightly high, and suggests that the shift of the quartz-feldspar boundary due to the An percentage using Von Platen's data is overemphasized.

The squares in Fig. 35 show groundmass analyses by Carmichael (1963) on two rhyolitic pitchstones and a rhyolitic welded tuff. In Fig. 35, numbers 1 and 2 contain quartz, and hence should give an estimate of the quartz-saturated feldspar boundary. Number 1, with a very low An percentage gives estimates both from the Ab/Or ratio of the minimum and the location of the quartz-feldspar boundary in the Ab-Or-Q system of water pressures quite near 2Kb, in agreement with the quartz-saturated feldspar boundary in Fig. 35. The location of number 2 in Fig. 35 suggests a water pressure of approximately 1.8Kb, but estimates in the Or-Ab-Q system give water pressures of 2 and 5Kb, using the An-free and An-adjusted methods, respectively. Coexisting feldspar data indicate that the lower pressure is the more reasonable. Hence, the lower pressure is accepted. Carmichael's sample number 3 has no quartz phenocrysts, but the low An percentages allows a determination to be made of the water pressure from the minimum or eutectic locations of Fig. 33. This gives a very low water pressure, again in agreement with the coexisting feldspar data.

Finally, the triangle in Fig. 35 represents the groundmass analysis of the oft-quoted coexisting feldspar-melt pair of Larsen (Larsen et al, 1938; Larsen and Cross, 1956). This rock contains no quartz, but the normative quartz percentage of the groundmass is high enough that it is thought that it is in fact not far from being saturated with quartz. As has been noted before, the coexisting feldspars indicate a low water pressure, and in fact this specimen has over the years become the "type" low water pressure feldspar-melt assemblage. A low water pressure is also consistent with the Or-Ab ratio of the groundmass, and is allowable in Fig. 35 depending on the closeness to quartz saturation.

Summarizing the above data, groundmass analyses, or calculated groundmass compositions, indicate that the quartz-saturated feldspar boundary gotten using Von Platen's data is reasonable and that melts coexisting with two feldspars and quartz can exist at significantly more An-rich compositions than would have been suggested by the 5Kb quartz-free experimental boundary. The data thus supports the concept of a doubling-back of the feldspar boundary in the quartz-saturated system. However, as a general rule, the agreement between the water pressure estimates using either coexisting feldspars or the melt location in the Or-Ab-An system, and estimates based on the quartz-feldspar boundary in the Or-Ab-Q system is not good, and in most cases, agreement is made better if the amount of shift toward the Q-corner of the quartz-feldspar boundary due to An addition is made smaller than Von Platen's data would indicate.

Natural Coexisting Feldspars

The orientation of the tie lines connecting coexisting feldspars in the Or-Ab-An system has long been regarded as an estimate of the water pressure on the system. As a rule, at constant temperature, the lower the water pressure on the system, the greater the Or percentage of the plagioclase and the An percentage of the alkali feldspar, and the greater the angle with which the projected tie line meets the Or-Ab sideline. Of the two feldspars, the coexisting feldspar data indicates that the Or percentage of the plagioclase is the most useful. In fact, very few coexisting feldspars have an alkali feldspar which has more than 4 percent An, suggesting that the side of the ternary feldspar solvus near the Or-rich end of the Or-Ab sideline is almost vertical.

Coexisting feldspars in quartz-saturated systems- that is, ones which contain quartz in equilibrium with the feldspars- are shown in Fig. 36. Most of these specimens are porphyritic volcanics of various kinds, as in the past it has been much easier to separate phenocrysts from groundmass in porphyritic rocks of this type relative to plutonic rocks.

The suspected low water pressure specimens (the two labelled tie lines), both from Larsen et al (1936, 1937, 1938), are quite obvious on the diagram. These will be used to illustrate an important point. The oft-quoted Larsen et al (1936, 1937, 1938) analysis of coexisting feldspars is shown by the heavy solid tie lines. The dashed line roughly parallel to the Ab-An sideline shows the optically determined compositional variation in the plagioclase, and the tie line has been connected to the bulk analysis of this plagioclase. The total rock composition

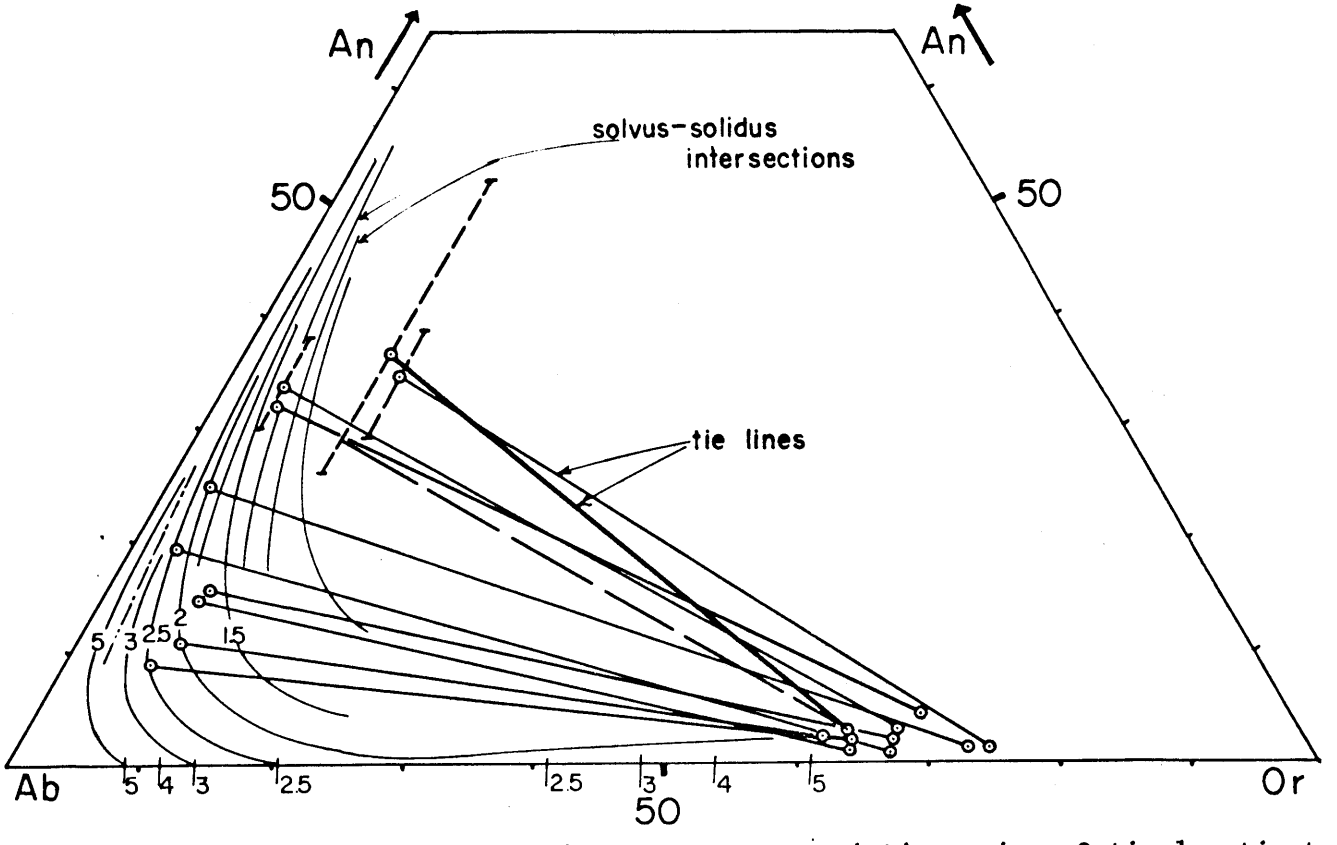


Fig. 36. Natural coexisting feldspars. Tie lines connect coexisting pairs. Optical estimate of range of composition of plagioclase member of pair shown by heavy short-dashed lines. Light solid lines show solvus-solidus intersections at various water pressures from microprobe analyses of feldspars from the Little Chief Stock, and from estimates of various authors based on the compositions of the coexisting melts in equilibrium with the feldspars. Intersections of solvus and solidus in Or-Ab system, using Wright-Orville solvus(Wright, 1964), shown for various water pressures. Water pressure values noted in Kb.

(not shown in figure) indicates that plagioclase would be the first to crystallize, followed by plagioclase and alkali feldspar. Thus, the bulk composition of the plagioclase is too calcic for the plagioclase that would have coexisted with alkali feldspar. Indeed, since the sanidine in this case is apparently not compositionally zoned, it would be most logical to place the tie line for simultaneous crystallization toward the more sodic plagioclase. This is indicated in the figure by the dashed tie line. The orientation of the tie line connecting the two coexisting feldspars is significantly changed.

Recent work on welded tuffs by Scott (1965), and Larsen et al (1936, 1937, 1938), suggest that the plagioclases in the rhyolitic or quartz latitic volcanics are often extremely zoned in a normal sense. Hence, since in most of the cases the bulk rock compositions plot well into the plagioclase field, the bulk data on the plagioclase will in general show the plagioclase as being excessively calcic, and suggest tie lines that in fact have too large intersection angles with the Ab-Or sideline. A similar result would be obtained by bulk analysis of the plagioclase phenocrysts of the stock. Other tie lines shown in Fig. 36 are from Carmichael (1963), Ewart (1965) and Larsen et al (1936, 1937, 1938).

Superimposed on the feldspar compositions and tie lines of Fig. 36 is a set of estimated solvus-solidus intersections. They have been tentatively located using the following data. First, along the Or-Ab sideline, solvus-solidus intersections were located graphically for the quartz saturated system using the lowering of the feldspar liquidus on saturation with quartz at various water pressures combined with the

Wright-Orville alkali feldspar solvus (Wright, 1964; Orville, 1963). Allowance was made for the roughly 10-14°Kb temperature change with total pressure of the solvus.

Within the ternary diagram, several tenuous lines of evidence were used to estimate the trend of the solvus-solidus intersections. The apparent equilibrium zoning trends of the plagioclase phenocrysts of the Little Chief stock were estimated in order to determine the origin of the reversals in zoning (see Fig. 39a). The dot-dash trend is that of a series of coexisting feldspars from a pegmatite (Spruce Pine pegmatite, Orville, 1956) which was at high water pressures and was apparently in equilibrium with quartz.

To place actual pressure values on the lines obtained, within the ternary diagram, the most consistent two feldspar plus melt water pressure determinations were used as obtained from the previous discussions of the Or-Ab-An and Or-Ab-Q systems. Of these various choices, number 1 of Fig. 35 is probably the most reliable, and number 2 and Ewart's results also quite reliable. These values are only rough estimates, but are thought to be good enough to give reasonable pressure estimates. The lowest pressure systems are probably the least accurate. Note that Fig. 36 is the least diagnostic at high water pressures.

A special effort was made to construct a diagram like Fig. 36 because it is thought that, of all the possible water pressure indicators the coexisting feldspar tie lines, and especially the Or percentage of the plagioclase, is probably the best, if it can be determined through textural means which plagioclase coexisted with which alkali feldspar.

The coexisting feldspars, especially in volcanic rocks which have a glassy or very fine-grained matrix, are the least likely to be altered. In volcanic rocks of this type, the feldspars are often fresh while the groundmass is extensively altered and hence changed in composition. The feldspars also have the advantage of preserving a record of their crystallization history so that alteration effects or changes in conditions can be detected.

## Petrogenesis of Stock

In the preceding portion of the thesis, the emphasis has been on the description of the various phases, their compositions, and distribution in the stock. In this section, the main emphasis will be on an attempt to determine the mechanisms which were responsible for the textures observed, and the pressures and temperatures that held sway during the various periods in the crystallization sequence of the stock. The basis of these estimates will be the phase systems just discussed.

There are several important features whose origin should be determined; namely, the transition from two-feldspar to one-feldspar crystallization, the abrupt steps and reversals in zoning of the plagioclase phenocrysts and the trend in the unstable portion of the sodic zones toward very low Or percentage (see Fig. 11). Initially, the two- to one-feldspar transition expressed as oligoclase rimming on sanidine will be treated using the data from DV56 and this will then be compared to the transition in other specimens. All the features noted above in the plagioclase phenocrysts are common to all the specimens, and hence have general application.

Two-Feldspar to One-Feldspar Transition

The crystallization sequence previously determined for specimen DV56 is as follows: The sanidine started to crystallize roughly at the same time that the oligoclase started to crystallize, and was definitely later than the outermost parts of the intermediate zone and associated reversals of the plagioclase phenocrysts. The oligoclase continued to crystallize after the sanidine had stopped crystallizing, so that the oligoclase rims formed on the sanidine phenocrysts. The oligoclase zones on the plagioclase phenocrysts crystallized throughout this whole interval, and hence if there was a sudden change in the physical conditions at the time of the two to one-feldspar transition, it should be recorded in the compositional variation within the stable portion of the oligoclase zone of the plagioclase phenocrysts.

Probe work on the oligoclase zones of the plagioclase phenocrysts shows no abrupt change in composition and the only visible change appears to be a slow steady decrease in the Or percentage of the oligoclase (Fig. 10 or Fig. 11). By comparing Fig. 11 with Fig. 36, it can be seen that the path in the Or-Ab-An system followed by the stable oligoclase crystallization (a to b of Fig. 11) suggests a steadily increasing water pressure. However, this in itself does not explain the two- to one-feldspar change. This must ultimately rest on the geometry of the phase relationships, perhaps by complications caused by the relationship of the feldspar boundary and the critical curve on the solvus.

The sequence of feldspar reactions and rimming observed in specimen DV56, which is a specimen typical of the interior portion of the north

phase of the stock, is very similar to the rapakivi-type rimming in which oligoclase rims both alkali feldspar and plagioclase phenocrysts. If one compares the analyses of the coexisting oligoclase and alkali feldspar from rapakivi granites (Stewart, 1959) with those from specimen DV56 (Fig. 38), it is seen that they are roughly similar. Coexisting feldspars from other specimens of the stock (summarized in Fig. 48) are even more similar. One slight difference is that there are no unrimmed alkali feldspar phenocrysts in the DV56-type specimens as there are in some rapakivi granites.

The crystallization model idealized by Stewart (1959) to explain this sequence of rimming relationships is shown in Fig. 37. In essence, it depends on the rate at which the plagioclase crystallizing in the system can take up Or. As the plagioclase crystallizes, corner A of the three phase triangle plag. + alkali feldspar + liquid (+ vapor phase + quartz in his version) sweeps toward the Or corner, as shown in the progression of isothermal sections $T_1$ - $T_2$ - $T_3$ - $T_4$. In a system with perfect equilibrium crystallization, if the bulk composition were located at point x, at $T_3$ for example, the AB side of the three phase field would pass across point x, and hence two feldspar plus liquid crystallization must give way to one feldspar plus liquid crystallization ($T_4$). In this case, the single feldspar would be plagioclase producing the oligoclase rims on the alkali feldspar cores. In is obvious, however, that many of the rapakivi granites with which Stewart is dealing crystallize at least in part fractionally, hence Stewart allows that the effective bulk composition of the system will move just to the right of point x, but the

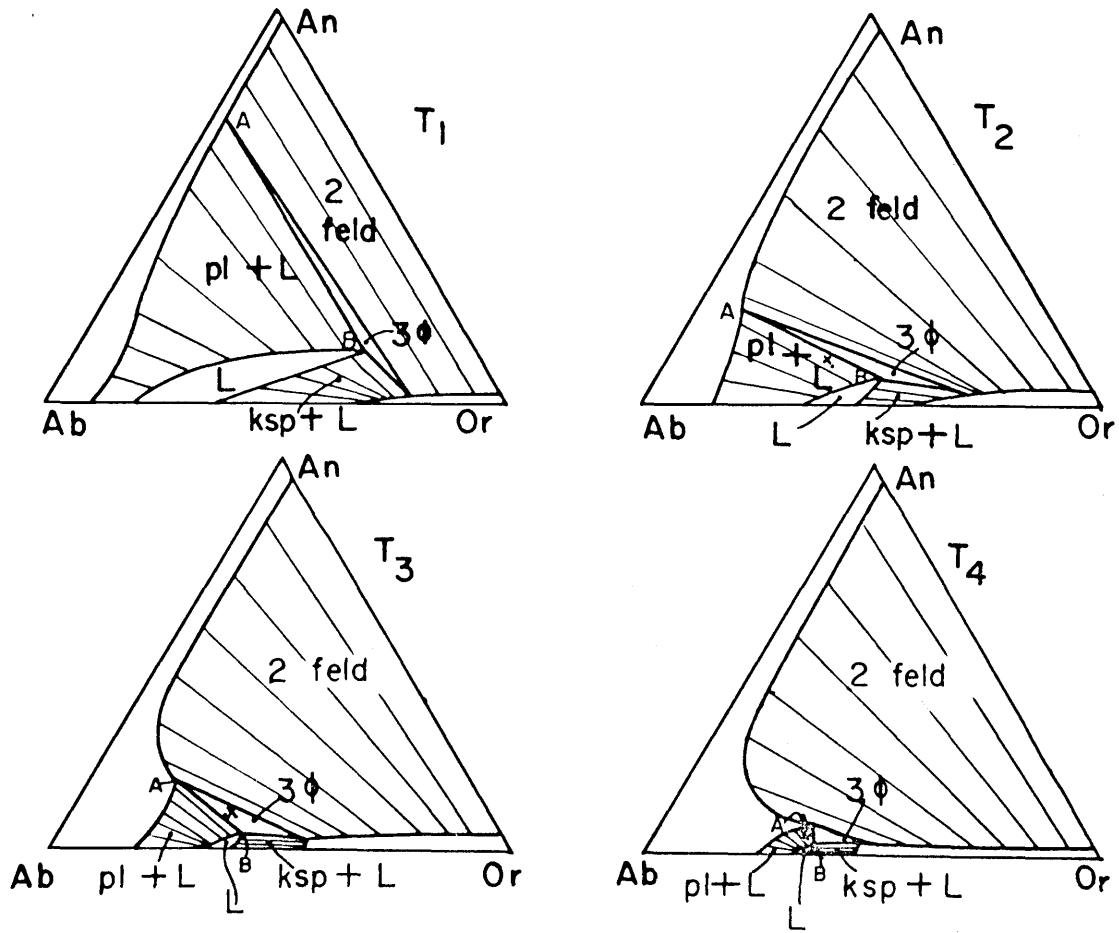


Fig. 37. Series of isothermal sections showing Stewart's model of the crystallization sequence of rapakivi feldspars. $T_1 > T_2 > T_3 > T_4$. pl=plagioclase, L=liquid, Ksp= K-rich feldspar, 3ϕ=3 phase region.

general geometry will still hold and the same result will occur; namely oligoclase rims on sanidine cores. He also notes that, according to this model, the composition of the plagioclase changes rapidly with small decreases in temperature, while the composition of the alkali feldspar does not change nearly as rapidly. He suggests that this might be a further cause of disequilibrium, since the real composition of the plagioclase would tend to lag behind the expected composition.

With the compositions observed in the Little Chief stock, this model may be tested somewhat more rigorously. Figure 38 shows the three phase triangles resulting from the feldspars of specimen DV56. The square is the calculated bulk composition of the rock, gotten from point counts of stained thin sections and cut slabs. The sequence of points labelled 1, 2, 3, 4, 5 and 6 are calculated liquid compositions at various stages of crystallization. Point 1 represents the liquid composition immediately after the most calcic plagioclase has crystallized; obtained by subtracting the proper amount of labradorite from the bulk composition. Point 2 represents the liquid after the andesite zones had crystallized. Point 3 is the composition of the liquid immediately before the two feldspars, oligoclase and sanidine, began to crystallize, but after the very small amount of plagioclase transitional between the andesine and oligoclase zones had crystallized on the plagioclase phenocrysts.

In the figure, the liquid composition is connected to the feldspar composition thought to be in equilibrium with it, which is labelled 1P, 3P, and so on, for the plagioclase and 3S or 4S for the sanidine. Hence the three phase triangle 3P-3S-3 represents the coexisting oligoclase,

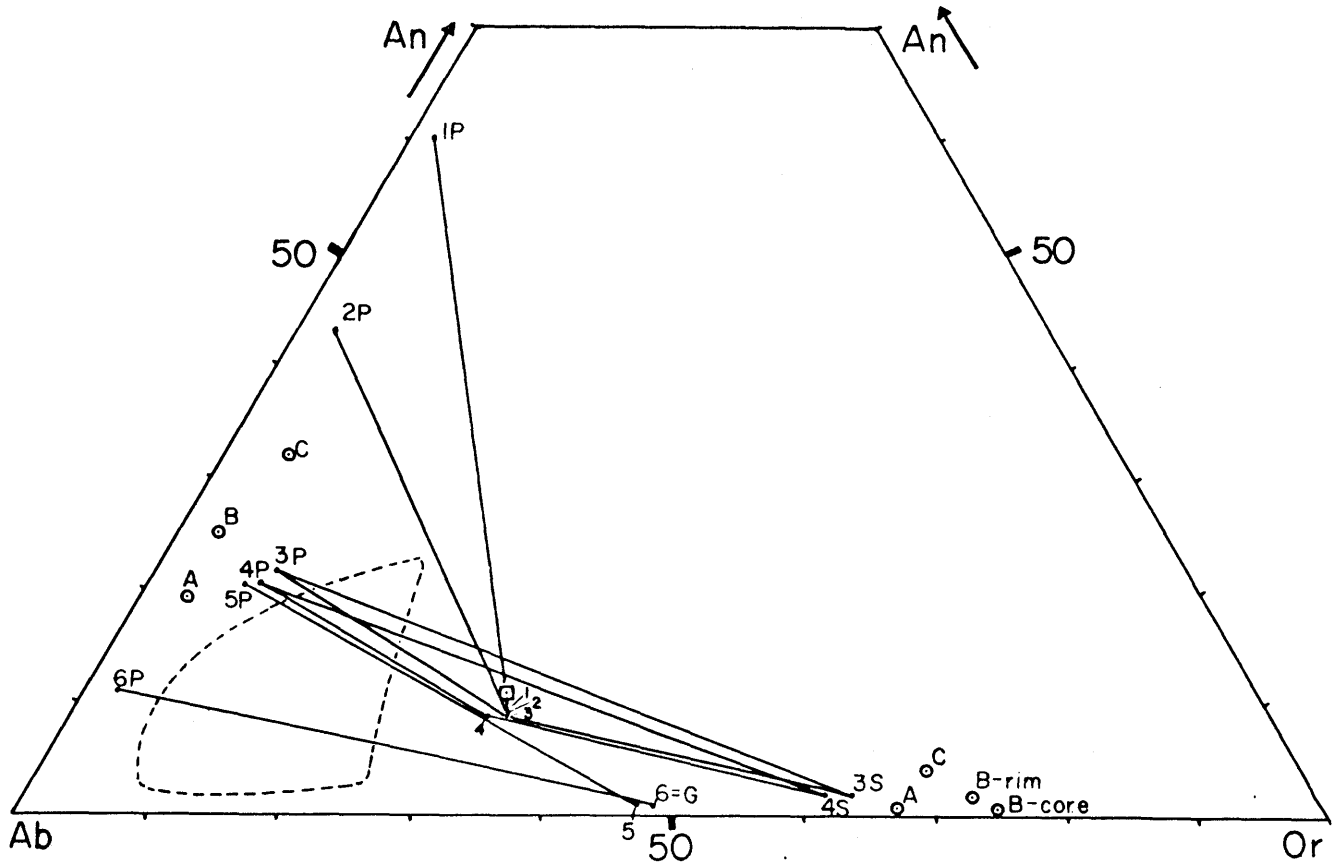


Fig. 38. Composition of coexisting feldspar(s) and melt from specimen DV56. Melt compositions given by numbers 1 to 6, plagioclase compositions given by 1P to 6P, sanidine compositions given by 3S and 4S. Tie lines connect coexisting melt and phases. Circles A, B, and C represent coexisting feldspars from rapakivi granites(Stewart, 1959). G=groundmass Area outlined indicates region in which no feldspar compositions were found from the Little Chief stock. Square shows bulk composition of specimen DV56.

sanidine and liquid at stage 3. Point 4 represents the best approximation of the composition of the liquid at the instant that sanidine stopped crystallizing. Point 5 is the calculated liquid composition after most of the plagioclase rims had crystallized, but just before the outer reversals and sodic plagioclase had crystallized, and finally, point 6 represents the liquid composition after all the phenocrysts had crystallized. This, then, is also the composition of the groundmass.

Referring back to Fig. 37, it is seen that the feldspars of the Little Chief stock show no evidence of the sweep of the plagioclase composition (A) toward the Or corner as suggested by Stewart. In fact, in the stock samples, the plagioclase composition moves in the opposite direction a slight amount on two-feldspar crystallization. Thus, during two-feldspar crystallization, the liquid-plagioclase tie line moves from 3-3P to 4-4P; toward the Ab corner.

There is no evidence in any of the probe work on the plagioclase phenocrysts that a plagioclase with a composition that fell in the outlined area of Fig. 38 ever existed, and there is no break in the oligoclase zones and rims that would allow resorption of a phase of this composition. In fact, on further crystallization, the Or percentage of the plagioclase decreases still further.

The compositional data suggest that crystallization passed from the three phase triangle 4-4P-4S to a two phase tie line 4-4P, but shows no evidence of any sudden change of physical conditions, and does not obviously allow Stewart's rapakivi model to apply in this case. It is possible that the combination of a shift of the two-feldspar boundary due to the suggested steady water pressure increase, and very rapid

crystallization of sanidine which would drive the melt composition toward the Ab-An sideline, could account for the change from two to one feldspar. If Von Platen's data, discussed previously,are correct, then the water pressure increase in the region of liquids 3 and 4 of Fig. 38, should drive the feldspar boundary toward the Or-Ab sideline due to the disappearance of the doubled back portion on the tentative boundary curve. This would drive the boundary curve in the opposite direction that the rapid crystallization of sanidine would tend to drive the melt.

The period of assimilation of basic material does not appear to be related to the change from two- to one-feldspar crystallization. In the interior portions of the north phase of the stock, the change took place before the period of assimilation. In the southern phase of the stock, the feldspars appear to have coexisted through the period of assimilation, and on to a time of crystallization of sodic oligoclase. There is no obvious relationship between the amount of material assimilated, as reflected in the percentage of calcic groundmass plagioclase, and the type and degree of reaction of the sanidine.

On the basis of textural relationships and probe data, the composition of the plagioclase which was crystallizing from the melt at the time that the sanidine started to react with the melt ranged from $An_{20}$ in specimen DV56(north phase interior), about $An_{18}$ in specimens DV151 and DV63(north phase exterior), about $An_{16}$ in specimens DV130 and DV55(late dikes in north phase interior), and about $An_{14}$ in specimen DV74(south phase). In the contact zones of both phases of the stock the sanidine appears to have been stable right up to the time of groundmass crystallization.

Plagioclase Zoning "Reversals"

The two most likely mechanisms of forming the large, abrupt oscillations or reversals (as previously defined) are: first, sudden variations in water pressure, and second, abrupt addition of calcic material to the system through assimilation of carbonate rocks.

In the light of the compositional and textural information on the early igneous phase of the stock, seen only as inclusions within the present stock, the second of the two possibilities seems to be the most likely. The extremely large reversals, which involve compositional changes of 35 percent An or more, the sudden appearance of calcic groundmass plagioclase, and the presence of diopside all favor the assimilation model. However, as noted before, the rapid return of the plagioclase compositions to the normal sodic compositions then requires that the system rapidly returned to normal, and it was suggested that this was caused by the intermixing of large amounts of normal magma with the contaminated magma at the margins of the magma chamber. The fact that the reversals make up a very small percentage of the rock supports this latter concept.

If this model is to account for the reversals seen in the stock plagioclase phenocrysts in general, then there must have been several stages of assimilation, as reversals are present in all the zones of the plagioclase phenocrysts. However, these reversals are much smaller in magnitude than the reversals noted in the early igneous phase, and seldom change the An percentage by more than 10 percent. What is more significant, however, is that these reversals are, without exception, located on the outermost edges of each of the respective compositional zones. This

implies a causal relationship between the formation of the reversals and the change from one compositional zone to another.

In order to test the first possibility listed above-namely reversal formation by water pressure variations-Fig. 39 has been constructed. In this figure, an attempt has been made to compare the detailed compositional changes seen in the reversals with the changes that are expected to take place given certain physical conditions.

The light background lines in Fig. 39a represent the path a crystallizing plagioclase would follow on cooling if the water pressure on the system remained constant, and if the plagioclase were in equilibrium with an alkali feldspar, melt, and fluid. Thus, each line represents the location of the solvus-solidus intersection in the Or-Ab-An system at a different water pressure. The lines were located in the following manner. The probe scan data on the plagiclase phenocrysts from various specimens was examined in great detail, and the compositional variations in those regions of the scans in which the composition was changing regularly and smoothly were plotted on a ternary feldspar diagram. The resulting lines through the respective data points are the background lines of Fig. 39a.

Admittedly, this is an exceedingly subjective method, since the decision must be made as to which portions of the scans to include and which to exclude. It is thought, nonetheless, that these lines approximate relatively constant water pressure solvus-solidus intersections in the Or-Ab-An system. They are consistent with previous estimates based on the simplest geometry of the phase system (Tuttle and Bowen, 1958).

The short heavy lines in Fig. 39a represent the initial compositional changes of the reversals; that is, the first abrupt change in composition from the sodic plagioclase of the broad outer zone to the more calcic plagioclase at the top of each reversal (from A to B in Fig. 39b). The trend of the lines is clearly at an angle to the approximate solvus-solidus intersection trends, and as the composition changes along these trends, the respective plagioclases intersect higher and higher water pressure solvus-solidus intersections in going from the sodic to the calcic portion of the reversals. This suggests that a very sudden increase in water pressure could have been responsible for this type of sudden compositional change.

If the compositional changes took place under relatively constant water pressure conditions, then the zoning should follow one of the background lines. In the simplest case this should be true in the assimilation model on the addition of An to the system. Thus this supports the water pressure change model for reversal formation. It is entirely possible that both models are correct, in that the calcic material that was assimilated contained more water than the magmatic rock which assimilated it.

This dual model of simultaneous assimilation and water pressure increase, followed by mixing with uncontaminated magma of normal water content, is thought to be the most realistic for the formation of the reversals. The respective variations in Or percentage and in An percentage would then be due to the interplay of these two factors.

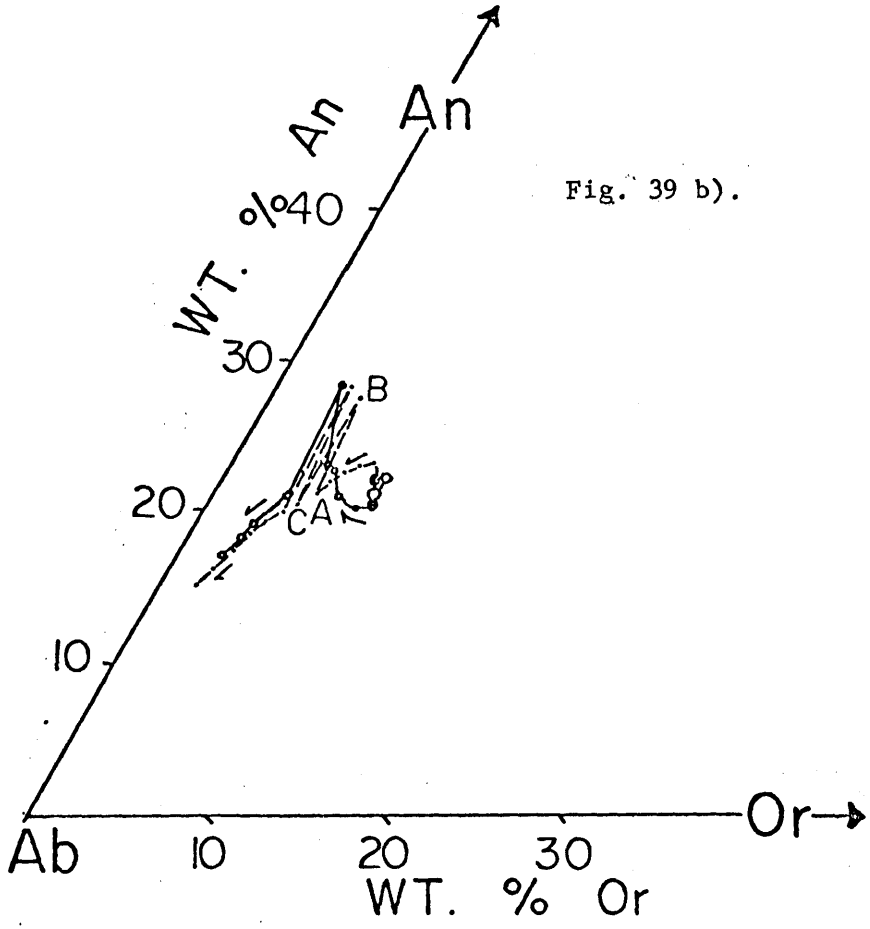


Fig. 39 b).

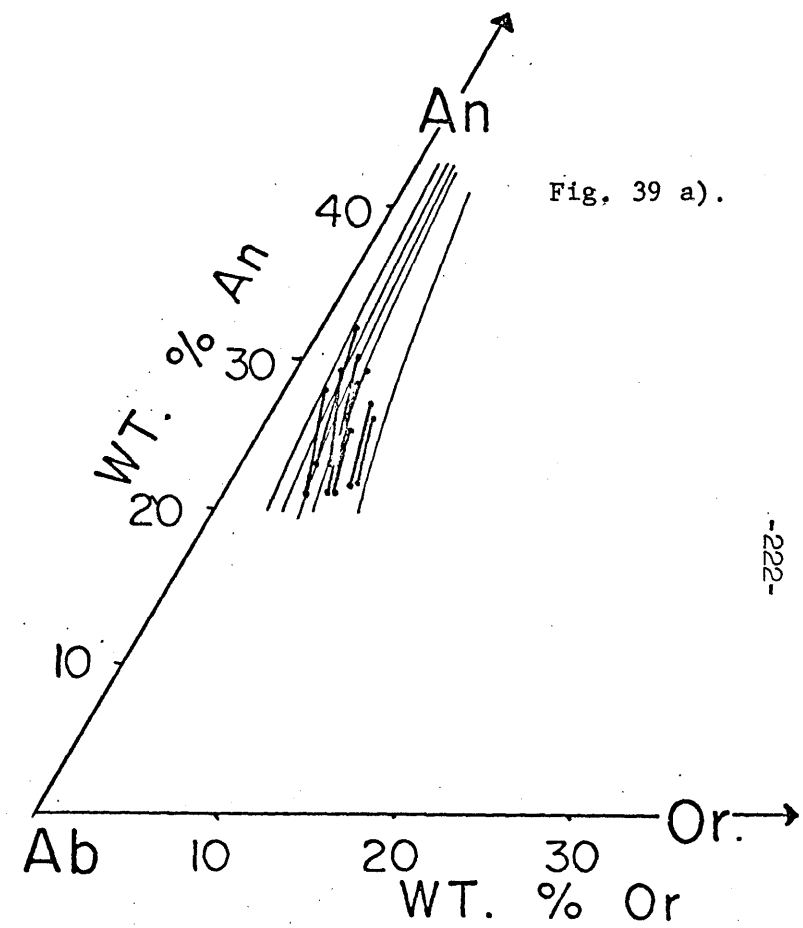


Fig. 39 a).



Fig. 39. b) Detailed compositional changes in outermost edges of sodic plagioclase zones of plagioclase phenocrysts, in unstable portion of phenocryst. Arrows show direction toward outer edge of phenocryst.

a) Initial change in composition of reversals(dark lines), from most sodic to most calcic plagioclase composition, superimposed on estimated solvus-solidus intersection trends at various water pressures(light lines) based on detailed probe scans on plagioclase grains.

Unstable Portion of Sodic Zones on the Plagioclase Phenocrysts

The outermost oligoclase zone of the plagioclase phenocrysts of specimen DV56 was divided into two sections, an inner stable and an outer unstable section. This two-fold division can be made in all the specimens of the stock which contain zoned plagioclase phenocrysts, and in general the thinner outer unstable portion contains the zoning reversals and can be characterized by a decrease in Or percentage toward the edge of the phenocryst. In Fig. 39b, the compositional variation in the unstable oligoclase portion of two plagioclase phenocrysts has been plotted in some detail. The general decrease in Or percentage and the superimposed reversals can be seen. Sanidine in some cases coexists with plagioclases with Or percentages of 2-3 percent so that the plagioclase compositional trend should approximate the solvus-solidus intersection.

Previous work on feldspars has given no hint of the existence of a trend of this sort. Outer sodic margins have been noted, but no information was available on the variation of the Or percentage. Hence the fact that a trend of this sort has not been previously reported may be due entirely to the analytical techniques and not to the true absence of the trend.

In terms of the probable distribution and water pressure values of the various solvus-solidus intersections shown in Fig. 36, the simplest interpretation of the above zonation is that the water pressure on the system steadily increased. However, taken at face value, this would indicate that water pressures in the neighborhood of 4 or 5Kb existed.

Water pressures of this magnitude are not compatible with the inferred depth of emplacement of the magma at this stage of its crystallization history. If the estimated total pressure of 2Kb or so of water pressure at the time of stable two-feldspar crystallization is correct, then the country rocks would have had to withstand an overpressure of 2 or 3Kb, which is not thought possible in the light of the previous results on the stock's structural relationships.

A second possibility which might account for the observed decrease in Or percentage is that of load pressure variations. As a rule, as the total pressure decreases, both the melting temperature of the feldspars and the temperature at the top of the solvus decrease. If they decrease at different rates, then the position of the solvus-solidus intersection will change and the amount of movement of the solvus-solidus intersection in the Or-Ab-An system will depend on the geometry of the system and the difference in the rates of temperature change.

The melting temperature of Ab changes at a rate of $14^{\circ}$/Kb total pressure change (Boyd and England, 1963). The rate of change of the top of the Or-Ab feldspar solvus with total pressure is roughly $14^{\circ}$/Kb (Yoder et al, 1956) as estimated using the solvus determined using the $\bar{2}01$ method. Using Orville's (1963) more recent solvus estimate, which is considered to be more accurate, the change becomes $10^{\circ}$/Kb.

If the $10^{\circ}$/Kb figure for the solvus is correct and holds for the part of the solvus near the sodic oligoclase compositional range, then the difference of rates of change between the solvus and the solidus is such that on load pressure decrease, the solvus-solidus intersection will move outward, or toward lower Or percentage in this compositional

range. This agrees with the observed compositional variation, and is compatible with a magma body moving upward in the crust as is expected of the stock's magma at this point. The problem is chiefly one of scale-it is not thought that load pressure changes can account for all the variation in Or percentage that is observed within the depth limitations put on the magma by the structural work and by the pressure estimates during the immediately preceding stage of stable two-feldspar crystallization. However, note that the decreasing load pressure model reinforces the increasing water pressure model until the time at which the two become equal.

However, there is another possibility. The general trend toward decreasing Or percentage in these very sodic plagioclases could be due to a real curvature of the solvus-solidus intersection caused by the so-called peristerite solvus. Traditionally, solvus-solidus intersections have been drawn, in the ternary feldspar diagram, such that the Or percentage increases with decreasing An percentage. However, there are no good data, as noted above, in this region (the trends in Fig. 39a are valid only for An percentages greater than 20 percent). The only work is that by Muir (1962), who made bulk analyses of successive fractions of coarse anorthoclase-potash andesine or oligoclase feldspar phenocrysts. However, these rocks were chosen for analysis because they were exceedingly dry systems, and hence the increasing Or percentage with decreasing An percentage observed in them is quite far removed from the trends that would be possible in the relatively fluid-rich system under study here.

There is very little information on the expected shape of the peristerite solvus. Most of the information on the observed solubility

gap (Ribbe and Van Cott, 1962; Ribbe, 1960; Brown, 1962), has been based on combinations of optical and X-ray methods, and again there is no information on the Or percentage of the system. It seems established that plagioclases in the compositional range of $An_{2-17}$ tend to unmix. Ribbe (1962) suggested that the plagioclases of composition closer to $An_{17}$ unmix to $An_{2.5}$ and $An_{20}$, while the more sodic plagioclases will unmix to phases of $An_{2.5}$ and $An_{30}$ composition. Tentative estimates of the temperature of the top of the peristerite solvus are roughly 600°C or higher, again assuming no effects due to the Or percentage of the plagioclase.

It is here suggested that, by analogy to the alkali feldspar solvus, the peristerite solvus increases in temperature as Or is added to the system and the compositions move into the ternary system. In the simplest case, the peristerite solvus would merge with the ternary feldspar solvus. This could produce the sequence of isothermal sections through the ternary solvus and below the solidus shown diagramatically in Fig. 40. At higher temperatures, above the two-phase peristerite solvus and in the region in which the solvus is truncated by the solidus, the solvus-solidus intersection on the plagioclase side could curve outward as shown. Crystallization at constant water pressure of two feldspars would then produce plagioclases in which the Or percentage decreased as the An percentage decreased. If the fluid pressure were high enough, and the system saturated with quartz, the solidus might intersect the two-phase peristerite region.

In this regard, a very unusual texture was noted in some plagioclase phenocrysts of specimen DV56. The plagioclase, normal in all

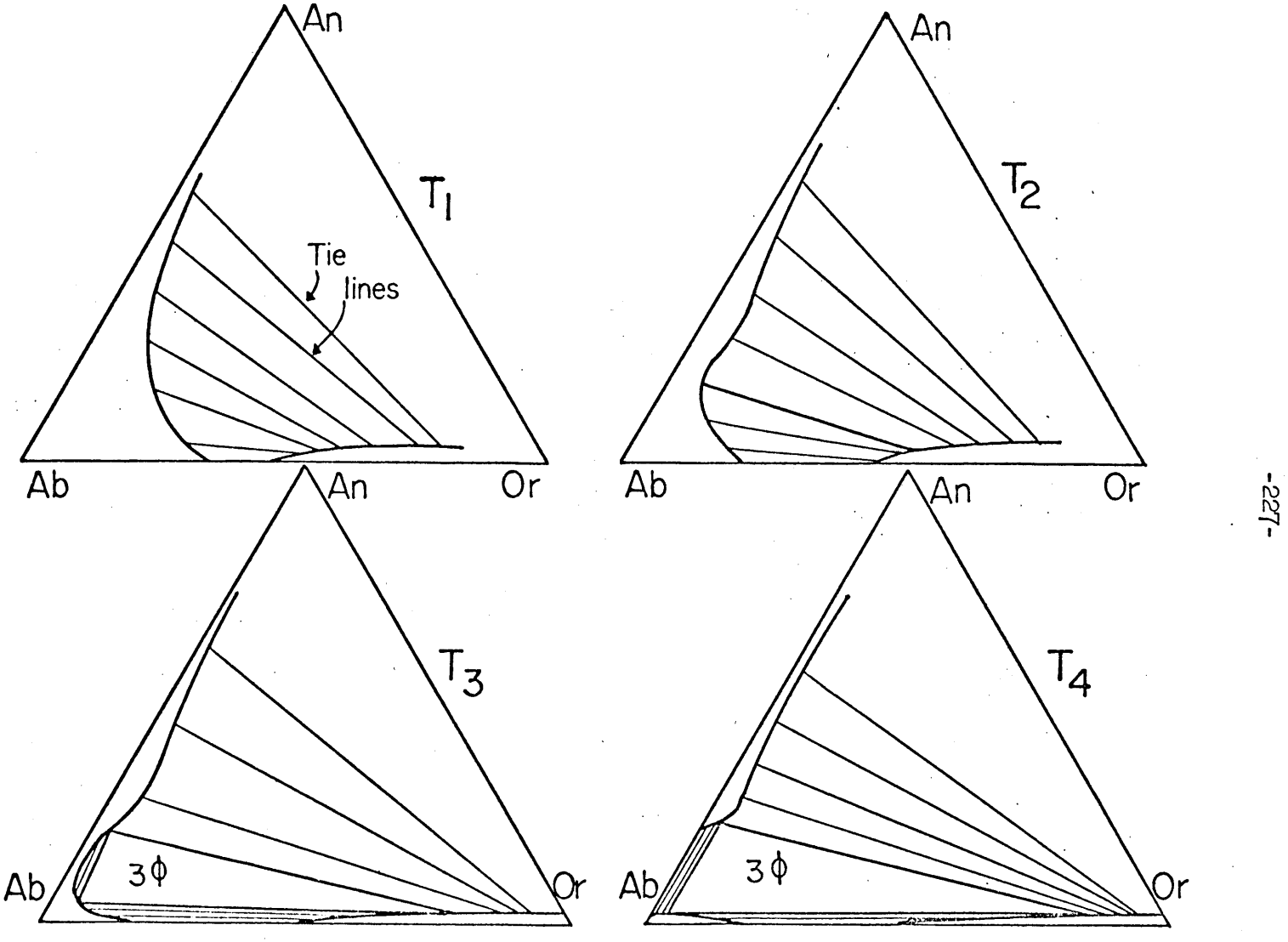


Fig. 40. Series of isothermal sections showing possible effect of peristerite solvus on ternary feldspar solvus. $T_1 \rangle T_2 \rangle T_3 \rangle T_4$. $3\phi$=3 phase region.

other respects, shows a very unusual worm-like extinction pattern in crossed nicols which is illustrated in Fig. 41b. This consists of interstitial worm-like areas of sodic plagioclase set in and often surrounding islands of a more calcic plagioclase which itself has very thin "overgrowths" of an intermediate plagioclase which occurs between the two phases. Several probe scans across these features are shown in Fig. 41a. These show that the composition of the calcic plagioclase islands (shaded) is $Or_{4-5}Ab_{73-74}An_{21-23}$, the worm-like interstitial area (clear) $Or_{2-3}Ab_{96-97}An_{1}$, and the overgrowth-like areas $Or_{1.5-2}Ab$ $Or_{1.5-2}Ab_{92-93}An_{5-6}$. The three compositions are labelled a, c, and b, respectively, in Fig. 41.

This texture occurs in the sodic zones of the plagioclase phenocrysts, and in the plagioclase rims on the sanidine phenocrysts; always inside the reversals and in that part of the sodic plagioclase zones which has been referred to as the stable portion.

The compositions observed-$An_{22}$, $An_{5}$, and $An_{1}$- are very similar to the compositions observed in peristerites, although the $An_{5}$ "selvage," which forms a very minor part of the peristerite, is unusual in combination with a second sodic phase. The transitions between the three phases, as shown by the probe scans, is abrupt in most cases, as would be expected.

A problem with the suggested peristerite origin for the observed texture is that the probable bulk composition of the plagioclase from which the peristerite was produced is in the range $An_{19-21}$, which is outside the limits noted thus far for peristerite formation. According to Brown (1960) no plagioclases with bulk compositions greater than

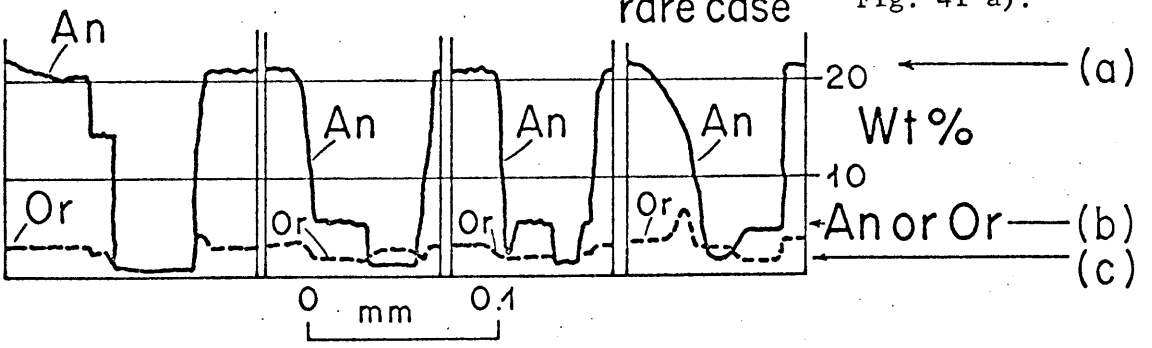


Fig. 41 a).

(a) Shaded area Fig. 41b
(b) "Overgrowth-like" composition
(c) "Interstitial" composition

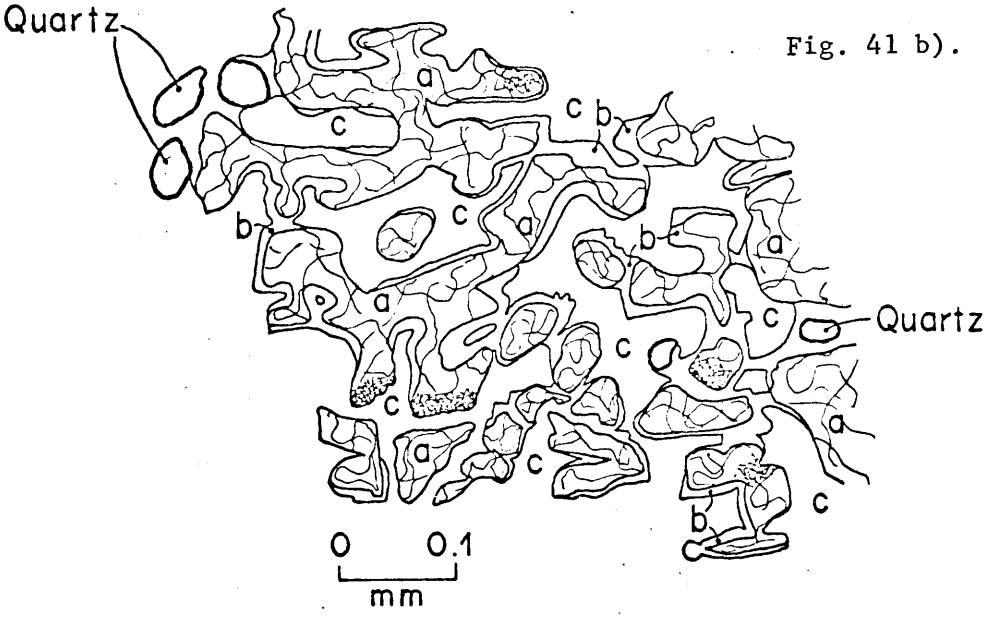


Fig. 41 b).

a— $An_{21}$ Shaded area

b—$An_5$ Overgrowth-like area

c—$An_1$ Interstitial area

Fig. 41 a). Probe scans across possible peristerite exsolution in sodic plagioclase phenocryst of specimen DV56.
b). Sketch of typical peristerite texture from same specimen as was scanned in Fig. 40 a).

$An_{18}$ have been found to have unmixed. However, if the peristerite solvus does expand as Or is added and the system becomes ternary, as suggested in Fig. 41, the limits noted by Brown may not hold.

Of the three methods outlined above for the origin of the compositional trends of the outer sodic plagioclase zones and rims, the two that would seem the most important are the load and water pressure changes. The existence of the "bulge" in the feldspar solvus is questionable and obviously needs further study to verify its existence. The water and load pressure changes are compatible with the upward movement of a magma body, probably unsaturated with respect to $H_2O$, into regions of lower load pressure and higher water concentrations. The evidence noted previously for the period of assimilation and water uptake during the time of reversal formation, which occurred during the period that the compositional variations under discussion were taking place, fits in very well with the expected load and water pressure changes.

Step-like Normal Plagioclase Zonation

Several hypotheses have been advanced in recent years to account for the step-like normal zonation in igneous plagioclase, and the two most likely possibilities appear to be the abrupt decrease of confining pressure as a magma ascends, or abrupt changes in fluid pressure.

Vance (1965), dealing with plagioclase which required the crystallization of calcic plagioclase, a period of resorption, and then the crystallization of a much more sodic plagioclase, favors the confining pressure change method. Since in general the depression of the liquidus and solvus with decrease in confining pressure eventually yields at best

a plagioclase of the same composition as originally (complete fractional crystallization) or a more calcic plagioclase (equilibrium crystallization), assuming that the solidus and liquidus retain their same shape, Vance suggests that in order to get a more sodic plagioclase the curvature of the solidus must be reduced. He justifies the flattening of the solidus by comparing Bowen's (1913) dry plagioclase system, with its very flat solidus, with Yoder's et al (1956) 5Kb $P_{H_2O} = P_{total}$ plagioclase system, which has a much more curved solidus.

While this method might conceivably produce a more sodic plagioclase, it does not appear capable of producing normal zoning "steps" of 15 percent An without also requiring excessively large changes in confining pressure and curvature of the solidus. A confining pressure change is the most logical way of producing the period of resorption, however, which preceded the crystallization of the more sodic plagioclase in Vance's case.

The sequence of crystallization in the plagioclase of the Little Chief stock, which consists of the crystallization of a calcic plagioclase immediately followed by the crystallization of a much more sodic plagioclase, with or without an intervening stage of resorption, is basically the same as that which Vance attempted to explain. The most logical way of crystallizing the more sodic plagioclase is by raising the liquidus by abrupt decreases in fluid pressure. Since the plagioclase liquidus is so sensitive to slight fluid pressure changes, large compositional gaps can be produced in this manner.

In order to test the suggestion that fluid pressure change is responsible for the compositional gaps in the plagioclase zoning, the

transitional portions of the plagioclase phenocrysts between the broad zones of roughly constant composition were scanned with the probe and plotted in Fig. 42. It is clear from the figure that in going from the intermediate to the sodic zones, shown by the larger symbols, the Or percentage of the transitional plagioclase increases abruptly in a series of steps, and does not follow a smooth path. This is most compatible with a succession of decreases in fluid pressure, as in this way the solidus is lifted and the Or percentage of the plagioclase increased. Large decreases in confining pressure would tend to decrease the Or percentage of sodic plagioclase as well as producing a more calcic plagioclase.

Plagioclase Crystallization Summary

In the light of the previous discussions, the most likely combination of processes which could yield the observed sequence of compositional zones in the plagioclase phenocrysts of the stock is summarized as follows. The reversal (or reversals) which occurred at the outer edges of the calcic plagioclase zones were probably formed by the assimilation of calcic wall rock material which may have contained more water than the magma itself. Immediate mixing of normal magma with the contaminated magma soon returned the crystallizing compositions to normal, but the fact of sudden assimilation and water pressure increase implies that the magma was at this time moving upward in the crust.

Continued upward movement resulted in decreases in confining pressure which promoted resorption of the existing plagioclase and eventually brought about fracturing of the roof rocks to the extent that

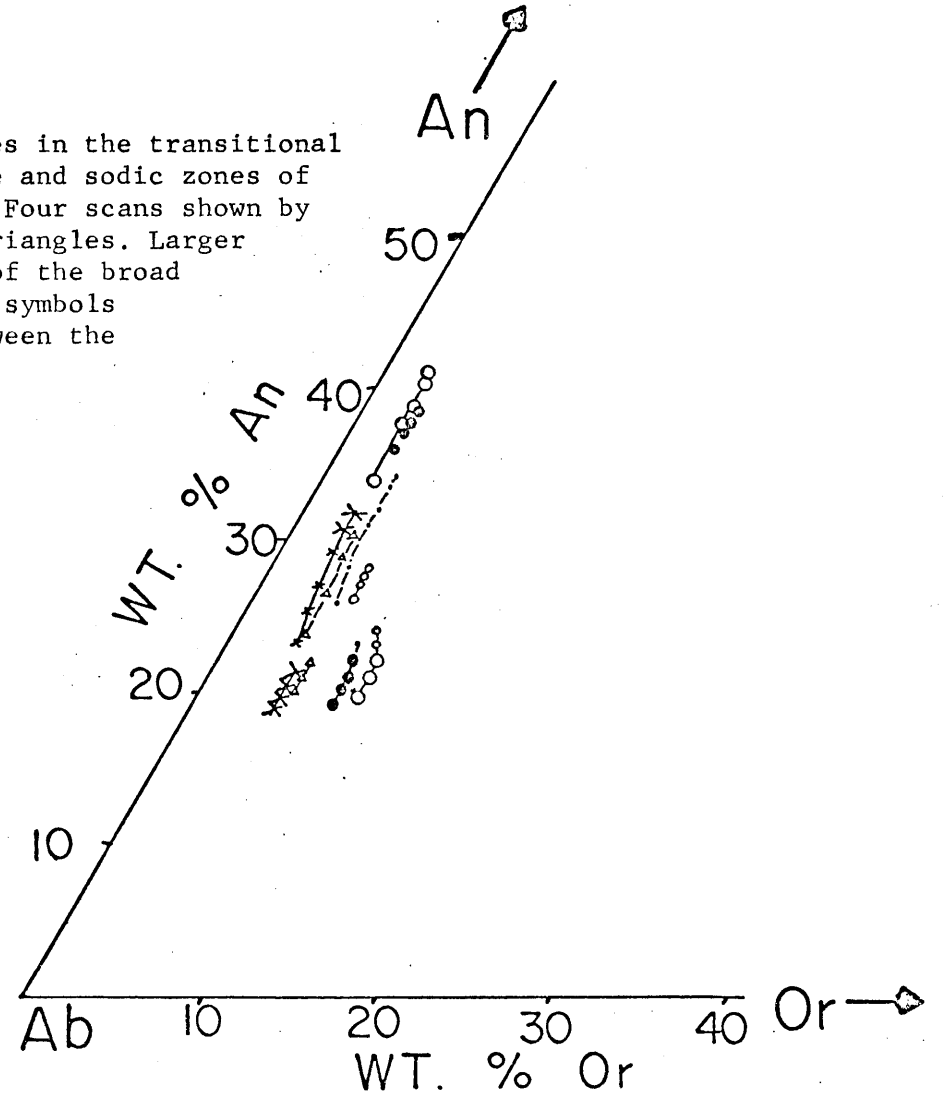


Fig. 42. Detailed compositional changes in the transitional zone between the intermediate and sodic zones of the plagioclase phenocrysts. Four scans shown by crosses, circles, dots and triangles. Larger symbol denotes compositions of the broad compositional zones, smaller symbols compositions in the gaps between the broad zones.

the fluid pressure rapidly decreased as the volatiles escaped. This requires that the fluid pressure was equal to the total pressure at this early stage in the crystallization history, which could be possible if $CO_2$ generated during assimilation was present, and also if fracturing opened the system to higher regions of much lower effective fluid pressure. Erratic, repeated volatile loss produced the abrupt increases in Or percentage seen in the transitional portions of the plagioclase phenocrysts. During the initial stages of upward movement, the magma was probably not saturated with volatiles and resorption could occur. Hence, during the first stages of upward movement, confining pressure effects would dominate, and during the latter stages fluid pressure effects would dominate.

Eventually, upward magma movement was halted and the physical conditions stabilized, producing the intermediate compositional zones. A similar sequence of events repeated itself to produce the next gap in zoning and the sodic compositional zones.

After crystallization of the stable portion of the sodic plagioclase zone, during which time sanidine coexisted with the plagioclase, upward movement was again initiated and the magma moved into regions of lower confining pressure and higher water concentration. Assimilation occurred, producing the reversals and the contaminated marginal phase of the magma chamber which is now seen as the early igneous phase inclusions. Continued upward movement led to fracturing of the roof, devolitatilization of the system which was definitely saturated with respect to volatiles at this point, and formation of the groundmass. During the period of upward movement, much of the replacement of the

sanidine took place. The dike swarms were probably produced at the time that the system was initially devolatilized.

## Bulk Chemical Trends

In terms of the bulk composition of the various samples, as calculated from the probe data combined with point counts of thin sections and stained rocks slabs, the following points can be made about the crystallization history of the stock. First, as is shown in Fig. 43, the bulk compositions in the Or-Ab-An system roughly define a trend in which the Or componant of the system steadily increases until compositions quite near $Or_{50}Ab_{50}$ are obtained. In the figure, the bulk rock composition is shown by the triangles, and the groundmass by the squares, with a tentative melt path shown for each pair.

The dots represent the bulk compositions of the various dike rocks, pegmatites and aplites. In the simplest case, these should represent melts tapped off the larger system in the later stages, and hence should fall along the gross trend for the system. A comparison of Fig. 43 with Fig. 45, on which the large number of calculated groundmass compositions have been plotted, shows that the groundmass data, as expected, roughly defines the same trend. The very calcic samples in Fig. 45, of the early igneous phase, have apparently been extensively modified by Ca addition, and it is felt that these do not lie on the major trend of the system.

The trend indicates a differentiating system-a fact in agreement with the zoning of the feldspars-in which the various specimens have been tapped off at various stages, and in which these various specimens

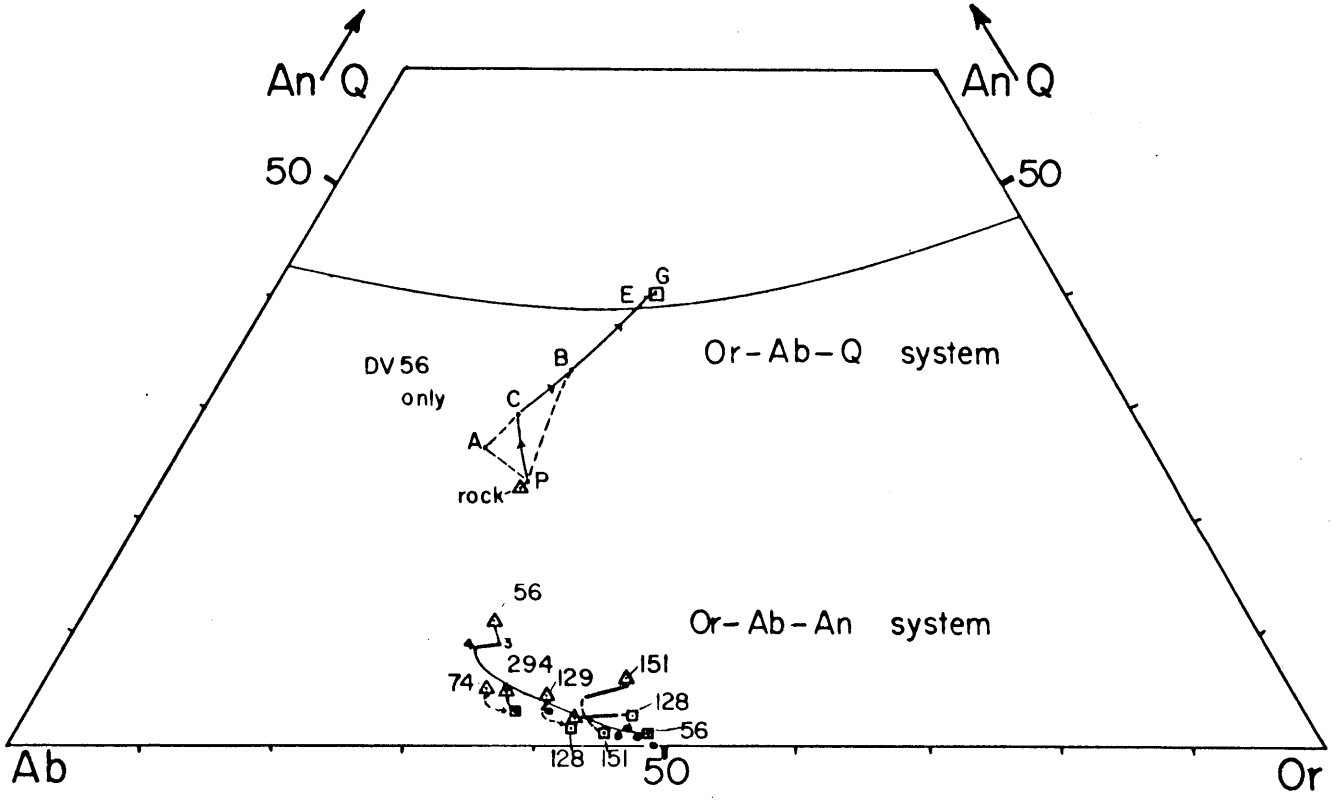


Fig. 43. Or-Ab-Q system. Calculated crystallization path for melt from specimen DV56. Solid line indicates most probable path. See text for detailed explanation. Dashed lines show limiting cases.

Or-Ab-An system. Calculated melt paths of various numbered specimens from the Little Chief Stock. Trend for DV56 calculated, trends for other specimens estimated using probe analyses and modal data. Arrows indicate compositional change with time. Triangle=bulk rock composition, square=groundmass composition. Heavy solid line portion indicates melts which were in equilibrium with two feldspars. Dots=bulk compositions of various dike rocks, pegmatites, and aplites.

have themselves differentiated in large degree. As a general rule, the interior portions of the north phase of the stock appears to represent the earlier stages of differentiation, the southern phase the intermediate stages, and the exterior part of the northern phase the end stages. The samples in the later stages of differentiation show the most extensive development of the patch perthite type sanidine replacement mechanism, the intermediate stages show a dominance of the direct replacement mechanism, and the initial stages show the resorption-rimming sequence.

The calculated trend of the differentiating melt of specimen DV56 is shown in some detail on Fig. 43. This is the only sample that has been calculated in detail, as it is the only specimen in which the phenocryst textures are simple enough to be accurately point counted. In the specimens which have the extensively replaced sanidine phenocrysts, it is not possible to reconstruct the original percentages of sanidine before the replacement stage with any accuracy.

The major fact to be noted in the melt path of specimen DV56 is that the time of crystallization of two feldspars, which occurred in the heavily-lined interval 3 to 4 (Or-Ab-An system, numbers as in Fig. 38) is such that the melt is very An-rich and falls in an area not usually expected to contain melts which coexist with two feldspars. However, a comparison of Fig. 34 with Fig. 43 indicates that this area is almost exactly that in which Von Platen's data indicates that the feldspar boundary occurs. Hence, this tends to support Von Platen's results, and further strengthens the concept of a doubling-back of the

feldspar boundary trend postulated in Fig. 34. The estimated areas in which melt plus two feldspars existed for the other specimens are also shown by the heavy lines, and these too indicate very Ab-An-rich melts relative to those that would have been allowed in the light of previous experimental work.

Fig. 43 also shows the calculated melt path for DV56 plotted in the Or-Ab-Q system. Three paths are shown. The path through A is calculated assuming that all the sanidine phenocrysts crystallized before any of the oligoclase, B is calculated assuming no oligoclase crystallized after the sanidine, while C is calculated assuming that part of the oligoclase crystallized with the sanidine and part after it. This latter is texturally the most reasonable, and is the path shown in the Or-Ab-An system. Two feldspars coexisted with each other in the section PC, and the orientation of the path relative to the feldspar cotectics of Fig. 33 is compatible with a slow steady increase of water pressure. However, the effect of An in the system on the location of the cotectic is an unknown factor. Using the data of Von Platen one could recreate the melt path shown for DV56 in Fig. 43.

## Estimate of Physical Conditions

Estimates of the physical conditions of stock crystallization may be made reliably for two periods of its crystallization history: The stage of two-feldspar phenocryst crystallization, and the stage of groundmass crystallization at the present level of exposure of the stock.

In the ideal case, the bulk composition of the groundmass should represent the composition of the melt that was in equilibrium with the feldspar phenocrysts during the time that the two feldspars crystallized together under relatively stable conditions. The previous discussions have shown that the period of stable two-feldspar crystallization was followed by a short period of unstable crystallization during which the reversals were formed, calcic material was assimilated, and sanidine reacted with the melt. All these changes would modify the ideal melt composition that was present during the stable two-feldspar crystallization stage and hence must be allowed for in using the groundmass compositions for estimates of the physical conditions.

Groundmass Crystallization Conditions

The calculated groundmass compositions are shown in Fig. 44 and 45, in the Or-Ab-Q and Or-Ab-An systems, respectively. The compositions of each of the different parts of the stock have been grouped together, and each point has been labelled with its specimen number.

It is immediately apparent that the different portions of the stock have different groundmass compositions. Thus, the outer portion of the north phase of the stock (squares) is the most quartz-rich, while the interior portion of the northern phase and the southern phase are quite similar and of intermediate quartz percentage, and the early igneous phase is quite quartz-poor.

In order to determine the physical conditions at the time of groundmass crystallization, it is necessary to find those samples in which the ideal melt which coexisted with the phenocrysts has itself differentiated to some degree so that while its bulk composition might represent the earlier melt, the quartz-alkali feldspar ratio and the Ab/Or ratio of the alkali feldspar would represent groundmass-time imposed conditions. For instance, in those specimens to which significant Ca and Mg have

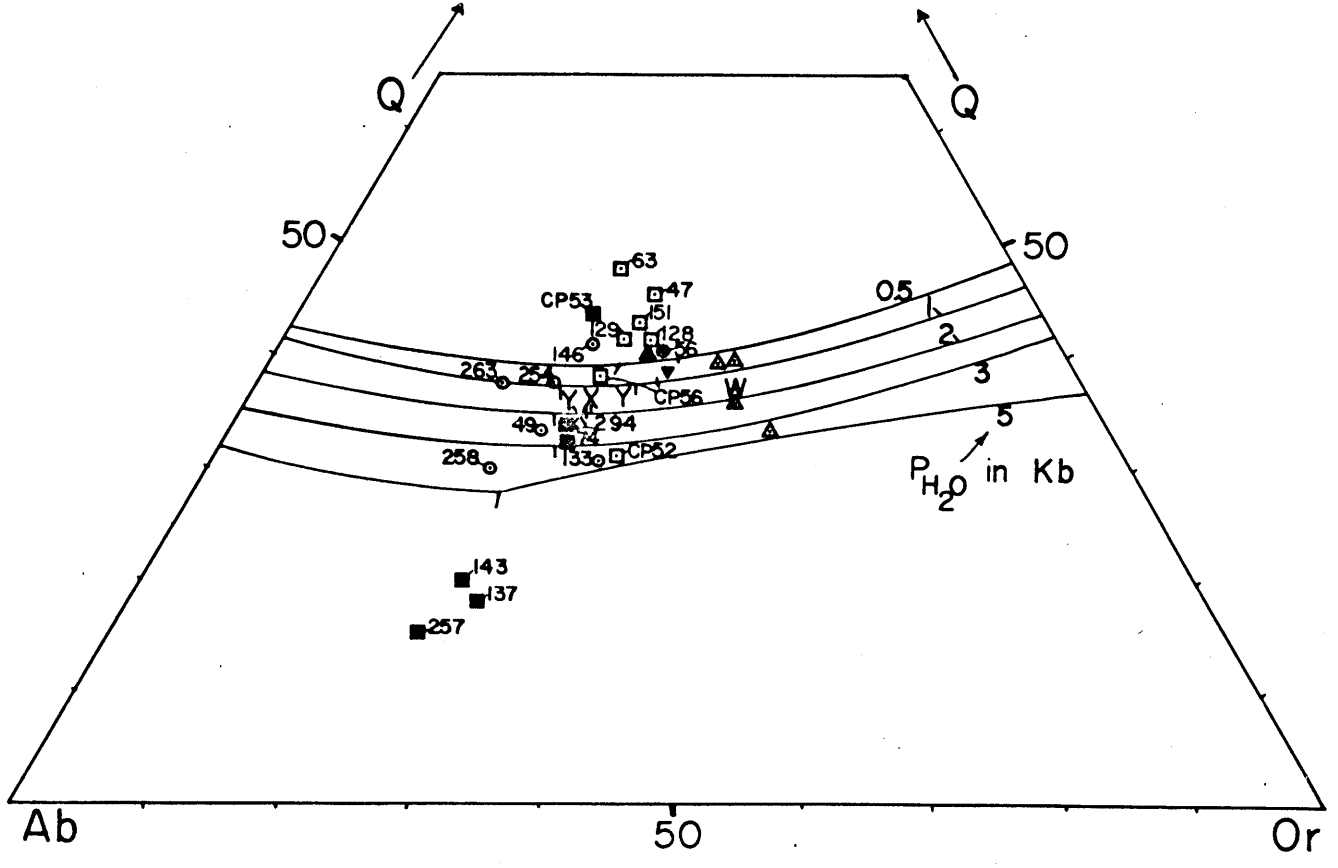


Fig. 44. Calculated bulk groundmass compositions of various stock specimens, plotted in Or-Ab-Q system. Quartz-feldspar boundaries at various water pressures shown(labelled in Kb.) by solid lines. Solid squares-south phase of stock, open squares-exterior north phase of stock, squares with cross(3 low-quartz specimens)-early igneous phase, open circles-interior north phase of stock, triangles-dikes in interior north phase of stock. Solid circle-Average of interior north phase compositions, solid triangle-average of dike and aplitic rocks, inverted triangle-average of exterior north phase of stock. See text for explanation of letters(X,X',Y,Y',and W).

Fig. 45. Calculated bulk groundmass compositions of various labelled stock specimens plotted in the Or-Ab-An system. Symbols as in Fig. 44.

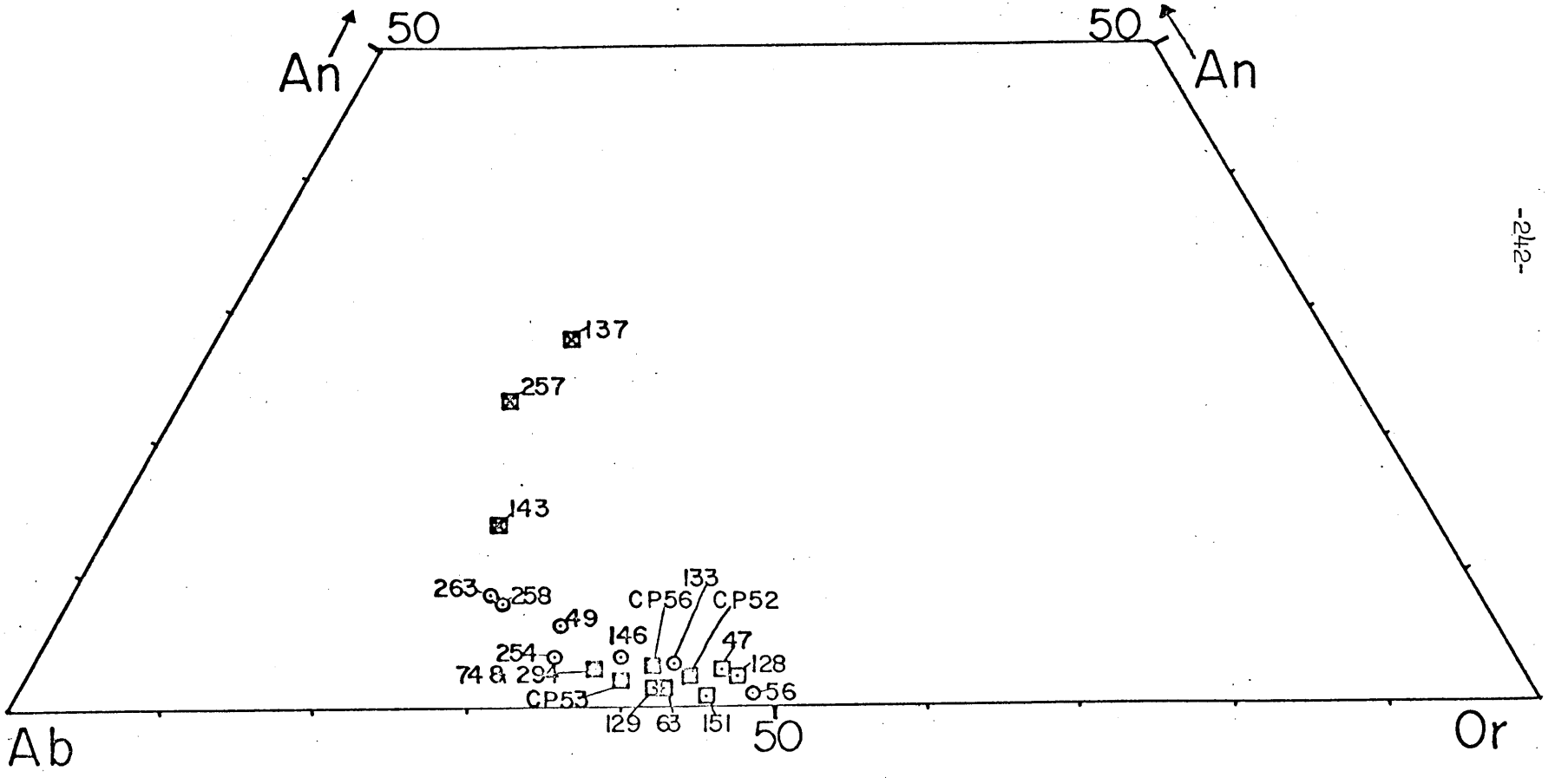

been added, it is obvious that at the time of groundmass crystallization, the crystallization sequence was the following: Crystallization of the labradoritic plagioclase, and then abrupt zoning of the plagioclase to sodic oligoclase compositions, and finally, cystallization of a single alkali feldspar and quartz. Thus the alkali feldspar is consistently later than the plagioclase. This is compatible with the Or-Ab-Q system at low water pressures since in these cases, the minimum on the quartz-feldspar boundary is on the alkali feldspar portion of the boundary, and any sequence that starts out with plagioclase and that succeeds in reaching the minimum must end up with only alkali feldspar and quartz. Since in all the stock specimens the alkali feldspar is later than the groundmass plagioclase, and since the plagioclase itself is zoned, we are dealing with a true differentiating system and hence we may subtract the plagioclase from the groundmass bulk composition to get an idea of the minimum melt composition.

Dealing first with the interior portion of the northern phase of the stock (circles, Fig. 44), the average groundmass melt composition after groundmass plagioclase subtraction plots in the area of the solid circle. Of the 8 calculated groundmasses used, 5 fall within 2 percent of the average point, and the two samples which deviate most, DV133 and 146, both occur very near the stock margin and close to the volatile rich northeast corner area of the stock. This point, along with the Or/Ab ratio, indicates a water pressure of roughly 0.4Kb and a temperature of 780°C.

A second reliable estimate of the groundmass composition may be

gotten from those phases tapped off the crystallizing system at the present level of emplacement--that is, the dikes of the contact sheath and dike swarm, the aplitic dikes, and the pegmatitic pods. Here no subtraction of plagioclase should be necessary. Their bulk compositions are shown in Fig. 46. The compositions for all the dikes were gotten by partial chemical analysis ($Na_2O$ and $K_2O$ by flame photometer, Cao by emission spectroscopy, $SiO_2$ by X-ray fluorescence), while the aplite and pegmatite compositions were calculated from probe data. The average bulk composition of the dike swarm dikes, and the dike sheath dikes, is essentially the same as the pegmatite and aplite compositions, and is shown in Fig. 44 by the solid triangle. On Fig. 44, this also indicates a water pressure just less than 0.5Kb.

The specimens from the exterior portion of the north phase of the stock, shown by the squares in Fig. 44 consistently have less than 4 percent plagioclase in the groundmass, and hence have not had significant addition of Ca-rich material as have the other specimens discussed. Only three of the groundmass analyses are accurate enough to be used to estimate the water pressure in the system at the time of groundmass crystallization. The two samples with arrows, DV63 and 47B, are good only for maximum estimate of the quartz percentage since the alkali rim material was not included in the groundmass point counts in these cases. The same is true for CP53. Using the three reliable analyses, a very low water pressure is indicated, in the vicinity of 0.3Kb. This is surprising in the light of the fact that this portion of the stock shows the most obvious evidence of large amounts of vapor phase. Of the three specimens used, DV128A should give the best groundmass pressure

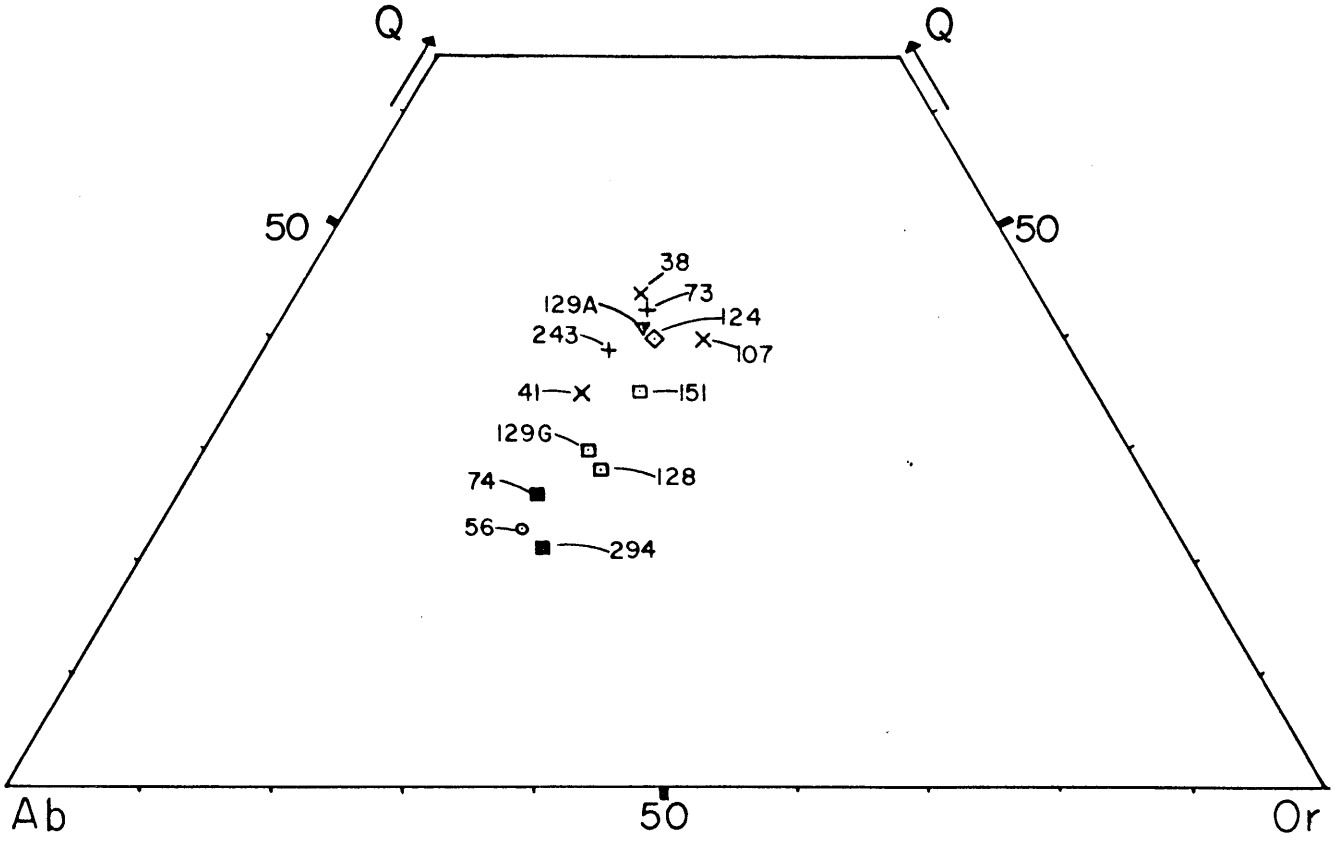


Fig. 46. Calculated bulk rock compositions of various labelled stock specimens plotted in the Or-Ab-Q system. Open squares-north phase exterior of stock. Solid squares-south phase of stock. Circle -interior north phase of stock. X-porphyry dike specimens. Inverted triangle-aplite dikes. Diamond-pegmatite. +-dike sheath rocks.

estimate since it is a very volatile-rich specimen and presumably equilibrated to the new pressure conditions.

The groundmass compositions of the southern phase of the stock, noted by the solid squares, result in the average value shown by the inverted solid triangle using the plagioclase subtraction method outlined above. This yields a pressure of just over 0.5Kb.

The consistency of results using the groundmass melt compositions obtained by subtraction of the groundmass plagioclase, and the results from the dikes and volatile rich phases, indicate that the water pressure of the system at the present level of emplacement was roughly 0.4-0.5Kb and the temperature roughly 770 to 790°C.

Total Pressure Estimate at Time of Groundmass Crystallization

A key to determining the amount of $CO_2$ in the vapor phase is the presence of wollastonite in one of the contact scarns. Experimental evidence on reactions which form this mineral in the presence of both $CO_2$ and $H_2O$, and the variation of this reaction in P-T space with the $H_2O/CO_2$ ratio of the vapor phase now exist.

Fig. 47 shows the variation of the reaction calcite + quartz goes to wollastonite + $CO_2$ in $P_{total}$- T space for various $H_2O/CO_2$ ratios. The diagram, from Winkler (1965, p. 30), was constructed by Winkler using Greenwood's (1962) data at $P_{total}$= 1 and 2Kb for the reaction, plus data on the reaction with $P_{total}$= $P_{H_2O}$ from Harker and Tuttle (1955). Since we are dealing with a very thin contact zone in this case, the temperature of the diagram will essentially be that at the contact of the stock.

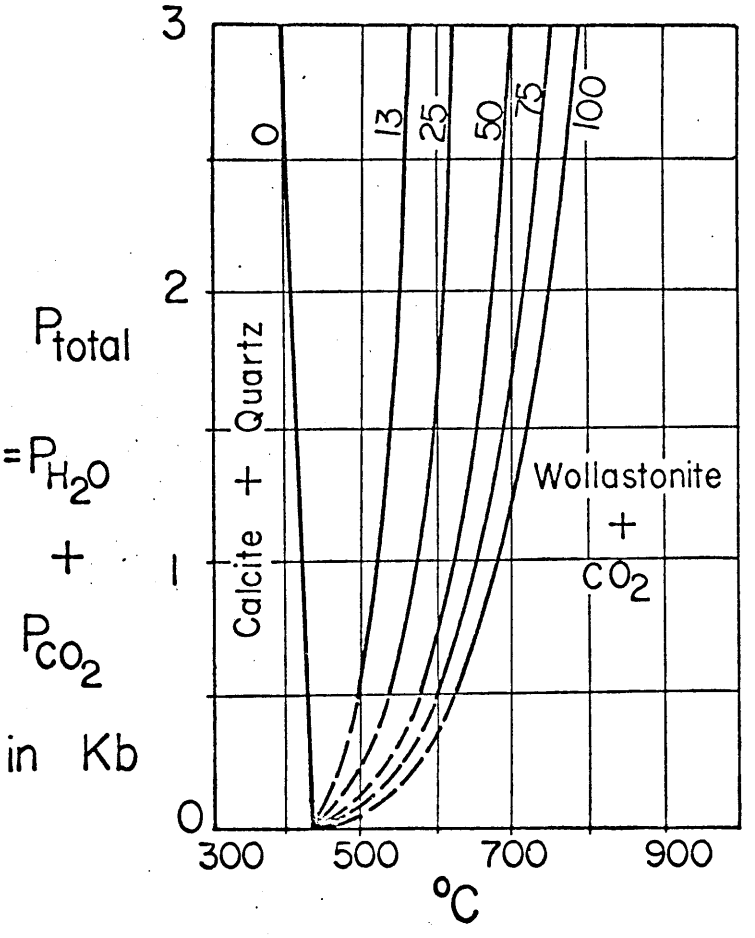


Fig. 47. Variation of reaction calcite + quartz = wollastonite + $CO_2$ with total pressure(in Kb.), mol percent $CO_2$ in vapor phase(labels on curves), and temperature. Figure from Winkler(1965) after data of Harker and Tuttle (1955) and Greenwood(1962).

Using Jaeger's heat flow calculations (1957), which assumed a vertical dike geometry of various thicknesses, treated only conduction, allowed for latent heat of crystallization, and finally assumed that the magma crystallized regularly inward from the walls, the temperature at the contact is roughly two-thirds of the magma temperature. At 0.5Kb, the water pressure estimated for the stock during groundmass crystallization at the present level of emplacement, the eutectic temperature in the Or-Ab-Q system is roughly 775°C. This is probably a maximum temperature since if perfect equilibrium did not occur the temperature would be lower as the system originally came from higher water pressures. This places the contact temperature at roughly 500°C plus the wall rock temperature before intrusion.

Taking the estimated contact temperature of 500°C, a $P_{H_2O}$ of the system of 0.5Kb, and various wall rock temperatures, Fig. 47 provides estimates of the mole fraction of $CO_2$ in the vapor phase. If the wall rock temperature were 100°C, then $P_{total}$ is about 0.9Kb and the vapor 40 percent $CO_2$. If the wall rock temperature were 50°C, then $P_{total}$ is about 0.7Kb and the vapor was roughly 20 percent $CO_2$. The latter probably is a more reasonable estimate.

Coexisting Feldspar Crystallization Conditions

In order to use the calculated groundmass compositions to determine the water pressures which existed at the time that the phenocrysts crystallized, any effects which occurred in the interval between groundmass and stable phenocryst crystallization must be removed. However, in practice, it is essentially impossible to remove these effects except by

relying on those specimens which seem to show the least evidence of the existence of these effects.

For instance, if one simply averages all the calculated groundmass compositions for the specimens of the interior portion of the north phase of the stock, the result is point Y in Fig. 44. This assumes that the plagioclase in the groundmass is part of the equilibrium assemblage and that, if any calcium addition did occur, it was not significant. Since the groundmass plagioclase percentages of four of these specimens are 17, 20, 27, and 30 percent, it seems most likely that this would have a significant effect on the bulk groundmass composition of these specimens. Hence, if these four high-An samples are neglected and an average based on the remaining three low An specimens, the result is Y' in Fig. 44, which is felt to be a more reasonable result. This yields a pressure of roughly 1-1.5Kb and a temperature roughly 700°C.

Similarly, averaging all the specimens from the south phase of the stock results in point X. Since none of these specimens have plagioclase percentages in the groundmass of greater than roughly 10 percent, there is no major problem here. However, two of the specimens, CP52 and CP53, are contact phase rocks in which it would be expected that the groundmass would have equilibrated with the conditions at the level of emplacement in the volatile-rich area. Hence, these would most likely give erroneous results. Also, specimen CP52 contains a large amount of very fine graphic quartz-feldspar intergrowth in the groundmass, and hence the point counting is very poor and quite likely the quartz percentage is underestimated. Using the remaining three

specimens, point X' is gotten. This yields a pressure of roughly 2Kb and a temperature of 680°C. Again, all samples in this case are low enough in An that it can be neglected.

The dark phenocryst-rich dikes which occur in the interior north phase of the stock have an exceedingly fine groundmass, and this groundmass could conceivably represent the most quenched melt available in any of the specimens seen. The probe determined groundmass compositions, which are only approximate, are plotted in Fig. 44 as the open triangles, and the average of four determinations is noted as point W. This suggests an approximate water pressure of 1-2Kb, but has an anomalously low Ab-Or ratio on the average. Optical studies indicate that biotite is present in the groundmass, and since a moving-spot technique was used it is entirely possible that some of the excess Or is in fact due to K counts gotten from the biotite.

The groundmass analyses of the northern phase exterior portions suggest that the rock has equilibrated to the new, groundmass crystallization conditions, and hence no estimate of earlier pressure conditions can be made.

Thus, on the basis of the groundmass compositions, estimated water pressure values of roughly 1-1.5Kb and 2Kb, respectively, are gotten for the interior north phase and the south phase of the stock.

A second method of estimating the water pressures in the system is to use the compositions of the coexisting feldspars in conjunction with Fig. 36 on which the various solvus-solidus intersections under quartz saturated conditions at various water pressures have been estimated.

Figure 48 shows the compositions of the coexisting feldspars determined in the various samples from the stock. The figure is so set up that for each sample, the first and last coexisting pair of feldspars is shown, and the arrows on the lines connecting the first and last plagioclase, etc., indicate the direction of zoning of the average of the crystals analysed going from center to edge of the crystals. Hence, there is an infinite number of tie lines between each pair of tie lines for a given sample.

The first thing that is apparent is that there are two groups of coexisting feldspars. The first is represented by DV56, which clearly crystallized at a lower water pressure than the other specimens. Judging from the examination of thin sections throughout the stock, this sample is representative of the coarse interior portion of the north phase of the stock.

The second group is clearly representative of a higher water pressure, and is made up of specimens from the exterior of the north phase of the stock, the south phase of the stock, and the dark porphyry dikes which occur within the interior portion of the north phase of the stock. The trend toward sodic plagioclase with low Or percentage in these specimens is very well shown in this figure.

In order to determine an actual water pressure, these feldspar compositions must be compared with Fig. 36. The assumption is made here that the quartz-saturated system can be used since in many of the specimens, the presence of the quartz trains in the alkali rims indicates that quartz crystallization initiated immediately after the

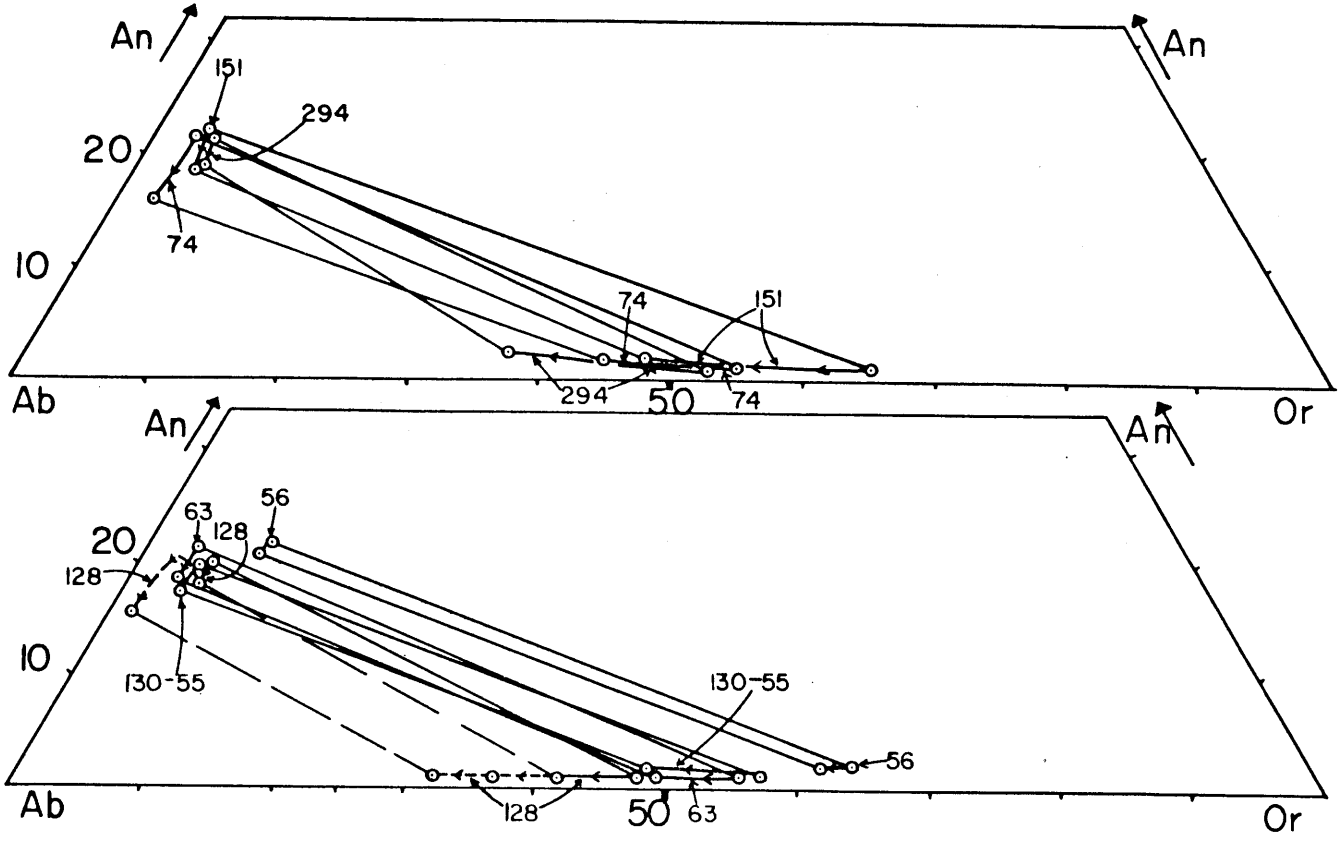


Fig. 48. Summary of coexisting feldspars from the Little Chief stock, plotted in the Or-Ab-An system. All data in weight percent. Tie lines connect first and last feldspars to coexist in any given specimen, arrows indicate direction of compositional change during two feldspar crystallization stage, in direction toward outer edge of phenocrysts. Numbers refer to specimen numbers.

phenocryst stage.

The data indicates that DV56 crystallized at roughly 1.3Kb water pressure, and this is thought to be a representative value for the interior portion of the north phase of the stock.

The values gotten for the rest of the feldspars indicate water pressures of roughly 2-2.5Kb for the bulk of the crystallization of the oligoclase plagioclase.

The estimated water pressures-roughly 1-1.5Kb for the interior portion of the north stock phase, and roughly 2-2.5Kb for the rest of the stock--are quite similar by either the groundmass method in the Or-Ab-Q system, or the coexisting feldspar method in the Or-Ab-An system. That the two methods agree is encouraging but not proof of the absolute correctness of the two methods. Of the two, it is felt that the coexisting feldspar method is potentially the more accurate since the feldspars are less susceptible to alteration than the groundmass, but it is obvious that considerable work must be done to calibrate the tentative solvus-solidus intersections more accurately.

The orientation of the tie lines in Fig. 48 are all relatively consistent except for those of DV128A, and the sodic tie line of DV294. The sanidine composition of DV128A is not particularly reliable due to the tendency of the crystals to form very coarse lamellar perthite, and hence the tie lines have been dashed. The plagioclase, despite its complexity, is thought to be reliable. The more sodic tie line of DV294 is probably not correct, as no true plagioclase phenocrysts were analysed; only those which were found in the megaphenocrysts and therefore which had the most sodic plagioclase. The sanidine composition is reliable.

# SUMMARY

## Crystallization Sequence

The crystallization sequence of all the feldspars may be subdivided into five stages as follows: 1) calcic plagioclase phenocrysts, 2) oligoclase + sanidine phenocrysts, 3) period of reversals on oligoclase plagioclase phenocrysts, and zoning to very sodic compositions, 4) removal of sanidine from equilibrium, and 5) groundmass crystallization stage. Stages 3) and 4) overlap, and both can be transitional into stage 5). Figure 49 summarizes the stock feldspar compositions.

The first stage consisted of the crystallization of zones of plagioclase with restricted compositions in normal zoning sequence with abrupt compositional breaks between the zones. In the rocks with the most An-rich bulk compositions, the plagioclase zoning sequence was $An_{60}$-$An_{42}$-$An_{20}$ (Fig. 49, $A_3$-$A_2$-$A_1$). This sequence is found only in the interior portion of the stock's north phase. In the rocks of intermediate bulk An percentage the plagioclase sequence was $An_{50}$-$An_{35}$-$An_{20}$ (Fig. 49, $B_2$-$B_1$), and in the lowest An percentage rocks it was $An_{40}$-$An_{20}$ ($B_2'$-$B_1$). Often, at the outermost edges of the various zones, abrupt reversals in zoning occur in which the plagioclase composition rapidly increases in An percentage and then decreases to the original composition (RA and RB). These reversals are invariably present on the outer edges of the $An_{20}$ zones. The volume percentage of plagioclase with greater than 30 percent An is usually less than 3 percent of the rock.

The next common stage throughout the stock is that of the

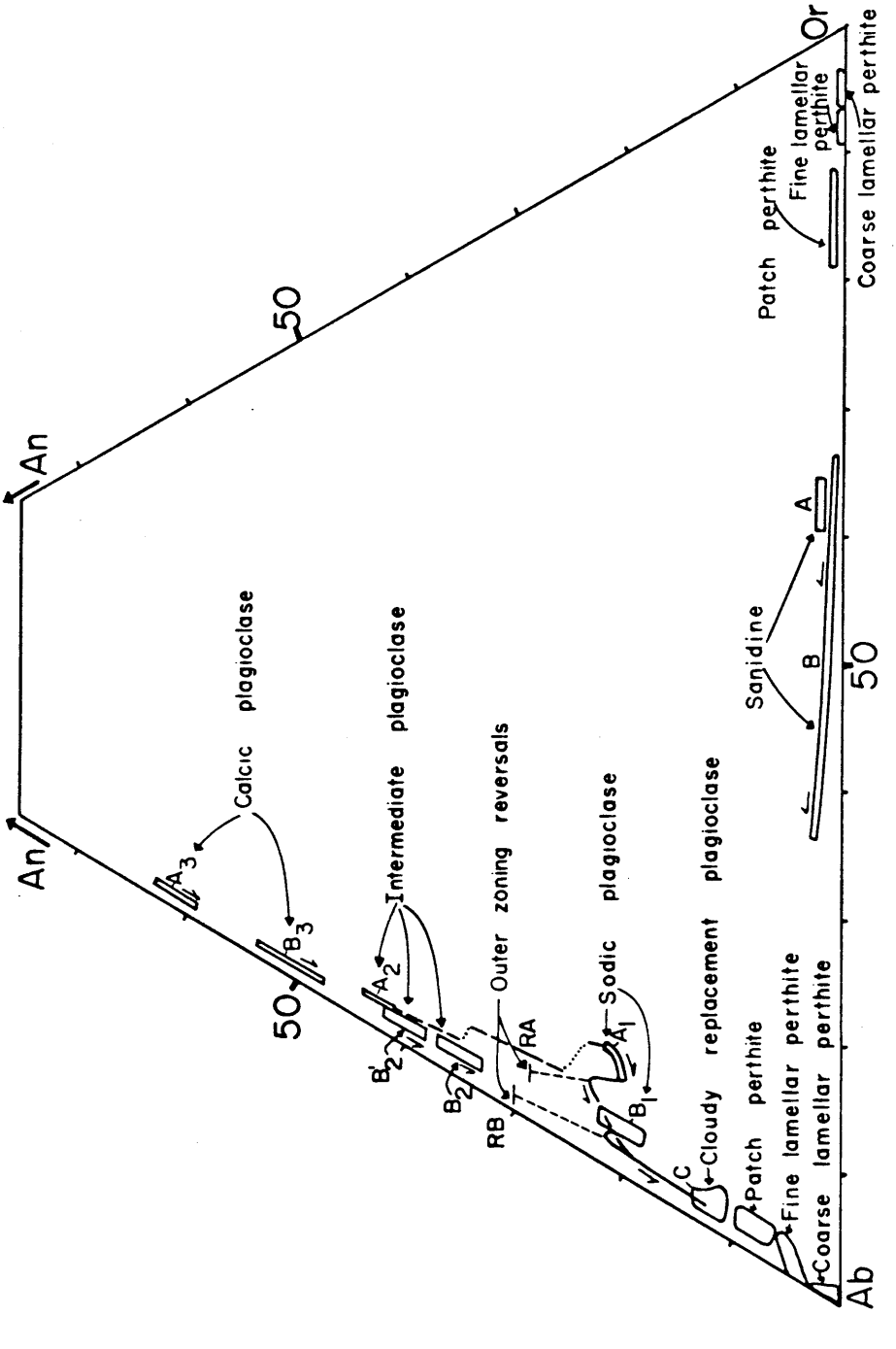


Fig. 49. Summary diagram of all analysed feldspars from the major phases of the Little Chief stock, plotted in weight percent in the Or-Ab-An system. See text for detailed explanation. Arrows show direction toward outer edge of phenocrysts.

crystallization of two feldspars; sanidine and oligoclase. The An percentage of the oligoclase, the last plagioclase of the sequence of zones noted above, is $An_{20}$ in almost all cases, but there are significant differences in the Or percentage ($A_1$ and $B_1$), indicating that the interior portions of the stock's north phase crystallized at significantly lower water pressures than the rest of the stock at this time. The sanidine zoned steadily from roughly $Or_{65}$ to $Or_{35}$ (A and B), with different specimens having different portions of this range. During the time of stable coexistence of oligoclase and sanidine, defined as that period of oligoclase crystallization in which the An percentage was essentially constant and the Or percentage changed very slowly per unit distance, if at all, the sanidine zoned very rapidly and grew very large relative to the plagioclase. This stage of stable two-feldspar crystallization accounts for 75 to 95 percent by volume of the phenocryst crystallization in all rocks except those of the north phase interior portion, in which the two feldspar stage accounts for perhaps 60 percent of the phenocryst crystallization.

The third stage of feldspar crystallization is that of plagioclase crystallization immediately after the stable period of oligoclase crystallization. In this stage, which accounts for less than 5 percent of phenocryst crystallization (not including the replacement stage in some rocks), the Or and An percent changed rapidly, the prominant reversals were formed and the relatively rapid zonation to Or-poor sodic oligoclase occurred ($A_1$ or $B_1$ to C, Fig. 49). The general pattern of the compositional change, in which the An percentage increases

then decreases, while the Or percentage is steadily decreasing, is shown on the figure. The reversals in most cases have maximum An percentage of $An_{30}$ and thus involve a change in An percentage of less than 10 percent. However, in the earliest igneous phase of the stock, now present only as inclusions in the later granite, the maximum An percentage of the reversals reaches $An_{55}$, an abrupt change of 35 percent An.

During the fourth stage, the sanidine reacted with the magma to yield oligoclase. In different parts of the stock, this reaction took place at different times relative to the plagioclase that was crystallizing from the melt at the same time. Thus, in the interior portion of the north stock phase, sanidine, after a brief period of resorption was rimmed by oligoclase, and this took place during the period of stable oligoclase crystallization so that sanidine was no longer crystallizing at the time the reversals and outermost sodic oligoclase crystallized. In the rest of the stock, however, sanidine reaction took place after the time the reversals formed, when the plagioclase was approaching the outermost sodic oligoclase compositions (C, Fig. 149). Thus sanidine coexisted with plagioclase through the reversal stage.

In the first case, sanidine was simply rimmed by stable $An_{20}$ oligoclase ($A_1$), and this latter accounted for roughly 30 percent by volume of phenocryst crystallization. In the second case, the sanidine was replaced by sodic oligoclase through a complex series of steps, and in this case the stable oligoclase ($B_1$) makes up less than 10 percent of the phenocrysts. The replacement mechanism varied and can be broken

down into two end member-types with all combinations present in the stock. In one end member-type, the sanidine was replaced directly by cloudy sodic oligoclase (C, Fig. 49) which formed rims around the clear sanidine cores. In the other, the sanidine exsolved into a patch perthite with compositions as shown in Fig. 49, and the Or-rich phase was progressively replaced by plagioclase of the same composition as the Ab-rich phase. This latter was itself replaced by sodic oligoclase (C) to eventually produce phenocrysts which consisted of cloudy sodic oligoclase with scattered patches of relict Or-phase. At the same time, in a few instances, sodic oligoclase crystallized directly from the melt onto the same phenocrysts, as well as on the true magmatic plagioclase phenocrysts already discussed. Much of the sodic oligoclase, especially that which replaced the outermost parts of the former sanidine phenocrysts, in turn formed antiperthite with less than 5 percent of an Or-rich phase.

The direct replacement sequence dominates in the southern phase of the stock, while the patch perthite replacement sequence dominates in the northern phase exterior portions. The replacement process took place at the time that the sodic oligoclase, with less than 17 percent An,was crystallizing on the plagioclase phenocrysts, and the end result of the replacement process was to form plagioclase with a sodic oligoclase composition. In general, the more sodic outer portions of the sanidine phenocrysts were replaced first, or went to patch perthite first.

In a few areas of the stock, a contact phase was formed in which the sanidine never went out of equilibrium with the melt, and no rimming

or replacement occurred.

The last stage of crystallization resulted in the formation of the groundmass in all parts of the stock. The dominant minerals of the groundmass were alkali feldspar (G, Fig. 49) and quartz which crystallized simultaneously, the alkali feldspar forming thin rims on all the phenocrysts at the beginning of this stage. In those portions of the stock which have significant plagioclase as part of the groundmass--namely, the early igneous phase, the interior north phase, and the south phase--the groundmass generation plagioclase nucleated about the same time as the reversals formed on the oligoclase zones of the plagioclase phenocrysts, reproduced the zoning of the outermost sodic plagioclase of the phenocrysts, and then was commonly rimmed by groundmass sanidine. Thus, the groundmass generation alkali feldspar is always later than the sodic oligoclase, no matter whether the oligoclase formed on the phenocrysts or as a second generation of crystals in the groundmass.

Features indicative of high volatile concentrations, as for instance, lobate quartz macrocrysts, micro pegmatitic patches in the groundmass, large pegmatitic pods, graphic groundmass textures, vugs, and coarse lamellar perthite (Fig. 49) tend in general to concentrate in the outer parts of the stock, and especially in the northeast corner of the north phase where rocks up to 30 percent vug are present. This in turn suggest a variation in the volatile concentration of the magma, with higher concentrations at the outer edges of the stock. At this stage in the crystallization it is certain that $P_{fluid} = P_{total}$.

The sequence of crystallization of the mafic minerals was as follows: Initially augite and magnetite, followed by hornblende, magnetite and biotite from the time of crystallization of the intermediate plagioclase zones onward. The growth rate of the mafic minerals was slow until the time of reversal formation and crystallization of the "unstable" period oligoclase and sodic oligoclase (stage 3 above), at which time very large amounts of hornblende and biotite crystallized very rapidly. In most of the area, during the groundmass crystallization stage, hornblende reacted to biotite.

Diopside rims formed on the large hornblende crystals in ten specimens from all phases of the stock, and in a few of these the diopside was in turn altered to biotite during groundmass crystallization. In the early igneous phase, the percentage of mafic minerals is as much as 20 percent of the rock, and diopside makes up half this in several cases. The diopside was formed by the assimilation of dolomite wall rock, a process that can be demonstrated at the present stock contacts against the Noonday Dolomite. The extreme reversals in the early igneous phase are also due to this period of assimilation. In several rocks from the present stock, a second generation of biotite formed in the groundmass which was relatively more Mg-rich than the normal igneous biotite that preceeded it, and dolomite assimilation is in part the reason for its formation.

Assimilation of the calcareous graywacke of the Kingston Peak Formation, at the present contacts, formed inclusions which are dominantly biotite and hornblende, with magnetite. Similar appearing clots of hornblende, biotite and magnetite are scattered throughout the stock

and are associated with sodic plagioclase, indicating that assimilation of rock like the Kingston Peak Formation took place close to the time of reversal formation on the oligoclase plagioclase zones.

In the very late stages of groundmass crystallization, $pO_2$ was relatively high, so that biotite reacted to magnetite and oxybiotite was formed close to the actual vugs. This may also in part have been the cause for the Mg-rich groundmass biotite generation noted above.

Petrogenesis

The changes in physical conditions which produced the observed compositional variations in the feldspar are summarized in the following section in the form of a short petrogenetic history of crystallization of the stock.

The step-like normal zonation in the plagioclase phenocrysts is due to the interplay of several factors. The compositional gaps between the calcic, intermediate and sodic plagioclase zones were chiefly caused by the progressive, sporadic decrease in volatile content of the system as it moved upward in the earth's crust. The reversals which immediately preceed the respective compositional gaps were formed by the assimilation of calcic material, probably of dolomitic composition, which contained more $H_2O$ than the magma and hence caused an increase in the $H_2O$ content of the magma. The plagioclase returned to "normal" compositions immediately after the reversal due to a combination of supersaturation of the An-component in the melt leading to rapid crystallization, and mixing of the contaminated magma with relatively uncontaminated magma. The probable sequence of events which led to each compositional gap is noted below.

Initial upward movement of the magma led to the assimilation of dolomitic material relatively rich in water. The contaminated outer portions of the magma chamber were mixed with the uncontaminated central part of the magma chamber due to turbulence in the magma chamber. The assimilation caused the generation of $CO_2$ which led to the condition of $P_{fluid} = P_{total}$, which in turn led to volatile release through extensive fracturing of the magma chamber roof. The magma then abruptly moved upward, decreasing the total pressure and allowing a brief period of resorption of the plagioclase crystals in some cases. However, on continued upward movement, the effect of rapid irregular loss of volatiles was dominant, causing the crystallization of much more sodic, Or-rich plagioclase. At the point that the magma came to rest temporarily, the next broad compositional zone in the plagioclase phenocrysts was formed.

This sequence of events accounts for all the features observed in the compositional variation of the plagioclase phenocrysts up to the formation of the sodic zone. During the last gap between the intermediate and sodic plagioclase zones, the volatile pressure decrease caused a shift of the feldspar boundary toward the interior of the ternary feldspar system so that, when the magma reached a stable position both sodic plagioclase and sanidine crystallized. At this point, the $H_2O$ pressure on the system is estimated to have been 1-1.5Kb in the "drier" parts of the magma chamber, and 2-2.5Kb in the "wetter" parts, at temperatures of roughly 710 and 680°C, respectively.

A similar sequence of events formed the complex outer compositional zonation of the sodic plagioclase zones, and the rapid crystallization

to form the groundmass. The groundmass formed during devolatilization of the system as the magma reached its present position. The reversal or reversals superimposed on the unstable portion of the sodic plagioclase zones are due to the assimilation of basic material which formed a contaminated marginal phase of the magma chamber now preserved as the early igneous phase inclusions. However, one important difference is that, during the period of unstable plagioclase crystallization, the Or percentage steadily decreased.

The observed compositional change could be due to a combination of an increase in water content combined with a decrease in total pressure; however, this leads to excessively high water pressures. Another possibility is that this trend is due to a natural outward curvature of the solvus-solidus intersection caused by the peristerite plagioclase solvus. This cannot be verified with the present data, but is a likely possibility. Using water pressure changes alone, large amounts of water would have to have been added to the magma to produce the observed compositions.

At various times during the crystallization of both the stable and unstable portions of the sodic plagioclase zones the sanidine was removed from equilibrium with the melt. In the "drier," most-calcic, and least-differentiated parts of the magma chamber the sanidine was slightly resorbed and then rimmed with oligoclase. The plagioclase that was crystallizing at the time the sanidine reacted with the melt was $An_{20}$ in composition in this case. In the "wetter," least-calcic and most-differentiated portions of the magma chamber the sanidine was directly replaced by sodic plagioclase or replaced through the patch

perthite mechanism. At this time, the coexisting plagioclase was $An_{16}$ to $An_{14}$ in composition. In some marginal parts of the present stock, the sanidine remained in equilibrium with the melt until groundmass crystallization started.

The cause for the transition from two to one feldspar crystallization appears to have been a shift of the feldspar boundary due to slow, steady water pressure increase combined with the very rapid crystallization of sanidine which changed the melt composition significantly. Stewart's model for the crystallization sequence of rapakivi granites, similar to that seen here, does not agree with the observed compositional changes in the feldspars of the stock.

The beginning of the period of unstable sodic plagioclase crystallization is roughly the time that the magma started to move upward from the position it occupied during stable plagioclase crystallization. Thus in the drier parts of the magma chamber, the sanidine was already out of equilibrium with the melt at this time. Structural evidence suggests that, at the time the reversals formed, the magma had at least reached the position of the base of the Pahrump Series--roughly 6000 feet below the present erosion level, or 13000 feet below the probably ground surface at the time of intrusion of the stock. At this time, the dike swarm in the Hanaupah Canyon area was injected. The distribution of replacement textures in the stock suggests that the magma had essentially reached its present level by the time that the $An_{16}$ plagioclase was forming. Thus part of the sanidine replacement took place when the stock magma was at its present position. Build-up of fluid pressure at this point led to roof fracture and devolatilization

of the system to form the "pressure-quench" groundmass.

The inhomogeneous water distribution in the magma chamber during the time of coexisting feldspar crystallization was changed to the very homogeneous water distribution seen during the time of groundmass crystallization, as reflected in the similar water pressure estimates gotten from the groundmass mineralogy throughout the stock. However, while the water pressure was the same throughout the stock at this time, the volume distribution of the separated vapor phase bubbles in the system was very inhomogeneous. Thus, great concentrations of the vapor phase are seen in the vug-rich northeast corner of the stock. This late migration of the vapor phase toward the exterior of the stock, and especially to the northeast corner where the volatiles were apparently able to escape from the magma chamber, resulted in the development of late textural features which modified the groundmass. Thus, going from the vapor-poor interior to the vapor-rich exterior of the stock, and also roughly in the order of formation, quartz megacrysts, quartz-alkali feldspar intergrowths, small pegmatitic pods, large pegmatitic pods, and coarse lamellar perthite were formed.

The effects of the vapor phase are most obvious in the dike rocks which originated from the stock. Here the phenocrysts were completely albitized, and the glassy matrix, on devitrification, was completely separated into spherulites of K-feldspar and interstitial areas of Na-feldspar and quartz. In some extreme cases, the Na-feldspar and quartz were also separated. This separation of phases is thought to be due to vapor phase transport in the presence of temperature gradients, as suggested by Orville (1963) and Burnham (oral communication).

The water pressure at the time of groundmass crystallization was consistently 0.4-0.5Kb, and the magma temperature therefore roughly 775°C. The presence of wollastonite at the stock contact suggests that the total pressure at this time was roughly 0.7Kb and the volatile phase consisted of roughly 25 percent $CO_2$.

A second generation of plagioclase crystallization was initiated at the time of assimilation of dolomitic material and formation of the reversals. The compositional variation in these plagioclase microcrystals exactly duplicates the outer zones of the plagioclase phenocrysts, starting at the "peak" of the reversals. This is thought to be due to a combination of the supersaturation of An-component in the melt and the change in bulk composition of the melt, both of which would tend to cause very rapid nucleation of relatively calcic plagioclase. This method is not the same as the pressure quence mechanism which caused the groundmass quartz and alkali feldspar crystallization.

The existence of coexisting feldspars which crystallized under different water pressure conditions indicates that water pressure variations existed in the magma chamber at depth. The great similarity in the sequence of events preserved in the compositional variations of plagioclases that crystallized under the different water pressures indicates that all parts of the magma chamber were in communication. Assuming that $P_{total} = P_{water}$ throughout the stock, then the difference of 1 to 1.5Kb between the different parts of the magma chamber would indicate a vertical magma chamber roughly 15000 feet in height which had the least differentiated material at the top, and the most differentiated material at depth.

A more likely alternative would be a relatively equant magma chamber in which parts of the magma were saturated with respect to water, and other parts unsaturated. The most likely distribution would be to have the least differentiated, "drier," unsaturated magma in the center of the magma chamber, surrounded by an envelope of differentiated, saturated magma. This agrees with the evidence of assimilation of relatively "wet" material at the margins, and is also borne out by the present distribution of textures in the stock. A distribution of this sort was first suggested by Kennedy (1955). In this case, the south phase and the exterior north phase of the stock would have been derived from the outer part of the magma chamber, while the interior north phase would have been derived from the inner part of the magma chamber. Using this model, the magma would have been at a depth of 20000 feet below the surface, or roughly 13000 feet below the present outcrop level, at the time of two-feldspar crystallization.

NORMS CALCULATED FROM PROBE ANALYSES AND MODAL DATA

| | | North phase interior | South phase | | North phase exterior | | | | | Early igneous phase | | |
|---|---|---|---|---|---|---|---|---|---|---|---|---|
| | | DV56 | DV74 | DV294 | DV129G | DV151 | DV63 | DV47B | DV128A | DV143B | DV137 | DV257B |
| Ground-mass | Or | 29 | 25 | 25 | 24.5 | 25.5 | 22 | 25 | 27 | 20.5 | 20.5 | 18.5 |
| | Ab | 30.5 | 40.5 | 40 | 33 | 31.5 | 29.5 | 28.5 | 30.5 | 50 | 42.5 | 49 |
| | An | 6.5 | 2 | 2 | 1 | 1 | 1 | 1.5 | 1.5 | 12 | 23.5 | 20.5 |
| | Q | 40 | 32.5 | 33 | 41.5 | 42 | 47.5 | 45 | 41 | 17.5 | 13.5 | 12 |
| Whole rock | Or | 25 | 26 | 28.5 | 28 | 29.5 | | | 30.5 | | | |
| | Ab | 45.5 | 45.5 | 47.5 | 40.5 | 33.5 | | | 40 | | | |
| | An | 8.5 | 3.5 | 3 | 3 | 3.5 | | | 1.5 | | | |
| | Q | 21 | 25 | 21 | 29 | 33.5 | | | 28 | | | |

GROUNDMASS NORMS CALCULATED FROM OPTICAL DATA

| | North phase interior | | | | | South phase | | | NORMS CALCULATED FROM WET CHEMICAL ANALYSES WHOLE ROCK: Dike rocks | | | Contact dike sheath | |
|---|---|---|---|---|---|---|---|---|---|---|---|---|---|
| | DV49 | DV133 | DV146 | DV258 | DV263 | CP53 | CP52 | CP56 | DV38C | DV41A | DV107 | DV243A | DV73 |
| Or | 22.5 | 28.5 | 23 | 20 | 17.5 | 22 | 29.5 | 25 | 26 | 26 | 32.5 | 26 | 27 |
| Ab | 41.5 | 39.5 | 34.5 | 46 | 40.5 | 33.5 | 38.5 | 35.5 | 30 | 38 | 27.5 | 34 | 30 |
| An | 4 | 2 | 2.5 | 6 | 5.5 | 1.5 | 1.5 | 2 | 0.5 | 2 | 1 | 2 | 1 |
| Q | 32 | 30 | 40 | 28 | 36.5 | 43 | 30.5 | 37.5 | 44 | 34 | 39 | 38 | 42 |

APPENDIX A NORMATIVE AND MODAL DATA
FROM VARIOUS STOCK SPECIMENS.

SELECTED MODES FROM THE LITTLE CHIEF STOCK-MAJOR SPECIMENS

volume percent

| | DV56 |
|---|---|
| sanidine pheno. | 10 |
| oligoclase rims | 11 |
| oligoclase zones on plag pheno. | 20.5 |
| intermediate zone on plag pheno. | 1.5 |
| calcic cores in plag pheno. | 0.5 |
| Gnd alkali feld. | 29 |
| Gnd quartz | 19.5 |
| hornblende | 3 |
| biotite | 2.5 |
| magnetite | 1.5 |
| sphene | <0.5 |
| apatite | <0.5 |
| vug | 0.5 |
| total | 100.5 |

| | DV74 |
|---|---|
| sanidine pheno. | 12 |
| cloudy plag rim | 5.5 |
| sodic plag pheno | 5.5 |
| calcic plag | 1 |
| Gnd alkali feld. | 37 |
| Gnd quartz | 24 |
| Gnd plag | 7.5 |
| hornblende | 4.5 |
| biotite | 1.0 |
| magnetite | 1.0 |
| sphene + apatite | 1.0 |
| total | 100.0 |

| | DV128A |
|---|---|
| sanidine pheno + perthite | 28.5 |
| plag pheno | 3 |
| alkali rims | 2 |
| Gnd alkali feld | 35 |
| Gnd quartz | 25 |
| Gnd plag | 1 |
| hornblende | 3 |
| biotite | 1 |
| magnatite | 1 |
| sphene + apatite | 0.5 |
| total | 100.0 |

| | DV151 |
|---|---|
| sanidine pheno + patch perthite | 27 |
| alkali rims | 5 |
| sodic plag zone on plag pheno. | 3 |
| calcic plag core in plag pheno. | 3 |
| Gnd alkali feld. | 26.5 |
| Gnd quartz | 28.5 |
| Gnd plag | 1 |
| hornblende | <0.5 |
| biotite | 3 |
| opaque | 1 |
| sphene | 1 |
| vug | 0.5 |
| total | 100.0 |

# APPENDIX B

## Analytical Techniques

### Electron Microprobe

The chemical analyses were made on an Applied Research Laboratory three-channel electron microprobe (EMX) equipped with pulse height analyzers on each channel. Ca and K were analyzed on two channels with LiF crystals, while Na was analyzed on the third channel using a KAP crystal. Data were printed out on an I.B.M. electric typewriter. All channels had sealed proportional gas-counter detectors.

### Sample Preparation

All analyzed specimens were in the form of polished thin section disks which were prepared by Mr. Rudolf von Huene, California Institute of Technology. A thick thin section, roughly 100 microns thick, was prepared and rough ground by ordinary polished section techniques. These were usually cut from the blanks left over from the normal thin sections that were examined in detail optically. Final grinding was done on a porous agate lap using levigated alumina powder by applying light pressure on a slow moving wheel for periods of five minutes or more. This was then polished using silk or Buehler Texmet with 0.5 micron diamond powder. Final polishes were obtained using silk or Texmet, wet, with tin oxide.

One inch diameter disks were then drilled from the polished thin sections. If the grain desired for analysis was located in the corner of the polished thin section, the corner was cut off and mounted on a one inch glass disk.

All sample disks were carbon coated using a graphite arc in an evacuated bell jar. It was found that coating times between 30 and 60 seconds produced the best results; these times gave colors on polished brass ranging from deep red-orange to purple. In applying the carbon coat, it is absolutely necessary that the sample be absolutely dry, as any moisture in the sample will cause the carbon coat to buckle under the electron beam.

As a rule, the grain or area of the polished disk to be analyzed was selected using a petrographic microscope, all other areas painted out with black conducting paint, and then each specific area photographed using a polaroid camera-petrographic microscope combination. This was necessary for detailed analysis, both in location of the desired area in the probe, and for the location of the specific probe spot or scan locations due to the very poor transmitted light optics of the ARL probe.

Experimental Conditions

All analyses were made using a sample current of 0.1 $\mu a$ and an operating voltage of 15 KV. Electron beam spot sizes varied as a function of the specimen being analysed, but in general it was found that under the above operating conditions no spot diameters of less than 3 $\mu$ could be used due to serious volatilization of the alkalis in the specimen.

All sample current readings were made on the individual specimens and not on reference specimens or on brass.

Three basic methods of analysis were used. To analyze specific

small areas, as for instance an individual perthite lamella, two or three 5 to 10 -diameter areas were analyzed for times of 10 seconds each, and the results averaged. To obtain compositional profiles, the mineral grain was scanned by making 10 second analyses at distances of 2 to 10 apart using various spot sizes. After each 10-second analysis, the sample was automatically moved in the chosen direction a specified amount and another analysis made. Finally, to obtain an average composition of a large, very inhomogeneous area, such as the groundmass of some of the dike rocks, a 50 to 100 spot was moved by hand regularly over the desired area for periods of 100 seconds. Several such 100 second analyses were averaged to obtain the final result.

Standards

All analyses were obtained by reference to standard curves. A standard curve for each end member feldspar was made by plotting background corrected counts per second vs. weight percent end member feldspar for a series of homogeneous analyzed feldspars obtained from Dr. J. V. Smith. Plagioclase and K-feldspar glasses from the Geophysical Laboratory were also used. In all cases, the sample current was read on the mineral grain itself.

The resulting three curves were then adjusted for day to day use by graphically shifting the curves relative to the counts obtained on a working standard. The working standards were themselves calibrated relative to the other standards and also analyzed chemically by Dr. D. R. Maynes. The three working standards were placed in the

same mount so that they could be constantly referred to during the time that various samples of unknown composition were being analyzed.

The secondary standards, and their compositions were:

Amelia Albite: $Or_{0.9}Ab_{99.0}An_{0.1}$ (Na)

Andesine, Kregarϕ, Norway: $Or_{4.1}Ab_{71.6}An_{23.3}$ (Ca)

Sanidine, Leilenkopf, Germany: $Or_{77.5}Ab_{19.0}An_{0.5}$ (K)

Daily operation was as follows: After a warm-up period, the uncorrected counts per second for the desired end member feldspar in each of the working standards was obtained by averaging the results of three 100-second counting periods. The various samples were then analyzed, and periodically the working standards were rerun for comparison purposes. In most cases, the working standards were run every 3 or 4 hours, but at times when the sample current was drifting due to filiment warpage, the standards were run more often. Finally, at the end of the day the working standards were rerun as before, and then backgrounds on each of the standards were obtained. It was found that, within counting rate errors, the background values were essentially unchanged from day to day, and backgrounds on samples were identical to backgrounds on the standards.

Graphical Procedures

The majority of the probe results were in the form of scans across various features of interest within the feldspar grains. These scans were plotted, as in Fig. 50, and the compositions then obtained by reference to the standard curves. In areas where the feldspar compositions varied widely in short distances, at least three adjacent spot analyses with closely similar counting rates were averaged to obtain

one reliable analysis. While this tended to mask minor variations in compositions, it was more useful in determining the more general compositional trends which were used to work out the feldspar crystallization history. This was necessary to allow for the fact that the area of the spot often overlapped phase boundaries, or because large compositional changes occurred in the width of the spot.

The first data scans were plotted by hand. However, it soon became apparent that the plotting time would not allow all the probe data to be reduced. Therefore, most of the later probe analyses were plotted by computer using the GMPLOT subroutine available in the CIT computer library. A program was written by Mr. R. S. Naylor, and modified by the author, which made the background corrections and determined the weight percent end member feldspars for each spot analysis. This information was then plotted to the nearest 1 percent by the GMPLOT subroutine.

Linear standard curves were used in this computer program. Because the actual standard curves for Or and An were slightly curved, this introduced predictable errors in certain compositional ranges of up to 1.5 percent Or or An which were corrected when the final compositional information was summarized.

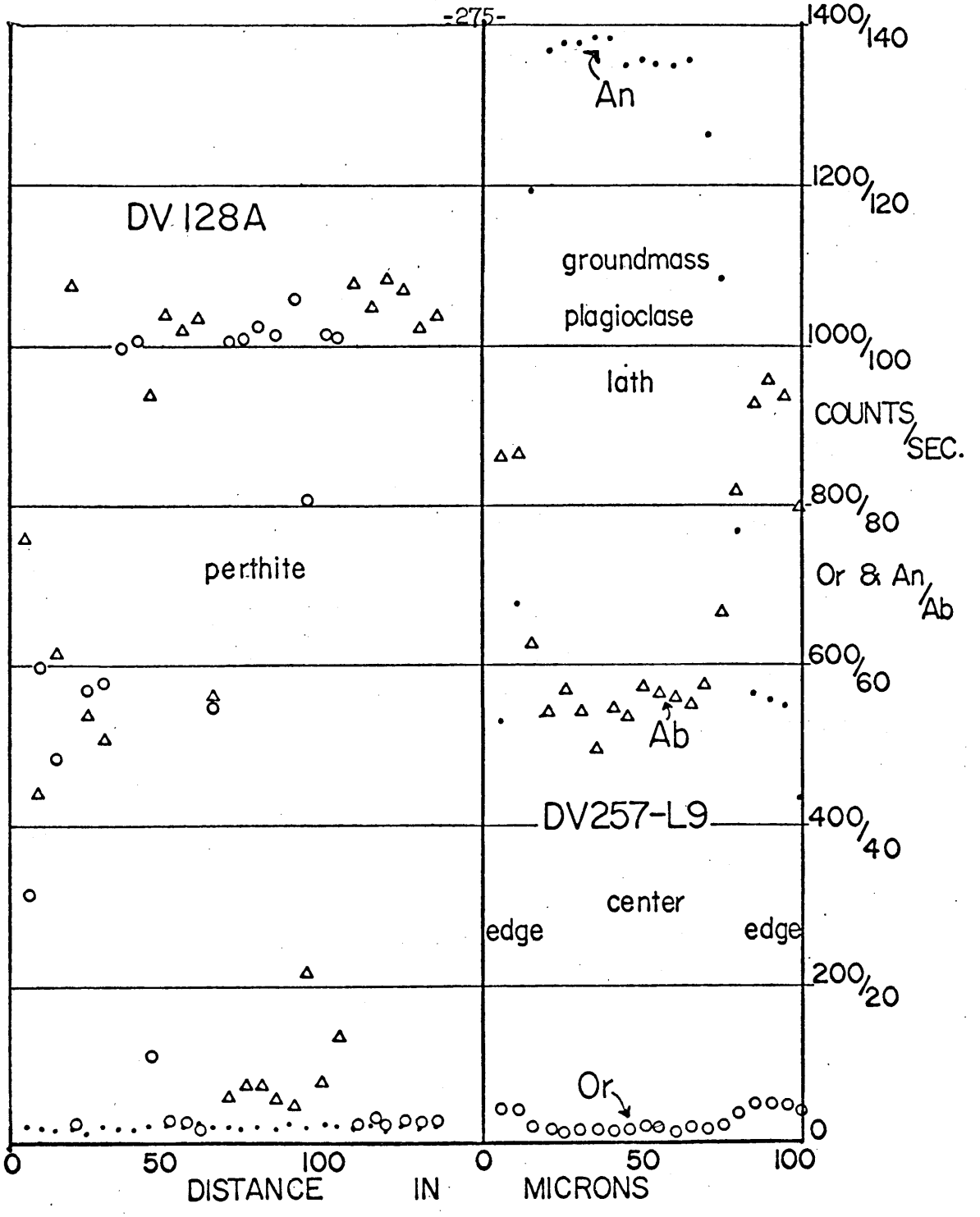


Fig. 50. Actual profiles obtained for three elements from scans across various typical feldspar phenocrysts or groundmass grains. Dots-An(Ca) counts per second(cps). Circles-Or(K) cps. Triangles-Ab(Na) cps. Scale for Ab(Na) cps 0-140. Scale for Or(K) and An(Ca) cps 0-1400.

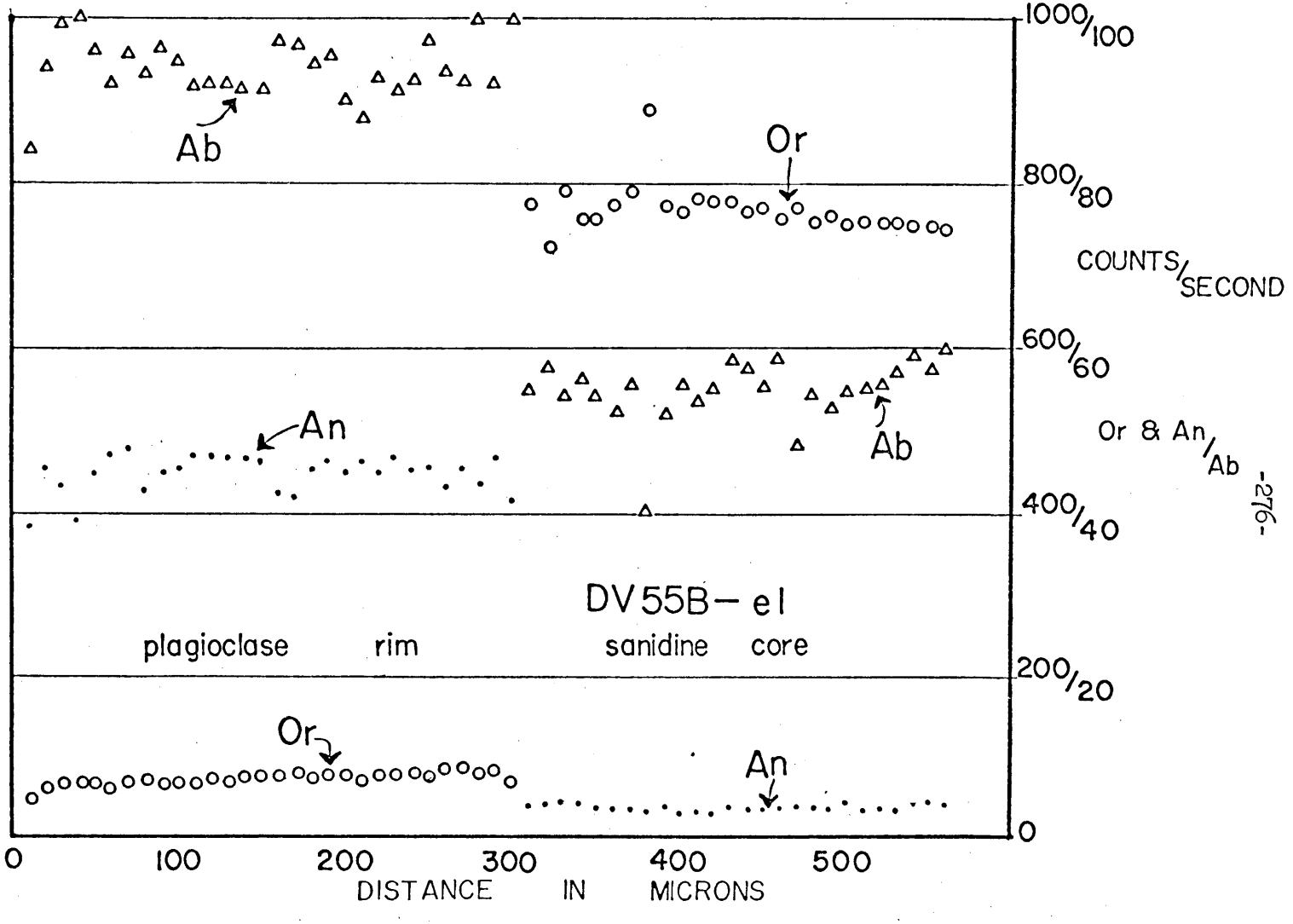




Fig. 50. see previous page.

REFERENCES

Albee, A.L., and M.A. Lanphere, 1962, Distribution of earlier and later Precambrian rocks in the Central Panamint Range: California (abs.) Geol. Soc. America, Cordilleran Section, Los Angeles, California.

Bowen, N.L., 1913, The melting phenomena of the plagioclase feldspars: Amer. Jour. Sci., 4th series, v. 35, p. 577-599.

Boyd, F.R., and J.L. England, 1963, Effect of pressure on the melting of diopside, $CaMgSi_2O_6$, and albite, $NaAlSi_3O_8$, in the range up to 50 Kb.: Jour. Geophys. Res., v. 68, p. 311-323.

Brown, W.L., 1960, The crystallographic and petrologic significance of peristeritic unmixing in the acid plagioclases: Zeit. F. Krist., v. 113, p. 330-344.

Carmichael, I.S.E., 1960, The feldspar phenocrysts from some Tertiary acid glasses: Min. Mag., v. 32, p. 537-608.

_____, 1963, The crystallization of the feldspar in volcanic acid liquids: Geol. Soc. London Quat. Jour., v. 119, p. 95-131.

Currie, J.B., 1956, Role of concurrent deposition and deformation of sediments in development of salt-dome graben structures: Am. Assoc. Petroleum Geologists Bull., v. 40, p. 1-16.

deSitter, L.U., 1956, Structural Geology: 1st Ed., McGraw-Hill Book Co. Inc., New York, 552 pp.

Ewart, A., 1965, Mineralogy and petrogenesis of the Whakamaru Ignimbrite in the Maraetai Area of the Taupo Volcanic Zone, New Zealand: New Zealand Jour. Geol. and Geophys., v. 8, p. 611-677.

Greenwood, H.J., 1962, Metamorphic reactions involving two volatile components: Carnegie Institute of Washington Yr. Book 61, p. 82-85.

Harker, A., 1954, Petrology for Students: 8th Ed., Cambridge Univ. Press, 283 pp.

Harker, R.I., and O.F. Tuttle, 1955, Studies in the system CaO-MgO-$CO_2$: Part I. Am. Jour. Sci., v. 253, p. 209-224.

Hazzard, J.C., 1937, Paleozoic section in the Nopah and Resting Springs Mountains, Inyo County, California: Calif. Div. Mines. Jour. Mines and Geology, v. 33, p. 273-339.

Hewett, D.F., 1940, New formation names to be used in the Kingston Range, Ivanpah Quadrangle, California: Washington Acad. Sci. Jour., v. 30, p. 239-240.

_____, 1956, Geology and mineral resources of the Ivanpah Quadrangle, California and Nevada: U.S. Geol. Survey Prof. Paper 275, 172 pp.

Hopper, R.H., 1947, Geologic section from the Sierra Nevada to Death Valley, California: Geol. Soc. America Bull., v. 58, p. 393-432.

Hunt, C.B., and D.R. Mabey, 1966, Stratigraphy and structure. Death Valley, California: U.S. Geol. Survey Prof. Paper 494A, 162 pp.

Jaeger, J.C., 1957, The temperature in the neighborhood of a cooling intrusive sheet: Am. Jour. Sci., v. 255, p. 306-318.

Johnson, B.K., 1957, Geology of a part of the Manly Peak Quadrangle, Southern Panamint Range, California: Univ. Calif. Publ. in Geol. Sciences, v. 30, p. 353-424.

Kennedy, G.C., 1955, Some aspects of the role of water in rock melts: Geol. Soc. America Spec. Paper 62, p. 489-503.

Lanphere, M.A., 1962, I. Geology of a part of the Wildrose Area, Panamint Range, California. II. Geochronologic studies in the Death Valley - Mojave region, California: Ph.D. Thesis, Calif. Inst. of Tech.

_____, G.J. Wasserberg, A.L. Albee, and G.R. Tilton, 1964, Redistribution of Strontium and Rubidium isotopes during metamorphism, World Beater Complex, Panamint Range, California: Isotopic and Cosmic Chemistry, North-Holland Publishing Co., Amsterdam, Chapter 20, 578 pp.

Larsen E.S. Jr., J. Irving, F.A. Gonyer, and E.S. Larsen, IIIrd, 1937, Petrologic results of a study of the minerals from the Tertiary volcanic rocks of the San Jaun region, Colorado: Am. Min., v. 22, p. 889-905

_____, _____, _____, and _____, 1938, Petrologic results of a study of the minerals from the Tertiary volcanic rocks of the San Jaun region, Colorado: Am. Min., v. 23, p. 227-257, p. 417-429.

Larsen, E.S., Jr., and W. Cross, 1956, Geology and petrology of the San Jaun region, southwestern Colorado: U.S. Geol. Survey Prof. Paper 258, 303 pp.

Luth, W.C., R.H. Jahns, and O.F. Tuttle, 1964, The granite system at pressures of 4 to 10 kilobars: Jour. Geophys. Res., v. 69, p. 759-773.

Muir, I.D., 1962, The paragenesis and optical properties of some ternary feldspars: Norsk. Geol. Tidsskr., v. 42, 2nd half, p. 477-492.

Murphy, F.M., 1932, Geology of a part of the Panamint Range, California: Calif. Div. Mines 27th Rept. of State Mineralogist, p. 329-355.

Murray, G.E., 1966, Salt sturctures of Gulf of Mexico Basin - a review: Am. Assoc. Petroleum Geologists Bull., v. 50, p. 439-478.

Nettleton, L.L., 1934, Fluid mechanics of salt domes: Am. Assoc. Petroleum Geologists Bull., v. 18, p. 1175-1204

_____, 1955, History of concepts of Gulf Coast salt-dome formation: Am Assoc. Petroleum Geologists Bull., v. 39, p. 2373-2383.

Noble, L.F., 1934, Rock formations of Death Valley, California: Science, new ser., v. 80, p. 173-178.

_____, and L.A. Wright, 1954, Geology of the Central and Ssuthern Death Valley region, California: Calif. Div. Mines. Bull 170, Chapter II, p. 143-160.

Nolan, T.B., 1929, Notes on the stratigraphy and structures of the northwest portion of Spring Mountains, Nevada: Am. Jour. Sci. 5th ser., v. 17, p. 461-472.

Orville, P.M., 1958, Feldspar investigations: Carnegie Institute of Washington Yr. Book 57, p. 206-209.

_____, 1963, Alkali ion exchange between vapor and feldspar phases: Am. Jour. Sci., v. 261, p. 201-237.

Parker, T.J., and A.N. McDowell, 1955, Model studies of salt-dome tectonics: Am. Assoc. Petroleum Geologists Bull., v. 39, p. 2384-2470.

Pirsson, L.V., 1915, The microscopical characters of volcanic tuffs - a study for students: Am. Jour. Sci., 4th ser., v. 40, p. 191-211.

Ribbe, P.H., 1960, An X-ray and optical investigation of the peristerite plagioclases: Am. Min., v. 45, p. 626 - 644.

_____, 1962, Observations on the nature of unmixing in peristerite plagioclases: Norsk. Geol. Tidssk., v. 42, p. 138-151.

_____, and van Cott, H.C., 1962, Unmixing in peristerite plagioclases observed by phase-contrast and dark-field microscopy: Canadian Min., v. 7, p. 278-290.

Ross, C.S., and R.L. Smith, 1961, Ash-flow tuffs: Their origin, geologic relations and identification: U.S. Geol. Survey Prof. Paper 366.

Scott, R.B., 1965, The Tertiary geology and ignimbrite petrology of the Grant Range, east central Nevada: Ph.D. Thesis, Rice University.

Shaw, H.R., 1963, Obsidian-$H_2O$ viscosities at 1000 and 2000 bars in temperature range 700° to 900°C: Jour. Geophys. Res., v. 68, p. 6337-6343.

_____, 1965, Comments on viscosity, crystal settling, and convection in granitic magmas: Am. Jour. Sci., v. 263, p. 120-152.

Silver, L.T., C.R. McKinney, and L.A. Wright, 1961, Some Precambrian ages in the Panamint Range, Death Valley, California: Abs., Geol. Soc. America, Sp. Paper 68, p. 55.

Spry, A., 1953, Flow structure and laminar flow in bostonite dykes at Armidale, New South Wales: Geol. Mag., v. 90, p. 248-256.

Stern, T.W., M.F. Newell, and C.B. Hunt, 1966, Uranium-lead and potassium-argon ages of parts of the Amargosa Trust complex, Death Valley, California: U.S. Geol. Survey Prof. Paper 550-B, p. 142-147.

Stewart, D.B., 1959, Rapakivi granite from eastern Penobscot Bay, Maine: Proc. 20th Internat'l Geol. Congr., Section XI -A, p. 293-320.

_____, and E.H. Roseboom, 1962, Lower temperature terminations of the three-phases region plagioclases-alkali feldspar-liquid: Jour. Petrology, v. 3, p. 280-315.

Stewart, J.H., 1966, Correlation of Lower Cambrian and some Precambrian strata in the southern Great Basin, California and Nevada: U.S. Geol. Survey Prof. Paper 550-C, p. 66-72.

Swift, H.R., 1947, Some experiments on cyrstal growth and solution in glasses: Am. Ceramic Soc. Jour., v. 30, p. 165-169.

_____, 1947, Effect of magnesia and alumina on rate of crystal growth in some soda-lime-silica glasses: Am. Ceramic Soc. Jour., v. 30, p. 170-174.

Troxel, B.W., 1966, Sedimentary features of the Upper Precambrian Kingston Peak Formation, Death Valley, California: Abs., Geol. Soc. America, Cordilleran Section, Reno, Nevada.

Trusheim, F., 1960, Mechanism of salt migration in Northern Germany: Am. Assoc. Petroleum Geologists Bull., v. 44, p. 1519-1540.

Tuttle, O.F., and N.L. Bowen, 1958, Origin of granite in the light of experimental studies in the system $NaAlSi_3O_8$ - $SiO_2$ - $H_2O$: Geol. Soc. America Mem. 74, 153 pp.

Vance, J.A., 1965, Zoning in igneous plagioclase: patchy zoning: Jour. Geol., v. 73, p. 636-651.

v. Platen, H., 1965, Kristallisation granitischer Schmelzen: Bert. zur Min. und Petrog., v. 11, p. 334-381.

Wallace, W.E., Jr., 1944, Structure of South Louisiana deep-seated domes: Am. Assoc. Petroleum Goelogists Bull., v. 28, p. 1249-1312.

Wasserberg, G.J., G.W. Wetherill, and L.A. Wright, 1959, Ages in the Precambrian terrane of Death Valley, California: Jour. Geol., v. 67, p. 702-708.

Winkler, H.G.F., 1947, Kristallgrösse und Abkühlung: Heidelberger Min. Petrog. Bertr., v. 1, p. 86-104.

_____, 1949, Crystallization of basaltic magma as recorded by variation of crystal size in dikes: Min. Mag., v. 28, p. 557-574.

_____, 1965, Petrogenesis of metamorphic rocks: Springer-Verlag, New York, Inc., 220 pp.

Wones, D.R., and H.P. Eugster, 1965, Stability of biotite: experiment thoery, and application: Am. Min., v. 50, p. 1228-1272.

Wright, T.L., 1964, The alkali feldspars of the Tatoosh Pluton in Mount Rainier National Park: Am. Min., v. 49, p. 715-735.

Wright, L.A., and B.W. Troxel, 1965, Limitations on strike-slip displacement along the Death Valley and Furnace Creek Fault Zones, California: Abs., Geol. Soc. America, annual Mtg., Kansas City, Mo.

_____, and _____, 1966, Strata of Late Precambrian age, Death Valley Region, California - Nevada: Am. Assoc. Petroleum Geologists Bull., v. 50, p. 846-857.

Wyllie, P.J., and O.F. Tuttle, 1961, Experimental investigation of silicate systems containing two volatile components, part II. The effect of $NH_3$ and HF, in addition to $H_2O$, on the melting temperatures of albite and granite: Am. Jour. Sci., v. 259, p. 128-143.

_____, and _____, 1959, Effect of carbon dioxide on the melting of granite and feldspars: Am. Jour. Sci., v. 257, p. 648-655.

_____, and _____, 1964, Experimental investigation of silicate systems containing two volatile components, Part III. The effect of $SO_3$, $P_2O_5$, HCl and $Li_2O$, in addition to $H_2O$, on the melting temperatures of Albite and granite: Am. Jour. Sci., v. 262, p. 930-939.

Yee, P.B., and A.I. Andrews, 1956, The relation of viscosity, nuclei formation, and crystal growth in titania-opacified enamel:

Am. Ceramic Soc. Jour., v. 39, p. 188-195.

Yoder, H.S., D.B. Stewart, and J.R. Smith, 1956, Ternary feldspars: Carnegie Inst. Washington Yr. Book 56, p. 206-214.

Yoder, H.S., C.E. Tilley, and J.F. Schairer, 1963, Pyroxenes and associated minerals in the crust and mantle: Carnegie Inst. Washington Yr. Book 62, p. 84- 95.